SISSA
Scuola
Internazionale
Superiore di
Studi Avanzati

Mathematics Area - PhD course in
Mathematical Analysis, Modelling, and Applications

Some results on mixing flows and on the blocking fire problem

Candidate:
Martina Zizza

Advisor:
Prof. Stefano Bianchini

Academic Year 2022-23

Contents

Introduction

This thesis is developed following two lines of research in analysis and applied mathematics: the study of mixing phenomena arising in a non-smooth setting and dynamic blocking problems of fire propagation.

The first part of this thesis is devoted to the study of mixing from the point of view of Ergodic Theory and the one of Fluid dynamics. The major result achieved here is the construction of infinitely many Exponential Mixers, that is divergence-free vector fields that have strong mixing properties. Moreover we give an example of a vector field which is weakly mixing but not strongly mixing.

The second part is devoted to the study of the Fire Problem first proposed by Bressan in 2007 [14]. Here, we study the properties of Optimal Blocking Strategies, proving Bressan's fire conjecture for spiral-like strategies.

Properties of Mixing BV vector fields

This part of the thesis will focus on the interplay between Ergodic Theory and Fluid Dynamics. A common feature between these two fields is the study of Mixing. In particular, in Ergodic Theory it is studied as a statistical behaviour of some dynamical system and in Fluid Dynamics it refers generally to the property of the motion of an incompressible fluid. Since the study of Mixing in Ergodic Theory has been widely developed [4, 23, 30, 32, 33, 36], the aim of this work is to understand the possible connections between these two branches of Mathematics, showing indeed that some ideas can be borrowed from Ergodic Theory in order to study the mixing properties of incompressible fluids. There is a quite recent interest in quantifying the degree of mixedness of an incompressible fluid and in producing deterministic examples of flows that achieve the optimal mixing: two of the most challenging open problems in the field are indeed Bressan Mixing Conjecture [1] and the deterministic Pierrehumbert Model [41]. Many approaches going from Probability to Geometric Measure Theory have been used in the recent years to solve some questions [3, 27, 37, 8], while the strong connection with Ergodic Theory could be a rich source of inspiration for new results.

Now, we consider a divergence-free vector field $b : \mathbb{R}^+ \times \mathbb{T}^d \to \mathbb{R}^d$ and the continuity equation

$$\partial_t \rho_t + D \cdot (\rho_t b_t) = 0, \quad \rho_{t=0} = \rho_0. \tag{0.0.1}$$

In recent year the following question has been addressed: is the solution ρ_t approaching weakly a constant as $t \to \infty$? The meaning of "approaching a constant" is usually formalized as

$$\rho_t \underset{t\to\infty}{\rightharpoonup} \fint \rho_0 \mathcal{L}^d \quad \text{weakly in } L^2, \tag{0.0.2}$$

($\mathcal{L}^d$ is the d-dimensional Lebesgue measure) since $\|\rho_t\|_{L^p}$ is constant (at least for positive solutions and sufficiently regular vector fields) and this is referred to as *functional mixing* (another notion of mixing is the *geometric mixing* introduced in [1], but for our purposes the functional mixing above is the most suitable, since it is related to Ergodic Theory).

Without any functional constraint on the space derivative Db_t, it is quite easy to obtain mixing in finite time: a well known example is [39]. A similar idea, used in a nonlinear setting, can be found in [2]. See also [**finite**] for completeness. The problem is usually formulated as follows: assume that $b \in L^\infty_{t,x} \cap L^\infty_t W^{s,p}_x$, what is the maximal speed of convergence in (0.0.2)?

This question has been addressed in several papers. In [3] the 2d-case has been throughly analyzed, and the main results are the explicit construction of mixing vector

fields when the initial data is fixed: the authors are able to achieve the optimal exponential mixing rate for the case $W^{1,p}$, $p > 1$, and study also the case $s < 1$ (mixing in finite time) and $s > 1$ (mixing at a polynomial rate). Recall that for $s = 1, p > 1$ the mixing is at most exponential [24], while the same estimate in $W^{1,1}$ (or equivalently BV) is still open [1]. In [**YaoZlatos**, 27] it is discussed the existence of universal mixers: that is divergence-free vector fields that mix *any* initial data. In particular, in [27] the authors construct a vector field which mixes at an exponential rate every initial data, and it belongs to $L^\infty_t W^{s,p}_x$ for $s < \frac{1+\sqrt{5}}{2}$, $p \in [1, \frac{2}{2s+1-\sqrt{5}})$. The autonomous 2d vector field is special, having an Hamiltonian structure: indeed in [11] the authors show that the mixing is polynomial with rate t^{-1} when $b \in \mathrm{BV}$.

In this paper we consider the different problem: how many vector fields are mixing? More precisely, we study the mixing properties of flows generated in the unit square $K = [0,1]^2$ by divergence-free vector fields $b : [0,1] \times K \to \mathbb{R}^2$ belonging to the space $L^\infty([0,1], \mathrm{BV}(K))$: to avoid problems at the boundary, we assume that the vector field b is divergence-free and BV when extended to whole $\mathbb{R}^2$. In order to shorten the notation, we will sometimes write $\mathrm{BV}(K)$, $K = [0,1]^2$ as the space $\mathrm{BV}(\mathbb{R}^2) \cap \{\mathrm{supp}\, b \subset K\}$.
All the results stated here can be extended to the case $x \in \mathbb{T}^2$ with minor modifications; our choice is in the spirit of [43].
In this setting, there exists a unique flow $t \to X_t \in C([0,1], L^1(K;K))$ (called Regular Lagrangian Flow (RLF)) of the ODE

$$\begin{cases} \frac{d}{dt} X_t(y) = b(t, X_t(y)), \\ X_{t=0}(y) = y, \end{cases}$$

which is measure-preserving and stable, see [6, 5] and Section 1.0.2. The idea here is to consider the $\mathcal{L}^2$-a.e. invertible measure preserving map $X_{t=1} : K \to K$ as an *automorphism* of the measure space $(K, \mathcal{B}(K), \mathcal{L}^2 \llcorner_K)$ and apply the tools of Ergodic Theory. Here and in the following $\mathcal{L}^2 \llcorner_K$ is the Lebesgue measure on K and $\mathcal{B}(K)$ are the Borel subsets of K. We call $G(K)$ the group of automorphisms of K. A non trivial additional difficulty is to retain that the maps under consideration are generated by a divergence-free vector field in $L^\infty_t \mathrm{BV}_x$.

There is a rich literature in Ergodic Theory that has deeply investigated the genericity properties of mixing for invertible and measure-preserving maps. We have to take into account that here *mixing behaviour*, or *mixing phenomena*, refers to different notion of mixing that are developed in Ergodic Theory (and recently they have been studied also in a Fluid Dynamics context). More precisely, let $T \in G(K)$ be an automorphism. We say that

- T is ***ergodic*** if for every $A \in \mathcal{B}(K)$

$$T(A) = A \quad \Rightarrow \quad \mathcal{L}^2(A) = 0 \text{ or } \mathcal{L}^2(A) = 1; \tag{0.0.3}$$

- T is ***weakly mixing*** if $\forall A, B \in \mathcal{B}(K)$

$$\lim_{n\to\infty} \frac{1}{n} \sum_{j=0}^{n-1} \left[\mathcal{L}^2(T^{-j}(A) \cap B) - \mathcal{L}^2(A)\mathcal{L}^2(B)\right]^2 = 0; \tag{0.0.4}$$

- T is ***(strongly) mixing*** if $\forall A, B \in \mathcal{B}(K)$

$$\lim_{n\to\infty} L^2(T^{-n}(A) \cap B) = \mathcal{L}^2(A)\mathcal{L}^2(B). \tag{0.0.5}$$

The genericity results concerning ergodic, weakly mixing and strongly mixing automorphisms are due mostly to Oxtoby and Ulam [40], Halmos [30, 31], Katok and Stepin [33] and Alpern [4]. They proved that the set of ergodic transformation is a residual (or comeagre) G_δ-set (i) in the set $G(K)$ with the *neighbourhood topology*[1] [31], (ii) in the set of measure-preserving homeomorphisms of a connected manifold with the strong topology[2] [40, 33]. Moreover, the weakly mixing automorphisms are a residual G_δ set [31, 33]. In 1976 Alpern showed that these problems are indeed connected by using the Annulus Theorem [4]. A different result holds for strongly mixing maps. It was shown firstly by Rokhlin in [42] (see [45] for an exposition of Rokhlin's work) and then by D. Ornstein [32] that (strongly) mixing maps are a first category set in the neighborhood topology.

In these settings, the genericity properties of measure-preserving (weakly) mixing or ergodic maps are fairly understood; to our knowledge a similar analysis has not been done for flows generated by vector fields with additional regularity requirements (e.g. $b \in L^\infty_t \operatorname{BV}_x$). The aim of our work is to extend the above genericity results to divergence-free vector fields whose Regular Lagrangian Flow is ergodic and weakly mixing (in dimension $d = 2$, but see the discussion below on the extension to every dimension $d \geq 3$).
We remark that here we are looking to genericity properties of mixing in the topological sense, and not a.e. mixing w.r.t. some probability measure in the space of vector fields (e.g. [9]): while there is some relation between the two notions, in general one result does not imply the other.

We consider $b \in L^\infty([0,1], \operatorname{BV}(K))$ be a divergence-free vector field.

Definition 0.0.1. We say that b is *ergodic (weakly mixing, strongly mixing)* if its unique Regular Lagrangian Flow evaluated at time $t = 1$ is ergodic (respectively weakly mixing, strongly mixing) as an automorphism.

0.0.1 Comparing weakly and strongly mixing behaviour

The definition of mixing vector fields was first given in [10], but there are examples of strongly mixing vector fields in previous literature. For instance, in [27] the authors give an explicit example of a strongly mixing vector field $b \in L^\infty([0,1], W^{s,p}(\mathbb{T}^d))$ for $s < \frac{1+\sqrt{5}}{2}$ and $p \in [1, \frac{1}{2s+1-\sqrt{5}})$ whose RLF at time $t = 1$ is the *Folded Baker's map*. We should remark that the advantage of the rough regularity of the vector field, especially in the case of the BV regularity, is that it allows for rigid *cut and paste* motions, since the flows originated by these vector fields do not preserve the property of a set to be connected. These constructions would be hard to reproduce for vector fields with higher regularity in time and space. Nevertheless, a stochastic approach (see for example [8]) investigates mixing vector fields with higher regularity, but does not furnish deterministic examples of vector fields with the desired mixing properties.

As we told above, the weakly mixing behaviour is *typical*, while strongly mixing vector fields are *few* in the sense of Baire Category Theorem (see also [4],[30],[32],[40],[42], and [45]). Nevertheless it is hard to give examples of weakly mixing automorphisms/ vector fields that are not strongly mixing.

The example we give in Chapter 2 is based on a work of Chacon [21], who constructed a weakly mixing automorphism that is not strongly mixing, in the

[1] The neighbourhood topology is indeed the convergence in measure, see Subsection 1.1.1.
[2] A sequence of maps $T_n \to T$ in the strong topology if $T_n \to T$ and $T_n^{-1} \to T^{-1}$ uniformly on K.

1	2	3	4
5	6	7	8
9	10	11	12
13	14	15	16

Figure 1: The grid on the torus with $k = 4$ and an enumeration of subsquares.

15	9	1	2
11	12	5	6
3	4	10	13
7	8	14	16

Figure 2: The automorphism U_4 sends the starting configuration into this final one.

one-dimensional space $([0,1], \mathcal{B}([0,1]), |\cdot|)$, where $|\cdot|$ is the one-dimensional Lebesgue measure. The importance of his work is that a general procedure to build up weakly mixing automorphisms that are not strongly mixing is given. Indeed his example easily extends to multiple dimensions, but we will focus on the dimension $d = 2$ to avoid technicalities and to provide some *visual* expressions of the vector fields under consideration. In particular we will construct a divergence-free vector field $b \in L^\infty([0,1], \mathrm{BV}(\mathbb{T}^2))$ whose Regular Lagrangian Flow $X(t)$, when evaluated at time $t = 1$, is a weakly mixing automorphism that is not strongly mixing.

The general idea here is the definition of a setting (see *Configurations* in Section 2.2) that helps to relate an automorphism, call it U, to the vector field b^U whose RLF at time $t = 1$ is U.

A *configuration* γ is a $n \times n$ matrix that takes values in the set $\{1, 2, \dots, n^2\}$. Moreover we ask that $\gamma_{ij} = \gamma_{hk}$ iff $i = h, j = k$. Every configuration indeed represents an enumeration of the subsquares of the torus of the grid $\mathbb{N} \times \mathbb{N}\frac{1}{n}$ (see Figures 1,2). A *movement* $T : \mathcal{C}(n) \to \mathcal{C}(n)$ is a one-to-one map from the space of configurations $\mathcal{C}(n)$ into itself, that is, it is a *permutations* of the subsquares of the grid $\mathbb{N} \times \mathbb{N}\frac{1}{n}$. Among movements the following are relevant for Chacon's example: simple exchange, sort, rotation (Section 2.2), and each one of them can be realized as the flow, evaluated at time $t = 1$, of some BV divergence-free vector field (see Subsection 2.2.1 and Figure 3).

The key example that one has to keep in mind while approaching this problem is the *15 puzzle* where one performs rigid movements on subsquares in order to reach the desired configuration (see Figure 4).

Chacon's method provides a sequence of automorphisms $\{U_k\}$ that are permutations of the subsquares of the grid $\mathbb{N} \times \mathbb{N}\frac{1}{k}$. To give an intuition, we fix for example $k = 4$ and we assume to enumerate squares as in Figure 1. Chacon's automorphism $U_4 \in G(\mathbb{T}^2)$ moves the previous enumeration of squares (the starting configuration) into the final configuration in Figure 2. Then he considers the limit map $U = \lim_{k\to\infty} U_k$, which is a

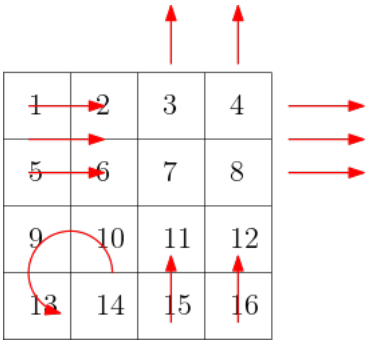

Figure 3: Vector fields on the torus that move rigidly the subsquares.

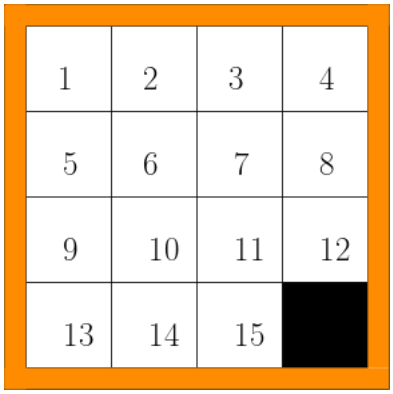

Figure 4: The 15 puzzle.

weakly mixing automorphism that is not strongly mixing (see Sections 2.1, 2.3).

Using Chacon's construction and the setting of configurations, we prove in particular the following result (Section 2.4):

Theorem 0.0.2. *There exists a divergence-free vector field $b^U \in L^\infty_t \mathrm{BV}_x$ whose RLF $X^U(t)$ when evaluated at time $t = 1$ is the Chacon's map U, that is b^U is a weakly mixing vector field that is not strongly mixing.*

We conclude remarking that all these constructions are possible assuming to work in $[0,1]^d$ instead of $\mathbb{T}^d$.

0.0.2 Residuality results for mixing BV vector fields.

Before our work [10], only few examples of deterministic mixing vector fields were known. In [10] we extended the genericity results mentioned above to divergence-free vector fields whose Regular Lagrangian Flow is ergodic and weakly mixing (in dimension $d = 2$, but see the discussion below on the extension to every dimension $d \geq 3$). Moreover, we constructed infinitely many exponentially mixing vector fields.

In the original setting (0.0.1), if $b_{t+1} = b_t$ (i.e., it is time periodic of period 1), then it is fairly easy to see that if b is strongly mixing as in the above definition then (0.0.2) holds, while for weakly mixing vector fields b it holds the weaker limit

$$\lim_{T\to\infty} \frac{1}{T} \int_0^T \left(\int_K \left(\rho_t - \fint \rho_0 \mathcal{L}^2 \right) \phi \mathcal{L}^2 \right)^2 dt = 0, \quad \forall \phi \in L^2(K).$$

This gives a precise connection between the *functional mixing* and the notion of mixing in Ergodic Theory.

The main result that we achieved is:

Theorem 0.0.3. *There exists a G_δ-subset $\mathcal{U} \subset L^1([0,1]; L^1(K)) \cap \{b : D \cdot b = 0\}$ containing all divergence-free vector fields in $L^\infty([0,1]; \mathrm{BV}(K))$ with the following properties:*

1. *the map Φ associating b with its RLF X_t,*

$$\Phi : \{b \in L^\infty_t \mathrm{BV}_x : D \cdot b_t = 0\} \to C([0,1], L^1(K)),$$

   can be extended as a continuous function to the G_δ-set $\mathcal{U}$;

2. *ergodic vector fields b are a residual G_δ-set in $\mathcal{U}$;*

3. *weakly mixing vector fields b are a residual G_δ-set in $\mathcal{U}$;*

4. *strongly mixing vector fields b are a first category set in $\mathcal{U}$;*

5. *exponentially (fast) mixing vector fields are a dense subset of $\mathcal{U}$.*

We will reasonably call the flow $X_t = \Phi(b)$, $b \in \mathcal{U}$, as the Regular Lagrangian Flow of b, even if we are outside the setting where RLF are known to be unique: however X_t is the unique flow which can be approximated by RLF of smoother vector fields b^n as $b^n \to b$ in L^1. The existence of such a set $\mathcal{U}$ is due to purely topological properties of metric spaces (Proposition 1.0.3).

Our proof adapts some ideas from [31] to our setting: we give an outline of Halmos' analysis. First of all, both ergodic automorphisms and weakly mixing automorphisms are a G_δ-set [30, 31]. Next, it is shown that the mixing properties are invariant under conjugation, i.e., if $T : [0,1] \to [0,1]$ is weakly/strongly mixing and $R : [0,1] \to [0,1]$ is an automorphism, then $R \circ T \circ R^{-1}$ is weakly/strongly mixing too. It remains to be proved that weakly mixing maps are dense: define a *permutation* as an automorphism of $[0,1]$ sending dyadic intervals (subintervals of $[0,1]$ with dyadic endpoints) into dyadic intervals by translation (in dimension greater than 1 the map translates dyadic subcubes). Cyclic permutations (i.e., permutations made by a unique cycle) of the same intervals are clearly conjugate. One of the key ingredients of Halmos' proof is that, for every non periodic automorphism (i.e., $T^n x \neq x$ for all n in a conegligible set of points x), there exists a cyclic permutation close to it in the neighbourhood topology, and by the previous observation about conjugation of permutations one deduces that if T is non-periodic then the maps of the form $R \circ T \circ R^{-1}$ form a dense set. In particular, the weakly mixing maps are a G_δ-set containing a non periodic map, hence this set is residual.

In our setting, the fact that ergodic/weakly mixing vector fields form a G_δ-subset of $\mathcal{U}$ is an easy consequence of the Stability Theorem for Regular Lagrangian Flows and the definition of the map Φ (see Point (1) and Proposition 1.1.10). Indeed, since both ergodic automorphisms and weakly mixing automorphisms are a G_δ-set [30, 31], then by the continuity of the map Φ associating b with the RLF X_t, ergodic and weakly mixing vector fields are a G_δ-set also. Unfortunately, we cannot use conjugation of a RLF X_t with an automorphism R of K, since in general $R \circ X_{t=1} \circ R^{-1}$ is not a RLF generated by $b \in L^\infty_t BV_x$ (or even $b \in \mathcal{U}$). However, we are able to prove the density in $\mathcal{U}$ of vector fields $b \in L^\infty_t \mathrm{BV}_x$ whose RLF is a cyclic permutation of subsquares of

K, which is the natural extension of the permutation of intervals used in [31]. More precisely, the map $T = X_{t=1}$ sends by a rigid translation subsquares of some rational grid $\mathbb{N} \times \mathbb{N}\frac{1}{D}$, where $D \in \mathbb{N}$, into subsquares of the same grid (it will be clear later that being dyadic as in [31] is not relevant, see Lemma 4.1.1 and Remark 4.1.3), and as a permutation of subsquares it is made by a single cycle. The precise statement is the following.

Theorem 0.0.4. *Let $b \in L^\infty([0,1], \mathrm{BV}(K))$ be a divergence-free vector field. Then for every $\epsilon > 0$ there exist $1 \ll D \in \mathbb{N}$, two positive constants C_1, C_2 and a divergence-free vector field $b^c \in L^\infty([0,1], \mathrm{BV}(K))$ such that*

$$||b - b^c||_{L^1(L^1)} \leq \epsilon, \quad ||\mathrm{Tot.Var.}(b^c)(K)||_\infty \leq C_1 ||\mathrm{Tot.Var.}(b)(K)||_\infty + C_2 \tag{0.0.6}$$

and the map $X^c_{t=1} : K \to K$, where $X^c_t : [0,1] \times K \to K$ is the flow associated with b^c, is a D^2-cycle of subsquares of size $\frac{1}{D}$.

The above approximation is the most technical part of the work we did, and it is the point which forces to state the theorem in $\mathcal{U}$ and not in the original space $b \in L^\infty_t \mathrm{BV}_x$: indeed, while achieving the density in the $L^1_{t,x}$-topology, the total variation increases because of the constants C_1, C_2 in (0.0.6). (It is possible to improve the first estimate of (0.0.6) to $\|b - b^c\|_{L^\infty L^1} \leq \epsilon$, see Remark 3.1.7, but to avoid additional technicalities we concentrate on the simplest results leading to Theorem 0.0.3.)

We remark that the above approximation result is sufficient to prove that strongly mixing vector fields are a set of first category (Proposition 1.1.10): indeed, Theorem 0.0.4 shows the density in $\mathcal{U}$ of divergence-free vector fields whose flow is made of periodic trajectories with the same period D^2. This observation is the key to obtain Point (4) of Theorem 0.0.3.

Looking at cyclic permutations of subsquares is an important step to obtain ergodic (and then weakly mixing and strongly mixing) vector fields: indeed, instead of studying the map $X^c_{t=1}$ (the RLF generated by b^c of Theorem 0.0.4 above) in the unit square K with the Lebesgue measure $\mathcal{L}^2$, it is sufficient to work in the finite space made of the centers of the subsquares

$$\Omega = \left\{ x = \left(\frac{k_1 - 1/2}{D}, \frac{k_2 - 1/2}{D} \right), k_1, k_2 = 1, \dots, D \right\}, \tag{0.0.7}$$

where the measure-preserving transformation $X^c_{t=1}$ reduces to a cyclic permutations. In particular in Ω it is already ergodic.

Since we cannot use the conjugation argument as we observed above, the final steps of the proof of Theorem 0.0.3 differ from the ones of [31]. Indeed we give a general procedure to perturb vector fields $b^c \in L^\infty_t \mathrm{BV}_x$ (whose RLF X^c_t at $t = 1$ is a cyclic permutation of subsquares) into ergodic vector fields b^e (strongly mixing vector fields b^s) still belonging to $L^\infty_t \mathrm{BV}_x$: here the explicit form of X^c plays a major role, allowing us to construct *explicitly* the perturbations to b^c (Sections 3.1.1,3.1.2).
The key idea is to apply the (rescaled) *universal mixer* vector field (introduced in [27]) whose RLF at time $t = 1$ is the *Folded Baker's map*

$$U = U_{\llcorner t=1} = \begin{cases} \left(-2x + 1, -\frac{y}{2} + \frac{1}{2}\right) & x \in \left[0, \frac{1}{2}\right), \\ \left(2x - 1, \frac{y}{2} + \frac{1}{2}\right) & x \in \left(\frac{1}{2}, 1\right], \end{cases} \qquad y \in [0,1], \tag{0.0.8}$$

to the subsquares of the grid $\mathbb{N} \times \mathbb{N}\frac{1}{D}$ given by Theorem 0.0.4.
In order to achieve ergodicity, it is sufficient to apply the universal mixer U inside

a single subsquare, because the action of $X^c_{t=1}$ is already ergodic in Ω being a cyclic permutation. Together with the fact that ergodic vector fields are a G_δ-set, this gives the proof of Point (2) of Theorem 0.0.3. The perturbation to achieve exponential mixing is more complicated, since we need to transfer mass across different subsquares. The idea is to apply the universal mixer U to adjacent couples of subsquares, a procedure which assures that the mass of ρ is eventually equidistributed among all subsquares. The exponential mixing is a consequence of the finiteness of Ω and the properties of U (see Proposition 3.1.10). This concludes the proof of Point (5) of Theorem 0.0.3, and since strongly mixing vector fields are a subset of weakly mixing vector fields we obtain also Point (3), concluding the proof of the theorem.

It should not be surprising that exponentially mixing vector fields are a dense subset of $\mathcal{U}$. Even if this G_δ contains vector fields whose behaviour is far from mixing (as for example horizontal shears) the key point is that any vector field can be approximated by *permutation vector fields*, which are the building blocks for any mixing behaviour. We point out that our construction does not provide any example of a smooth mixing vector field: an interesting open question is the construction of a time-periodic vector field with smooth regularity in space, since the one constructed in [9] does not satisfy the periodicity in time.

A completely analogous result can be obtained in any dimension by adapting the above steps, at the cost of additional heavy technicalities. In this work we decided to sketch the proof of the key estimates (i.e., the ones requiring new ideas) in the general case (see Subsection 4.1.1).

0.1 Structure of the proof of Theorem 0.0.3

Approximations of flows by permutations

The approximation through divergence-free vector fields b whose flow at $t = 1$ is a permutation of squares has been already studied in [43] in the context of generalized flows for incompressible fluids. Indeed the starting point of Chapter 4 is Lemma 4.1.1, whose statement is almost identical to Lemma 4.3 of [43]: it says that if T is a smooth map sufficiently close to identity, there exists an arbitrarily close flow σ_t, $t \in [0, 1]$, such that $\sigma_{t=0} = T$ and $\sigma_{t=1}$ maps affinely rectangles whose edges are on a dyadic grid into rectangles belonging to the same grid. Even if the ideas of the proof are completely similar to the original ones, we choose to make them more explicit (see also Remark 4.1.3 for some comments on the original proof).

At this point the proof diverges from [43], due to the fact that in his case one has to control the L^2-norm of the vector field while here we need to build a perturbation of a vector field (not of a map) and to estimate its BV_x-norm. In Lemma 4.2.3 we prove that the perturbation σ_t constructed in the above paragraph (i.e., in Lemma 4.1.1) can be encapsulated inside the flow X_t so that the resulting vector field is close in $L^\infty_t L^1_x$ and remains in $L^\infty_t \mathrm{BV}_x$ if the grid is sufficiently small, always under the assumption that X_t is close to identity.

We finally arrive to the approximation theorem through permutations (Theorem 4.4.1), which we think that can have an independent interest:

Theorem 0.1.1. *Let $b \in L^\infty([0,1]; BV(K))$ be a divergence-free vector field. Then for every $\epsilon > 0$ there exist $\delta', C_1, C_2 > 0$ positive constants, $D \in \mathbb{N}$ arbitrarily large and a divergence-free vector field $b^\epsilon \in L^\infty([0,1]; BV(K))$ such that*

1. $\operatorname{supp} b^\epsilon_t \subset\subset K^{\delta'} = [\delta', 1-\delta']^2$,

2. *it holds*

$$\|b-b^\epsilon\|_{L^\infty(L^1)} \leq \epsilon, \quad ||\text{Tot.Var.}(b^\epsilon)(K)||_\infty \leq C_1||\text{Tot.Var.}(b)(K)||_\infty + C_2, \quad (0.1.1)$$

3. *the map $X^\epsilon{}_{\llcorner t=1}$ generated by b^ϵ at time $t=1$ translates each subsquare of the grid $\mathbb{N}\times\mathbb{N}\frac{1}{D}$ into a subsquare of the same grid, i.e., it is a permutation of squares.*

We remark that in the statement of Theorem 4.4.1 it is also assumed that there exists $\delta > 0$ such that for $\mathcal{L}^1$-a.e. $t \in [0,1]$, $\operatorname{supp} b_t \subset\subset K^\delta$. This is for technical reason, as standard approximation methods allows to deduce the Theorem 0.1.1 above from Theorem 4.4.1.

The starting point of its proof is to divide the time interval $[0,1]$ into subintervals $[t_i, t_{i+1}]$ and apply the previous perturbations (Lemma 4.1.1) to b_t, $t \in [t_i, t_{i-1}]$. We however need an additional mechanism in order to obtain a permutation of subsquares and not a piecewise affine map at $t=1$, as it would be the case if we only use the perturbations above.

The introduction of this new perturbation is done in Section 4.3: the idea is that if a measure preserving map T is diagonal with rational eigenvalues, then there exists a subgrid and a map R made by two rotations such that $T \circ R$ maps subsquares of the new grid into subsquares instead of rectangles (Lemma 4.3.1). The key point is that the total variation of the new map is bounded independently on the grid size, while the L_1-norm converges to 0 as the grid becomes smaller and smaller. This gives better BV estimates than the construction of [43]. In the proof of the theorem, this rotation mechanism has to act differently in each subrectangle. The procedure illustrated in Figure 5) has to be done during the time evolution. The interesting part of the above theorem is the form of the estimate for the Total Variation in (0.1.1). The constant C_1 comes out from the approximation argument of Shnirelman: it means that the total variation of the piecewise affine approximation is, as expected, of the order of Tot.Var.(b_t): we believe that this constant C_1 can be optimized, but it is not necessary here, because the hard term is the one leading to C_2. Indeed, the second constant comes from the rotation mechanism: performing a rotation inside a rectangle costs, in terms of the total variation, as the area of the rectangle see Lemma 2.2.13).

From permutations of subsquares to ergodic/exponential mixing

The advantage of having a flow X_t such that $X_{t=1}$ is a permutations of subsquares is that its action is sufficiently simple to perturb in order to achieve a desired property. Nevertheless it requires some smart constructions, since in any case we need to control the L^1-distance and the BV norm.

The first step is to perturb a permutation of subsquares into a cyclic permutation of subsquares, i.e., a permutation made of a single cycle: this is clearly a necessary condition for ergodicity. Roughly speaking, the idea is to exchange two adjacent subsquares belonging to different cycles in order to merge them. We do this operation in two steps. In Lemma 3.1.4 it is shown that one can arbitrarily refine the grid $\mathbb{N}\times\mathbb{N}\frac{1}{D}$ into $\mathbb{N}\times\mathbb{N}\frac{1}{DM}$ so that each cycle of length k in the original grid becomes a cycle of length kM^2 in the new one. Moreover the perturbation is going to 0 in $L^\infty_t L^1_x$ as $M\to\infty$ and its $L^\infty \operatorname{BV}_x$ is arbitrarily small when D is large.
The above result allows now to exchange sets of size $(DM)^{-1}$ when merging cycles: this is done in Proposition 3.1.5. This proposition faces a new problem: in the previous case the exchange of subsquares of size $(DM)^{-1}$ occurs within the same subsquare of size D^{-1}: the latter is only deformed during the evolution and hence the merging can

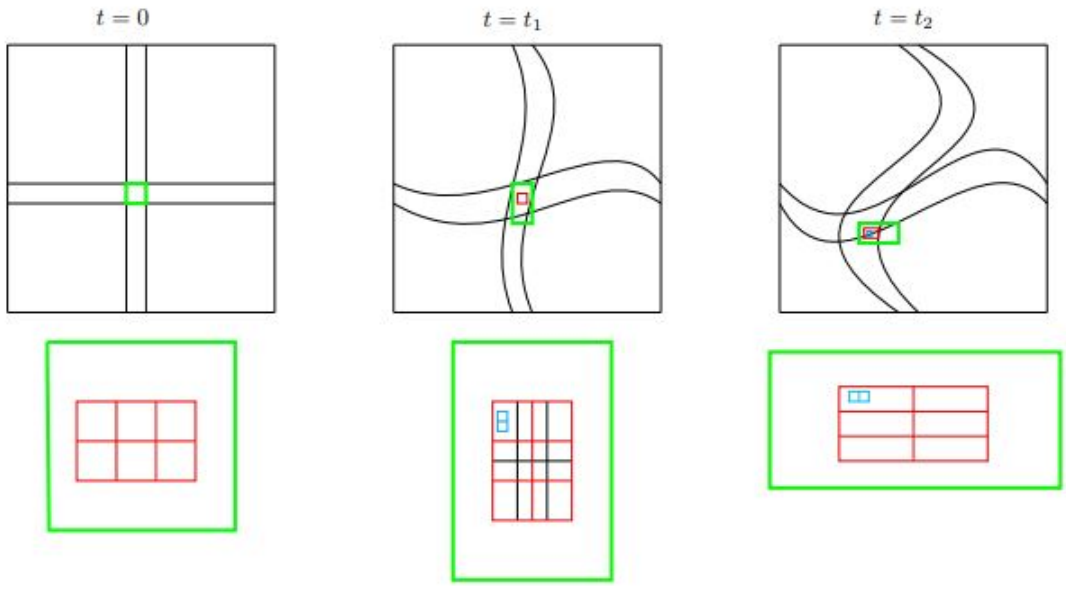

Figure 5: A graphic explanation of the action of rotations: the three top frames above shows the evolution of curves at different times t_i, where the perturbation of Lemma 4.1.1 takes care of transforming the green square affinely into the green rectangles. The three bottom frames is the action of the rotation on a finer grid: the red rectangle is chosen so that the action of the affine map $X_{t=t_1}$ coincides with a rotation by $\pi/2$ (as a set, but the black grid (image through an affine map) is not the image of the red grid after a rotation), and then the red grid is mapped into itself when composed with a rotation of $\pi/2$ inside the red rectangle. At the next step, one chooses again a finer grid (the light blue one) to perform the same transformation, so that the blue grid is mapped into itself.

be done in the whole time interval $[0,1]$. In the case of Proposition 3.1.5, instead, we are exchanging subsquares of size $(DM)^{-1}$ which are then shifted away during the flow, since they belong to different subquares of the grid D^{-1}. This requires to do the exchange sufficiently fast (i.e., during the time where they share a common boundary, Remark 3.1.7), or to freeze the evolution for an interval of time $[0,\delta]$ and perform the exchanges here and then let the flow permuting the subsquares to evolve during the remaining time interval $[\delta,1]$. We choose for simplicity this second line, being easier and not changing the final result: notice however that now the constant M plays the role of controlling the constant δ^{-1}, appearing because the exchange action occurs in the time interval $[0,\delta]$.

Once we have a cyclic permutation of subsquares, the perturbation to get an ergodic vector field is straighforward.

To achieve the exponential mixing, instead, we need to transfer mass across different subsquares, and hence we face again the problem of Proposition 3.1.5 above: we let the mixing action occurs in an interval of time where the evolution is frozen, and then let the cyclic permutation to act in the time interval $[\delta,1]$ (see also Remark 3.1.11). The idea is again to use the universal mixer (0.0.8) to exchange mass across to nearby subsquares. The additional difficulty here is that in order to avoid resonant phenomena we mix all squares with 2 neighboring ones, so that by simple computations the Markov

Shift obtained through this map is exponentially mixing, Proposition 3.1.10.

To collect all the above results into a proof of Point (5) of Theorem 0.0.3 is not difficult at this point, and we devote a section (Section 3.1.3 and Corollary 1.1.11) to shows how to merge these result and get the desired statement.

0.1.1 Structure of The Thesis

In this section we indicate how the material presented in the introduction is organized in the thesis.

In Chapter 1, after listing some of the notation used in the paper, we give a short overview of BV functions (Section 1.0.1) and Regular Lagrangian Flows (Section 1.0.2), proving the extension of the continuous dependence to a complete set $\mathcal{U}$ in Proposition 1.0.3 (providing the proof of Point (1) of Theorem 0.0.3) and stating some technical estimates on composition of maps (Theorem 1.0.4 and (1.0.3), (1.0.4)) and on the vector field (2.2.5) generating a rotation (Lemma 2.2.13).

In Section 1.1 we collect some classical results in Ergodic Theory which are needed for Theorem 0.0.3, and also give the proof of the G_δ-properties of the set of ergodic/weakly mixing vector fields of Theorem 0.0.3. First we introduce the basic definitions, then in Section 1.1.1 we clarify the relation with the neighborhood topology and the L^1-topology used in Theorem 0.0.3.
In Section 1.1.2 we restate in our setting the well known fact that weakly mixing are a G_δ-set, as well as the first category property of strongly mixing vector fields (Proposition 1.1.10). The proof of the remaining parts of Theorem 0.0.3 is a corollary of the previous statement (Corollary 1.1.11), if we know that the strongly mixing vector fields are dense.
The construction of exponential mixing vector fields is based on the analysis of Markov Shift: in Section 1.1.3 we give the results which are linked to our construction.

In Chapter 2 we give an example of a weakly mixing vector field which is not strongly mixing. Here the construction is based on the work of Chacon 2.1.3, who gave a general method for constructing weakly mixing automorphisms.

In Chapter 3 we present the proof of the the density of exponentially mixing vector fields, under the assumption that permutation flows are dense in $L^1_t \mathrm{BV}_x$ w.r.t. the $L^1_{t,x}$-norm. We decide to put first this construction because it is in some sense independent on the proof of the density of permutation flows: the idea is that different functional settings can be studied by changing this last part (i.e., the density of permutation flow), while keeping the construction of approximation by permutations more or less the same. The first statement is Lemma 3.1.4 which allows to partition the subsquares of a given cycle into smaller subquares still belonging to the same cycle. The usefullness of this estimate is shown in Proposition 4.1.4, where we need to exchange mass only on an area which is of order M^{-2}, and hence obtaining that the perturbation is small in $L^1_{t,x}$ and $L^\infty_t BV_x$ (Proposition 3.1.8 of Remark 3.1.7 addresses the problem of exchanging two subquares during the evolution, a refinement not needed for the proof of Theorem 0.0.3). The last two subsection address the density of ergodic vector fields (Proposition 3.1.9) and of exponentially mixing vector fields (Proposition 3.1.10): the basic idea is the same (i.e., perturb the cyclic permutation). Section 3.1.3 shows at this point how the assumptions of Corollary 1.1.11 are verified, concluding the proof of Theorem 0.0.3 under the assumption of the density of vector fields whose flow is a permutation of subsquares.

The last Chapter 4, proves the cornerstone approximation result, i.e., the density of vector fields whose flow at $t = 1$ is a permutation of subsquares, Theorem 4.4.1 (whose

statement is the same of Theorem 0.1.1).
In Section 4.1 we approximate a smooth flow close to identity with a BV flow which is locally affine in subrectangles: Lemma 4.1.1 considers the 2d-case as in [43], while the needed variations for the d-dimensional case are in Section 4.1.1.
The BV estimates for such perturbed flow are studied in Section 4.2. A preliminary result (Lemma 4.2.1) takes care of the conditions that the area of the subsquares has to be a dyadic rational, while the key estimates are in Lemma 4.2.3: an important fact is that as the grid becomes finer the perturbation becomes smaller.
An ingredient for obtaining a flow which is a permutation of subsquares is the use of rotations: in Section 4.3 we study these elementary transformations.
The main approximation theorem, Theorem 4.4.1, is stated and proved in Section 4.4. Its proof uses all the ingredients of the previous sections, and an additional argument on how to encapsulate rotations in order to control the total variation.

Chapter 1

Preliminaries and notation

In this chapter we collect some preliminary and technical results that will be used in the main body of this thesis. More in details, we will introduce BV functions and Ambrosio Theory [6] on the existence and uniqueness of flows of weakly differentiable vector fields in the subsections 1.0.1 and 1.0.2. In Section 1.1 we will present the group of automorphism and the sketch of the proof of genericity of weakly mixing automoprhisms. Finally, in the subsection 1.1.3 we will present some tools from the theory of Markov shifts that will be used to prove the density of strongly mixing vector fields.

First, a list of standard notations used throughout this paper.

- $\Omega \subset \mathbb{R}^n$ denotes in general an open set; $\mathcal{B}(\Omega)$ denotes the σ-algebra of Borel sets of Ω;
- $\mathrm{dist}(x, A)$ is the distance of x from the set $A \subset \Omega$, defined as the infimum of $|x - y|$ as y varies in A;
- $\forall A \subset \Omega$, $\mathring{A}$ denotes the interior of A and ∂A its boundary, moreover, if $\epsilon > 0$, then A^ϵ is the ϵ-neighbourhood of A, that is

$$A^\epsilon = \{x \in \Omega : \mathrm{dist}(x, \partial A) \leq \epsilon\};$$

- $\mathcal{M}_b(\Omega)$ bounded Radon measures;
- if $\nu \in \mathcal{M}_b(\Omega)$ then $\|\nu\|$ denotes its total variation;
- $\mathrm{BV}(\Omega)$ is the set of functions with bounded variation, and if $u \in \mathrm{BV}(\Omega)$ we will use instead Tot.Var.(u) to denote $\|Du\|$;
- $\mathcal{L}^d$ denotes the d-dimensional Lebesgue measure on $\mathbb{R}^d$, and $\mathcal{H}^k$ the k-dimensional Hausdorff measure;
- $K = [0, 1]^2$ is the unit square;
- all vector fields b are divergence-free and BV when extended to the whole $\mathbb{R}^2$. In order to shorten the notation, it will sometimes be written $\mathrm{BV}(K)$, $K = [0, 1]^2$ as the space $\mathrm{BV}(\mathbb{R}^2) \cap \{\mathrm{supp}\, b \subset K\}$;
- $\mathcal{L}^2 \llcorner_K$ denotes the normalized Lebesgue measure on K;

- let $b : [0,1] \times \mathbb{R}^2 \to \mathbb{R}^2$, and let $t, s \in [0,1]$ then we denote by $X(t,s,x)$ a solution of
$$\begin{cases} \dot{x}(t) = b(t, x(t)) \\ x(s) = x, \end{cases}$$
moreover we will use $X(t)(x)$ or (alternatively $X_t(x)$) for $X(t,0,x)$ (in our setting as a flow the function $X(t,s,x)$ is unique a.e.);

- (S, Σ, μ) denotes a locally compact separable metric space where μ is a normalized complete measure;

- $G(S)$ denotes the space of automorphisms of S.

1.0.1 BV functions

In this subsection we recall some results concerning functions of bounded variation. For a complete presentation of the topic, see [7]. Let $u \in \mathrm{BV}(\Omega; \mathbb{R}^m)$ and $Du \in \mathcal{M}_b(\Omega)^{n \times m}$ the $n \times m$-valued measure representing its distributional derivative. We recall the decomposition of the measure Du

$$Du = D^{\mathrm{cont}}u + D^{\mathrm{jump}}u = D^{\mathrm{a.c.}}u + D^{\mathrm{cantor}}u + D^{\mathrm{jump}}u,$$

where $D^{\mathrm{cont}}u, D^{\mathrm{a.c.}}u, D^{\mathrm{cantor}}u, D^{\mathrm{jump}}u$ are respectively the continuous part, the absolutely continuous part, the Cantor part and the jump part of the measure. We also recall that for $u \in BV(\Omega)$ the following estimate on the translation holds: for every $C \subset \Omega$ compact and $z \in \mathbb{R}^n$ such that $|z| \leq \mathrm{dist}(C, \partial\Omega)$

$$\int_C |u(x+z) - u(x)| dx \leq \left| \sum_{i=1}^{n} z_i D_i u \right| (C^{|z|}). \tag{1.0.1}$$

1.0.2 Regular Lagrangian Flows

Throughout the paper we will consider divergence-free vector fields $b : [0,1] \times K \to \mathbb{R}^2$ in the space $L^\infty([0,1]; \mathrm{BV}(K))$ (in short $b \in L^\infty_t \mathrm{BV}_x$) such that $\mathrm{supp}(b_t) \subset\subset \mathring{K}$ for $\mathcal{L}^1$-a.e. $t \in [0,1]$: it is standard to extend the analysis to divergence-free BV-vector fields in $\mathbb{R}^2$ with support in K. When the velocity field b is Lipschitz, then its *flow* is well-defined in the classical sense, indeed it is the map $X : [0,1] \times K \to K$ satisfying

$$\begin{cases} \frac{d}{dt} X_t(x) = b(t, X_t(x)); \\ X_0(x) = x. \end{cases}$$

But when we allow the velocity fields to be discontinuous (as in our case BV regular in space) we can still give a notion of a flow (namely the *Regular Lagrangian Flow*). These flows have the advantage to allow rigid *cut and paste* motions, since they do not preserve the property of a set to be connected. More in detail, we give the following

Definition 1.0.1. Let $b \in L^1([0,1] \times \mathbb{R}^2; \mathbb{R}^2)$. A map $X : [0,1] \times \mathbb{R}^2 \to \mathbb{R}^2$ is a *Regular Lagrangian Flow* (RLF) for the vector field b if

1. for a.e. $x \in \mathbb{R}^2$ the map $t \to X_t(x)$ is an absolutely continuous integral solution of
$$\begin{cases} \frac{d}{dt} x(t) = b(t, x(t)); \\ x(0) = x. \end{cases}$$

2. there exists a positive constant C independent of t such that

$$\mathcal{L}^2(X_t^{-1}(A)) \leq C\mathcal{L}^2(A), \quad \forall A \in \mathcal{B}(\mathbb{R}^2).$$

DiPerna and Lions proved existence, uniqueness and stability for Sobolev vector fields with bounded divergence [26], while the extension to the case of BV vector fields with divergence in L^1 has been done by Ambrosio in [6]. When dealing with divergence-free vector fields b the unique Regular Lagrangian Flow $t \to X_t$ associated with b is a flow of measure-preserving maps, main objects of investigations in Ergodic Theory. In the sequel we will build flows of measure-preserving maps originating from divergence-free vector fields; more precisely, if a flow $X : [0,1] \times K \to K$ is invertible, measure-preserving for $\mathcal{L}^1$-a.e. t and the map $t \to X_t$ is differentiable for $\mathcal{L}^1$-a.e. t and $\dot{X}_t \in L^1(K)$, then the *vector field associated with* X_t is the divergence-free vector field defined by

$$b_t(x) = b(t,x) = \dot{X}_t(X_t^{-1}(x)). \tag{1.0.2}$$

Theorem 1.0.2 (Stability, Theorem 6.3 [5])**.** *Let $b_n, b \in L^\infty([0,1], \mathrm{BV}(K))$ be divergence-free vector fields and let X^n, X be the corresponding Regular Lagrangian Flows. Assume that*

$$||b_n - b||_{L^1_{t,x}} \to 0 \quad \text{as } n \to \infty,$$

then

$$\lim_{n\to\infty} \int_K \sup_{t\in[0,1]} |X_t^n(x) - X_t(x)|dx = 0.$$

In this setting we can extend the family of vector fields we consider to a Polish subspace of $L^1_{t,x}$ in which we still have a notion of uniqueness. This extension allows us to apply Baire Category Theorem for the results of genericity that we will give for weakly mixing vector fields.

Proposition 1.0.3 (Extension)**.** *Let*

$$\Phi : \{b \in L^\infty_t \mathrm{BV}_x : D \cdot b_t = 0\} \subset \{b \in L^1([0,1], L^1(K)), D \cdot b_t = 0\} \to C([0,1], L^1(K))$$

the map that associates b with its unique Regular Lagrangian Flow X_t. Then Φ can be extended as a continuous function to a G_δ-set $\mathcal{U}$ containing $\{b \in L^\infty_t \mathrm{BV}_x : D \cdot b_t = 0\}$.

This proposition proves Point (1) of Theorem 0.0.3.

Proof. We recall that for every $f : A \to Z$ continuous where $A \subset W$ is metrizable and Z is a complete metric space, there exists a G_δ-set $A \subset G$ and a continuous extension $\tilde{f} : G \to Z$ (Proposition 2.2.3, [35]). Thus we have to prove the continuity of the map Φ which follows by

$$\begin{aligned}\|\Phi(b^n) - \Phi(b)\|_{C_t L^1_x} &= \sup_{t\in[0,1]} \int_K \left|X_t^n(x) - X_t(x)\right|dx \\ &\leq \int_K \sup_{t\in[0,1]} \left|X_t^n(x) - X_t(x)\right|dx.\end{aligned}$$

This concludes the proof. □

We will also use the following tools to prove the main approximation theorems of the paper. The first one gives a rule to compute the total variation of the composition of vector fields, while the second one is a direct computation of the cost, in terms of the total variation of the vector field whose flow rotates rectangles.

Theorem 1.0.4 (Change of variables, Theorem 3.16, [7]). *Let Ω, Ω' two open subsets of $\mathbb{R}^n$ and let $\phi : \Omega \to \Omega'$ invertible with Lipschitz inverse, then $\forall u \in BV(\Omega')$ the function $v = u \circ \phi$ belongs to $BV(\Omega)$ and*

$$\text{Tot.Var.}(v) \leq \text{Lip}(\phi^{-1})^{n-1}\text{Tot.Var.}(u).$$

Corollary 1.0.5. *Let $\Omega, \Omega' \subset \mathbb{R}^n$ be two open sets where $\partial\Omega'$ is Lipschitz and let $\phi : \bar{\Omega} \to \bar{\Omega}'$ invertible with Lipschitz inverse, then $\forall u \in BV(\mathbb{R}^n)$ the function*

$$v = \begin{cases} u \circ \phi & x \in \Omega, \\ 0 & \text{otherwise}, \end{cases}$$

belongs to $BV(\mathbb{R}^n)$ and

$$\begin{aligned} \text{Tot.Var.}(v)(\mathbb{R}^n) &\leq \text{Lip}(\phi^{-1})^{n-1}\big(\text{Tot.Var.}(u)(\Omega') + \|\text{Tr}(u, \partial\Omega')\|_{L^1(\mathcal{H}^{n-1}\llcorner_{\partial\Omega'})}\big) \\ &= \text{Lip}(\phi^{-1})^{n-1}\text{Tot.Var.}(u_{\llcorner\Omega'})(\mathbb{R}^n). \end{aligned}$$

In the following, we have often to study the properties of the vector field b_3 associated with the composition $Y_3(t)$ of two smooth measure preserving flows $t \mapsto Y_i(t)$, $i = 1, 2$, with associated vector fields b_1, b_2. By direct computation

$$\begin{aligned} b_3(t, Y_3(t, y)) &= \partial_t Y_1(t, Y_2(t, y)) = b_1(t, Y_3(t, y)) + \nabla Y_1(t, Y_2(t, y))b_2(t, Y_2(t, y)), \\ b_3(t, x) &= b_1(t, x) + \nabla Y_1(t, Y_2(t, Y_3^{-1}(t, x)))b_2(t, Y_2(t, Y_3^{-1}(t, x))) \\ &= b_1(t, x) + \nabla Y_1(t, Y_1^{-1}(t, x))b_2(t, Y_1^{-1}(t, x)). \end{aligned} \tag{1.0.3}$$

Hence using Theorem 1.0.4 we conclude that (being $Y_1 \circ Y_2$ measure preserving too)

$$\begin{aligned} \text{Tot.Var.}(b_3) &\leq \text{Tot.Var.}(b_1) + \text{Lip}(Y_1)^{n-1}\text{Tot.Var.}(DY_1(t)b_2) \\ &\leq \text{Tot.Var.}(b_1) + \|\nabla Y_1\|_\infty^n \text{Tot.Var.}(b_2) + \|\nabla Y_1\|_\infty^{n-1}\|b_2\|_\infty \text{Tot.Var.}(DY_1(t)). \end{aligned} \tag{1.0.4}$$

Throughout the paper we will extensively use a flow rotating rectangles and the vector field associated with it. More precisely we define the *rotation flow* $r_t : K \to K$ for $t \in [0, 1]$ in the following way: call

$$V(x) = \max\left\{\left|x_1 - \frac{1}{2}\right|, \left|x_2 - \frac{1}{2}\right|\right\}^2, \quad (x_1, x_2) \in K.$$

Then the *rotation field* is $r : K \to \mathbb{R}^2$

$$r(x) = \nabla V^\perp(x), \tag{1.0.5}$$

where $\nabla^\perp = (-\partial_{x_2}, \partial_{x_1})$ is the orthogonal gradient. Finally the rotation flow r_t is the flow of the vector field r, i.e., the unique solution to the following ODE system:

$$\begin{cases} \dot{r}_t(x) = r(r_t(x)), \\ r_0(x) = x. \end{cases} \tag{1.0.6}$$

This flow rotates the cube counterclockwise of an angle $\frac{\pi}{2}$ in a unit interval of time.

Lemma 1.0.6. *Let $R \subset \mathbb{R}^2$ a rectangle of sides $a, b > 0$. Consider the rotating flow*

$$R_t = \chi^{-1} \circ r_t \circ \chi,$$

where $\chi : R \to K$ is the affine map sending R into the unit cube and r_t is the rotation flow defined in (2.2.5). Let b_t^R the divergence-free vector field associated with R_t. Then

$$\text{Tot.Var.}(b_t^R)(\mathbb{R}^2) = 4a^2 + 4b^2, \quad \forall t \in [0, 1].$$

Proof. The potential V generating the rotation of $\pi/2$ in this case is the function

$$V(x) = \max\left\{\frac{b}{a}\left(x_1 - \frac{a}{2}\right)^2, \frac{a}{b}\left(x_2 - \frac{b}{2}\right)^2\right\},$$

where we assume that $R = [0,a] \times [0,b]$, so that the vector field is given by

$$r(x) = \nabla^\perp V = \begin{cases} \left(0, \frac{2b}{a}\left(x_1 - \frac{a}{2}\right)\right) & |x_1| \geq \frac{b}{a}|x_2|, 0 \leq x_1 \leq a, \\ \left(-\frac{2a}{b}\left(x_2 - \frac{b}{2}\right), 0\right) & |x_1| < \frac{b}{a}|x_2|, 0 \leq x_2 \leq b. \end{cases}$$

Hence by elementary computations

$$\|D^{\text{cont}} r\| = a^2 + b^2, \quad \|D^{\text{jump}} r\| = 3a^2 + 3b^2,$$

and then we conclude. Recupera dim di questo. □

1.1 Ergodic Theory

We will consider flows of divergence-free vector fields from the point of view of Ergodic Theory. Even if we apply the results to the case $(K, \mathcal{B}(K), \mathcal{L}^2{\llcorner}_K)$ in this section we will give the notions of ergodicity and mixing in more general spaces [23, Chapter 1]. More precisely, let (Ω, Σ, μ) be a locally compact separable metric space where μ is complete and normalized, that is $\mu(\Omega) = 1$.

Definition 1.1.1. An *automorphism* of the measure space (Ω, Σ, μ) is a one-to-one map $T : \Omega \to \Omega$ bi-measurable and measure-preserving, that is

$$\mu(A) = \mu(T(A)) = \mu(T^{-1}(A)), \quad \forall A \in \Sigma.$$

We call $G(\Omega)$ the group of automorphisms of the measure space (Ω, Σ, μ).

Definition 1.1.2. A *flow* $\{X_t\}$, $t \in \mathbb{R}$, is a one-parameter group of automorphisms of (Ω, Σ, μ) such that for every $f : \Omega \to \mathbb{R}$ measurable, the function $f(X_t(x))$ is measurable on $\Omega \times \mathbb{R}$.

Definition 1.1.3. Let $T : \Omega \to \Omega$ an automorphism. Then

- T is ***ergodic*** if for every $A \in \Sigma$

$$T(A) = A \quad \Rightarrow \quad \mu(A) = 0 \text{ or } \mu(A) = 1; \tag{1.1.1}$$

- T is ***weakly mixing*** if $\forall A, B \in \Sigma$

$$\lim_{n\to\infty} \frac{1}{n} \sum_{j=0}^{n-1} \left[\mu(T^{-j}(A) \cap B) - \mu(A)\mu(B)\right]^2 = 0; \tag{1.1.2}$$

- T is ***(strongly) mixing*** if $\forall A, B \in \Sigma$

$$\lim_{n\to\infty} \mu(T^{-n}(A) \cap B) = \mu(A)\mu(B). \tag{1.1.3}$$

Remark 1.1.4. It is a well-known and quite elementary fact that strongly mixing $\Rightarrow$ weakly mixing $\Rightarrow$ ergodic.

We can give the analogous definitions for the flow:

Definition 1.1.5. Let $\{X_t\}$ a flow of automorphisms. Then

- $\{X_t\}$ is ***ergodic*** if for every $A \in \Sigma$

$$X_t(A) = A \quad \Rightarrow \quad \mu(A) = 0 \text{ or } \mu(A) = 1; \tag{1.1.4}$$

- $\{X_t\}$ is ***weakly mixing*** if $\forall A, B \in \Sigma$

$$\lim_{t\to\infty} \int_0^t \left[\int_\Omega \chi_A(X_{-s}(x))\chi_B(x)d\mu - \mu(A)\mu(B) \right]^2 ds = 0; \tag{1.1.5}$$

- $\{X_t\}$ is ***(strongly) mixing*** if $\forall A, B \in \Sigma$

$$\lim_{t\to\infty} \int_\Omega \chi_A(X_{-t}(x))\chi_B(x)d\mu = \mu(A)\mu(B). \tag{1.1.6}$$

Let now $T \in G(\mathbb{T}^2)$, then the Kolmogorov Koopman operator (see Chapter 1 in [23]) $U_T : L^2(\mathbb{T}^2) \to L^2(\mathbb{T}^2)$ is defined as

$$U_T f(x) \doteq f(T(x)), \quad \forall f \in L^2(\mathbb{T}^2). \tag{1.1.7}$$

We observe that any operator U_T of the form considered has eigenfunctions $f = \text{const}$ corresponding to the eigenvalue 1. Then we have the following:

Theorem 1.1.6 (Mixing, Theorem 2 [23])**.** *T is weakly mixing iff U_T has no eigenfunctions which are not constants.*

1.1.1 The neighbourhood topology as a convergence in measure.

To get a genericity result it is necessary to identify the correct topology on $G(\Omega)$. Following the work of Halmos [31] we define the *neighbourhood topology* as the topology generated by the following base of open sets: let $T \in G(\Omega)$ then

$$N(T) = \{S \in G(\Omega) : |T(A_i) \triangle S(A_i)| < \epsilon, \quad i = 1, \dots, n\},$$

where $\epsilon > 0$ and $A_i \in \Sigma$ are measurable sets.

Since for our purposes we will consider the L^1 topology on $G(\Omega)$, we recall the following

Proposition 1.1.7. *Let $\{T_n\}, T \subset G(\Omega)$ and assume that $T_n \to T$ in measure. Then $T_n \to T$ in the neighbourhood topology. Conversely, if $T_n \to T$ in the neighbourhood topology, then T_n converges to T in measure.*

Since in our case Ω is a compact set, then the convergence in measure is equivalent to the convergence in L^1: hence we will use the L^1 topology for maps as in Proposition 1.0.3.

We will be concerned with flows of vector fields extended periodically to the real line, that is $b(t+1) = b(t)$. Even if X_t is not a flow of automorphisms, the quantities in the r.h.s. of (1.1.5),(1.1.6) can be computed and are related to the mixing properties of $T = X_{t=1}$. Also the ergodic properties of $T = X_1$ are equivalent to an ergodic property of X_t.

Let $\{X_s\}_{s\in[0,1]}$ be a family of automorphisms of Ω such that $s \to X_s$ is continuous (hence uniformly continuous) with respect to the neighborhood topology of $G(\Omega)$. Let $T = X_{t=1}$ and define

$$X_t = X_s \circ T^n = T^n \circ X_s, \quad t = n + s, s \in [0, 1).$$

Lemma 1.1.8. *The following hold*

1. *if T is ergodic then for every set $A \in \Sigma$*
$$\fint_0^t \chi_{X_s(A)} ds \to_{L^1} |A|;$$
2. *T is weakly mixing iff for every $A, B \in \Sigma$*
$$\lim_{t\to\infty} \fint_0^t \left[|X_s(A) \cap B| - |A||B|\right]^2 ds = 0;$$
3. *T is mixing iff $\forall A, B \in \Sigma$*
$$\lim_{t\to\infty} \left|X_t(A) \cap B\right| = |A||B|.$$

The proof of this lemma is given in Appendix 4.4, since we believe it is standard and not strictly related to our results.

Definition 1.1.9. Let $b \in L^\infty([0,1], \mathrm{BV}(\mathbb{R}^2))$, $\operatorname{supp} b_t \subset K$, be a divergence-free vector field. We will say that b is ergodic (weakly mixing, strongly mixing) if its unique RLF X_t evaluated at $t = 1$ is ergodic (respectively weakly mixing, strongly mixing).

1.1.2 Genericity of weakly mixing

Let $\mathcal{U}$ be the G_δ-subset of $L^1_{t,x}$ where the Regular Lagrangian Flow can be uniquely extended by continuity (Proposition 1.0.3). The first statement has the same proof of [Theorem 2, [31]] and [Page 77,[32]]:

Proposition 1.1.10. *The set of ergodic/weakly-mixing vector fields is a G_δ-set in $\mathcal{U}$, the set of strongly mixing is a first category set.*

We repeat the proof for convenience only for weakly/strongly mixing, the case for ergodic vector fields is completely analogous [30].

Proof. Since the map $\tilde{\Phi}(b)(t = 1) = T(b)$ defined in Proposition 1.0.3 is continuous from $\mathcal{U}$ into $L^1(K, K)$, it is enough to prove that the set of weakly mixing maps is a G_δ. For simplicity we define a new topology on $G(K)$ that coincides with the neighbourhood topology known as *Von Neumann strong neighbourhood topology*. Given $T \in G(K)$, define a linear operator $T : L^2(K, \mathbb{C}) \to L^2(K, \mathbb{C})$ by
$$(Tf)(x) = f(Tx) \quad \forall f \in L^2(K, \mathbb{C})$$
such that $||Tf||_{L^2} = ||f||_{L^2}$ (being T measure-preserving). Consider f_i a countable dense subset in L^2: a base of open sets in the strong neighbourhood topology is given by
$$N(T) = \{S \in G(K) : ||Tf_i - Sf_i||_2 \le \epsilon, \quad i = 1, \dots, n\}.$$
Then we define
$$E(i, j, m, n) = \left\{T \in G(K) : \left|(T^n f_i, f_j) - (f_i, 1)(1, f_j)\right| < 2^{-m}\right\},$$
where $(\cdot, \cdot)$ denotes the scalar product in L^2. Simply observing that $T \to (Tf, g)$ is continuous in the strong neighbourhood topology then by Proposition 1.1.7 it follows that $E(i, j, n, m)$ is open in $L^1(K, K)$, and then
$$G = \bigcap_{i,j,m} \bigcup_n E(i, j, m, n)$$

is a G_δ-set. By the Mixing Theorem [Theorem 2, page 29, [23]] G coincides with the set of weakly mixing maps in $L^1(K,K)$. Indeed if T is not mixing, then there exists $f \neq 0$ and a complex eigenvalue $\lambda \in \{|z| = 1, z \neq 0, 1\}$ such that $Tf = \lambda f$. We can assume that f is orthogonal to the eigenvector 1, that is $(f,1) = 0$, and also that $||f||_2 = 1$. Now choose i such that $||f - f_i|| \leq \epsilon$ for some ϵ to be chosen later and take $f_j = f_i$. Then

$$\begin{aligned}
1 &= |(T^n f, f) - (f,1)(f,1)| \\
&\leq |(T^n f, f) - (T^n f, f_i)| + |(T^n f, f_i) - (T^n f_i, f_i)| + |(T^n f_i, f_i) - (f_i,1)(1,f_i)| \\
&\quad + |(f_i,1)(1,f_i) - (f,1)(f_i,1)| + |(f,1)(1,f_i) - (f,1)(f,1)| \\
&\leq 2||f - f_i||_2 + 2||f_i||_2||f - f_i||_2 + |(T^n f_i, f_i) - (f_i,1)(1,f_i)|,
\end{aligned}$$

so since $||f_i||_2 \leq 1 + \epsilon$ we get that

$$1 \leq 2\epsilon + 2(1+\epsilon)\epsilon + |(T^n f_i, f_i) - (f_i,1)(1,f_i)|.$$

With the choice of $\epsilon > 0$ small enough we get that $\frac{1}{2} \leq |(T^n f_i, f_i) - (f_i,1)(1,f_i)|$, that is $T \notin G$. This concludes the proof of the first part of the statement.
We next prove that the set of strongly mixing vector fields is a first category set. Let $A \subset K$ be a measurable set such that $|A| = \frac{1}{2}$. Then define the F_σ-set

$$F = \bigcup_n \bigcap_{k>n} \left\{ T \in G(K) : \left| |(T^{-k}(A) \cap A)| - \frac{1}{4} \right| \leq \frac{1}{5} \right\}.$$

Clearly strongly mixing maps are contained in F by definition and therefore strongly mixing vector fields are contained in $\tilde{F} = \tilde{\Phi}^{-1}(t=1)(F)$. This $\tilde{F}$ is a set of first category: indeed consider the set

$$\bigcup_{k>n} \tilde{\Phi}^{-1}(t=1) \left(\left\{ T \in G(K) : \left| |(T^{-k}(A) \cap A)| - \frac{1}{4} \right| \leq \frac{1}{5} \right\} \right)^c. \tag{1.1.8}$$

By our main result (Theorem 4.4.1) $\forall b \in \mathcal{U}$ for all $n \in \mathbb{N}$ there exists $k > n$ and $b^p \in L^\infty_t(\mathrm{BV}_x)$ such that the RLF $X^p_{t=1}$ associated with b^p evaluated at $t = 1$ is a permutation of subsquares of period k. Hence

$$\bigcup_{k>n} \{b \in L^\infty_t(\mathrm{BV}_x) \text{ permutation of period } k\}$$

is dense and contained in (1.1.8), so that we conclude that (1.1.8) is open and dense for all n, i.e., F is of first category. □

Corollary 1.1.11. *Assume that the set*

$$SM = \{b \in \mathcal{U} : b \text{ is strongly mixing}\}$$

is dense in $\mathcal{U}$. Then the set of weakly mixing vector fields is residual.

Proof. Elementary. □

Our aim will be to prove the assumption of the above corollary, which together with Proposition 1.1.10 will conclude the proof of Theorem 0.0.3 once we show that the dense set of strongly mixing vector fields are actually exponentially mixing.

Remark 1.1.12. The above situation, namely

- b strongly mixing is dense in $\mathcal{U}$,
- b weakly mixing is second category in $\mathcal{U}$,

is in some sense the best situation we can hope in $\mathcal{U}$. Indeed, the strongly mixing vector fields are a set of first category and then it is not a "fat" set. On the other hand, the weakly mixing vector fields would be a "fat" set once we know their density, which one deduces from the density of the strongly mixing vector fields.

1.1.3 Markov Shifts

When dealing with finite spaces $X = \{1, \dots, n\}$ and processes whose outcome at time k depends only on their outcome at time $k-1$ it is easier to determine some statistical properties of the dynamical system, as ergodicity and mixing (see for a reference [36],[44]). More precisely let $B(n) = \{\theta : \mathbb{Z} \to X\}$ the space of sequences and define a cylinder

$$C(m, k_1, \dots, k_r) = \Big\{\theta \in B(n) : \theta(m+i) = k_{i+1},\ i = 0, \dots, r-1\Big\}$$

where $m \in \mathbb{Z}$ and $k_i \in X$. Therefore, since the Borel σ-algebra on $B(n)$ is generated by disjoint union of cylinders, we can define a probability measure μ on $B(n)$ simply determining its value on cylinders. A *Markov measure* μ is a probability measure on $B(n)$ for which there exist $p_i > 0, P_{ij} \geq 0$, $i, j = 1, \dots n$, with

$$\sum_i p_i = \sum_j P_{ij} = 1, \quad \sum_i p_i P_{ij} = p_j,$$

such that

$$\mu(C(m, k_1, \dots, k_r)) = p_{k_1} P_{k_1 k_2} \dots P_{k_{r-1} k_r}$$

for every cylinder $C(m, k_1, \dots, k_r)$. The P_{ij} are called *transition probabilities* and $P = (P_{ij})$ is the *transition matrix*. The transition matrix is a stochastic matrix, that is $\sum_j P_{ij} = 1$ for every i. Now define $P_{ij}^{(m)}$ the coefficients of the matrix P^m.

Definition 1.1.13. A matrix P with positive coefficients is *irreducible* if $\forall i, j$ there exists m such that $P_{ij}^{(m)} > 0$.

Definition 1.1.14. A matrix P with positive coefficients is *aperiodic* if there exists m such that $P_{ij}^{(m)} > 0\ \forall i, j$.

A *Markov shift* is a map $\sigma : (B(n), \mu) \to (B(n), \mu)$ such that

$$\sigma(\theta)(i) = \theta(i+1), \quad \forall \theta \in B(n).$$

Then it can be proved that $\sigma_\sharp \mu = \mu$. We conclude this subsection with the following results on ergodicity and mixing properties of Markov shifts (see [44], Chapter 7).

Proposition 1.1.15 (Ergodicity)**.** *The following are equivalent:*

1. $\sigma : (B(n), \mu) \to (B(n), \mu)$ *is ergodic;*
2. P *is irreducible;*
3. $\lim_{m \to \infty} \frac{1}{m} \sum_{k=0}^{m-1} P_{ij}^{(k)} = p_j$.

Proposition 1.1.16 (Mixing)**.** *The following are equivalent:*

1. $\sigma : (B(n), \mu) \to (B(n), \mu)$ *is strongly mixing;*
2. P *is aperiodic;*
3. $\lim_{m\to\infty} P_{ij}^{(m)} = p_j$.

Chapter 2

Mixing BV vector fields

In this chapter we present the construction of a divergence free BV weakly mixing vector field (see [46]) that is not strongly mixing. The example is based on the fact that the Canonical Chacon map, which is a weakly mixing automorphism that is not strongly mixing, can be connected to the identity, that is it is the time-1 map of the flow of some divergence-free vector field.

Before [10] only few examples of divergence-free vector fields with good mixing properties were known. A fundamental example was provided in [27] where the authors constructed the time-periodic divergence-free vector field $u \in L^\infty_t([0,1], BV_x(\mathbb{R}^2))$ whose flow $T_t : [0,1] \times K \to K$ of measure-preserving maps realizes at time $t = 1$ the *folded Baker's map*, that is

$$T = T_{\llcorner t=1} = \begin{cases} \left(-2x+1, -\frac{y}{2} + \frac{1}{2}\right) & x \in \left[0, \frac{1}{2}\right), \\ \left(2x-1, \frac{y}{2} + \frac{1}{2}\right) & x \in \left(\frac{1}{2}, 1\right], \end{cases} \qquad y \in [0,1], \tag{2.0.1}$$

(see Theorem 1, [27]). In reality, the construction in [27] gives a Sobolev Regular vector field, but for our analysis we need simply the BV regularity. The action of this automorphism can be represented as in Figure 2. The fundamental idea of the authors is to prove that the map T is the time-1 map of the RLF of some divergence-free vector field. A similar analysis can be performed for more complicated automorphisms, as the Canonical Chacon's automorphism. Here the vector fields that play a role perform more complicated *movements* in order to obtain the precise behaviour of the map. We remark that the analysis, that we perform in dimension 2, can be easily extended to any dimension. In the next section we present the Canonical Chacon's Transformation in dimension 1: this is the starting point of our analysis. In Section 2.2 we present

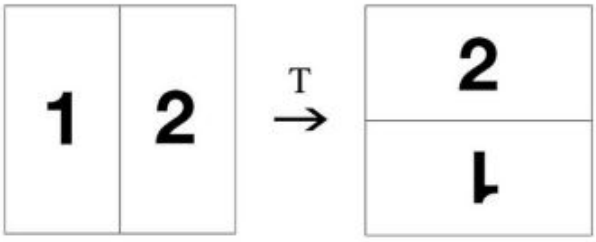

Figure 2.1: The action of the automorphism U on the unit square K.

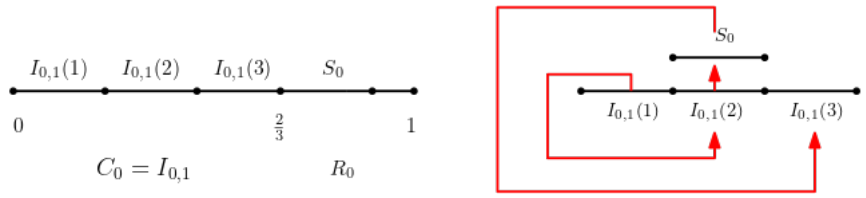

Figure 2.2: In the left figure the Column C_0, in the right figure the geometric representation of the action of the automorphism T_1.

the vector fields that act on the 2-dimensional torus as simple movements (rotation, sort, exchange). In Section 2.3 we present the two dimensional version of the Chacon map, and finally, in Section 2.4 we give the explicit construction of a weakly mixing BV vector field which is not strongly mixing, providing a proof of Theorem 0.0.2.

2.1 Canonical Chacon's Transformation

We present here the one dimensional canonical Chacon's Transformation [21], that can be easily extended to higher dimension (see for example Section 2.3 for the two dimensional): indeed, this construction is based on a general geometric approach which consists in mapping subintervals of the same length linearly onto each other (see also [22] for further reference). Let us consider $I = [0, 1]$ and let $|\cdot|$ be the Lebesgue measure. The aim is to construct a weakly mixing automorphism $T \in G(I)$ which is not strongly mixing.

Definition 2.1.1. A *column* C is a finite sequence of disjoint subintervals $J \subset I$ called *levels*. The number of levels in a column is its *height* h.

We define a family of automorphisms $\{T_k\}_k \subset G(I)$ by induction. Let C_0 be the column $C_0 \doteq I_{0,1} = \left[0, \frac{2}{3}\right)$, and let the *remaining set* be $R_0 = \left[\frac{2}{3}, 1\right]$. The height of the column C_0 is $h_0 = 1$, since it has a unique level $I_{0,1}$. We divide C_0 into three disjoint subintervals with same length: $I_{0,1}(1) = \left[0, \frac{2}{9}\right)$, $I_{0,1}(2) = \left[\frac{2}{9}, \frac{4}{9}\right)$, $I_{0,1}(3) = \left[\frac{4}{9}, \frac{2}{3}\right)$. We call *spacer* the interval $S_0 = \left[\frac{2}{3}, \frac{8}{9}\right)$ and $R_1 = R_0 \setminus S_0$. We observe that the spacer has the same length of $I_{0,1}(j)$ for $j = 1, 2, 3$. We put the spacer on the top of the middle interval $I_{0,1}(2)$ (see Figure 2.2). We define the piecewise linear map $T_1 : I \to I$ in the following way:

$$\begin{cases} T_1(I_{0,1}(1)) = I_{0,1}(2), \\ T_1(I_{0,1}(2)) = S_0, \\ T_1(S_0) = I_{0,1}(3). \end{cases}$$

In the set $I \setminus (I_{0,1}(1) \cup I_{0,1}(2) \cup S_0)$ the map T_1 is defined in such a way that T_1 is invertible and measure-preserving (for simplicity we can assume $T_1(I_{0,1}(3)) = I_{0,1}(1)$ and $T_1 = id$ otherwise). A useful notation to represent T_1 in a simpler way is using the language of permutations, that is

$$T_{1 \llcorner [0,1] \setminus R_1} = \begin{pmatrix} I_{0,1}(1) & I_{0,1}(2) & I_{0,1}(3) & S_0 \\ I_{0,1}(2) & S_0 & I_{0,1}(1) & I_{0,1}(3) \end{pmatrix}. \tag{2.1.1}$$

We construct the column C_1 of height $h_1 = 3h_0 + 1 = 4$ putting one on the top of the other the intervals in the order $I_{0,1}(1), I_{0,1}(2), S_0, I_{0,1}(3)$: the intervals are arranged so that each point is located below its image (see Figure 2.3). We rename the levels $I_{1,1} = I_{0,1}(1), I_{1,2} = I_{0,1}(2), I_{1,3} = S_0, I_{1,4} = I_{0,1}(3)$.

Figure 2.3: The column C_1 in which the levels are arranged one on top the other.

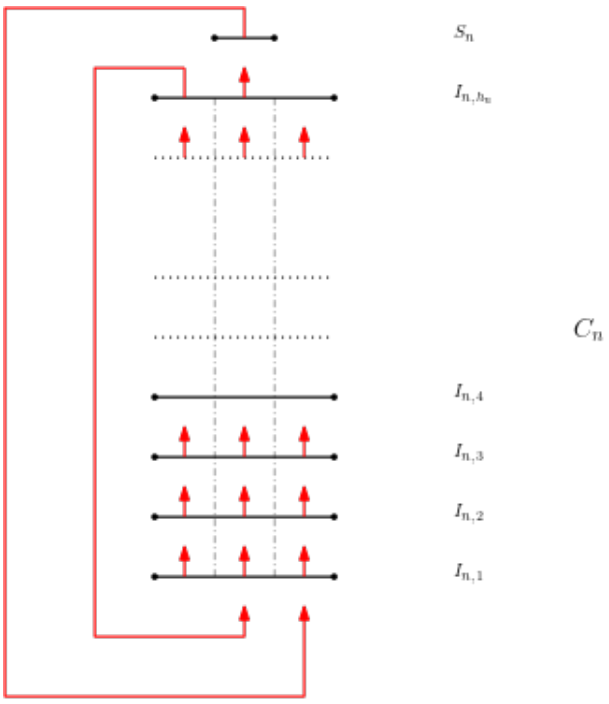

Figure 2.4: A column C_n and the action of the automorphism T_{n+1}.

The inductive step is performed in the following way: we start with a column C_n made of $h_n = 3h_{n-1} + 1$ levels $I_{n,1}, I_{n,2}, \ldots, I_{n,h_n}$. We divide each level into three disjoint consecutive subintervals of the same length, that is $I_{n,j} = I_{n,j}(1) \cup I_{n,j}(2) \cup I_{n,j}(3)$ for $j = 1, \ldots, h_n$. We consider the set $R_n = \left[\frac{3^{n+1}-1}{3^{n+1}}, 1\right]$ and we construct $S_n = \left[\frac{3^{n+1}-1}{3^{n+1}}, \frac{3^{n+2}-1}{3^{n+2}}\right]$, with $|S_n| = \frac{2}{3^{n+2}} = |I_{n,j}(i)|$ for $j = 1, \ldots, h_n$, $i \in \{1, 2, 3\}$ and we put it on the top of the middle interval $I_{n,h_n}(2)$ of the bottom level I_{n,h_n} (see Figure 2.4). We finally define the piecewise linear map T_{n+1} in the following way:

$$\begin{cases} T_{n+1}(I_{n,j}(i)) = I_{n,j+1}(i) \quad \forall j = 1, \ldots h_n - 1, \quad \forall i \in \{1, 2, 3\}, \\ T_{n+1}(I_{n,h_n}(1)) = I_{n,1}(2), \\ T_{n+1}(I_{n,h_n}(2)) = S_n, \\ T_{n+1}(I_{n,h_n}(3)) = I_{n,1}(1), \\ T_{n+1}(S_n) = I_{n,1}(3), \\ T_{n+1} = \text{id} \quad \text{otherwise.} \end{cases}$$

The new column C_{n+1} of height $h_{n+1} = 3h_n + 1$ is obtained arranging the levels starting from the bottom $I_{n,1}(1), I_{n,2}(1), \ldots I_{n,h_n}(1), I_{n,1}(2), I_{n,2}(2), \ldots I_{n,h_n}(2), S_n, I_{n,1}(3), \ldots, I_{n,h_n}(3)$.

We rename them as $I_{n+1,j}$ $j = 1, \dots, h_{n+1}$ following the same order of the levels and we define $R_{n+1} = R_n \setminus S_n$.

Definition 2.1.2. The Canonical Chacon's map is the automorphism $T = \lim_{n\to\infty} T_n$.

Observe that the limit map T is well defined, invertible and measure-preserving, indeed one can easily check that $T_{n+1} = T_n$ on $\left(\cup_{j=1}^{h_n-1} I_{n,j}\right)^c$.

Theorem 2.1.3 (Chacon [21])**.** *T is weakly mixing but not strongly mixing.*

We will give a proof of this theorem in the case of two dimensional examples (see Proposition 2.3.2).

2.2 Configurations and movements

In this subsection we introduce the notion of rows, columns and configurations. The advantage of this abstract description is to simplify the action of two-dimensional automorphisms on the torus as the composition of a finite number of *movements*, where each one can be described as the flow (evaluated at time $t = 1$) of a divergence-free BV vector field.

Definition 2.2.1. A row $r(i)$ of *length* $n \in \mathbb{N}$ and index $i \in \mathbb{N}$ is a integer-valued $1 \times n$ matrix

$$r(i) = (i, j_1 \quad i, j_2 \quad \dots \quad i, j_n),$$

where $j_1, j_2, \dots, j_n \in \mathbb{N}$.

Definition 2.2.2. A column $c(j)$ of *length* $n \in \mathbb{N}$ and index $j \in \mathbb{N}$ is a integer-valued $n \times 1$ matrix

$$c(j) = \begin{pmatrix} i_1, j & i_2, j & \dots & i_n, j \end{pmatrix}^T,$$

where $i_1, i_2, \dots, i_n \in \mathbb{N}$.

Definition 2.2.3. A configuration γ of *size* $n \in \mathbb{N}$ is a integer-valued $n \times n$ matrix, where the entries $\gamma_{i,j} \in \{1, 2, \dots, n^2\}$ and $\gamma_{i,j} = \gamma_{h,k}$ iff $i = h, j = k$. We can denote γ both *by rows* as $\gamma = (r(1), r(2), \dots, r(n))^T$ and *by columns* $\gamma = (c(1), c(2), \dots, c(n))$. We call $\mathcal{C}(n)$ the *space of configurations* of size n.

Remark 2.2.4. One can easily observe that $\sharp\mathcal{C}(n) = n^2!$, being γ all possible permutations of $\{1, 2, \dots, n^2\}$.

Definition 2.2.5. Let $\gamma \in \mathcal{C}(n)$ be a configuration. Two entries $\gamma_{i,j}$, $\gamma_{i',j'}$ are *adjacent* if $|i' - i| = 1$ and $j' = j$ or $i' = i$ and $|j' - j| = 1$.

Definition 2.2.6. A movement is a bijective map $S : \mathcal{C}(n) \to \mathcal{C}(n)$.

Definition 2.2.7 (Simple exchange)**.** Let $\gamma \in \mathcal{C}(n)$ and let $\gamma_{i,j}$, $\gamma_{i',j'}$ be two adjacent entries. For simplicity we can assume $i' = i + 1, j' = j$ according to Definition 2.2.5. A *simple exchange* is a map $E_s(i, j; i+1; j) : \mathcal{C}(n) \to \mathcal{C}(n)$ that exchanges the two entries, that is

$$E_s(i,j;i+1;j) \begin{pmatrix} \dots & \dots & \dots & \dots & \dots \\ i,1 & \dots & i,j & \dots & i,n \\ i+1,1 & \dots & i+1,j & \dots & i+1,n \\ \dots & \dots & \dots & \dots & \dots \end{pmatrix} = \begin{pmatrix} \dots & \dots & \dots & \dots & \dots \\ i,1 & \dots & i+1,j & \dots & i,n \\ i+1,1 & \dots & i,j & \dots & i+1,n \\ \dots & \dots & \dots & \dots & \dots \end{pmatrix}$$

Definition 2.2.8 (Sort)**.** Let $\gamma \in \mathcal{C}(n)$ and let $i \in \mathbb{N}$ be some fixed row index. Let $j, j' \in \mathbb{N}$ with $j < j'$. Then the *sort* operation on columns is $S_c(i; j, j') : \mathcal{C}(n) \to \mathcal{C}(n)$ defined by

$$S_c(i;j,j') \begin{pmatrix} \dots & \dots & \dots & \dots & \dots & \dots & \dots \\ \dots & i,j & i,j+1 & \dots & i,j'-1 & i,j' & \dots \\ \dots & \dots & \dots & \dots & \dots & \dots & \dots \end{pmatrix} = \begin{pmatrix} \dots & \dots & \dots & \dots & \dots & \dots & \dots \\ \dots & i,j' & i,j & i,j+1 & \dots & i,j'-1 & \dots \\ \dots & \dots & \dots & \dots & \dots & \dots & \dots \end{pmatrix}.$$

Similarly, if $i, i', j \in \mathbb{N}$ and $i < i'$ $S_r(i, i'; j) : \mathcal{C}(n) \to \mathcal{C}(n)$ is defined by

$$S_r(i,i';j) \begin{pmatrix} \dots & \dots & \dots \\ \dots & i,j & \dots \\ \dots & i+1,j & \dots \\ \dots & \dots & \dots \\ \dots & i',j & \dots \\ \dots & \dots & \dots \end{pmatrix} = \begin{pmatrix} \dots & \dots & \dots \\ \dots & i',j & \dots \\ \dots & i,j & \dots \\ \dots & \dots & \dots \\ \dots & i'-1,j & \dots \\ \dots & \dots & \dots \end{pmatrix}. \tag{2.2.1}$$

Example 2.2.9. We give the example of some configuration γ and the new configuration $S_c(1; 2, 4)(\gamma)$ obtained by exchanging rows:

$$\gamma = \begin{pmatrix} 1 & 2 & 3 & 4 \\ 5 & 6 & 7 & 8 \\ 9 & 10 & 11 & 12 \\ 13 & 14 & 15 & 16 \end{pmatrix} \qquad S_c(1;2,4)(\gamma) = \begin{pmatrix} 1 & 4 & 2 & 3 \\ 5 & 6 & 7 & 8 \\ 9 & 10 & 11 & 12 \\ 13 & 14 & 15 & 16 \end{pmatrix}.$$

Remark 2.2.10. We observe that if $j = 1$ and $j' = n$ then the sort operation is simply a shift. Since we will work on the torus, the shifts are easier to perform than sort movements. In particular we will see that the cost of a shift, in terms of the total variation, is lower than the cost of a sort movement.

Definition 2.2.11 (Rotation)**.** Let $\gamma \in \mathcal{C}(n)$ and let $i \geq 2$ and $j < n$. Then the counterclockwise rotation $R^-_{i,j} : \mathcal{C}(n) \to \mathcal{C}(n)$ is the following map

$$R^-_{i,j} \begin{pmatrix} \dots & \dots & \dots & \dots \\ \dots & i-1,j & i-1,j+1 & \dots \\ \dots & i,j & i,j+1 & \dots \\ \dots & \dots & \dots & \dots \end{pmatrix} = \begin{pmatrix} \dots & \dots & \dots & \dots \\ \dots & i-1,j+1 & i,j+1 & \dots \\ \dots & i-1,j & i,j & \dots \\ \dots & \dots & \dots & \dots \end{pmatrix}, \tag{2.2.2}$$

while the clockwise rotation $R^+_{i,j} : \mathcal{C}(n) \to \mathcal{C}(n)$ is the following map

$$R^+_{i,j} \begin{pmatrix} \dots & \dots & \dots & \dots \\ \dots & i-1,j & i-1,j+1 & \dots \\ \dots & i,j & i,j+1 & \dots \\ \dots & \dots & \dots & \dots \end{pmatrix} = \begin{pmatrix} \dots & \dots & \dots & \dots \\ \dots & i,j & i-1,j & \dots \\ \dots & i,j+1 & i-1,j+1 & \dots \\ \dots & \dots & \dots & \dots \end{pmatrix}. \tag{2.2.3}$$

Example 2.2.12. We give the example of some configuration γ and the new configuration $R^-_{2,3}(\gamma)$ obtained by a counterclockwise rotation:

$$\gamma = \begin{pmatrix} 1 & 2 & 3 & 4 \\ 5 & 6 & 7 & 8 \\ 9 & 10 & 11 & 12 \\ 13 & 14 & 15 & 16 \end{pmatrix} \qquad R^-_{2,3}(\gamma) = \begin{pmatrix} 1 & 2 & 4 & 8 \\ 5 & 6 & 3 & 7 \\ 9 & 10 & 11 & 12 \\ 13 & 14 & 15 & 16 \end{pmatrix}.$$

2.2.1 Flows of vector fields associated with movements

From now on we will consider the two dimensional torus $\mathbb{T}^2 = [0,1]^2$ with periodic boundary conditions. The idea of this subsection is to apply the previous description via configurations, rows and columns to the two dimensional torus. In particular our aim is to find vector fields whose flow acts on the torus as the movements previously defined (Sort, Exchange, Rotation) and we want to give some estimates on their total variation. We remark here that the BV regularity of the vector fields make possible all these constructions, allowing for rigid *cut and paste motions*, in the spirit of [10] and [27].

Following the notation introduced in [10] we define a flow that rotates subrectangles of $\mathbb{T}^2$ and the vector field associated with it. More precisely we define the *rotation flow* $r_t : \mathbb{T}^2 \to \mathbb{T}^2$ for $t \in [0,1]$ in the following way: call

$$V(x) = \max\left\{\left|x_1 - \frac{1}{2}\right|, \left|x_2 - \frac{1}{2}\right|\right\}^2, \quad (x_1, x_2) \in \mathbb{T}^2.$$

Then the *rotation field* is $r : \mathbb{T}^2 \to \mathbb{R}^2$

$$r(x) = \nabla^\perp V(x), \tag{2.2.4}$$

where $\nabla^\perp = (-\partial_{x_2}, \partial_{x_1})$ is the orthogonal gradient. Finally the rotation flow r_t is the flow of the vector field r, i.e. the unique solution to the following ODE system:

$$\begin{cases} \dot{r}(t,x) = r(r(t,x)), \\ r(0,x) = x. \end{cases} \tag{2.2.5}$$

This flow rotates the unit square $[0,1]^2$ counterclockwise of an angle $\frac{\pi}{2}$ in a unit interval of time. We recall here Lemma 2.6 in [10] that gives the cost, in terms of the total variation, of the rotation of a rectangle:

Lemma 2.2.13. *Let $Q \subset [0,1]^2$ be a rectangle of sides $a, b > 0$. Consider the rotating flow on the torus*

$$(R_Q)(t,x) = \chi_Q^{-1} \circ r(t) \circ \chi_Q(x), \quad \text{if } x \in Q.$$

where $\chi_Q : Q \to [0,1]^2$ is the affine map sending Q into $[0,1]^2$ and $r(t)$ is the rotation flow defined in (2.2.5)*. Let $b(t)^{R_Q}$ the divergence-free vector field associated with $(R_Q)(t)$ (extended to 0 outside the rectangle Q). Then*

$$\text{Tot.Var.}(b^R(t))(\mathbb{T}^2) = 4a^2 + 4b^2, \quad \forall t \in [0,1].$$

Let us fix now some $k \in \mathbb{N}$ giving the size of the partition, and let us consider the grid given by $\mathbb{N} \times \mathbb{N}\frac{1}{k}$ made of squares of side $\frac{1}{k}$. We consider the subsquares $Q_{i,j} = [\frac{j-1}{k}, \frac{j}{k}] \times [\frac{k-i}{k}, \frac{k-i+1}{k}]$ and we identify each subsquare with an entry γ_{ij} of some configuration $\gamma \in \mathcal{C}(k)$. A horizontal stripe $H_i = [0,1] \times [\frac{k-i}{k}, \frac{k-i+1}{k}]$ is a row, while a vertical stripe $V_j = [\frac{j-1}{k}, \frac{j}{k}] \times [0,1]$ is a column. We observe that if $Q_{i,j}$ and $Q_{i',j'}$ are adjacent subsquares (that is, they share a common side), then $\gamma_{i,j}$ and $\gamma_{i',j'}$ are adjacent entries (Definition 2.2.5). From now on we will identify every $\gamma \in \mathcal{C}(k)$ with an enumeration of the subsquares of the torus, and any movement $T : \mathcal{C}(k) \to \mathcal{C}(k)$ with an automorphism $T : \mathbb{T}^2 \to \mathbb{T}^2$that sends rigidly every subsquare of the grid $\mathbb{N} \times \mathbb{N}\frac{1}{k}$ into another one of the same grid. We start introducing the vector fields whose RLF,

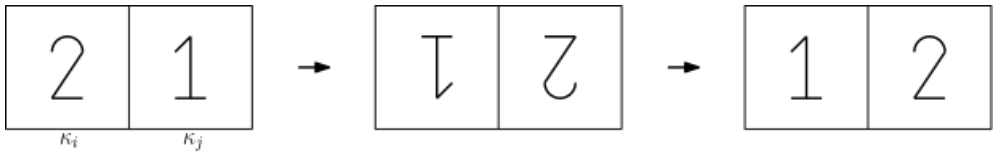

Figure 2.5: A transposition between two squares is an exchange.

when evaluated at time $t = 1$, are movements.

We first recall the transposition vector field, first introduced in [10]. Let κ_i, κ_j be two adjacent squares of size $\frac{1}{k}$ and let $Q = \kappa_i \cup \kappa_j$, then the *transposition flow* between κ_i, κ_j is $T(t)(\kappa_i, \kappa_j) : [0,1] \times \mathbb{T}^2 \to \mathbb{T}^2$ defined as

$$T(t)(\kappa_i, \kappa_j) = \begin{cases} \chi^{-1} \circ r(4t) \circ \chi & x \in \mathring{Q},\ t \in \left[0, \frac{1}{2}\right], \\ \chi_i^{-1} \circ r(4t) \circ \chi_i & x \in \mathring{\kappa}_i,\ t \in \left[\frac{1}{2}, 1\right], \\ \chi_j^{-1} \circ r(4t) \circ \chi_j & x \in \mathring{\kappa}_j,\ t \in \left[\frac{1}{2}, 1\right], \\ x & \text{otherwise}, \end{cases} \tag{2.2.6}$$

where the map $\chi : Q \to \mathbb{T}^2$ is the affine map sending the rectangle Q into the torus $\mathbb{T}^2$, χ_i, χ_j are the affine maps sending κ_i, κ_j into the torus $\mathbb{T}^2$ and r is the rotation flow (2.2.5). This invertible measure-preserving flow has the property to exchange the two subsquares in the unit time interval (Figure 3.1). Moreover, by the computations done in Lemma 2.2.13, we can estimate the total variation of the vector field $b^T(t)(\kappa_i, \kappa_j)$ associated with $T(t)(\kappa_i, \kappa_j)$ (recall 1.0.2) as

$$\text{Tot.Var.}(b^T(t)(\kappa_i, \kappa_j))(\mathbb{T}^2) \leq 4\frac{20}{k^2}. \tag{2.2.7}$$

We also observe that also L^∞ estimates on the vector field are easily available: indeed

$$\|b^T(\kappa_i, \kappa_j)\|_{L^\infty_{t.x}} \leq 4\frac{2}{k}. \tag{2.2.8}$$

Definition 2.2.14 (Simple exchange vector field)**.** Let us fix $i, i' \leq k$ with $|i - i'| = 1$ and $j \leq k$ (or alternatively $i \in \mathbb{N}$ and $j, j' \in \mathbb{N}$ with $|j - j'| = 1$). The simple exchange *vector field* is $b(t)(i, j; i', j) \in L^\infty_t \,\mathrm{BV}_x$ such that, if $X(i, j; i', j)$ is its RLF evaluated at time $t = 1$, then

$$X(i, j; i', j)(\mathbb{T}^2) = E_s(i, j; i', j)(\gamma), \quad \forall \gamma \in \mathcal{C}(k). \tag{2.2.9}$$

The construction of this vector field is easy: fix for example $i' = i + 1$. Then take the two adjacent subsquares Q_{ij} and $Q_{i+1,j}$ and perform a transposition between them $T(t)(Q_{i,j}, Q_{i+1,j})$. Then define

$$b(t)(i, j; i + 1, j) = b^T(t)(Q_{ij}, Q_{i+1,j}).$$

Clearly one has

$$\|b(i, j; i + 1, j)\|_{L^\infty_{t,x}} \leq \frac{8}{k}, \qquad \text{Tot.Var.}(b(t)(i, j; i + 1, j))(\mathbb{T}^2) \leq 4\frac{20}{k^2}. \tag{2.2.10}$$

Similarly we have

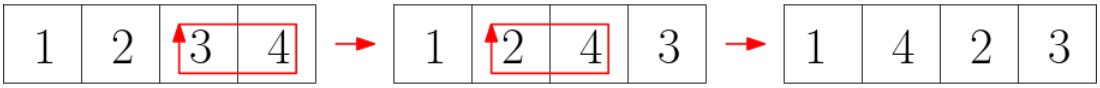

Figure 2.6: An example of a sort vector fields on a horizontal stripe of the torus. Here $j = 2, j' = 4$. The transpositions to be performed are $j' - j = 2$.

Definition 2.2.15 (Sort vector field)**.** Let $i \leq k$ be some fixed row index. Let $j, j' \leq k$ with $j < j'$. Then the *sort vector field* (on columns) is $b^{S_c}(i; j, j')(t) \in L^\infty_t \, \mathrm{BV}_x$ such that, if $X^{S_c}(i; j, j')$ is its RLF evaluated at time $t = 1$ then

$$X^{S_c}(i; j, j')(\mathbb{T}^2) = S_c(i; j, j')(\gamma), \quad \forall \gamma \in \mathcal{C}(k). \tag{2.2.11}$$

Remark 2.2.16. Similarly one has the sort vector field on rows $b^{S_r}(i, i'; j)(t)$ for some $i < i' \leq k$, $j \leq k$.

To construct a sort vector field (on columns, but the construction for rows is identical), we fix $\gamma \in \mathcal{C}(k)$, a row index i and two columns indices $j < j'$. The idea is to perform $j' - j$ exchanges between squares (recalling that an exchange is a transposition). For clarity see Figure 2.6 and compare with Example 2.2.9. We define the flow in the following way:

$$X^{S_c}(i; j, j')(t) = \begin{cases} T_{(j'-j)t}\left(Q_{i(j'-1)}, Q_{ij'}\right) & \text{for } t \in \left[0, \frac{1}{j'-j}\right], \\ T_{(j'-j)t-1}\left(Q_{i(j'-2)}, Q_{i(j'-1)}\right) & \text{for } t \in \left[\frac{1}{j'-j}, \frac{2}{j'-j}\right], \\ \dots \\ T_{(j'-j)t-(j'-j-2)}\left(Q_{i(j+1)}, Q_{i(j+2)}\right) & \text{for } t \in \left[\frac{j'-j-2}{j'-j}, \frac{j'-j-1}{j'-j}\right], \\ T_{(j'-j)t-(j'-j-1)}\left(Q_{ij}, Q_{i(j+1)}\right) & \text{for } t \in \left[\frac{j'-j-1}{j'-j}, 1\right], \\ x \quad \text{otherwise.} \end{cases} \tag{2.2.12}$$

By definition one has

$$b^{S_c}(i; j, j')(t) = \dot{X}^{S_c}(i; j, j')(t) \circ X^{S_c}(i; j, j')^{-1}(t), \tag{2.2.13}$$

so that

$$\sup_{t,x} |b^{S_c}(i; j, j')(t, x)| \leq \sup_{t,x} |\dot{X}^{S_c}(i; j, j')(t, x)| \leq (j - j')\frac{8}{k} \leq 8,$$

being the rotation vector field of the order of the side of subsquares. This implies that

$$\|b^{S_c}(i; j, j')\|_{L^\infty_t L^\infty_x} \leq 8. \tag{2.2.14}$$

Similarly one has, for every $t \in [0, 1]$

$$\text{Tot.Var.}(b^{S_c}(t)(i; j, j'))(\mathbb{T}^2) \leq (j' - j) \cdot 4 \cdot 4 \left(\frac{4}{k^2} + \frac{1}{k^2}\right) \leq \frac{80}{k}. \tag{2.2.15}$$

Remark 2.2.17. Recalling Remark 2.2.10 we observe that for the shift operation (that is $j' = k$ and $j = 1$) we can consider another vector field, exploiting the structure of the torus. We will still denote it as the sort vector field, but

$$b(t, x)(i; 1, k) = \begin{cases} \frac{1}{k}, & \text{if } x \in H_i, \\ 0 & \text{otherwise.} \end{cases} \tag{2.2.16}$$

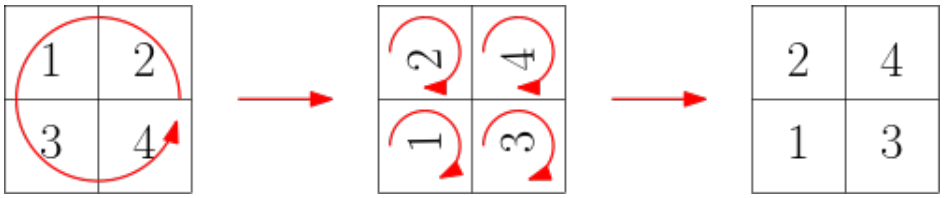

Figure 2.7: Action of the counterclockwise rotation vector field, where $k = 2$, $i = 2$, $j = 1$.

So we have instead the following estimates:

$$\|b(i,1,k)\|_{L^\infty_{t,x}} \leq \frac{1}{k}, \qquad \|\text{Tot.Var.}(b(i,1,k)(\mathbb{T}^2)\|_\infty \leq 2\frac{1}{k}. \tag{2.2.17}$$

This tells us that both the shift vector field and the sort vector field have total variation of the order of the side of the squares of the grid.

Definition 2.2.18 (Rotation vector field)**.** Let $2 \leq i \leq k$ and $j \leq k-1$. Then the counterclockwise rotation vector field is $b^-(i,j) \in L^\infty_t \,\mathrm{BV}_x$ such that, if $X^-(i,j)$ is its RLF evaluated at time $t = 1$, then

$$X^-(i,j)(\mathbb{T}^2) = R^-_{ij}(\gamma), \quad \forall \gamma \in \mathcal{C}(k). \tag{2.2.18}$$

The clockwise rotation vector field is $b^+(i,j) \in L^\infty_t \,\mathrm{BV}_x$ such that, if $X^+(i,j)$ is its RLF evaluated at time $t = 1$, then

$$X^+(i,j)(\mathbb{T}^2) = R^+_{ij}(\gamma), \quad \forall \gamma \in \mathcal{C}(k). \tag{2.2.19}$$

We write here just the counterclockwise case since the other one is identical. Here we have that, if we fix i, j as in the definition, we call $Q = Q_{(i-1)j} \cup Q_{ij} \cup Q_{i(j+1)} \cup Q_{(i-1)(j+1)}$, then

$$X^-(i,j)(t) = \begin{cases} \chi_Q^{-1} \circ r_{2t} \circ \chi_Q, & x \in \mathring{Q}, t \in \left[0, \frac{1}{2}\right], \\ \chi_{lm}^{-1} \circ r_{2t}^{-1} \circ \chi_{lm}, & x \in \mathring{Q}_{lm}, t \in \left[\frac{1}{2}, 1\right], l = i, m = j, j+1, \text{ or } l = i-1, m = j, j+1, \\ x \quad \text{otherwise}, \end{cases} \tag{2.2.20}$$

where χ is the affine map sending Q into $\mathbb{T}^2$ and χ_{lm} is the affine map sending Q_{lm} into $\mathbb{T}^2$. Again, one has

$$|\dot{X}^-(i,j)(t,x)| \leq \frac{2}{k}, \tag{2.2.21}$$

from which one gets

$$\|b^-(i,j)\|_{L^\infty_{t,x}} \leq \frac{2}{k}, \qquad \text{Tot.Var.}(b^-(t)(i,j))(\mathbb{T}^2) \leq 2 \cdot 4 \left(\frac{4}{k^2} + \frac{4}{k^2}\right), \quad \forall t. \tag{2.2.22}$$

In the Figure 2.7 an example of the action of a clockwise rotation vector field.

Remark 2.2.19. If $X : [0,1] \times \mathbb{T}^2 \to T^2$ is one of the flows previously considered (simple exchange, sort/shift, rotation), then, if k is the side of the squares in which the torus is tiled, one has

$$\|\dot{X}\|_{L^\infty_t L^\infty_x} \leq \max\left(\frac{8}{k}, \frac{(j-j')8}{k}, \frac{2}{k}\right) \tag{2.2.23}$$

We remark also that, if b is a vector field associated with a movement, then, $\forall t \in [0,1]$, it holds

$$\|\text{Tot.Var.}(b)(\mathbb{T}^2)\|_\infty \leq \max\left(\frac{80}{k^2}, (j-j')\frac{80}{k^2}, \frac{64}{k^2}\right), \tag{2.2.24}$$

which follows by the second of (2.2.10),(2.2.15) and the second of (2.2.22).

2.3 Two dimensional construction

Our aim is the construction of a weakly mixing vector field which is not strongly mixing, that is a divergence-free vector field $b \in L^\infty([0,1], \mathrm{BV}(\mathbb{T}^2))$ whose RLF $X_{\llcorner t=1}$ when evaluated at time $t = 1$ is a weakly mixing automorphism of $\mathbb{T}^2$ but not a strongly mixing automorphism. The idea is to adapt Chacon's one-dimensional construction of Subsection 2.1 and decompose the map into simple movements (Section 2.2), described as the flow of some divergence-free BV vector field (Subsection 2.2.1). Also in this case the fundamental idea is to define U as the limit of a family of automorphisms $\{U_k\}_k$.

Let us consider the two dimensional torus $\mathbb{T}^2$ as the unit square $Q_1 = Q_{1,1} = [0,1]^2$ with the canonical identification of boundaries. Using the notation via configurations (see Section 2.2) we say that Q_1 can be identified with the configuration $\gamma_1 = (1) \in \mathcal{C}(1)$. We define $h_1 = 0$ and we divide the square $Q_1 = Q_{1,1}$ into four identical subsquares each one of side $\frac{1}{2}$, more precisely: $Q_{1,1} = Q_{1,1}(1) \cup Q_{1,1}(2) \cup Q_{1,1}(3) \cup R_1$ where $Q_{1,1} = [0, \frac{1}{2}] \times [\frac{1}{2}, 1]$, $Q_{1,1}(2) = [\frac{1}{2}, 1] \times [\frac{1}{2}, 1]$ and $Q_{1,1}(3) = [0, \frac{1}{2}] \times [0, \frac{1}{2}]$. Clearly $R_1 = [\frac{1}{2}, 1] \times [0, \frac{1}{2}]$. We define U_1 on these subsquares in such a way that

$$U_1(Q_{1,1}(1)) = Q_{1,1}(2), \quad U_1(Q_{1,1}(2)) = Q_{1,1}(3) \tag{2.3.1}$$

and U_1 is measure-preserving and invertible on $Q_{1,1}$. More precisely, we define U_1 as

$$U_1(x) = \begin{cases} x + (\frac{1}{2}, 0) & \text{if} \quad x \in \mathring{Q}_{1,1}(1), \\ x + (-\frac{1}{2}, -\frac{1}{2}) & \text{if} \quad x \in \mathring{Q}_{1,1}(2), \\ x + (0, \frac{1}{2}) & \text{if} \quad x \in \mathring{Q}_{1,1}(3), \\ x & \text{otherwise.} \end{cases} \tag{2.3.2}$$

We put $h_2 = 4h_1 + 3$ and we rename the subsquares $Q_{1,1}(i)$ as $Q_{2,1} = Q_{1,1}(1), Q_{2,2} = Q_{1,1}(2), Q_{2,3} = Q_{1,1}(3)$. We look at this via configurations: let us take $\gamma_2 \in \mathcal{C}(2)$, for example

$$\gamma_2 = \begin{pmatrix} 1 & 2 \\ 3 & 4 \end{pmatrix}. \tag{2.3.3}$$

Then we can easily represent $U_1(\gamma_2)$ as

$$U_1(\gamma_2) = \begin{pmatrix} 3 & 1 \\ 2 & 4 \end{pmatrix}. \tag{2.3.4}$$

Here we see the advantage of the representation via configurations, which is more immediate. We continue our construction dividing each subsquare $Q_{2,i}$ with $i \in \{1,2,3\}$ into 4 subsquares of side equal to $\frac{1}{4}$: $Q_{2,i} = Q_{2,i}(1) \cup Q_{2,1}(2) \cup Q_{2,1}(3) \cup Q_{2,i}(4)$ and we divide also $R_1 = R_1(1) \cup R_1(2) \cup R_1(3) \cup R_2$ into 4 subsquares (see Figure 2.8). We define the map U_2 in the following way

$$U_2(x) = \begin{cases} U_1(x) & \text{if} \quad x \in \mathring{Q}_{2,1} \cup \mathring{Q}_{2,2}, \\ x + (\frac{1}{4}, \frac{1}{2}) & \text{if} \quad x \in \mathring{Q}_{2,3}(1), \\ x + (\frac{1}{4}, 0) & \text{if} \quad x \in \mathring{Q}_{2,3}(2), \\ x + (\frac{3}{4}, \frac{1}{4}) & \text{if} \quad x \in \mathring{Q}_{2,3}(3), \\ x + (\frac{1}{4}, 0) & \text{if} \quad x \in \mathring{Q}_{2,3}(4), \\ x + (-\frac{1}{2}, \frac{1}{4}) & \text{if} \quad x \in \mathring{R}_1(1), \\ x + (-\frac{1}{2}, \frac{1}{4}) & \text{if} \quad x \in \mathring{R}_1(2), \\ x + (-\frac{1}{2}, \frac{3}{4}) & \text{if} \quad x \in \mathring{R}_1(3), \\ x & \text{otherwise,} \end{cases} \tag{2.3.5}$$

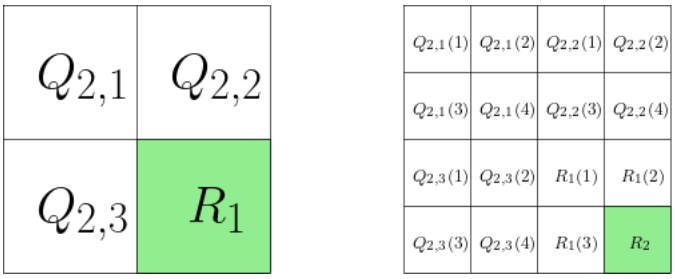

Figure 2.8: Subdivisions of the two dimensional torus.

or, via configurations, fixing some $\gamma_4 \in \mathcal{C}(4)$ we get

$$U_2 \begin{pmatrix} 1 & 2 & 5 & 6 \\ 3 & 4 & 7 & 8 \\ 9 & 10 & 13 & 14 \\ 11 & 12 & 15 & 16 \end{pmatrix} = \begin{pmatrix} 15 & 9 & 1 & 2 \\ 13 & 14 & 3 & 4 \\ 5 & 6 & 10 & 11 \\ 7 & 8 & 12 & 16 \end{pmatrix}. \tag{2.3.6}$$

We put $h_3 = 4h_2 + 3 = 15$ and we rename the squares as

$$\begin{aligned} Q_{3,1} \doteq Q_{2,1}(1) \to Q_{3,2} \doteq Q_{2,2}(1) \to Q_{3,3} \doteq Q_{2,3}(1) \to \\ \to Q_{3,4} = Q_{2,1}(2) \to \cdots \to Q_{3,14} \doteq Q_{2,3}(3) \to Q_{3,15} \doteq R_1(3), \end{aligned}$$

with the property that if $Q_{3,i} \to Q_{3,i+1}$ then $U_2(Q_{3,i}) = Q_{3,i+1}$.

The inductive step is the following: at the n-th step we have $Q_{n,1}, \dots Q_{n,h_n}$ subsquares each one of area $\frac{1}{4^{n-1}}$ and side $l_n = \frac{1}{2^{n-1}}$. We divide each subsquare into 4 identical subsquares: $Q_{n,i} = Q_{n,i}(1) \cup Q_{n,i}(2) \cup Q_{n,i}(3) \cup Q_{n,i}(4)$ and we divide also R_{n-1} into 4 identical subsquares $R_{n-1} = R_{n-1}(1) \cup R_{n-1}(2) \cup R_{n-1}(4) \cup R_n$. We put $h_{n+1} = 4h_n + 3 = 4^n - 1$ and we define the map U_n in the following way:

$$U_n(x) = \begin{cases} U_{n-1}(x) \text{ if } x \in \mathring{Q}_{n,1} \cup \cdots \cup \mathring{Q}_{n,h_n-1}, \\ x + (\frac{5}{4^{n-1}} - 1, 1 - \frac{1}{2^{n-1}}) \text{ if } x \in \mathring{Q}_{n,h_n}(1), \\ x + (\frac{1}{4^{n-1}}, 0) \text{ if } x \in \mathring{Q}_{n,h_n}(2), \\ x + (\frac{3}{4^{n-1}}, \frac{1}{4^{n-1}}) \text{ if } x \in \mathring{Q}_{n,h_n}(3), \\ x + (\frac{1}{4^{n-1}}, 0) \text{ if } x \in \mathring{Q}_{n,h_n}(4), \\ x + (-1 + \frac{1}{2^{n-1}}, \frac{2^n-3}{4^{n-1}}) \text{ if } x \in \mathring{R}_{n-1}(1), \\ x + (\frac{1}{2^{n-1}} - 1, \frac{2^n-3}{4^{n-1}}) \text{ if } x \in \mathring{R}_{n-1}(2), \\ x + (\frac{1}{2^{n-1}} - 1, \frac{2^n-1}{4^{n-1}}) \text{ if } x \in \mathring{R}_{n-1}(3), \\ x \text{ otherwise .} \end{cases} \tag{2.3.7}$$

We underline that, by definition, we have that

$$U_n(x) = U_{n-1}(x) \text{ if } x \in Q_{n,1} \cup \cdots \cup Q_{n,h_n-1}. \tag{2.3.8}$$

Finally we rename the squares as follows:

$$\begin{aligned} Q_{n+1,1} \doteq Q_{n,1}(1) \to Q_{n+1,2} \doteq Q_{n,2}(1) \to \dots Q_{n+1,h_n} \doteq Q_{n,3}(1) \to \\ \to \cdots \to Q_{n+1,4h_n+2} \doteq Q_{n,h_n}(3) \to Q_{n+1,h_{n+1}} \doteq R_n(3), \end{aligned}$$

with the property that if $Q_{n+1,i} \to Q_{n+1,i+1}$ then $U_n(Q_{n+1,i}) = Q_{n+1,i+1}$.

finally we define $U = \lim_{n\to\infty} U_n$ (well defined by condition 2.3.8). Then the following propositions hold:

Proposition 2.3.1. *The map U is measure-preserving and ergodic.*

The proof of the proposition relies on the notion of *sufficient semi-rings*, that can be taken from [22].

Proposition 2.3.2. *The map U is a weakly mixing automorphism of $\mathbb{T}^2$ that is not strongly mixing.*

Proof. The idea of the proof is the same of Chacon (see [21]). Indeed: take for example a subsquare $Q_n = Q_{n,i}$ with n sufficiently large. We will prove that

$$|U^{h_k}(Q_n) \cap Q_n| = \frac{1}{4}|Q_n| > |Q_n|^2, \quad \forall k \geq n. \tag{2.3.9}$$

We first recall that $U = \lim_{n\to\infty} U_n$ and that $U_{n+1} = U_n$ on $Q_{n+1,1} \cup Q_{n+1,2} \cup \cdots \cup Q_{n+1,h_{n+1}-1}$. We remember that $Q_n = Q_{n,i}(1) \cup Q_{n,i}(2) \cup Q_{n,i}(3) \cup Q_{n,i}(4)$, so

$$\begin{aligned}
U_n^{h_n}(Q_{n,i}(1)) &= Q_{n,i}(2),\\
U_n^{h_n}(Q_{n,i}(2)) &= Q_{n,i-1}(3),\\
U_n^{h_n}(Q_{n,i}(3)) &= Q_{n,i-1}(4),\\
U_n^{h_n}(Q_{n,i}(4)) &= Q_{n,i-1}(1).
\end{aligned}$$

This implies that

$$|U_n^{h_n}(Q_n) \cap Q_n| = \frac{1}{4}|Q_n|,$$

for any Q_n sublevel of the n-th column. Since (2.3.8) holds and also $U_n^{h_n}(Q_{n,i}(1)) = Q_{n,i}(2)$, one has

$$|U^{h_n}(Q) \cap Q| \geq \frac{1}{4}|Q|.$$

In particular, if one considers $k \geq n$ and takes a sublevel Q_k of the k-th column, one gets similarly

$$|U^{h_k}(Q_k) \cap Q_k| \geq \frac{1}{4}|Q_k|.$$

We observe now that any level Q_n of the n-th column has 4^{k-n} copies into the k-th column. For example, if $k = n+1$ one gets $Q_n = Q_{n+1}^1 \cup Q_{n+1}^2 \cup Q_{n+1}^3 \cup Q_{n+1}^4$. But then

$$\begin{aligned}
|U^{h_{n+1}}(Q_n) \cap Q_n| &= \sum_{j=1}^{4} |U^{h_{n+1}}(Q_{n+1}^j) \cap Q_n| \geq \sum_{j=1}^{4} |U^{h_{n+1}}(Q_{n+1}^j) \cap Q_{n+1}^j|\\
&\geq \sum_{j=1}^{4} \frac{1}{4}|Q_{n+1}^j| = \frac{1}{4}|Q|.
\end{aligned}$$

More in general

$$\begin{aligned}
|U^{h_k}(Q_n) \cap Q_n| &= \sum_{Q' \text{ copies}} |U^{h_k}(Q') \cap Q_n| \geq \sum_{Q' \text{ copies}} |U^{h_k}(Q') \cap Q'|\\
&\geq \sum_{Q' \text{ copies}} \frac{1}{4}|Q'| = \frac{1}{4}|Q|.
\end{aligned}$$

This gives a diverging sequence $\{k\}$ and a set Q_n for which the strongly mixing condition does not hold (if one simply requires that $|Q_n| < \frac{1}{4}$), therefore U cannot be strongly

mixing (see Definition 1.1.3). Whereas U is weakly mixing. Indeed, by the previous proposition, U is measure-preserving and ergodic. By Theorem 1.1.6 we have to prove that if $f \in \mathcal{L}^2(\mathbb{T}^2)$ is an eigenfunction of $\mathcal{U}_U$ of eigenvalue λ, with $|\lambda| = 1$, then $f = c$ for some constant c. By Lemma 2 of [23] (chapter 1, page 14), we need only to prove that $\lambda = 1$. Since f is non-zero on a set of positive measure, for every $\epsilon > 0$ there exists a constant k such that the set

$$A = \{x : |f(x) - k| < \epsilon\}$$

has positive measure. By the property of sufficient semi-rings (see again [22]) there exists a subsquare $Q = Q_{n,i}$ such that

$$\frac{|Q \cap A|}{|Q|} > \frac{7}{8}. \tag{2.3.10}$$

As in the previous computations, since $Q = Q_{n,i}(1) \cup Q_{n,i}(2) \cup Q_{n,i}(3) \cup Q_{n,i}(4)$, using that U is measure-preserving, $U^{h_n}(Q_{n,i}(1)) = Q_{n,i}(2)$, $U^{2h_n+1}(Q_{n,i}(1)) = Q_{n,i}(3)$ and that the inequality (2.3.10) holds, we obtain that there exists a point $x \in A \cap Q$ such that $U^{h_n}(x) \in A \cap Q$, and that there exists $y \in A \cap Q$ such that $U^{2h_n+1}(y) \in A \cap Q$. Indeed, by (2.3.10) we have that $|Q_{n,i}(2) \cap A| > \frac{1}{8}|Q|$ and for the same reason that

$$|Q_{n,i}(1) \cap A| > \frac{1}{8}|Q|,$$

therefore, by applying the map U^{h_n} one gets

$$|Q_{n,i}(2) \cap U^{h_n}(A)| > \frac{1}{8}|Q|,$$

which implies that

$$|(Q \cap A) \cap U^{h_n}(Q \cap A)| > 0.$$

An analogous argument proves that

$$|(Q \cap A) \cap U^{2h_n+1}(Q \cap A)| > 0.$$

Therefore

$$|f(x) - k| < \epsilon, \quad |\lambda^{h_n} f(x) - k| < \epsilon, \quad |f(y) - k| < \epsilon, \quad |\lambda^{2h_n+1} f(y) - k| < \epsilon. \tag{2.3.11}$$

So by the previous equations we have that

$$\lambda^{h_n} = \frac{k + \delta_2}{k + \delta_1}, \quad \lambda^{2h_n+1} = \frac{k + \delta_4}{k + \delta_3}$$

with $|\delta_i| < \epsilon$ for every i. That is

$$\lambda = \frac{(k + \delta_4)(k + \delta_1)^2}{(k + \delta_3)(k + \delta_2)^2}, \tag{2.3.12}$$

and since this hold for every $\epsilon > 0$, we conclude that $\lambda = 1$. □

The maps U_n can be decomposed into simple movements, using the notations of configurations.

We have the following

Proposition 2.3.3. *For every $n \geq 2$ the map U_n can be expressed as*

$$U_n = U_{n-1} \circ V_n, \tag{2.3.13}$$

where $V_n : \mathcal{C}(2^n) \to \mathcal{C}(2^n)$ and

$$\begin{aligned} V_n =& E_s(2^n, 2^n - 3; 2^n, 2^n - 2) \circ R^+(2^n, 2^n - 3) \circ R^+(2^n, 2^n - 3) \circ \\ & \circ S_c^2(2^n - 1; 2^n - 3, 2^n) \circ R^-(2^n, 2^n - 3) \circ S_c(2^n; 2^n - 3, 2^n - 1). \end{aligned} \tag{2.3.14}$$

Proof. For understanding the situation we first fix $n = 1$, and the starting configuration

$$\gamma = \begin{pmatrix} 1 & 2 & 5 & 6 \\ 3 & 4 & 7 & 8 \\ 9 & 10 & 13 & 14 \\ 11 & 12 & 15 & 16 \end{pmatrix},$$

We first apply V_1 finding

$$\begin{pmatrix} 1 & 2 & 5 & 6 \\ 3 & 4 & 7 & 8 \\ 9 & 10 & 13 & 14 \\ 11 & 12 & 15 & 16 \end{pmatrix} \xrightarrow{S_c(4;1,3)} \begin{pmatrix} 1 & 2 & 5 & 6 \\ 3 & 4 & 7 & 8 \\ 9 & 10 & 13 & 14 \\ 15 & 11 & 12 & 16 \end{pmatrix} \xrightarrow{R^-(4,1)} \begin{pmatrix} 1 & 2 & 5 & 6 \\ 3 & 4 & 7 & 8 \\ 10 & 11 & 13 & 14 \\ 9 & 15 & 12 & 16 \end{pmatrix} \xrightarrow{S_c^2(3;1,4)}$$

$$\begin{pmatrix} 1 & 2 & 5 & 6 \\ 3 & 4 & 7 & 8 \\ 13 & 14 & 10 & 11 \\ 9 & 15 & 12 & 16 \end{pmatrix} \xrightarrow{(R^+(4,1))^2} \begin{pmatrix} 1 & 2 & 5 & 6 \\ 3 & 4 & 7 & 8 \\ 15 & 9 & 10 & 11 \\ 14 & 13 & 12 & 16 \end{pmatrix} \xrightarrow{E_s(4,1;1,2)} \begin{pmatrix} 1 & 2 & 5 & 6 \\ 3 & 4 & 7 & 8 \\ 15 & 9 & 10 & 11 \\ 13 & 14 & 12 & 16 \end{pmatrix}.$$

Then by applying U_1 to the last configuration

$$\begin{pmatrix} 1 & 2 & 5 & 6 \\ 3 & 4 & 7 & 8 \\ 15 & 9 & 10 & 11 \\ 13 & 14 & 12 & 16 \end{pmatrix} \xrightarrow{U_1} \begin{pmatrix} 15 & 9 & 1 & 2 \\ 13 & 14 & 3 & 4 \\ 5 & 6 & 10 & 11 \\ 7 & 8 & 12 & 16 \end{pmatrix},$$

to compare with (2.3.6). For a generic $n \in \mathbb{N}$, one has to observe that, recalling (2.3.8), one has

$$U_n(x) = U_{n-1}(x) \text{ if } x \in Q_{n,1} \cup \cdots \cup Q_{n,h_n-1}. \tag{2.3.15}$$

with $h_n = 4^{n-1} - 1$. We list a series of useful observations:

- consider a configuration $\gamma \in \mathcal{C}(2^n)$, then the map V_n acts only on the subsquares

$$Q_{n+1,h_n}, Q_{n+1,2h_n}, Q_{n+1,2h_n+1}, Q_{n+1,3h_n+1}, Q_{n+1,3h_n+2}, Q_{n+1,4h_n+2}, Q_{n+1,4h_n+3}, R_n; \tag{2.3.16}$$

- $Q_{n,1} \cup \cdots \cup Q_{n,h_n-1}$ in equation 2.3.15 correspond to the following subsquares of the refined grid

$$Q_{n+1,1}, Q_{n+1,2}, \ldots, Q_{n+1,h_n-1}, Q_{n+1,h_n+1}, Q_{n+1,h_n+2}, \ldots, Q_{n+1,2h_n-1},$$

$$Q_{n+1,2h_n+2}, Q_{n+1,2h_n+3}, \ldots, Q_{n+1,3h_n-1}, Q_{n+1,3h_n}, \ldots Q_{n+1,3h_n+3},$$

$$Q_{n+1,3h_n+4}, \ldots Q_{n+1,4h_n+1};$$

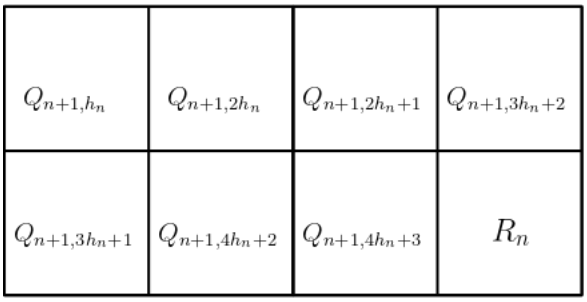

Figure 2.9: The adjacent subsquares Q_{n,h_n} and R_{n-1} and their refinement.

- therefore we have to check $U_{n-1} \circ V_n$ only on the subsquares of (2.3.16);
- we recall that, by the enumeration chosen, $U_n(Q_{n+1,i}) = Q_{n+1,i+1}$ and $U_n(Q_{n+1,h_{n+1}}) = Q_{n+1,1}$;
- we recall also that

$$U_{n-1}(Q_{n,h_n}) = Q_{n,1} = Q_{n+1,1} \cup Q_{n+1,h_n+1} \cup Q_{n+1,2h_n+2} \cup Q_{n+1,3h_n+3}, \quad (2.3.17)$$

and

$$U_{n-1} \llcorner R_{n-1} = Id. \quad (2.3.18)$$

That is, since $Q_n = Q_{n+1,h_n} \cup Q_{n+1,2h_n} \cup Q_{n+1,3h_n+1} \cup Q_{n+1,4h_n+2}$, then

$$\begin{aligned} &Q_{n+1,h_n} \overset{U_{n-1}}{\to} Q_{n+1,1}, \\ &Q_{n+1,2h_n} \overset{U_{n-1}}{\to} Q_{n+1,h_n+1}, \\ &Q_{n+1,3h_n+1} \overset{U_{n-1}}{\to} Q_{n+1,2h_n+2}, \\ &Q_{n+1,4h_n+2} \overset{U_{n-1}}{\to} Q_{n+1,3h_n+3}. \end{aligned} \quad (2.3.19)$$

Finally, we consider the adjacent subsquares Q_{n,h_n} and R_{n-1} in Figure 12 and their refinement (equation 2.3.16) on which V_n acts.
Then the action of V_n is the following

$$\begin{aligned} &Q_{n+1,h_n} \to Q_{n+1,2h_n}, \\ &Q_{n+1,2h_n} \to Q_{n+1,2h_n+1}, \\ &Q_{n+1,2h_n+1} \to Q_{n+1,3h_n+1}, \\ &Q_{n+1,3h_n+1} \to Q_{n+1,3h_n+2}, \\ &Q_{n+1,3h_n+2} \to Q_{n+1,4h_n+2}, \\ &Q_{n+1,4h_n+2} \to Q_{n+1,4h_n+3}, \\ &Q_{n+1,4h_n+3} \to Q_{n+1,h_n}, \\ &R_n \to R_n, \end{aligned}$$

as described in Figure 13. Thus the map V_n acts only on the sublevels $Q_{n+1,i}$ of the $n+1$-column, not on the sublevels $Q_{n,i}$ of the n-th column. Finally we recall that, by the enumeration chosen, by using the observation (2.3.17) and the definition of U_{n-1} in equations (2.3.19) one finally has

$$Q_{n+1,h_n} \overset{V_n}{\longrightarrow} Q_{n+1,2h_n} \overset{U_{n-1}}{\longrightarrow} Q_{n+1,h_n+1} = U_n(Q_{n+1,h_n}),$$

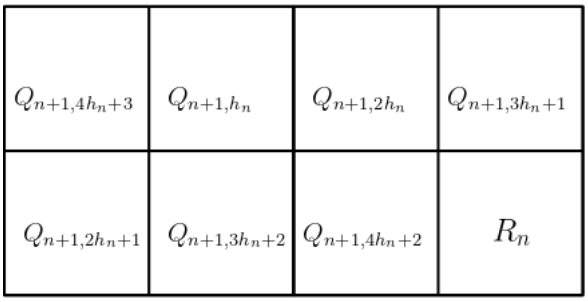

Figure 2.10: The action of V_n on the refinement of Q_{n,h_n} and R_n.

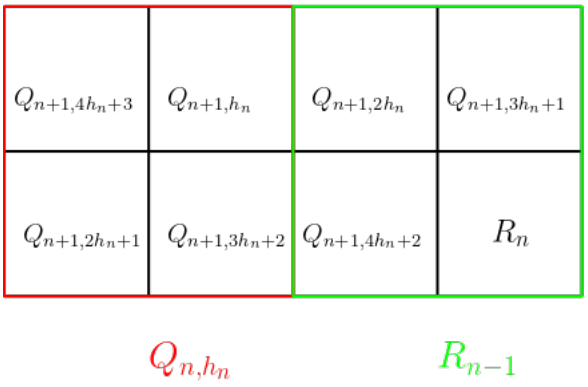

$$Q_{n+1,2h_n} \xrightarrow{V_n} Q_{n+1,2h_n+1} \xrightarrow{U_{n-1}} Q_{n+1,2h_n+1} = U_n(Q_{n+1,2h_n}),$$
$$Q_{n+1,2h_n+1} \xrightarrow{V_n} Q_{n+1,3h_n+1} \xrightarrow{U_{n-1}} Q_{n+1,2h_n+2} = U_n(Q_{n+1,2h_n+1}),$$
$$Q_{n+1,3h_n+3} \xrightarrow{V_n} Q_{n+1,4h_n+2} \xrightarrow{U_{n-1}} Q_{n+1,3h_n+3} = U_n(Q_{n+1,3h_n+3}),$$

and so on. □

We will use similar ideas to recover the flow of the weakly mixing vector field in the next section.

Remark 2.3.4. The interested reader can observe that $\forall n$ the map U_n is a cyclic permutation of subsquares of the same area (see [10] for the definitions). This observation is in the spirit of the result proved by Halmos in [31] that states that weakly mixing automorphisms are a residual G_δ-set in $G(\mathbb{T}^2)$ with the L^1-topology. A key ingredient for the proof is to show that cyclic permutations of subsquares are dense in $G(\mathbb{T}^2)$ with the L^1-topology. In [10] similar ideas are used to recover that weakly mixing vector fields are dense with respect to the $L^1_t L^1_x$-topology. In this paper we are doing a different thing: we are considering those automorphisms/vector fields that are weakly mixing but not strongly mixing, fixing a specific cyclic permutation. Therefore we cannot deduce from the previous computations the density of weakly mixing automorphisms.

2.4 The weakly mixing vector field

In this final section we provide a weakly mixing vector field $b^U \in L^\infty_t \mathrm{BV}_x$ whose RLF $X^U(t)$ evaluated at time $t = 1$ is the map U constructed in the previous section.

Our aim is to construct a flow X^n with $n \geq 2$ that, evaluated at time $t = 1$, gives the map V_n introduced in (2.3.14). We first consider $\gamma_2 \in \mathcal{C}(2)$: we can take to fix the ideas

the configuration (2.3.3). We start defining the following flow $X^1 : [0,1] \times \mathbb{T}^2 \to \mathbb{T}^2$ as

$$X^1(t) = \begin{cases} T(2t)(Q_{2,1}, Q_{2,2}), & t \in [0, \frac{1}{2}], \\ T(2t-1)(Q_{2,1}, Q_{2,3}) \circ T(1)(Q_{2,1}, Q_{2,2}), & t \in [\frac{1}{2}, 1]. \end{cases} \tag{2.4.1}$$

where the $Q_{2,i}$ $i = 1, 2, 3$ are the subsquares defined in the previous section. One can easily see that $X^1(1)(\gamma_2) = U_1(\gamma_2)$.

Building block flow. Let us consider the two adjacent subsquares Q_{n,h_n}, R_{n-1} of side $\frac{1}{2^n}$ for some $n \in \mathbb{N}$ and consider their subdivisions into the sublevels $Q_{n+1,i}$ as in Proposition 2.3.3. We look for a flow $X^n(Q_{n,h_n}, R_{n-1})[0,1] \times \mathbb{T}^2 \to \mathbb{T}^2$ that moves the subsquares within the time interval $[0,1]$ with the property that $X^n(Q_{n,h_n}, R_{n-1})(1) = V_n$. We define therefore $X^n(Q_{n,h_n}, R_{n-1})(t)$ as

$$X^n(Q_{n,h_n}, R_{n-1})(t) = \begin{cases} X^{S_c}(2^{n+1}; 2^{n+1}-3, 2^{n+1}-1)(7t) & t \in [0, \frac{1}{7}], \\ X^{-}(2^{n+1}, 2^{n+1}-3)(7t-1) \circ X^n(Q_{n,h_n}, R_{n-1})(\frac{1}{7}) & t \in [\frac{1}{7}, \frac{2}{7}], \\ X^{S_c}(2^{n+1}-1; 2^{n+1}-3, 2^{n+1})(7t-2) \circ X^n(Q_{n,h_n}, R_{n-1})(\frac{2}{7}) & t \in [\frac{2}{7}, \frac{3}{7}], \\ X^{S_c}(2^{n+1}-1; 2^{n+1}-3, 2^{n+1})(7t-3) \circ X^n(Q_{n,h_n}, R_{n-1})(\frac{3}{7}) & t \in [\frac{3}{7}, \frac{4}{7}], \\ X^{+}(2^{n+1}, 2^{n+1}-3)(7t-4) \circ X^n(Q_{n,h_n}, R_{n-1})(\frac{4}{7}) & t \in [\frac{4}{7}, \frac{5}{7}], \\ X^{+}(2^{n+1}, 2^{n+1}-3)(7t-5) \circ X^n(Q_{n,h_n}, R_{n-1})(\frac{5}{7}) & t \in [\frac{5}{7}, \frac{6}{7}], \\ X(2^{n+1}, 2^{n+1}-3; 2^{n+1}, 2^{n+1}-2)(7t-6) \circ X^n(Q_{n,h_n}, R_{n-1})(\frac{6}{7}) & t \in [\frac{6}{7}, 1]. \end{cases}$$

Let us call

$$b^n(Q_{n,h_n}, R_{n-1})(t,x) \doteq \dot{X}^n(Q_{n,h_n}, R_{n-1})(t, (X^n)^{-1}(t,x)).$$

Then we have the following

Proposition 2.4.1. *There exist two positive constants $C_1, C_2 > 0$ such that the following estimates hold:*

$$\|\dot{X}^n\|_{L^\infty_t L^\infty_x} \leq \frac{C_1}{2^n}, \tag{2.4.2}$$

$$\|TV(b^n)(\mathbb{T}^2)\|_{L^\infty} \leq \frac{C_2}{2^{2n}}. \tag{2.4.3}$$

Proof. Let us fix $t \in [0,1]$, then by (2.2.23), since the sort operation occurs for a maximum of 4 adjacent subsquares, that is $j - j' = 3$, we have that

$$\|\dot{X}^n\|_{L^\infty_t L^\infty_x} \leq \frac{7 \cdot 24}{2^n} = \frac{C_1}{2^n}.$$

To prove the second estimate we observe that, by (2.2.24), since again the sort operation occurs between at most 4 squares, one has

$$|\text{Tot.Var.}(b^n)(t)(\mathbb{T}^2)| \leq 7 \cdot \frac{240}{2^{2n}} = \frac{C_2}{2^{2n}}, \tag{2.4.4}$$

which concludes the proof. □

Finally we can define the flow $X^U(t)$ as

$$X^U(t) = \begin{cases} X^1(2t-1) \circ X^U(\frac{1}{2}) \quad t \in [\frac{1}{2}, 1], \\ X^2(Q_{2,3}, R_1)(4t-2) \circ X^U(\frac{1}{4}) \quad t \in [\frac{1}{4}, \frac{1}{2}], \\ \dots \\ X^n(Q_{n,4h_n}, R_{n-1})(2^n t - 2^n + 2) \circ X^U(2^{-n}) \quad t \in [2^{-n}, 2^{-n+1}], \\ \dots \quad . \end{cases} \tag{2.4.5}$$

One can observe that the map $X^U : [0,1] \times \mathbb{T}^2 \to \mathbb{T}^2$ is well-defined, $X^U \in C([0,1]; L^1(\mathbb{T}^2))$ and differentiable $\mathcal{L}^1$-a.e. t and for every $t \in [0,1]$ it is an invertible and measure-preserving map from the torus into itself. We also remark that for every $x \in \mathbb{T}^2$ we have that $\lim_{t\to 0} X^U(t,x) = x$, which tells us that X^U is a flow. Therefore, by (1.0.2) one can define the divergence-free vector field $b^U(t,x) \doteq \dot{X}^U(t, (X^U)^{-1}(t,x))$.

Proposition 2.4.2. *The divergence-free vector field b^U lives in the space $L^\infty_t \mathrm{BV}_x$. Moreover, its RLF $X^U(1)$ when evaluated at time $t = 1$ is the map U, that is b^U is a weakly mixing vector field that is not strongly mixing.*

Proof. Let us fix $t \in [2^{-n}, 2^{-n+1}]$. Then

$$b^U(t,x) = 2^n \dot{X}^n(Q_{n,4h_{n-1}+3}, R_{n-1})(2^n t - 2^n + 2, (X^U)^{-1}(t,x)).$$

Therefore

$$\begin{aligned} \|b^U(t)\|_{L^1_x} &= 2^n \int_{\mathbb{T}^2} |\dot{X}^n(Q_{n,4h_{n-1}+3}, R_{n-1})(2^n t - 2^n + 2, (X^U)^{-1}(t,x))| dx \\ &= 2^n \int_{\mathbb{T}^2} |\dot{X}^n(Q_{n,4h_{n-1}+3}, R_{n-1})(2^n t - 2^n + 2, y)| dy \qquad (2.4.6) \\ &\leq 2^n |Q_{n,4h_{n-1}+3} \cup R_{n-1}| \|\dot{X}^n(Q_{n,4h_{n-1}+3}, R_{n-1})\|_{L^\infty_t L^\infty_x} \qquad (2.4.7) \\ &\leq 2^n \cdot 2 \cdot 2^{-n} \frac{C_1}{2^n} \leq 2C_1, \qquad (2.4.8) \end{aligned}$$

where (2.4.6) follows by the fact that $X^U(t)$ is measure-preserving, (2.4.7) by the fact that X^n acts only on $Q_{n,4h_n} \cup R_{n-1}$ and (2.4.8) follows by (2.4.2). To compute the total variation of b^U, we observe that, for every $t \in [0,1]$ one has

$$\dot{X}^U(t, (X^U)^{-1}(t,x)) = 2^n \dot{X}^n(2^n t - 2^n + 2, (X^n)^{-1}(2^n t - 2^n + 2, x)),$$

so that $|\text{Tot.Var.}(b^U(t)(\mathbb{T}^2)| = 2^n |\text{Tot.Var.}(b^n(t)(\mathbb{T}^2)|$. By using (2.4.3), one has that, if $t \in [2^{-n}, 2^{-n+1}]$

$$|\text{Tot.Var.}(b^U(t)(\mathbb{T}^2)| = 2^n |\text{Tot.Var.}(b^n(t)(\mathbb{T}^2)| \leq 2^n \frac{C_2}{2^{2n}},$$

which implies that

$$\|\text{Tot.Var.}(b^U)(\mathbb{T}^2)\|_{L^\infty} \leq C_2.$$

To conclude the proof we have to show that the map $X^U(1) = U$ is the Chacon's map introduced in Section 2.3. More precisely, we have to prove that

$$X^1(1) \circ X^2(Q_{2,3}, R_1)(1) \circ \cdots \circ X^n(Q_{n,4h_{n-1}+3}, R_{n-1})(1) = U_n.$$

This easily follows by Proposition 2.3.3 observing that the map $X^1(1) = U_1$ and $X^n(Q_{n,4h_{n-1}+3}, R_{n-1})(1) = V_n$. □

Chapter 3

Density of Strongly Mixing vector fields

In this chapter we present the approximation result by cyclic permutation vector fields: that is, every vector field can be approximated by a divergence-free vector field whose RLF at time $t = 1$ is a cyclic permutation of subsquares. This is the content of Section 3.1. In subsection 3.1.1 we prove the density of ergodic divergence-free vector field by perturbing any cyclic permutation vector field with the Universal Mixer [27]. Finally In Section 3.1.2 we prove the density of strongly mixing vector fields, combining the previous result on ergodic vector fields with the theory of Markov Shifts.

3.1 Cyclic permutations of squares

We start by recalling some basic facts about permutations. Denote by S_n the set of permutations of the elements $\{1, \dots, n\}$.

Definition 3.1.1. Let $\sigma \in S_n$ be a permutation and $k \leq n \in \mathbb{N}$. We say that σ is a *k-cycle* c (or simply a *cycle*) if there exist k distinct elements $a_1, \dots, a_k \in \{1, \dots, n\}$ such that

$$\sigma(a_i) = a_{i+1}, \quad \sigma(a_k) = a_1, \quad \sigma(x) = x \quad \forall x \neq a_1, \dots, a_k.$$

We identify the permutation with the ordered set $c = (a_1 a_2 \dots a_k)$. The number k is the *length* of the cycle. We say that c is *cyclic* if $k = n$. We call *transpositions* the 2-cycles.

Definition 3.1.2. Let c_1, c_2 be the cycles $c_1 = (a_1 \dots a_t)$ and $c_2 = (b_1 \dots b_s)$. We say that c_1, c_2 are *disjoint* cycles if $a_i \neq b_j$ for every $i = 1, \dots, t$, $j = 1, \dots, s$.

Recall the following result.

Theorem 3.1.3. *Every permutation $\sigma \in S_n$ is the product of disjoint cycles.*

From now on we will address flows X_t of divergence-free vector fields such that $X_{t=1}$ is a permutation of squares of size $\frac{1}{D}$.

Let us fix the size $D \in \mathbb{N}$ of the grid in the unit square K. We enumerate the D^2 subsquares of the grid and we consider S_{D^2} the set of the permutations of $\{\kappa_1, \dots, \kappa_{D^2}\}$. We say that two squares (ore more in general two rectangles) are *adjacent* if they have a common side. We will use also the word *adjacent* for cycles: two disjoint cycles of

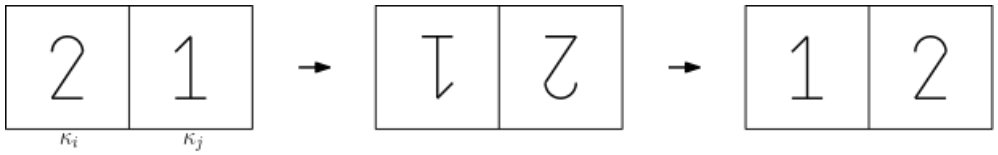

Figure 3.1: The action of the *transposition flow* T_t.

squares c_1, c_2 are adjacent if there exist $\kappa_1 \in c_1$, $\kappa_2 \in c_2$ adjacent subsquares. Two *adjacent* squares can be *connected* by a transposition, which can be defined simply as an exchange between the two squares: let κ_i, κ_j two adjacent squares of size $\frac{1}{D}$ and let $R = \kappa_i \cup \kappa_j$, then the *transposition flow* between κ_i, κ_j is $T_t(\kappa_i, \kappa_j) : [0,1] \times K \to K$ defined as

$$T_t(\kappa_i, \kappa_j) = \begin{cases} \chi^{-1} \circ r_{4t} \circ \chi & x \in \mathring{R},\ t \in \left[0, \frac{1}{2}\right], \\ \chi_i^{-1} \circ r_{4t} \circ \chi_i & x \in \mathring{\kappa}_i,\ t \in \left[\frac{1}{2}, 1\right], \\ \chi_j^{-1} \circ r_{4t} \circ \chi_j & x \in \mathring{\kappa}_j,\ t \in \left[\frac{1}{2}, 1\right], \\ x & \text{otherwise,} \end{cases} \tag{3.1.1}$$

where the map $\chi : R \to K$ is the affine map sending the rectangle R into the unit square K, χ_i, χ_j are the affine maps sending κ_i, κ_j into the unit square K and r is the rotation flow (2.2.5). This invertible measure-preserving flow has the property to exchange the two subsquares in the unit time interval (Figure 3.1). Moreover, by the computations done in Lemma 2.2.13, we can say that

$$\text{Tot.Var.}(\dot{T}_t(\kappa_i, \kappa_j))(\bar{R}) \leq \frac{20}{D^2}. \tag{3.1.2}$$

Lemma 3.1.4. *Let $b \in L_t^\infty(\mathrm{BV}_x)$ be a divergence-free vector field and assume that its flow at time $t = 1$, namely $X_{\llcorner t=1}$, is a k-cycle of squares of the grid $\mathbb{N} \times \mathbb{N}\frac{1}{D}$ where $k, D \in \mathbb{N}$. Then for every $M = 2^p$, there exists $b^c \in L_t^\infty(\mathrm{BV}_x)$ divergence-free vector field such that*

$$||b - b^c||_{L^\infty(L^1)} \leq \mathcal{O}\left(\frac{1}{D^3 M}\right),$$

$$||\text{Tot.Var.}(b^c - b)(K)||_\infty \leq \mathcal{O}\left(\frac{1}{D^2}\right),$$

and the map $X_{t=1}^c : K \to K$ is a kM^2-cycle of squares of size $\frac{1}{DM}$, where $X_t^c : [0,1] \times K \to K$ is the flow associated with b^c.

Here and in the following we will write $T(\kappa_i) = \kappa_j$ meaning that T is a rigid translation of κ_i to κ_j. This to avoid cumbersome notation.

Proof. Let us call $T \doteq X_{t=1}$: being a cycle, there exist $\{\kappa_1, \dots, \kappa_k\} \subset \{1, \dots, D^2\}$ such that

$$T(\kappa_i) = \kappa_{i+1}, \quad T(\kappa_n) = \kappa_1, \quad T(x) = x \quad \text{otherwise.}$$

Now fix some $M = 2^p$ and divide each subsquare κ_i into M^2 subsquares κ_i^j with $j = 1, \dots, M^2$. Since T is a translation of subsquares and choosing cleverly the labelling $j \to \kappa_i^j$, then we have also $T(\kappa_i^j) = \kappa_{i+1}^j$ so that T is a permutation of subsquares κ_i^j. More precisely, it is the product of M^2 disjoint cycles of length k. The idea is to connect these cycles with transpositions in order to have a unique cycle of length kM^2: we will need a parturbation inside κ_1.

Divide the M^2 subsquares of κ_1 into $\frac{M^2}{2}$ couples $R_h^2 = \kappa_1^j \cup \kappa_1^{j'}$ with $h = 1, \dots, \frac{M^2}{2}$ and $\kappa_1^j, \kappa_1^{j'}$ are adjacent squares. In the time interval $\left[0, \frac{1}{2}\right]$ perform $\frac{M^2}{2}$ transpositions, one in each R_h^2, that is

$$X_t^c(x) = X_t \circ T_t^2(x), \quad t \in \left[0, \frac{1}{2}\right],$$

where the flow $T^2 : \left[0, \frac{1}{2}\right] \times K \to K$

$$T_t^2 \llcorner_{R_h^2} \doteq T_{2t}(\kappa_1^j, \kappa_1^{j'}) \quad \text{and} \quad T_t^2(x) = x \text{ otherwise},$$

is the transposition flow (3.1.1) between κ_1^j and $\kappa_1^{j'}$ as defined in (3.1.1) above. Then for $t \in \left[0, \frac{1}{2}\right]$ fixed,

$$\text{Tot.Var.}(b_t^c - b_t)(\kappa_1) \leq \mathcal{O}(1) 2 \frac{M^2}{2} \frac{20}{M^2 D^2},$$

where we have used (3.1.2). We observe that at this time step we have obtained $\frac{M^2}{2}$ disjoint $2k$-cycles.

In the time interval $\left[\frac{1}{2}, \frac{3}{4}\right]$ we divide the unit square into squares $R_h^4 = R_j^2 \cup R_{j'}^2$ with $h = 1, \dots, \frac{M^2}{4}$ where $R_j^2, R_{j'}^2$ are adjacent (in particular there exist $\kappa_1^j \subset R_j^2, \kappa_1^{j'} \subset R_{j'}^2$ adjacent squares). Now we perform $\frac{M^2}{4}$ transpositions of squares connecting the two rectangles $R_j^2, R_{j'}^2$ as in Figure 3.2. More precisely we define for $t \in \left[\frac{1}{2}, \frac{3}{4}\right]$

$$X_t^c(x) = X_t \circ T_t^4(x), \quad t \in \left[\frac{1}{2}, \frac{3}{4}\right],$$

where the flow $T^4 : \left[\frac{1}{2}, \frac{3}{4}\right] \times K \to K$

$$T_t^4 \llcorner_{R_h^4} \doteq T_{4t-2}(\kappa_1^j, \kappa_1^{j'}) \quad \text{and} \quad T_t^4(x) = x \text{ otherwise},$$

is the transposition flow (3.1.1) between κ_1^j and $\kappa_1^{j'}$. Again,

$$\text{Tot.Var.}(b_t^c - b_t)(\kappa_1) \leq \mathcal{O}(1) 4 \frac{M^2}{4} \frac{20}{M^2 D^2}.$$

Repeating the procedure (see Figure 3.2),

1. at the $2i-1$-th step we divide our initial square κ_1 into $\frac{M^2}{2^{2i-1}}$ rectangles (made of two squares of obtained at the step $2(i-1)$) so that we perform 2^{2p-i} transpositions of subsquares κ_1^j in the time interval $\left[\sum_{j=1}^{2i-2} \frac{1}{2^j}, \sum_{j=1}^{2i-1} \frac{1}{2^j}\right]$;

2. at the $2i$-th step, we divide our initial square κ_1 into $\frac{M^2}{2^{2i}}$ squares (made of 2 rectangles of the previous step) so that we perform 2^{2p-i} transpositions of subsquares κ_1^j in the time interval $\left[\sum_{j=1}^{2i-1} \frac{1}{2^j}, \sum_{j=1}^{2i} \frac{1}{2^j}\right]$.

In both cases we find in the interval $\left[\sum_{j=1}^{i-1} \frac{1}{2^j}, \sum_{j=1}^{i} \frac{1}{2^j}\right]$ that

$$\text{Tot.Var.}(b_t^c - b_t)(\kappa_1) \leq \mathcal{O}(1) 2^i \frac{M^2}{2^i} \frac{20}{M^2 D^2}.$$

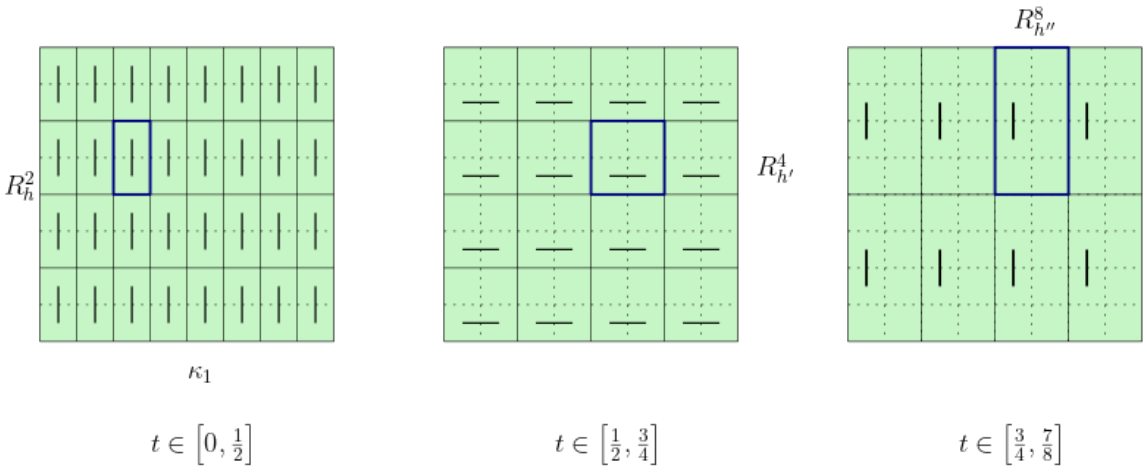

Figure 3.2: Subdivision of the initial square κ_1 into subrectangles/subsquares where transpositions (the bars) occurr between subsquares $\kappa_i^j \subset R_j^{2i}, \kappa_i^{j'} \subset R_{j'}^{2i}$ of side $\frac{1}{DM}$ (dotted lines). Notice that at the first/third step the initial square κ_1 is divided into rectangles (see Point (1) of the procedure), while at the second step it is divided into squares (see Point (2)).

Call $t_i = \sum_{j=1}^{i} 2^{-j}$. We will prove that the map $X(1, t_i) \circ X^c{\llcorner}_{t=t_i}$ is a permutation given by the product of $\frac{M^2}{2^i}$ disjoint $2^i k$-cycles simply by induction on i.

The case $i = 1$ is immediate from the definition. So let us assume that the property is valid for i and call $c_1, c_2, \dots, c_{\frac{M^2}{2^i}}$ the disjoint $2^i k$-cycles made of rectangles of subsquares as in Figure 3.2, where we have ordered them in such a way that c_{2h-1}, c_{2h} with $h = 1, \dots, \frac{M^2}{2^{i+1}}$ are adjacent along the long side. Then fix a couple of adjacent cycles, for simplicity c_1, c_2. Then

$$\begin{aligned} c_1 &= (\kappa_1^1 \quad \dots \quad \kappa_{2^i k}^1), \\ c_2 &= (\kappa_1^2 \quad \dots \quad \kappa_{2^i k}^2), \end{aligned}$$

and assume that there exist j, j' such that $\kappa_j^1, \kappa_{j'}^2$ are the adjacent subsquares in which we perform the transposition. By simply observing that

$$X^c{\llcorner}_{t=t_{i+1}}(x) = X^c{\llcorner}_{t=t_i}(x) + \int_{t_i}^{t_{i+1}} b^c(s, X_s^c(x))ds,$$

we deduce that, when restricted to $c_1 \cup c_2$, the map $X(1, t_{i+1}) \circ X^c{\llcorner}_{t_{i+1}}$ is the following permutation

$$\begin{pmatrix} \kappa_1^1 & \dots & \kappa_{j-1}^1 & \kappa_j^1 & \dots & \kappa_{2^i k}^1 & \kappa_1^2 & \dots & \kappa_{j'-1}^2 & \kappa_{j'}^2 & \dots & \kappa_{2^i k}^2 \\ \kappa_2^1 & \dots & \kappa_{j'}^2 & \kappa_{j+1}^1 & \dots & \kappa_1^1 & \kappa_2^2 & \dots & \kappa_j^1 & \kappa_{j'+1}^2 & \dots & \kappa_1^2 \end{pmatrix}.$$

Clearly this is a single cycle of length $2^{(i+1)k}$, and it is supported on a rectangle.

The procedure stops at $t = \sum_{j=1}^{2p} \frac{1}{2^j}$ when we have obtained a unique $M^2 k$-cycle. Summing up, for t fixed

$$\text{Tot.Var.}(b_t^c - b)(K) \leq \mathcal{O}(1)\frac{20}{D^2},$$

that is

$$||\text{Tot.Var.}(b_t^c - b_t)(K)||_\infty \leq \mathcal{O}\left(\frac{1}{D^2}\right).$$

We conclude with the $L_t^\infty L_x^1$ estimate of the vector field: to do this computation it is necessary to observe that b_t and b_t^c differ only in the couples of adjacent squares in which we perform the transpositions. Using (1.0.3) and simple estimates on the rotation (2.2.4) we obtain, for $t \in [t_{i-1}, t_i]$ fixed,

$$\|b_t^c - b_t\|_1 \leq \mathcal{O}(1)\frac{M^2}{2^i}2^i\frac{2}{DM}\frac{2}{D^2M^2} \leq \mathcal{O}\left(\frac{1}{D^3M}\right),$$

which concludes the proof. □

We state now the approximation result by vector fields whose flow at time $t = 1$ is a unique cycle.

Proposition 3.1.5. *Let $b \in L_t^\infty(\mathrm{BV}_x)$ be a divergence-free vector field and assume that $b_t = 0$ for $t \in [0, \delta]$, $\delta > 0$, and its flow at time $t = 1$, namely $X_{\llcorner t=1}$, is a permutation of squares of the grid $\mathbb{N} \times \mathbb{N}\frac{1}{D}$ where $D \in \mathbb{N}$. Then for every $M = 2^p \gg 1$ there exists a divergence-free vector field $b^c \in L_t^\infty(\mathrm{BV}_x)$ such that*

$$||b - b^c||_{L^1(L^1)} \leq \mathcal{O}\left(\frac{1}{DM^3}\right), \quad ||\text{Tot.Var.}(b_t^c - b_t)(K)||_\infty \leq \mathcal{O}\left(\frac{1}{\delta M^2}\right)$$

and the map $X_1^c : K \to K$, being $X_t^c : [0,1] \times K \to K$ is the flow associated with b^c, is a M^2D^2-cycle of subsquares of size $\frac{1}{DM}$.

Proof of Proposition 3.1.5. Let us fix $\epsilon > 0$ and consider $M = 2^p$ to be chosen later. Let $C \doteq X_{\llcorner t=1}$ be a permutation, which we write by Theorem (3.1.3)

$$C = (\kappa_1^1 \dots \kappa_{k_1}^1)(\kappa_1^2 \dots \kappa_{k_2}^2) \dots (\kappa_1^n \dots \kappa_{k_n}^n) = c_1 \dots c_n,$$

where $\sum_{i=1}^n k_i \leq D^2$. Define $c_{n+1}, \dots c_N$, $N = D^2 - \sum_i k_i + n$, the 1-cycles representing the subsquares that are sent into themselves. By the previous lemma we can also assume that $C_{\llcorner c_i}$ $i = 1, \dots, N$ is a cyclic permutation of subsquares a_{jk}^i, $j = 1, \dots, M^2$, of the grid $\mathbb{N} \times \mathbb{N}\frac{1}{MD}$. To find a D^2M^2 cycle we should consider all the couples of adjacent subsquares (of size $\frac{1}{MD}$), and then we should connect them by transpositions in a precise way.

Fix c_1 and consider

$$C^1 = \{c_h \neq c_1 \text{ s.t. } c_h \text{ adjacent to } c_1\} = \{c_1^1, \dots, c_{|C^1|}^1\}.$$

Now for every $c_j^1 \in C^1$ define by induction the disjoint families of cycles

$$C_j^2 = \{c_h \notin \{c_1\} \cup C^1 \cup C_1^2 \cup \dots \cup C_{j-1}^2 \text{ s.t. } c_h \text{ is adjacent to } c_j^1\},$$

and call

$$C^2 = C_1^2 \cup \dots \cup C_{|C^1|}^2 = \{c_1^2, \dots, c_{|C^2|}^2\}.$$

At the $i-1$-th step we have

$$C^{i-1} = \{c_1^{i-1}, \dots, c_{|C^i|}^{i-1}\}.$$

and, for every $c_j^{i-1} \in C^{i-1}$,

$$C_j^i = \{c_h \notin \{c_1\} \cup C^1 \cup C^2 \cup \cdots \cup C^{i-1} \cup C_1^i \cup \dots C_{j-1}^i \text{ s.t. } c_h \text{ is adjacent to } c_j^{i-1}\}.$$

The procedure ends when we have arranged all c_i into sets C^i, and hence for some $K \in \mathbb{N}$ we obtain $C^{K+1} = \emptyset$ (see Figure 3.3). Indeed, by contradiction assume that $|\{c_1\} \cup C^1 \cup C^2 \cup \cdots \cup C^K| < N$. Then this set has a boundary, i.e., there exists a cycle $c \notin \{c_1\} \cup C^1 \cup C^2 \cup \cdots \cup C^K$ adjacent to a cycle of $\{c_1\} \cup C^1 \cup C^2 \cup \cdots \cup C^K$, which is a contradiction by definition.

The partition

$$C(c_1) = \{c_1\} \cup C^2 \cup \dots C^K$$

has the natural structure of a directed tree: indeed every two cycles $c_i \in C^i$, $c_j \in C^j$ are connected by a unique sequence of cycles: the direction of each edge is given by the construction $c_j^{i-1} \to c_h$ whenever $c_h \in C_j^i$. This tree-structure gives us a selection of the $N-1$ couples of subsquares κ_i^j of disjoint cycles c_i in which we can perform a transposition among the subsquares a_{jk}^i to connect all of them in a unique D^2M^2-cycle. More precisely, for every connected couple c_j^{i-1}, c_h such that $c_h \in C_j^i$, there exist cubes $\kappa \in c_j^{i-1}, \kappa' \in c_h$, and hence there are adjacent subsquares $a \subset \kappa, a' \subset \kappa'$ of size $1/(MD)$: assuming $M \geq 4$, we can take a, a' not being on the corners of κ, κ', respectively.

Let $T_t : [0,\delta] \times K \to K$ be the transposition flow (3.1.1) acting in the selected $N-1$ couples of subsquares a, a' reparametrized on the time interval $[0,\delta]$ and define (being $X_t = \mathrm{id}$ for $t \in [0,\delta]$)

$$X_t^c(x) = \begin{cases} T_t(x) & t \in [0,\delta], \\ X_t \circ T_\delta(x) & t \in [\delta, 1]. \end{cases} \tag{3.1.3}$$

The transposition is well defined: indeed it can happen that c_i, c_j, c_k are adjacent cycles and the couples of adjacent squares (of size $\frac{1}{D}$) are κ_i, κ_j and κ_i, κ_k (where $\kappa_i \in c_i, \kappa_j \in c_j$ and $\kappa_k \in c_k$), that is: κ_i is in common. But since the transposition occurs between subsquares of size $\frac{1}{DM}$ nor belonging to the corners, it is always guaranteed that the transpositions act on disjoint subsquares. By using the explicit formula (2.2.4) we get that for $t \in [0,\delta]$

$$||b_t^c - b_t||_1 \leq \frac{\mathcal{O}(1)}{\delta}\left(\frac{N-1}{D^3M^3}\right) \leq \frac{\mathcal{O}(1)}{\delta}\left(\frac{1}{DM^3}\right),$$

while for $t \in [\delta, 1]$ it clearly holds $b_t^c = b_t$. Coupling these last two estimates we get the $L_t^1 L_x^1$ estimate:

$$||b - b^c||_{L^1(L^1)} \leq \mathcal{O}\left(\frac{1}{DM^3}\right),$$

for $\delta << 1$ and M sufficiently large.

Next we compute the total variation for $t \in [0,\delta]$: by using (3.1.2), we get

$$\text{Tot.Var.}(b_t^c)(K) \leq \frac{N-1}{\delta}\frac{20}{M^2D^2} \leq \frac{1}{\delta}\frac{20}{M^2},$$

while for $t \in [\delta, 1-\delta]$ we find

$$\text{Tot.Var.}(b_t^c)(K) = \text{Tot.Var.}(b_t)(K),$$

therefore

$$||\text{Tot.Var.}(b_t^c - b_t)(K)||_\infty \leq \mathcal{O}\left(\frac{1}{\delta M^2}\right).$$

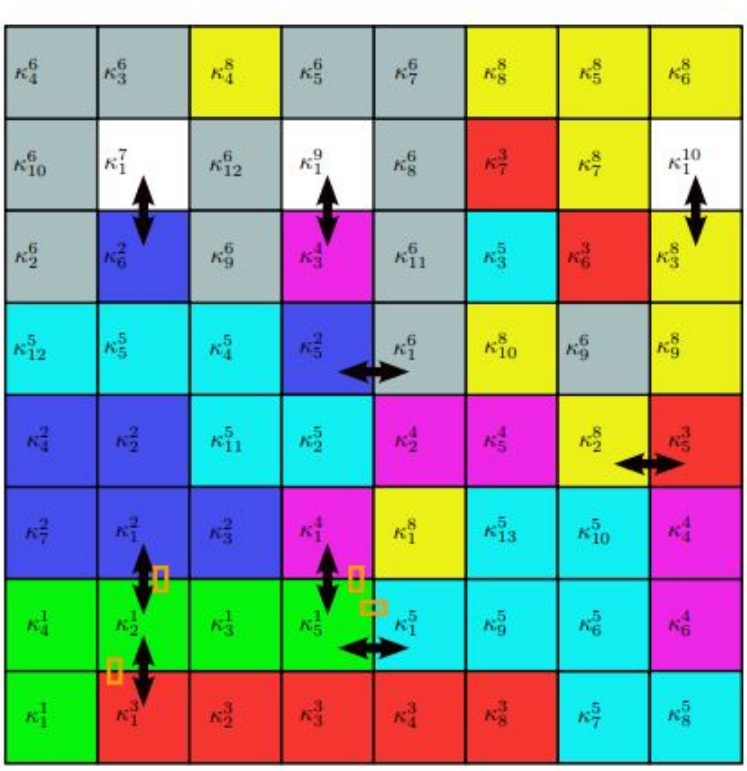

Figure 3.3: Concatenation of cycles in a specific example, Remark 3.1.6. The orange subrectangles are the couples of a^i_{jk} on which the transposition T_t of (3.1.3) acts.

To conclude we have to prove that X_1^c is a unique cycle, which follows by the tree-structure of the selection of adjacent cycles. The end points of the tree are clearly cycles. By recurrence, assume that c_j^{i-1} is connected to cycles γ_h, each one made of all squares belonging to $c_h \in C_j^i$ and all subsequent cycles to c_h. It is fairly easy to see that the transposition merging c_j^{i-1} to each $c_h \in C_j^i$ generates a unique cycles γ_j^i, made of the cubes of c_j^{i-1} and all γ_h. We thus conclude that the map X_1^c is a cycle of size M^2D^2. □

Remark 3.1.6. An example of how the proof works is in Figure 3.3: the decomposition in cycles is

$$C = (\kappa_1^1 \dots \kappa_5^1)(\kappa_1^2 \dots \kappa_7^2)(\kappa_1^3 \dots \kappa_8^3)(\kappa_1^4 \dots \kappa_6^4)(\kappa_1^5 \dots \kappa_{13}^5)(\kappa_1^6 \dots \kappa_{12}^2)(\kappa_1^7)(\kappa_1^8 \dots \kappa_{10}^8)(\kappa_1^9)(\kappa_1^{10}).$$

The black arrow indicates the adjacent subsquares where the exchanges are performed: the tree of concatenation is then

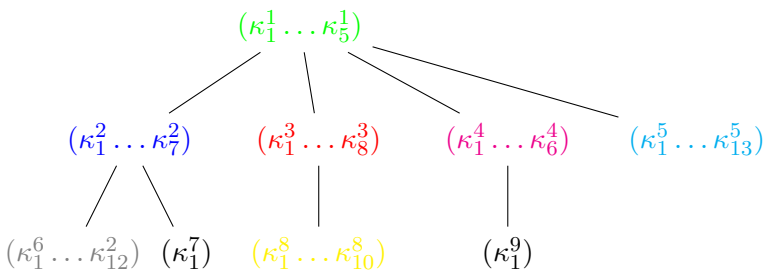

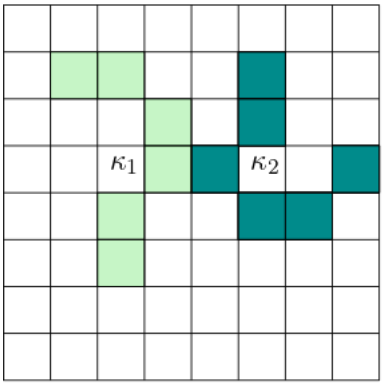

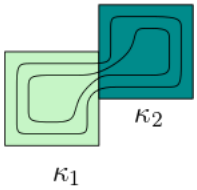

Figure 3.4: The two adjacent cycles c_1 (light green) and c_2 (blue) touch in κ_1 and κ_2, which exchange their mass during the time evolution.

Note that in the subsquares $(\kappa_2^1, \kappa_1^2), (\kappa_2^1, \kappa_1^3)$ and $(\kappa_5^1, \kappa_1^4), (\kappa_5^1, \kappa_1^5)$ the exchange occurs actually in the subsquares $(a_{2j}^1, a_{1\ell}^2), (a_{2j'}^1, a_{1\ell'}^3)$ and $(a_{5k}^1, a_{1\ell''}^4), (a_{5k'}^1, a_{1,\ell'''}^5)$, so that it is always acting on different couples of subsquares.

Remark 3.1.7. The construction of the cyclic flow (3.1.3) gives us only the $L_t^1 L_x^1$ estimate on the vector fields, which is what we need for our genericity result. We can get the more refined estimate in $L_t^\infty L_x^1$ allowing for mass flowing (when performing the transposition) during the time evolution of the flow X_t (see Figure 3.4). In this case, the time spent by the squares of size $(MD)^{-1}$ to transfer the mass is of order $(MD)^{-1}$, so that the vector field moving it should be of the order

$$\frac{\text{length}}{\text{time}} = \mathcal{O}(1), \quad \text{acting on a region of area } \frac{N-1}{(MD)^2} \leq M^{-2}. \tag{3.1.4}$$

Hence the $L_t^\infty L_x^1$ estimate can be obtained by (1.0.3) as

$$\|b_t^c - b_t\|_1 \leq \mathcal{O}(1) M^{-2},$$

while the total variation estimate becomes

$$\text{Tot.Var.}(b_t^c - b_t) = \mathcal{O}(1) \frac{D}{M}.$$

The statement one can prove is then the following.

Proposition 3.1.8. *Let $b \in L_t^\infty(\mathrm{BV}_x)$ be a divergence-free vector field and assume that its flow at time $t = 1$, namely $X_{\llcorner t=1}$, is a permutation of squares of the grid $\mathbb{N} \times \mathbb{N}\frac{1}{D}$ where $D \in \mathbb{N}$. Then for every $\epsilon > 0$ there exist $M = 2^p$ and $b^c \in L_t^\infty(\mathrm{BV}_x)$ a divergence-free vector field such that*

$$||b_t^c - b_t||_{L^1} \leq \mathcal{O}(M^{-2}) \leq \epsilon, \quad \text{Tot.Var.}(b_t^c - b_t)(K) \leq \mathcal{O}(D/M),$$

and the map $X_{t=1}^c : K \to K$, being $X_t^c : [0,1] \times K \to K$ the flow associated with b^c, is a M^2D^2-cycle of subsquares of size $\frac{1}{DM}$.

3.1.1 Density of ergodic vector fields

Starting from the cyclic permutation we have built in the previous section, we construct an ergodic vector field arbitrarily close to a given vector field in $L_t^\infty \mathrm{BV}_x$. The density

of ergodic vector fields is not strictly relevant for the genericity result of weakly mixing vector fields, but it can be considered as a simple case study for the construction of strongly mixing vector fields. Moreover it will give a direct proof of Point (2) of Theorem 0.0.3.

We will use the *universal mixer* that has been constructed in [27]: it is the time periodic divergence-free vector field $u \in L^\infty_t([0,1], BV_x(\mathbb{R}^2))$ whose flow $U_t : [0,1]\times K \to K$ of measure-preserving maps realizes at time $t = 1$ the *folded Baker's map*, that is

$$U = U_{\llcorner t=1} = \begin{cases} \left(-2x+1, -\frac{y}{2}+\frac{1}{2}\right) & x \in \left[0, \frac{1}{2}\right), \\ \left(2x-1, \frac{y}{2}+\frac{1}{2}\right) & x \in \left(\frac{1}{2}, 1\right], \end{cases} \qquad y \in [0,1], \tag{3.1.5}$$

(see Theorem 1, [27]).

Proposition 3.1.9. *Let $b \in L^\infty_t(\mathrm{BV}_x)$ and let X_t be its RLF, and assume that $X_{t=1}$ is a cyclic permutation of squares of the grid $\mathbb{N}\times\mathbb{N}\frac{1}{D}$. Then there exists $b^e \in L^\infty_t(\mathrm{BV}_x)$ divergence-free ergodic vector field such that*

$$\begin{aligned} &||b - b^e||_{L^\infty(L^1)} \leq \mathcal{O}\left(\frac{1}{D^2}\right), \\ &||\mathrm{Tot.Var.}(b^e)(K)||_\infty \leq ||\mathrm{Tot.Var.}(b)(K)||_\infty + \mathcal{O}\left(\frac{1}{D^2}\right). \end{aligned} \tag{3.1.6}$$

Proof. Let us call $T = X_{\llcorner t=1}$ and $\kappa_1, \dots, \kappa_{D^2}$ the subsquares of the grid where the numbering is chosen such that

$$T(\kappa_i) = \kappa_{i+1}, \quad T(\kappa_n) = \kappa_1.$$

Let us define

$$X^e_t = \begin{cases} X_t \circ U^1_t & x \in \kappa_1, \\ X_t & \text{otherwise}, \end{cases}$$

where the flow $U^1_t = \theta^{-1} \circ U_t \circ \theta$ and θ is the affine map from κ_1 to K, i.e. ,$\theta(x,y) = (Dx, Dy)$.

We first prove the ergodicity of $T^e = X^e{}_{\llcorner t=1}$. Assume by contradiction that T^e is not ergodic, then there exists a measurable set B such that $T^e(B) = B$ and $0 < |B| < 1$. We claim that $|B \cap \kappa_1| > 0$. Indeed, since $|B| > 0$ there exists i such that $|B \cap \kappa_i| > 0$. If $i = 1$ we have nothing to prove, if not, since T^e is measure-preserving, then $|T^e(B \cap \kappa_i)| > 0$. But

$$0 < |T^e(B \cap \kappa_i)| = |T^e(B) \cap T^e(\kappa_i)| = |B \cap \kappa_{i+1}|$$

(we have used that the set B is invariant) and re-applying the map T^e sufficiently many times we have the claim. Moreover, $|B \cap \kappa_1| < \frac{1}{D^2}$. If not, that is $|B \cap \kappa_1| = \frac{1}{D^2}$, then $|B \cap \kappa_i| = \frac{1}{D^2}$ for every $i = 1, \dots, D^2$, again by using the fact that B is invariant and that $T^e(\kappa_i) = \kappa_{i+1}$ and $T^e(\kappa_{D^2}) = \kappa_1$. But now

$$|B| = \sum_{i=1}^{D^2} |B \cap \kappa_i| = \sum_{i=1}^{D^2} \frac{1}{D^2} = 1,$$

which is a contradiction, since $|B| < 1$. Now, the fact that $0 < |B \cap \kappa_1| < \frac{1}{D^2}$ implies that $U^1_1(B \cap \kappa_1) \neq B \cap \kappa_1$ because U^1_1 is mixing (and thus ergodic). But this is a

contradiction because $T^e(B \cap \kappa_1) = B \cap \kappa_2$ and applying to both of them T^{D^2-1} we find that

$$U_1^1(B \cap \kappa_1) = T^{D^2-1}(T^e(B \cap \kappa_1)) = T^{D^2-1}(B \cap \kappa_2) = (T^e)^{D^2-1}(B \cap \kappa_2) = B \cap \kappa_1,$$

where we have used that $T^{D^2} = Id$. To prove the estimates (3.1.6) we have to observe first that U_t acts only on κ_1, then that it is the composition of two rotations (see [Figure 1, [27]]), that is Tot.Var.$(\dot{U}_t(U_t^{-1}))(\bar{\kappa}_1) \leq \mathcal{O}\left(\frac{1}{D^2}\right)$ (see again Lemma 2.2.13). □

3.1.2 Density of strongly mixing vector fields

As in the previous section, we use the density of cyclic permutations to show that the vector fields whose flow is strongly mixing are dense in $\mathcal{U}$ with the $L^1_{t,x}$-topology. Again we use the universal mixer constructed in [27]. The main result here is the following

Proposition 3.1.10. *Let $b \in L^\infty_t(\mathrm{BV}_x)$ and let X_t be its RLF, and assume that $b_t = 0$ for $t \in [0, 2\delta]$ and $X_{t=1}$ is a cyclic permutation of squares of the grid $\mathbb{N} \times \mathbb{N}\frac{1}{D}$, $D = 2^p$. Then there exists $b^s \in L^\infty_t(\mathrm{BV}_x)$ divergence-free strongly mixing vector field such that*

$$\begin{aligned} &||b - b^s||_{L^1(L^1)} \leq \mathcal{O}\left(\frac{1}{\delta D}\right), \\ &||\text{Tot.Var.}(b^s)(K)||_\infty \leq ||\text{Tot.Var.}(b)(K)||_\infty + \mathcal{O}\left(\delta^{-1}\right). \end{aligned} \tag{3.1.7}$$

In the proof it is shown that the mixing is actually exponential, in the sense that for every set in a countable family of sets $\{B_i\}_i$ generating the Borel σ-algebra it holds

$$\left|T^q(B_i) \cap B_j\right| - |B_i||B_j| = \mathcal{O}(1)c_{ij}^q, \quad c_{ij} < 1.$$

Proof. Let us call $T = X_{\llcorner t=1}$ and $\kappa_1, \dots, \kappa_{D^2}$ the subsquares of the grid where the numbering is chosen such that

$$T(\kappa_i) = \kappa_{i+1}, \quad T(\kappa_{D^2}) = \kappa_1.$$

If $\{1, \dots, D^2\} \ni \ell \mapsto j(\ell) \in \{1, \dots, D^2\}$ is an enumeration of κ_i such that $\kappa_{j(\ell)}, \kappa_{j(\ell+1)}$ are adjacent, consider the rescaled universal mixer $U_t^{\ell,\ell+1}$ acting on $\kappa_\ell, \kappa_{\ell+1}$ in the time interval $[0, \delta]$, whose generating vector field $b^{U^{\ell,\ell+1}}$ satisfies the estimates

$$\|b_t^{U^{\ell,\ell+1}}\|_{L^1} = \mathcal{O}(1)\frac{1}{\delta}\frac{1}{D^3}, \quad \text{Tot.Var.}(b_t^{U^{\ell,\ell+1}}) = \mathcal{O}(1)\frac{1}{\delta}\frac{1}{D^2}.$$

The idea is to define the a new vector field as in (3.1.3)

$$X_t^s(x) = \begin{cases} M_t(x) & t \in [0, 2\delta], \\ X_t \circ M_{2\delta}(x) & t \in [2\delta, 1], \end{cases}$$

where the map M_t, $t \in [0, 2\delta]$, is defined as follows:

$$M_t(x) = \begin{cases} U_t^{\ell,\ell+1}(x) & t \in [0, \delta], \ell \text{ even}, \\ U_t^{\ell,\ell+1}(x) & t \in [\delta, 2\delta], \ell \text{ odd}. \end{cases}$$

The estimates (3.1.7) follows as in Proposition 3.1.9, so we are left with the proof that $T^s = X_1^s$ is strongly mixing.

The map T^s is the composition of 3 maps $T_3 \circ T_2 \circ T_1$ acting as follows (all indexes should be intended modulus D^2):

1. T_1 is the folded Baker's map U acting on the couples $\ell, \ell+1$, $\ell = 0, 2, \dots$ even;
2. T_2 is the folded Baker's map U acting on the couples $\ell, \ell+1$, $\ell = 1, 3, \dots$ odd;
3. T_3 is a cyclic permutation $\ell \to j^{-1}(j(\ell)+1)$.

We first compute the evolution of a rectangle a of the form

$$a = 2^{-p}[k, k+1] \times 2^{-p'}[k', k'+1]\frac{1}{D}, \quad k = 0, \dots, 2^p D-1,\ k' = 0, \dots, 2^{p'} D-1,\ p, p' \in \mathbb{N}.$$

By definition of U (3.1.5) we obtain that if $p \geq 1$ then the map T_1 does not split a into disjoint rectangles, i.e.

$$T_1 a = 2^{1-p}[\tilde{k}, \tilde{k}+1] \times 2^{-p'-1}[\tilde{k}', \tilde{k}'+1]\frac{1}{D}, \quad \tilde{k} = 0, \dots, 2^{p-1} D-1, \tilde{k}' = 0, \dots, 2^{p'+1} D-1,$$

and the same happens for T_2:

$$T_2 a = 2^{1-p}[\hat{k}, \hat{k}+1] \times 2^{-p'-1}[\hat{k}', \hat{k}'+1]\frac{1}{D}, \quad \hat{k} = 0, \dots, 2^{p-1} D-1, \hat{k}' = 0, \dots, 2^{p'+1} D-1.$$

Hence if

$$a = 2^{-2p}[k, k+1] \times 2^{-2p'}[k', k'+1]\frac{1}{D}, \quad k = 0, \dots, 2^{2p} D-1,\ k' = 0, \dots, 2^{2p'} D-1,\ p, p' \in \mathbb{N}, \tag{3.1.8}$$

then

$$T_2 \circ T_1 a = 2^{2(1-p)}[\check{k}, \check{k}+1] \times 2^{-2(p'+1)}[\check{k}', \check{k}'+1]\frac{1}{D}, \quad \check{k} = 0, \dots, 2^{2(p-1)} D-1, \check{k}' = 0, \dots, 2^{2(p'+1)} D-1,$$

and being the action of T_3 just a permutation, the final form $T^s a = T_3 \circ T_2 \circ T_1 a$ is again a rectangle.
When $p = 0$, instead the rectangle a is mapped into two rectangles belonging to two different subsquares κ, κ'

$$T_1 a = [\tilde{k}_1, \tilde{k}_1 + 1] \times 2^{-p'-1}[\tilde{k}'_1, \tilde{k}'_1 + 1]\frac{1}{D} \cup [\tilde{k}_2, \tilde{k}_2 + 1] \times 2^{-p'-1}[\tilde{k}'_2, \tilde{k}'_2 + 1]\frac{1}{D},$$

and the action of T_2 divides $T_1 a$ into 4 rectangles of horizontal length $1/D$ belonging to 4 different subsquares. As before, T_3 just shuffles them into new locations.
The same happens when considering $(T^s)^{-1}$: if $p' \leq 1$ and a is given by (3.1.8) then $(T^s)^{-1} a$ is still a rectangle of side $2^{-2(p+1)} \times 2^{-2(p'-1)}\frac{1}{D}$, while for $p' = 0$ it is split into 4 rectangles with vertical size equal to $1/D$.

In particular, starting from two squares a, a' of side $(2^{-2p} D)^{-2}$, for $q \geq p$ the set $(T^s)^q a$ is made of disjoint rectangles whose horizontal side is D^{-1}, and $(T^s)^{-q} a'$ is made of disjoint rectangles whose vertical side is D^{-1}. Hence if the masses of $(T^s)^q a$, $(T^s)^{-q'} a'$ inside κ_i are $m_i(q)$, $m'_i(-q')$, then by Fubini

$$\mathcal{L}^2\big((T^s)^q a \cap (T^s)^{-q'} a'\big) = \sum_{i=1}^{D^2} D^2 m_i(q) m'_i(-q').$$

In order to prove the strong mixing it is enough to show that

$$m_i(q) \to \frac{\mathcal{L}^2(a)}{D^2},\ m'_i(-q') \to \frac{\mathcal{L}^2(a')}{D^2} \quad q, q' \to \infty.$$

Actually, we will show that the above convergence is exponential, which implies that the mixing is exponential. We prove the above exponential convergence for $m_i(q)$, the other being completely similar.

Once $(T^s)^q a$ has become a rectangle of horizontal side $1/D$, the distribution of mass by T^s is computed by the action of the following matrices on the vector $(m_i)_i$:

1. the matrix A_1 corresponding to the map T_1,

$$(A_1)_{\ell'\ell} = \frac{1}{2}\begin{cases}\delta_{\ell'\ell} + \delta_{\ell'(\ell-1)} & \ell' = 0, 2, \dots, \\ \delta_{\ell'(\ell+1)} + \delta_{\ell'\ell} & \ell' = 1, 3, \dots;\end{cases}$$

2. the matrix A_2 corresponding to the map T_2,

$$(A_2)_{\ell'\ell} = \frac{1}{2}\begin{cases}\delta_{\ell'\ell} + \delta_{\ell'(\ell+1)} & \ell' = 0, 2, \dots, \\ \delta_{\ell'(\ell-1)} + \delta_{\ell'\ell} & \ell' = 1, 3, \dots;\end{cases}$$

3. the permutation matrix A_3 corresponding to T_3.

Being the Markov process generated by the matrix $P = A_3A_2A_1$ finite dimensional, exponential mixing is equal to strong mixing, and we prove directly that P has a simple eigenvalue of modulus 1 whose eigenvector is necessarily the uniform distribution $(1/D^2, 1/D^2, \dots)$: in particular this gives that P is aperiodic (Definition 1.1.14 and Proposition 1.1.16). Indeed, for $v \in \mathbb{C}^D$ one considers the functional $|v|$, and by simple computations it holds $|A_3v| = |v|$ and

$$|A_1v| = |v| \quad \text{iff} \quad v_\ell = v_{\ell+1} \text{ for } \ell = 0, 2, \dots,$$

$$|A_2v| = |v| \quad \text{iff} \quad v_\ell = v_{\ell+1} \text{ for } \ell = 1, 3, \dots.$$

Hence the unique v such that $|Av| = |v|$ is $v = (1/D^2, 1/D^2, \dots)$, and 1 is a simple eigenvector. □

Remark 3.1.11. As in Remark 3.1.7, one could let the Bakers map to act during the time evolution of X_t, but in this case the distance in $L^\infty L^1$ would be of order 1. The problem is that the maps T_1, T_2 are acting on the whole set $K = [0, 1]^2$, and the vector field $b^s_t - b_t$ is of order 1 as in (3.1.4).

3.1.3 Proof of the density of strongly mixing vector fields

We are now ready to prove the density of strongly mixing vector fields in $\mathcal{U}$, which implies the statement by Corollary 1.1.11. It will be obtained through the following steps.

1. Let $b \in \mathcal{U}$: by the very construction of the set $\mathcal{U}$ (Proposition 1.0.3), we can assume that $b \in L^\infty_t \mathrm{BV}_x$. Fix $\epsilon > 0$.

2. By the continuity of translation in L^1, we can take $0 < \delta \ll 1$ such that defining

$$b^\delta = \begin{cases} 0 & t \in [0, 3\delta), \\ \frac{1}{1-3\delta} b_{(t-3\delta)/(1-3\delta)} & t \in [3\delta, 1], \end{cases}$$

it holds

$$\|b^\delta - b\|_{L^1_{t,x}} < \frac{\epsilon}{4}.$$

Since

$$\|\text{Tot.Var.}(b^\delta)\|_\infty = \frac{1}{1-3\delta}\|\text{Tot.Var.}(b)\|_\infty$$

then $b^\delta \in \mathcal{U}$. Clearly we can also assume that b^δ is compactly supported in K.

3. Use Theorem 4.4.1 to approximate b^δ in $[3\delta, 1]$ with a vector field $b^{\epsilon\delta} \in L^\infty_t \operatorname{BV}_x \subset \mathcal{U}$ such that
$$\|b^\delta - b^{\epsilon\delta}\|_{L^1_{t,x}} < \frac{\epsilon}{4},$$
and such that its RLF is a permutation of squares of size D^{-1}. We can assume that
$$D \gg \frac{1}{\epsilon\delta}. \tag{3.1.9}$$

4. Apply Lemma 3.1.4 together with Proposition 3.1.5 to $b^{\epsilon\delta}$ for $t \in [2\delta, 1]$ obtaining a new vector field $b^{\epsilon\delta c} \in L^\infty_t \operatorname{BV}_x \subset \mathcal{U}$ such that
$$\|b^{\epsilon\delta} - b^{\epsilon\delta c}\|_{L^1_{t,x}} \leq \mathcal{O}\left(\frac{1}{DM}\right) < \frac{\epsilon}{4}$$
for $M = 2^{p'} \gg 1$, and such that its RLF is a single cycle of squares of size $(DM)^{-1}$.

5. Finally, apply Proposition 3.1.10 to $b^{\epsilon\delta c}$ in $t \in [0, 1]$ obtaining a strongly (exponentially) mixing vector field $b^{\epsilon\delta cs} \in L^\infty_t \operatorname{BV}_x \subset \mathcal{U}$ such that
$$\|b^{\epsilon\delta c} - b^{\epsilon\delta cs}\|_{L^1_{t,x}} \leq \mathcal{O}\left(\frac{1}{\delta D}\right) < \frac{\epsilon}{4}$$
by using (3.1.9).

We thus conclude that for every $b \in L^\infty_t \operatorname{BV}_x$ and $\epsilon > 0$ there is a vector field $b^s \in L^\infty_t \operatorname{BV}_x$ exponentially mixing such that
$$\|b - b^s\|_{L^1_{t,x}} < \epsilon,$$
which is our aim.

Chapter 4

Permutation Flow

In this Chapter we prove the key tool of this paper, namely the approximation in $L^1_{t,x}$ of any BV vector field with another BV vector field such that its flow at $t = 1$ is a permutation of subsquares, i.e., it is a rigid translation of subsquares of a grid partition of $K = [0, 1]^2$. The approach is inspired by [43], with the additional difficulty that we need to control the BV norm of the approximating vector field. We will address also the d-dimensional case, explaining the additional technicalities needed to prove the same approximation result in the general case. In Section 4.1 we prove the Shnirelman Lemma and we correct a mistake in [43]. In Subsection 4.1.1 we analyze the construction in any dimension. In Sections **??** we prove some BV estimates useful for the main theorem, whose proof is given in Section 4.4.

This chapter is divided into two parts: in the first one we collect some preliminary estimates which will be used as building blocks in the proof of the main theorem, while in the second part we state the main approximation theorem and give its proof.

4.1 Affine approximations of smooth flows

The next lemma is almost the same of [43, Lemma 4.3]. In order to follow the original Shnirelman's Lemma we require the subrectangles in the next lemma to be dyadic (i.e., their corners belong to a dyadic partition, see Remark 4.1.3 however), but we notice that the proof of the main theorem works in the same way just asking subrectangles with rational coordinates to be mapped affinely onto subrectangles with rational coordinates. At the end this section we will address the same lemma in the general case $d > 2$, which in the original paper is not proved.
Let T be a measure-preserving diffeomorphism $T : [0, 1]^2 \to [0, 1]^2$ of class C^3 and such that $T = \mathrm{id}$ in a neighborhood of $\partial[0, 1]^2$. Assume that it is close to the identity, i.e., there exists $\delta > 0$ sufficiently small such that $||T - \mathrm{id}||_{\mathcal{C}^1} \leq \delta$.

Lemma 4.1.1. *There exists $N \in \mathbb{N}$, $N = 2^p$, and a path of measure-preserving invertible maps $t \to \sigma_t$ piecewise smooth w.r.t. the time variable t such that $\sigma_0 = T$ and σ_1 maps arbitrarily small dyadic rectangles $P_{ij} \in \mathbb{N} \times \mathbb{N}\frac{1}{N} = K_N$ (meaning that their boundaries are in the net K_N) affinely onto dyadic rectangles $\tilde{P}_{ij} \in K_N$.*
Moreover, the map σ is of the form

$$\sigma_t = T \circ \xi_{3t} \mathbb{1}_{[0,1/3]}(t) + \zeta_{3t-1} \circ T \circ \xi_1 \mathbb{1}_{[1/3,2/3]}(t) + \eta_{3t-2} \circ \zeta_1 \circ T \circ \xi_1 \mathbb{1}_{[2/3,1]}(t). \quad (4.1.1)$$

where $\xi, \eta : [0,1] \times [0,1]^2 \to [0,1]^2$ are piecewise smooth and $\zeta : [0,1] \times [0,1]^2 \to [0,1]^2$ is smooth, so that for every $t \in [0,1]$, the map σ_t is piecewise smooth on each subrectangle κ and it extends continuously on $\bar{\kappa}$.
Finally, the space differential $D\sigma_1$ of $\sigma_{t=1}$ is a constant diagonal matrix in each subrectangle.

The number N is used in the next results in order to have that the perturbation is arbitrarily small in $L^1_{t,x}$.

Proof. The proof is given in 3 steps:

1. first by an arbitrarily small perturbation of the final configuration we make sure the area of the regions which will be mapped into rectangles is dyadic;
2. secondly we perturb along horizontal slabs in order to have that vertical sections of the slabs are mapped into vertical segments;
3. finally we perturb vertical slabs so that the image of particular rectangles are rectangles and vertical segments remains vertical segments.

The composition of all 3 maps with T as in (4.1.1) will be the movement σ_t. We will use the notation

$$[0,1]^2 \ni (x_1, x_2) \mapsto T(x_1, x_2) = (z_1, z_2) \in [0,1]^2$$

to avoid confusion between the final coordinates and the initial ones. When piecing together maps which are defined in closed sets with piecewise regular boundaries, we will neglect the negligible superposition of boundaries for simplicity: this slight inaccuracy should not generate confusion.
Step 0: initial grid and perturbation. For $N_0 = 2^{p_0} \gg 1$ define the horizontal and vertical slabs

$$H_j = [0,1] \times 2^{-p_0}[j-1, j], \quad V_i = 2^{-p_0}[i-1, i] \times [0,1], \quad i, j = 1, \dots, 2^{p_0}.$$

The image of the horizontal lines

$$x_1 \mapsto T(x_1, x_2)$$

can be written as graphs of functions

$$z_1 \mapsto g(z_1, x_2),$$

and divides every vertical slab V_i into $N_0 = 2^{p_0}$ parts

$$\tilde{\omega}_{ij} = \Big\{(i-1)2^{-p_0} \le z_1 \le i2^{-p_0}, g(z_1, (j-1)2^{-p_0}) \le z_2 \le g(z_1, j2^{-p_0})\Big\}.$$

Let $\zeta_t : [0,1]^2 \to [0,1]^2$ be a measure preserving flow, moving mass across the boundary of $\tilde{\omega}_{ij}$: we can assume w.l.o.g that the mass flow $\phi_{ij,i'j'}$ across the boundary from $\tilde{\omega}_{ij}$ to $\tilde{\omega}_{i'j'}$ occurs in the relative interior of $\partial\tilde{\omega}_{ij} \cap \partial\tilde{\omega}_{i'j'}$. The measure preserving condition requires that

$$\phi_{ij,(i-1)j} + \phi_{ij,(i+1)j} + \phi_{ij,i(j+1)} + \phi_{ij,i(j-1)} = 0.$$

Set $T' = \zeta_1 \circ T$ and consider the new curves

$$z_1 \mapsto g'(z_1, x_2), \quad \text{Graph}\, g' = T'([0,1] \times \{x_2\}).$$

Let $\tilde\omega'_{ij}$ be the new regions

$$\tilde\omega'_{ij}=\Big\{(i-1)2^{-p_0}\le z_1\le i2^{-p_0}, g'(z_1,(j-1)2^{-p_0})\le z_2\le g'(z_1,j2^{-p_0})\Big\},$$

whose new area is

$$\mathcal{L}^2(\tilde\omega'_{ij})=\phi_{ij,i(j-1)}+\phi_{ij,i(j+1)}.$$

Starting with $\tilde\omega'_{11}$, we move a mass $\phi_{11,12}<2^{-p_0-p_1}\ll 1$ so that

$$\mathcal{L}^2(\tilde\omega'_{11})=2^{-p_0-p_1}n_{11}\in 2^{-p_0-p_1}\mathbb{N}.$$

Hence a mass $-\phi_{11,21}$ is flowing to the region $\tilde\omega_{21}$. Assuming that we have

$$\mathcal{L}^2(\tilde\omega'_{i1})=2^{-p_0-p_1}n_{i1}\in 2^{-p_0-p_1}\mathbb{N},$$

and that the mass flowing by $\phi_{i1,i2},\phi_{i1,(i+1)1}$ is $<2^{-p_1}$, we consider two cases:

1. if $\phi_{i1,(i+1)1}\in 2^{-p_0-p_1}[0,1)$, then we flow a mass $\phi_{(i+1)1,(i+1)2}\in 2^{-p_0-p_1}[0,1)$ so that
$$\mathcal{L}^2(\tilde\omega'_{(i+1)1})=2^{-p_0-p_1}n_{(i+1)1}\in 2^{-p_1}\mathbb{N},$$
and the flow to the right is then
$$\phi_{(i+1)1,(i+2)i}=\phi_{i1,(i+1)i}-\phi_{(i+1)1,(i+1)2}\in(-1,1)2^{-p_0-p_1},$$
by the balance and because they have different sign;
2. if $\phi_{i1,(i+1)1}\in 2^{-p_0-p_1}(-1,0)$, then we flow a mass $\phi_{(i+1)1,(i+1)2}\in 2^{-p_0-p_1}(-1,0)$ and obtain the same estimate.

The last term $\tilde\omega'_{N_01}$ is computed by conservation: indeed

$$\sum_i\phi_{i1,i2}=0,$$

and then

$$\mathcal{L}^2(T'([0,1]\times[0,2^{-p_0}])=2^{-p_0}=\sum\mathcal{L}^2(\tilde\omega'_{i1})=2^{-p_0-p_1}\sum_{i=0}^{2^{p_0}-1}n_{i1}+\mathcal{L}^2(\tilde\omega'_{N_01}),$$

so that

$$\mathcal{L}^2(\tilde\omega'_{N_01})=2^{-p_0-p_1}\left(2^{p_1}-\sum_{i=0}^{2^{p_0}-1}n_{i1}\right)\in 2^{-p_0-p_1}\mathbb{N}.$$

The estimate of ϕ_{N_01,N_02} is automatic from the flow $\phi_{(N_0-1)1,N_01}$.

The above procedure is then repeated for each region

$$T([0,1]\times 2^{-p_0}[j-1,j])=\bigcup_{i=1}^{N_0}\tilde\omega_{ij},$$

and the flow across each boundary is $\le 2^{-p_0-p_1}$: the conservation of the measure of $T([0,1]\times[0,j]2^{-p_0})$ yields that the last element $\tilde\omega_{N_0j}$ is again dyadic.

From now on we work with the map $T'=\zeta_1\circ T$.

Step 1: perturbation along horizontal slabs. Consider the curves

$$z_2\mapsto(T')^{-1}(z_1,z_2),$$

which can be parameterized as

$$x_2 \mapsto f'(z_1, x_2)$$

being T' close to the identity in C^1. In each H_j we can determine uniquely the value

$$x_{1,j}(z_1) = \fint_{(j-1)2^{-p_0}}^{j2^{-p_0}} f'(z_1, x_2)dx_2, \tag{4.1.2}$$

and since T' is close to identity, again every map $z_1 \mapsto x_{1,j}(z_1)$ is invertible: denote its inverse by $z_{1,j}(x_1)$.

In particular, we consider the values

$$x_{1,ij} = x_{1,j}(i2^{-p_0}). \tag{4.1.3}$$

By (4.1.2) it follows that

$$\big(x_{1,ij} - x_{1,(i-1)j}\big)2^{-p_0} = \mathcal{L}^2\big((T')^{-1}(\tilde{\omega}'_{ij})\big) \in 2^{-p_0-p_1}\mathbb{N}, \tag{4.1.4}$$

so that we deduce that the elements $x_{1,ij}$ are dyadic, i.e., $x_{1,ij} \in 2^{-p_1}\mathbb{N}$ (being $x_{1,0j} = 0$).

Consider the family of ordered curves parametrized by $x_1 \in [0,1]$

$$[0,1] \times [j-1, j]2^{-p_0} \ni t, x_2 \mapsto f'_{j,t}(x_1, x_2) = (1-t)x_1 + tf'(z_{1,j}(x_1), x_2),$$

and let $\xi_{j,t} : [0,1]\times[j-1,j]2^{-p_0} \to [0,1]\times[j-1,j]2^{-p_0}$ be the unique measure preserving map mapping each segment $\{x_1\} \times [j-1, j]2^{-p_0}$ into the image of $(f'_{j,t}(x_1, x_2), x_2)$, $x_2 \in [j-1, j]2^{-p_0}$. This map is uniquely defined by the balance of mass, which reads as

$$\int_{(j-1)2^{-p_0}}^{(\xi_{j,t})_2(x_1,x_2)} \partial_{x_1} f'_{j,t}(x_1, w)dw = x_2 - (j-1)2^{-p_0}. \tag{4.1.5}$$

Being $f'_{j,t}$ close to the identity, $\xi_{j,t}$ is smooth and close to the identity.

Let $\xi_t : [0,1]^2 \to [0,1]^2$ be the measure preserving map obtained by piecing together the maps $\xi_{j,t}$. By construction the map $T'' = T' \circ \xi_1$ maps each vertical segment $\{x_1\} \times [j-1, j]2^{-p_0}$ into the vertical segment

$$\{z_{1,j}(x_1)\} \times \big[g'(z_{1,j}(x_1), (j-1)2^{-p_0}), g'(z_{1,j}(x_1), j2^{-p_0})\big].$$

Step 2: construction of the affine maps. The next step is to rectify the pieces of curves

$$[i-1, i]2^{-p_0} \ni z_1 \mapsto g_j(z_1) = g'(z_1, j2^{-p_0}), \tag{4.1.6}$$

which are the horizontal slab of the sets $\tilde{\omega}'_{ij}$. Fixing a vertical slide v_i, one considers the unique measure preserving map $\eta_{i,t} : [i-1, i] \times [0,1] \to [i, i-1] \times [0,1]$ such that the segments (4.1.6) are mapped into vertical segments and such that maps the curve $g_j([i-1, i]2^{-p_0})$ into the curve

$$\begin{aligned} g'_{t,ij}(z_1) &= (1-t)g'(z_1, j2^{-p_0}) + t\fint_{(i-1)2^{-p_0}}^{i2^{-p_0}} g'(w, j2^{-p_0})dw \\ &= (1-t)g'(z_1, j2^{-p_0}) + tz_{2,ij}. \end{aligned} \tag{4.1.7}$$

In each $\tilde{\omega}'_{ij}$ this map is uniquely determined by the balance

$$\int_{(i-1)2^{-p_0}}^{(\eta_{i,t})_2(z_1,z_2)} \big(g'_{t,ij}(w) - g'_{t,i(j-1)}(w)\big)dw = \text{constant},$$

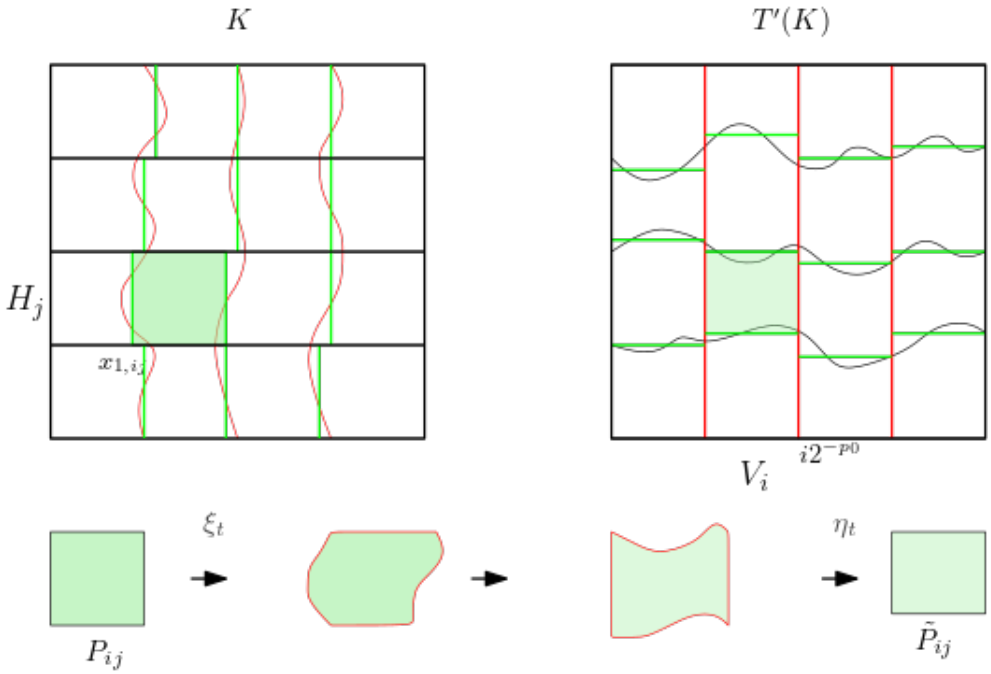

Figure 4.1: The action of σ_t in Lemma 4.1.1: first the map ξ_t moves the mass in H_j in order to map the vertical green segments into the counterimages of the vertical red segments; then the map T acts and the horizontal black boundaries of H_j becomes the black curves, but vertical segments remain vertical; finally the action of η_t rectifies the horizontal boundaries, while keeping vertical segments vertical.

while the vertical coordinate is affine in each vertical segment.

Let $\eta_t : [0,1]^2 \to [0,1]^2$ be the measure preserving map obtained by piecing together the maps $\eta_{i,t}$.

Conclusion. Up to a time scaling, the map we are looking for is

$$\sigma_t = T \circ \xi_t \mathbf{I}_{[0,1]}(t) + \zeta_{t-1} \circ T \circ \xi_1 \mathbf{I}_{[1,2]}(t) + \eta_{t-2} \circ \zeta_1 \circ T \circ \xi_1 \mathbf{I}_{[2,3]}(t).$$

It is clearly measure preserving and at $t = 3$ it maps affinely the rectangles with dyadic coordinates

$$P_{ij} = \left[x_{1,(i-1)j}, x_{1,ij}\right] \times [j-1, j]2^{-p_0}$$

into the rectangles with dyadic coordinates

$$\tilde{P}_{ij} = [i-1, i]2^{-p_0} \times \left[z_{2,i(j-1)}, z_{2,ij}\right].$$

The values $x_{1,ij}$, $z_{2,ij}$ are given by (4.1.3), (4.1.7) and belong to $2^{-p_1}\mathbb{N}$. Thus $N_1 = N$ is the number of the statement.

The fact that σ_t is piecewise smooth and it extends continuously to the boundary of each P_{ij} are immediate from the construction, and its smallness follows by observing that as p_0, p_1 diverge the maps ξ, ζ, η converge to the identity. □

Being the rectangles dyadic in the grid $\mathbb{N} \times \mathbb{N}\frac{1}{N}$, then we have the following

Corollary 4.1.2. *Every subsquare of the grid $\mathbb{N} \times \mathbb{N}\frac{1}{N}$ is sent by σ_1 affinely by a diagonal matrix onto a subrectangle with rational coordinates.*

Remark 4.1.3. The previous lemma also tells us that the map σ_1 is piecewise affine, in particular there exists $N = 2^{p_1} \in \mathbb{N}$ refinement of the grid such that σ_1 maps each κ subsquare of the grid $\mathbb{N} \times \mathbb{N}\frac{1}{N}$ affinely by a diagonal matrix onto a subrectangle q with rational coordinates. It's false, in general, that q has dyadic rational coordinates as stated in [43, Lemma 4.3]. More precisely, the previous lemma states that each

$$P_{ij} = [x_{1,(i-1)j}, x_{1,ij}] \times [j-1, j]2^{-p_0}$$

is sent into

$$\tilde{P}_{ij} = [i-1, i]2^{-p_0} \times [z_{2,i(j-1)}, z_{2,ij}],$$

where $x_{1,(i-1)j}, x_{1,ij}, z_{2,i(j-1)}, z_{2,ij}$ are dyadic. Call $\Delta x = x_{1,ij} - x_{1,(i-1)j}$ and $\Delta z = z_{2,ij} - z_{2,i(j-1)}$. Then by (4.1.4) $\Delta x = 2^{-p_1} n_{ij}$ with $n_{ij} \in \mathbb{N}$. Up to translation the perturbed map σ_1 (4.1.1) can be written as

$$\sigma_{1 \llcorner P_{ij}} = \begin{pmatrix} \frac{2^{-p_0}}{\Delta x} & 0 \\ 0 & 2^{p_0}(\Delta z) \end{pmatrix}.$$

Take a subsquare $\kappa = [h-1, h]2^{-p_1} \times [k-1, k]2^{-p_1} \subset P_{ij}$, then $q = \sigma_{1 \llcorner P_{ij}}(\kappa) = \left[\frac{2^{-p_0}}{n_{ij}}, 2^{p_0 - p_1}(\Delta z)\right]$, which is dyadic only with further requirements on n_{ij}. For a more detailed analysis consider H_j and call $\Delta x_i = x_{1,ij} - x_{1,(i-1)j} = 2^{-p_1} n_{ij}$, where $i = 1, \dots 2^{p_0}$. If we assume that every subsquare of the grid $\mathbb{N} \times \mathbb{N}\frac{1}{N}$ is sent into a dyadic rectangle then we find the conditions

$$n_{ij} = 2^{m_{ij}}, \quad \forall i, j.$$

This condition tells us that, being measure-preserving,

$$\sigma_{1 \llcorner P_{ij}} = \begin{pmatrix} 2^{-p_0 + p_1 - m_{ij}} & 0 \\ 0 & 2^{p_0 - p_1 + m_{ij}} \end{pmatrix},$$

that is, all possible matrices are of the form

$$\begin{pmatrix} 1 & 0 \\ 0 & 1 \end{pmatrix} \quad \begin{pmatrix} \frac{1}{2} & 0 \\ 0 & 2 \end{pmatrix} \quad \begin{pmatrix} 2 & 0 \\ 0 & \frac{1}{2} \end{pmatrix} \quad \begin{pmatrix} \frac{1}{4} & 0 \\ 0 & 4 \end{pmatrix} \quad \dots \quad .$$

This condition is not compatible with the fact that σ_1 is an approximation of the original map T, which has been chosen to be close to the identity.

Remark 4.1.4. From the previous lemma it easily follows that, if N is the size of the grid, then every rectangle contained in the unit square K is sent by the perturbed flow into a union of rectangles.

Remark 4.1.5. To use Theorem 1.0.4 we observe that in our case the change of variables ϕ is given by the flow X_t. In particular, since X_t is close to the identity with all its derivatives, the costant C_{X_t} given by the previous theorem, is $C_{X_t} \leq (1+\delta)^{d-1}$ ($d = 2$ here).

4.1.1 The d-dimensional case

The analysis of the general case can be done as follows.

The starting point is the following approximation assumption in $d-1$-dimension.

Assumption 4.1.6. If the $\mathcal{L}^{d-1}$-measure-preserving diffeomorphism $T : [0,1]^{d-1} \to [0,1]^{d-1}$ is sufficiently close to the identity and equal to id in a neighborhood of $\partial[0,1]^{d-1}$, then there exists $N \in \mathbb{N}$, $N = 2^p$, and a measure-preserving piecewise smooth invertible map σ close to T such that $T \circ \sigma$ maps dyadic rectangles $P_{ij} \in \frac{\mathbb{N}^{d-1}}{N}$ onto dyadic rectangles $\tilde{P}_{ij} \in \frac{\mathbb{N}^{d-1}}{N}$ by a diagonal linear map (up to a translation).

The above assumption is true for $d = 3$: indeed if σ_t is the map of Lemma 4.1.1 and T is any $\mathcal{L}^2$-measure-preserving diffeomorphism $T : [0,1]^2 \to [0,1]^2$, as in the previous assumption, then $\sigma = T^{-1} \circ \sigma_{t=1}$ does the job.

Now let $T : [0,1]^d \to [0,1]^d$ be a diffeomorphism sufficiently close to the identity and equal to the identity near $\partial[0,1]^d$ (Figure 4.2). We will not address the perturbation ζ used to obtain dyadic parallelepipeds (Step 0 of the proof above), being the idea completely similar to the $2d$-case. We will also neglect the time dependence (i.e., how to split $t \in [0,1]$ into time intervals where the different maps are acting), because it is a fairly easy extension of the $2d$ case.

Step 1. Consider the curves

$$z_d \mapsto T^{-1}(z_1, \dots, z_d).$$

The first step is to perturb T to a map T' in order to have that the above curves are segments along the x_d-direction in each slab $x_d \in [k_d, k_d + 1]/N$ (Figure 4.3).
Being T close to the identity, the surface $T^{-1}(\{z_{d-1} = \text{const.}\})$ is parameterized by $x_1, \dots, x_{d-2}, x_d$, and then in each strip

$$(x_1, \dots, x_{d-2}) = \text{const.}, \quad x_{d-1} \in [0,1],\ x_d \in [k_d, k_d + 1]\frac{1}{N}$$

one can use the same measure preserving map ξ_1 defined in Step 1 of the proof of Lemma 4.1.1 above to obtain a perturbation $\hat{T} = T \circ \xi$ such that

$$\hat{T}^{-1}(\{z_{d-1} = \text{const.}\}) \cap \big\{x_d \in [k_d, k_d + 1]/N\big\}$$

is independent of x_d, in the sense that it is the graph of a function depending only on $x_1, \dots, x_{d-2}$ times the segment $x_d \in [k_d, k_d + 1]/N$.
Disintegrate the Lebesgue measure $\mathcal{L}^d$ as

$$\mathcal{L}^d \llcorner_{\{x_d \in [k_d, k_d+1]/N\}} = \int \Big[a(x_1, \dots, x_{d-2}, z_{d-1}) dx_1 dx_{d-2} dx_d\Big] dz_{d-1},$$

according to the partition $\hat{T}^{-1}(z_{d-1} = \text{const})$ (the density a does not depend on x_d because the surfaces contains the segments along x_d), and consider the 2-dimensional surfaces

$$\hat{T}^{-1}(z_{d-1} = \text{const}) \cap \{x_1, \dots, x_{d-3} = \text{const}\}.$$

We use the same map ξ_1 of Step 1 of the proof above to rectify the curves

$$z_d \mapsto f(x_1, \dots, x_{d-3}, z_{d-2}, z_{d-1}; z_d) = (\hat{T})^{-1}(z_{d-2}, z_{d-1} = \text{const}) \\ \cap \{x_1, \dots, x_{d-3} = \text{const}\} \cap \{x_d \in [k_d, k_d + 1]/N\}.$$

The main difference w.r.t. the maps (4.1.2), (4.1.5) is that instead of the Lebesgue measure we use the density $a(x_1, \dots, x_{d-2}, z_{d-1})$. Eventually, the composition of the two maps above gives a new map $\check{T}$ such that $(\check{T})^{-1}(z_{d-2}, z_{d-1} = \text{const})$ is a $(d-2)$-dimensional surface made of the graph of a function depending on $x_1, \dots, x_{d-3}$ times the segment $x_d \in k_d, k_d + 1]/N$.

The argument is then repeated in the $d-2$-regions $(\check{T})^{-1}(z_{d-2}, z_{d-1} = \text{const})$ (i.e., disintegrate the Lebesgue measure and shift along the x_{d-3} direction to rectify $(\check{T})^{-1}(z_{d-3}, \dots, z_{d-1} = \text{const})$, and so on until we obtain that a new map T' such that

$$(T')^{-1}(\{z_1, \dots, z_{d-1} = \text{const.}\}) \cap \big\{x_d \in [k_d, k_d + 1]/N\big\}$$

is independent on x_d. This means that lines along the z_d are mapped back into N segments of length $1/N$ along x_d.

Step 2. Differently from the $2d$ case, it is not enough to perturb the vertical slab as in Step 2, since the sets $(T')^{-1}(\{z_k = \text{const.}\})$ are not of (piecewise) the form $\{x_k = \text{const.}\}$. Observe however that in each slab $\{x_d \in [k_d, k_d + 1]/N\}$ the map

$$(x_1, \dots, x_{d-1}) = (T'_{k_d})^{-1}(z_1, \dots, z_{d-1})$$

is well defined, where $(T')^{-1}_{k_d}$ denotes the first $(d-1)$-components of $(T')^{-1}$ restricted to $\{x_d \in [k_d, k_d+1]/N\}$: we have used the property that segments along z_d are mapped back into segments along x_d.

We use Assumption 4.1.6 to get a map $\sigma_{k_d} : [0,1]^{d-1} \to [0,1]^{d-1}$ such that $T''_{k_d} = T'_{k_d} \circ \sigma_{k_d}$ maps affinely parallepipeds of a grid $\mathbb{N}^{d-1}/(NN_1)$, $N_1 = 2^{p_1}$, into cubes of the same grid: we can take $N_1 \gg 1$ in order to be independent of k (Figure 4.4).
Hence the map T''_{k_d} maps parallelepipeds of the form

$$\prod_{i=1}^{d-1} \frac{[k_i, k_i + 1]}{NN_1} \times \frac{[k_d, k_d + 1]}{N}$$

into regions for the form

$$\left\{z_d \in \big[g(x_1, \dots, x_{d-1}, k_d/N), g(x_1, \dots, x_{d-1}, (k_d + 1)/N)\big], z_i \in \prod_{i=1}^{d-1} \frac{[k'_i, k'_i + 1]}{NN_1}\right\},$$

and up to a translation it is a linear diagonal map in the first $d-1$ coordinates and segments along x_d remains along x_d.

Step 3. Piecing together the maps T''_{k_d}, we obtain a measure preserving map $\bar{T}$ close to T with the properties listed at the end of the previous step. We will use the fact that it is affine in the first $(d-1)$ coordinates to use a map similar η_1 of Step 2 of the proof of Lemma 4.1.1 to rectify the set

$$\bar{T}(\{x_d \in [k_d, k_d + 1]/N\}) \cap \big\{z_j \in [k'_j, k'_j + 1]/(NN_1), j = 1, \dots, d-1\big\}.$$

It is defined as the unique measure preserving map $G(z_1, \dots, z_{d-1})$ of the form

$$G(z_1, \dots, z_{d-1}) = \Big(G_1(z_1, \dots, z_{d-1}), G_2(z_2, \dots, z_{d-1}), \dots, G_{d-1}(z_{d-1}), G(z_1, \dots, z_d)\Big).$$

Note that since z_d enters in the last component, segments along z_d are mapped into segments along z_d, and the triangular form of the map assures its uniqueness (Figure 4.5).

The last part of the analysis is to deduce that if a measure preserving transformation $\tilde{T} = G \circ \bar{T} : [0,1]^d \to [0,1]^d$ is such that $\tilde{T}$ is of triangular form then it is the identity: we have rescaled every rectangle to a cube by linear scaling.
If the map has this triangular form, we conclude that the measure preserving condition reads as

$$\prod_{i=1}^{d} \partial_i \tilde{T}_i(x_i, \dots, x_d) = 1,$$

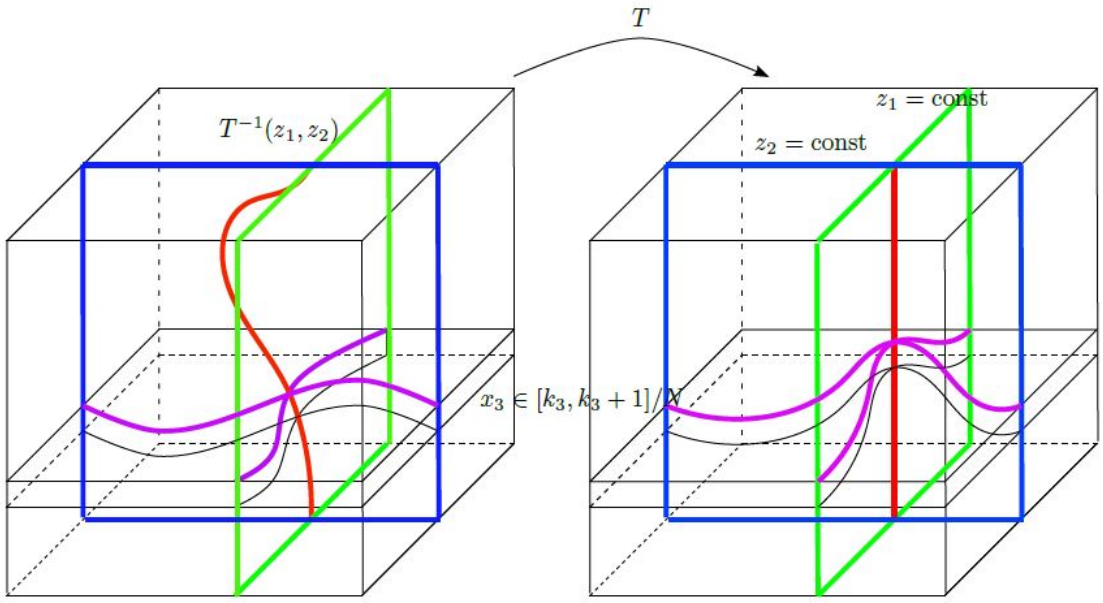

Figure 4.2: Starting point: the map $T : [0,1]^3 \to [0,1]^3$ maps the slap $x_3 \in [k_3, k_3+1]/N$ into a $3d$-set with purple intersections, and $T^{-1}(z_1, z_2)$ is the red curve at the left.

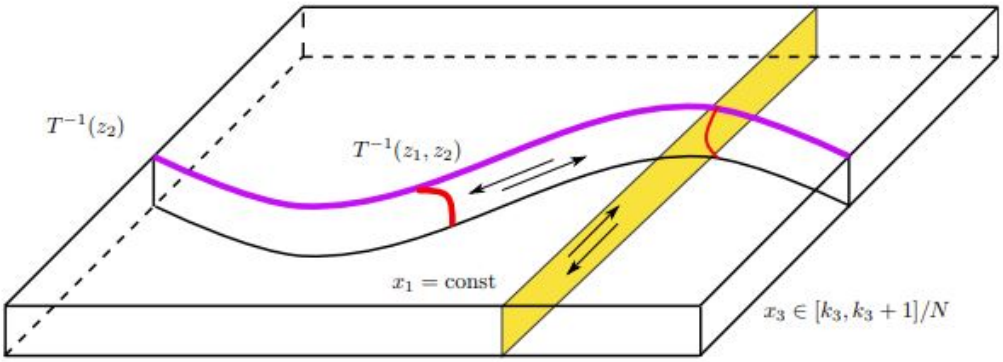

Figure 4.3: First move the mass in the yellow $2d$-rectangle $x_1 = \text{const}$ so that its intersection with $T^{-1}(z_2)$ is vertical in $x_3 \in [k_3, k_3 + 1]/N$, next move the mass along $T^{-1}(z_2)$ so that $T^{-1}(z_1, z_2)$ is vertical in $x_3 \in [k_3, k_3 + 1]/N$.

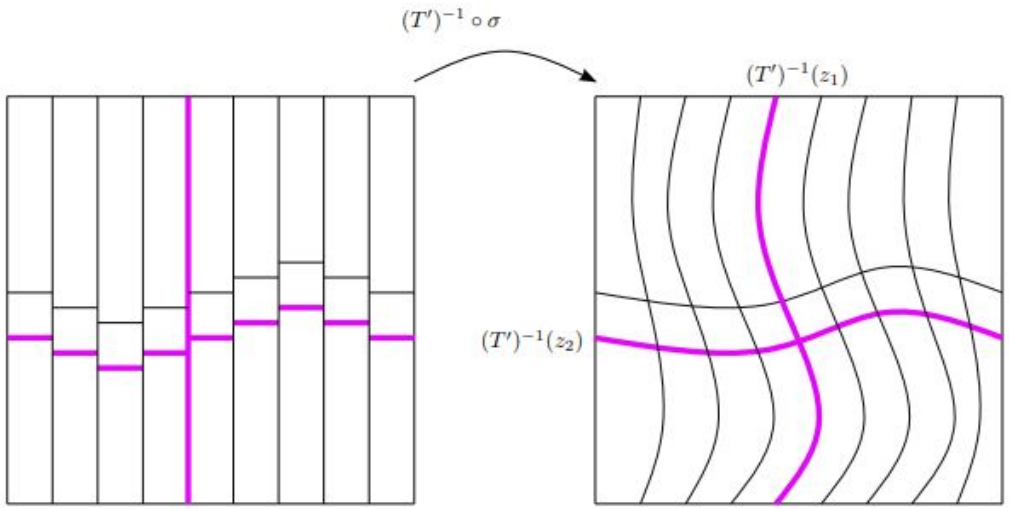

Figure 4.4: The recurrence assumption yields a map σ which maps affinely subsquares into rectangles: in the picture it is shows how it acts before the composition with T' (see also Figure 4.1).

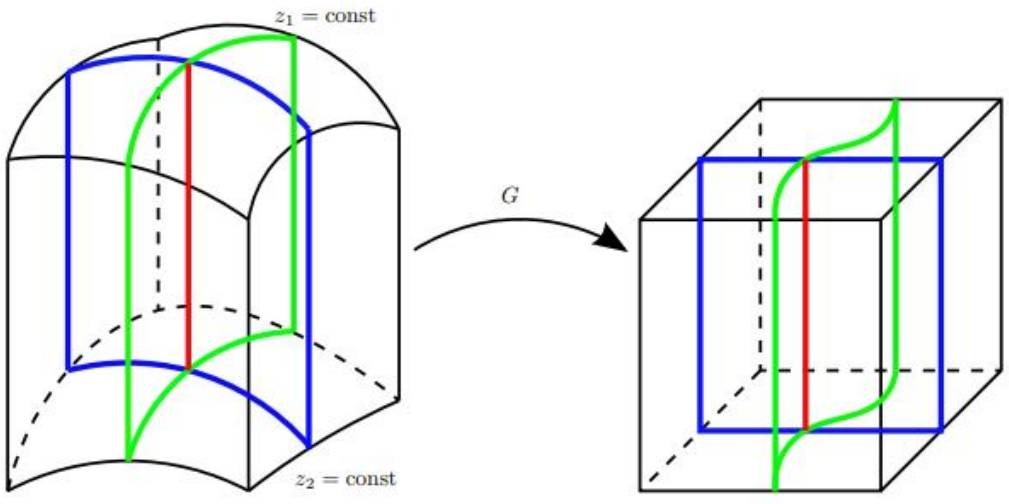

Figure 4.5: The last step is to map the subcubes deformed in the direction x_3 into parallelepipeds such that the Lebesgue measure is preserved and the map G is of triangular form: these conditions imply that $\tilde{T} = G \circ \bar{T}$ is affine.

which together with

$$\int \partial_i \tilde{T}_i(x_i, \dots, x_d) dx_i = 1$$

gives $\partial_i T_i(x_i, \dots, x_d) = 1$, i.e., that the map is the identity.

4.2 BV estimates of perturbations

Let $X_t : K \to K$ be a smooth flow of measure-preserving diffeomorphisms and assume

$$\|X_t - \mathrm{id}\|_{C^3}, \|X_t^{-1} - \mathrm{id}\|_{C^3} \leq \wp, \tag{4.2.1}$$

with $\wp \ll 1$. Call $T(x) = X_{t=1}(x)$, and let $N = 2^{p_0} \in \mathbb{N}$ be the dimension of the grid given by Lemma 4.1.1. In this section we compute the BV norms of the perturbations of the form (4.1.1) constructed in Lemma 4.1.1.

We first address the action of the map ζ_t on $X(t)$. Define the perturbed flow

$$t \mapsto X_t'(x) = \zeta_t \circ X_t(x).$$

Lemma 4.2.1. *There exists a perturbation ζ_t as required by Step 0 of Lemma 4.1.1 such that if v is its associated vector field then*

$$\|\zeta_t - \mathrm{id}\|_{C_0} + 2^{-p_0}\|\nabla\zeta_t - \mathrm{id}\|_{C_0} + 2^{-2p_0}\|\nabla^2\zeta_t\|_{C_0} \leq \mathcal{O}(1)2^{-p_1},$$

$$\|v\|_{C_0} + 2^{-p_0}\|\nabla v\|_{C_0} + 2^{-2p_0}\|\nabla^2 v\|_{C^0} \leq \mathcal{O}(1)2^{-p_1}.$$

for p_1 sufficiently large.

Proof. The request of Step 0 of Lemma 4.1.1 is that the flow across the each region $\tilde{\omega}_{ij}$ is 0 (plus the dyadic condition on the new region $\tilde{\omega}_{ij}$). Hence the problem reduces in finding a suitable incompressible flow with a given boundary flux: we will construct a flow generated by a vector field constant in time.

Consider a function v_n on $\partial\omega_{ij}$ such that

- its support is at distance 2^{-p_0-2} from the corners of $\tilde{\omega}_{ij}$,
- the integral on each of the regular sides is the required flux $\phi_{ij,i'j'}$,
- $\|v_n\|_\infty, 2^{-p_0}\|v_n'\|, 2^{-2p_0}\|v_n''\| \leq \mathcal{O}(1)2^{-p_1}$, where v_n' is the derivative of v_n.

Its existence follows from the fact that ω_{ij} is close to a square of side 2^{-p_0}, being X close to the identity. The last point is a consequence of the fact that $|\phi_{ij,i'j'}| \leq 2^{-p_0-p_1}$.

The integral of v on $\partial\tilde{\omega}_{ij}$ is a potential function p, which is constant in the 2^{-p_0-2}-neighborhood of every corner and such that

$$\|p\|_{C_0}, 2^{-p_0}\|p'\|_{C_0}, 2^{-2p_0}\|p''\|_{C_0}, 2^{-3p_0}\|p'''\|_{C_0} \leq \mathcal{O}(1)2^{-p_0-p_1},$$

where p', p'' are its first and second derivative.

Extend p to a C^2-function inside $\tilde{\omega}_{ij}$: since this extension can be required to vary in a region of size 2^{-p_0-2}, we get

$$\|p\|_{C_0} \leq \mathcal{O}(1)2^{-p_0-p_1}, \quad \|\nabla p\|_{C_0} \leq \mathcal{O}(1)\frac{2^{-p_0-p_1}}{2^{-p_0-2}} = \mathcal{O}(1)2^{-p_1},$$

$$\|\nabla^2 p\|_{C_0} \leq \mathcal{O}(1)\frac{2^{-p_0-p_1}}{2^{-2p_0-4}} = \mathcal{O}(1)2^{p_0-p_1}.$$

$$\|\nabla^3 p\|_{C_0} \leq \mathcal{O}(1)\frac{2^{-p_0-p_1}}{2^{-3p_0-6}} = \mathcal{O}(1)2^{2p_0-p_1}.$$

In particular the vector field $v = \nabla^\perp p$ satisfies the statement, and if ζ_t is the flow generated by v then the same holds by the estimates

$$\|\zeta_t - \mathrm{id}\|_{C^0} \leq \|v\|_{C_0} t, \quad \|\nabla\zeta_t - \mathrm{id}\|_{C^0} \leq e^{\|\nabla v\|_{C_0} t} - 1,$$
$$\|\nabla^2\zeta(t)\|_{C^0} \leq e^{\|\nabla v\|_{C_0} t}\|\nabla^2 v\|_{C_0}\|\nabla\zeta\|^2_{C_0},$$

with $p_1 \gg 1$. □

Corollary 4.2.2. *If b' is the vector field associated with $X'_t = \zeta_t \circ X_t$, then*

$$\|b'_t - b_t\|_{C_1} \leq \mathcal{O}(1)2^{2p_0-p_1}.$$

Proof. From the formula (1.0.3)

$$b'(t,x) - b(t,x) = v(x) + \big(\nabla\zeta_t(t,\zeta_t^{-1}(x)) - \mathrm{id}\big)b(t,x),$$

where $v(x)$ is the time independent vector field associated with ζ_t. Hence from the previous lemma

$$\begin{aligned}\|b'(t) - b(t)\|_{C^1} &\leq \|v\|_{C^1} + \mathcal{O}(1)\|\zeta_t - \mathrm{id}\|_{C^2}\|b\|_{C^1}\\ &\leq \mathcal{O}(1)2^{2p_0-p_1}.\end{aligned}$$

□

Define the **perturbed flow** $t \to \tilde{X}_t$ as

$$\tilde{X}_t(x) = \begin{cases} X'(t,0,\xi_t(x)) & t \in \left[0,\frac{1}{2}\right],\\ X'(t,1,\eta(t,1,w(x))) & t \in \left[\frac{1}{2},1\right],\end{cases}$$

where ξ_t and η_t are given by formula (4.1.1) of Lemma 4.1.1 (here since the map ζ is not needed we rescale ξ_t, η_t with $t \in [0,1/2]$) and

$$w(x) = \eta_1 \circ T' \circ \xi_{\frac{1}{2}}(x), \quad T' = \zeta_1 \circ T.$$

Call $\tilde{b}_t$ the vector field associated with $\tilde{X}_t$.

Lemma 4.2.3 (BV estimates)**.** *There exists a positive constant $C = C(\wp)$ such that*

$$\|b - \tilde{b}\|_{L^\infty(L^1)} \leq \frac{C\wp}{N}, \quad \|\mathrm{Tot.Var.}(\tilde{b})\|_\infty \leq C\|\mathrm{Tot.Var.}(b)\|_\infty + \frac{C\wp}{N}. \tag{4.2.2}$$

Proof. From Corollary 4.2.2, we have that (for $p_1 \gg 1$)

$$\|b - b'\|_{C^1} \leq \mathcal{O}(1)2^{2p_0-p_1} \ll \frac{\wp}{N},$$

so that we are left to prove (4.2.2) with b' in place of b:

$$\|b' - \tilde{b}\|_{L^\infty(L^1)} \leq \frac{C\wp}{N}, \quad \|\mathrm{Tot.Var.}(\tilde{b}_t)\|_\infty \leq C\wp.$$

We will prove the above estimates for $t \in [0,1/2]$, i.e., only for $X'_t \circ \xi_t$, being the analysis of $X'(t,1,\eta(t,1,w(x)))$ completely analogous.

We start by observing that there exists a constant $C > 0$ such that

$$\|\dot{\xi}_t\|_\infty \leq \frac{C\wp}{N}.$$

Indeed, the map $\xi_t^i = \xi_t \llcorner_{H_i}$ is given by the formulas (see Step 1 of the proof of Lemma 4.1.1)

$$\xi_{1,t}^i(x_1,x_2) = f'_{i,2t}(x_1,\xi_t^i(x_1,x_2)) = (1-2t)x_1 + 2tf'(z_{1,i}(x_1),\xi_{2,t}^i(x_1,x_2)),$$

$$\int_{(i-1)2^{-p_0}}^{\xi_{2,t}^i(x_1,x_2)} \partial_{x_1} f'_{i,2t}(x_1,w)dw = x_2 - (i-1)2^{-p_0}.$$

Since it holds by (4.2.1)

$$\|f'\llcorner_{H_i} - \mathrm{id}\|_{C^3}, \|z_{1,i} - \mathrm{id}\|_{C^3} \leq \mathcal{O}(\wp), \tag{4.2.3}$$

then

$$\|f'_{i,2t}(x_1,w) - x_1\|_{C_3} \leq \mathcal{O}(\wp).$$

Hence the function

$$F(t,x_1,x_2,\xi) = \int_{(i-1)2^{-p_0}}^{\xi_2} \partial_{x_1} f'_{i,2t}(x_1,w)dw - x_2 + (i-1)2^{-p_0}$$

satisfies

$$\|F(t,x_1,x_2,\xi) - (\xi_2 - x_2)\|_{C^2} = \left\| \int_{(i-1)2^{-p_0}}^{\xi_2} \big(\partial_{x_1} f'_{i,2t}(x_1,w) - 1\big)dw \right\|_{C_2} \leq \frac{\mathcal{O}(\wp)}{N}.$$

By the Implicit Function Theorem we deduce that

$$\|\xi_{2,t}^i - x_2\|_{C^2} \leq \frac{\mathcal{O}(\wp)}{N},$$

and in particular

$$\|\dot\xi_{2,t}^i\|_{C^0}, \|\nabla\dot\xi_{2,t}^i\|_{C^0} \leq \frac{\mathcal{O}(\wp)}{N}.$$

Similarly

$$\|\xi_{1,t}^i - x_1\|_{C^2} \leq \frac{\mathcal{O}(\wp)}{N},$$

and then

$$\|\dot\xi_{1,t}^i\|_{C^0}, \|\nabla\dot\xi_{1,t}^i\|_{C^0} \leq \frac{\mathcal{O}(\wp)}{N}.$$

We next estimate the total variation of the vector field

$$v_t = \dot\xi_t(\xi_t^{-1}(x)).$$

We will use the following elementary formulas:

$$\partial_{z_1} f'(z_1,x_2) = \frac{1}{\partial_{z_2} X_2^{-1}(z_1,z_2(z_1,x_2))} \tag{4.2.4}$$

$$\partial_{x_2} f'(z_1,x_2) = \frac{\partial_{z_2}(X_1)^{-1}(z_1,z_2(z_1,x_2))}{\partial_{z_2}(X_2)^{-1}(z_1,z_2(z_1,x_2))}, \quad X_2(z_1,z_2(z_1,x_2)) = x_2, \tag{4.2.5}$$

$$\partial_{x_1} z_1 = \frac{1}{\fint_{(i-1)2^{-p_0}}^{i2^{-p_0}} \partial_{z_1} f'(z_{1,i}(x_1),w)dw},$$

from which it follows

$$\sum_i ||\partial_{z_1} f'(z_{i,1},x_2)\partial_{x_1} z_{i,1} - 1||_{L^1(H_i)} + \sum_i \|\partial_{x_2} f'(z_{i,1},x_2)\|_{L^1(H_i)} \leq C||\mathrm{Tot.Var.}(b)(K)||_\infty.$$

Indeed

$$\begin{aligned}||\partial_{z_1} f'(z_{i,1}, x_2)\partial_{x_1} z_{i,1} - 1||_{L^1(H_i)} &\le ||\partial_{x_1} z_{i,1}||_\infty ||\partial_{z_1} f'(z_{i,1}, x_2) - 1||_{L^1(H_i)} \\ &\quad + ||\partial_{x_1} z_{i,1} - 1||_{L^1(H_i)} \\ &\le C||\partial_{z_1} f'(z_{i,1}, x_2) - 1||_{L^1(H_i)} \\ &\quad + C\left\| \fint_{(i-1)2^{-p_0}}^{i2^{-p_0}} \partial_{z_1} f'(z_{i,1}, x_2)dw - 1 \right\|_{L^1(H_i)} \\ &\le C||\partial_{z_1} f'(z_{i,1}, x_2) - 1||_{L^1(H_i)},\end{aligned}$$

therefore, by (4.2.4), we get

$$\begin{aligned}&\sum_i ||\partial_{z_1} f'(z_{i,1}, x_2) - 1||_{L^1(H_i)} + \sum_i \|\partial_{x_2} f'(z_{i,1}, x_2)\|_{L^1(H_i)} \\ &\quad \le C||\nabla(X^{-1} - Id)||_1 \le C\int_0^1 \text{Tot.Var.}(b_s)(K)ds \le C||\text{Tot.Var.}(b)(K)||_\infty.\end{aligned}$$

By the Implicit Function Theorem we recover the following estimate for $|\nabla\dot{\xi}|$:

$$\begin{aligned}|\nabla\dot{\xi}| &\le C\bigg(|\partial_{x_1} f'(z_{1,i}(x_1), \xi_2) - 1| + \int_{(i-1)2^{-p_0}}^{\xi_2} |\partial_{x_1}^2 f'(z_{1,i}(x_1), w)|dw \\ &\qquad + \|\nabla f'(z_{1,i}(x_1), \xi_2)\|_{C^1}\big(|\dot{\xi}| + |\nabla\xi| + |\dot{\xi}||\nabla\xi|\big)\bigg) \\ &\le C|\partial_{x_1} f'(z_{1,i}(x_1), \xi_2) - 1| + \frac{\mathcal{O}(\wp)}{N}.\end{aligned}$$

Hence

$$\|\nabla\dot{\xi}\|_1 \le C\|\text{Tot.Var.}(b)(K)||_\infty + \frac{\mathcal{O}(\wp)}{N}.$$

For the jump part, we estimate the vector v_t at the boundaries of H_i: from the definition

$$\begin{aligned}\xi_t(x_1, (i-1)2^{-p_0}) &= (1-2t)x_1 + 2tf'\big(z_{1,i}(x_1), (i-1)2^{-p_0}\big), \\ \xi_t(x_1, i2^{-p_0}) &= (1-2t)x_1 + 2tf'\big(z_{1,i}(x_1), i2^{-p_0}\big),\end{aligned}$$

We consider only the second one, being the analysis of the first completely similar. Differentiating $\xi_t(x_1, i2^{-p_0})$ w.r.t. t and using the definition of $z_{1,i}(x_1)$ we have

$$\begin{aligned}\dot{\xi}_t(x_1, i2^{-p_0}) &= 2\big(f'\big(z_{1,i}(x_1), i2^{-p_0}\big) - x_1\big) \\ &= 2\bigg(f'\big(z_{1,i}(x_1), i2^{-p_0}\big) - \fint_{(i-1)/N}^{i/N} f'\big(z_{1,i}(x_1), w\big)dw\bigg).\end{aligned}$$

and then

$$\begin{aligned}|\dot{\xi}_t(x_1, i/N)| &\le 2\int_{(i-1)/N}^{i/N} \big|\partial_{x_2} f'(z_{1,i}(x_1), w)\big|dw \\ &\le C\int_{(i-1)/N}^{i/N} \big|\partial_{z_2}(X_1)^{-1}(z_{1,i}(x_1), z_2(z_{1,i}(x_1), w))\big|dw.\end{aligned}$$

Hence, by (4.2.3) and from the definition of $z_2(z_1, x_2)$ in (4.2.5) we have that

$$\big\|(z_{1,i}(x_1), z_2(z_{1,i}(x_1), x_2)) - \text{id}\big\|_{C^1} \le \frac{\mathcal{O}(\wp)}{N},$$

so that using

$$\big\{\big(z_{1,i}(x_1), z_2(z_{1,i}(x_1), x_2)\big), (x_1, x_2) \in H_i\big\} = X_1(H_i),$$

we have

$$\begin{aligned}
&\int_0^1 |\dot\xi_t(x_1, i/N)|dx_1 \\
&\le C\int_0^1 \int_{(i-1)/N}^{i/N} \big|\partial_{z_2}(X_1)^{-1}(z_{1,i}(x_1), z_2(z_{1,i}(x_1), x_2))\big| dx_1 dx_2 \qquad (4.2.6)\\
&\le C\int_{X_1(H_i)} \big|\partial_{z_2}(X_1)^{-1}(z_1, z_2)\big| dz.
\end{aligned}$$

Again, since the change of variable which associate t, x_1 with its position w_1 on the jump line $[0,1]\times\{i/N\}$ is given by

$$t, x_1 \mapsto w_1 = (1-2t)x_1 + 2tf'(z_{1,i}(x_1), i/N),$$

up to a constant $1+\mathcal{O}(\wp)/N$ (again by (4.2.3)) the first integral in (4.2.6) corresponds to the jump part of $\dot\xi(x_1, i/N)$ on $[0,1]\times\{i/N\}$ when extended to 0 outside H_i.

The same estimate holds for the jump of $\dot\xi_t(x_1, (i-1)2^{-p_0})$ on $[0,1]\times\{(i-1)/N$.

We conclude that

$$\|D^{\text{jump}}v\| \le C\sum_i \int_{X(H_i)} \big|\partial_{z_2}(X_1)^{-1}(z_1, z_2)\big| dz \le C\|\text{Tot.Var.}(b)\|_\infty.$$

We thus deduce

$$\text{Tot.Var.}(v_t) \le C\|\text{Tot.Var.}(b)\|_\infty + \frac{\mathcal{O}(\wp)}{N}.$$

Collecting all estimates we have:

L^1 estimate. Fix $t \in \big[0, \frac{1}{2}\big]$. From (1.0.3) it follows that

$$|\tilde b_t(x) - b_t(x)| \le \|\dot\xi_t\|_\infty |\nabla X_t'((X')_t^{-1}(x)| \le \frac{C\wp}{N}.$$

BV estimate. Again from (1.0.3)

$$\text{Tot.Var.}(\tilde b_t - b_t) \le \text{Tot.Var.}\big(\nabla X_t(X_t^{-1}(x))\dot\xi_t(\tilde X_t^{-1}(x))\big),$$

so that we have to compute the total variation of

$$\nabla X_t(X_t^{-1}(x))\dot\xi_t(X_t^{-1}(x)).$$

By using Theorem 1.0.4 we have

$$\begin{aligned}
\text{Tot.Var.}\big(\nabla X_t(X_t^{-1})\dot\xi_t(\tilde X_t^{-1})\big) &\le \text{Lip}(X_t)\text{Tot.Var.}\big(\nabla X_t\dot\xi_t(\xi_t^{-1})\big)\\
&\le \text{Lip}(X_t)\text{Tot.Var.}(\nabla X_t)\|\dot\xi_t\|_\infty\\
&\quad + \text{Lip}(X_t)\|\nabla X_t\|_\infty\text{Tot.Var.}(\dot\xi_t\circ\xi_t^{-1})\\
&= \text{Lip}(X_t)\text{Tot.Var.}(\nabla X_t)\|\dot\xi_t\|_\infty\\
&\quad + \text{Lip}(X_t)\|\nabla X_t\|_\infty\text{Tot.Var.}(v_t).
\end{aligned}$$

The first term can be estimated by

$$\text{Tot.Var.}(\nabla X_t)\|\dot\xi_t\|_\infty \le \frac{\mathcal{O}(\wp)}{N},$$

while the second term is controlled by

$$\|\nabla X_t\|_\infty \text{Tot.Var.}(v_t) \leq C\|\text{Tot.Var.}(b)||_\infty + \frac{\mathcal{O}(\wp)}{N}.$$

This is the statement. □

Remark 4.2.4. The above estimates can be obtained also for the d-dimensional case, since the maps used in that case is a composition of maps of the $2d$ case: the estimates are completely similar (but a lot more complicated).

Remark 4.2.5. We notice here that the constant C in front of the total variation is larger than 1: this fact is one of the reasons why we need to work in the G_δ-set $\mathcal{U}$.

4.3 BV estimates for rotations

In this part we address the analysis of rotations: these are needed because the map of Lemma 4.1.1 maps affinely subrectangles into subrectangles, while we need squares translated into squares.
The approach here differs from the one of [43, Lemma 4.5], because the rotations used in that paper have a BV norm which is not bounded by the area (Lemma 4.3.1) and instead it depends on the size of the squares (actually it blows up when the size of the squares goes to 0).

Let $N = 2^{p_0}, p_0 \in \mathbb{N}$, and $\sigma_1 : K \to K$ be respectively the dimension of the grid and the map given by Lemma 4.1.1.

Lemma 4.3.1. *There exists $M \in \mathbb{N}$ and a flow $\bar{R}_t : K \to K$ invertible, measure-preserving and piecewise smooth such that the map $\sigma_1 \circ \bar{R}_1$ translates each subsquare of the grid $\mathbb{N} \times \mathbb{N}\frac{1}{M}$ into a subsquare of the same grid, i.e., it is a permutation of squares.*

In particular note that $\nabla(\sigma_1 \circ \bar{R}_1)$ is the identity inside each subsquare κ.

Proof. Fix κ a subsquare of the grid $\mathbb{N} \times \mathbb{N}\frac{1}{N}$ and call $q = \sigma_1(\kappa)$ its image. Since $\sigma_1 \llcorner \kappa$ is an affine measure-preserving map of diagonal form, then, up to translations,

$$\sigma_1(x) = \begin{pmatrix} \lambda_1 & 0 \\ 0 & \lambda_2 \end{pmatrix} x, \qquad \forall x \in \kappa,$$

where $\lambda_1, \lambda_2 \in \mathbb{Q}_{>0}$ and $\lambda_1\lambda_2 = 1$. Therefore the rectangle q has horizontal side of length $\frac{\lambda_1}{N}$ and vertical side of length $\frac{1}{\lambda_1 N}$. Decompose now the square κ into rectangles R_{ij} with $i = 1, \dots, \frac{1}{l_1}$ and $j = 1, \dots, \frac{1}{l_2}$ with horizontal side of length $\frac{l_1}{N}$ and vertical side of length $\frac{l_2}{N}$. The numbers $\frac{1}{l_1}, \frac{1}{l_2} \in \mathbb{N}$ are chosen such that $\lambda_1 = \frac{l_2}{l_1}$, i.e., $\sigma_1(R_{ij}) = R_{ij}^\perp$, where $R_{ij}^\perp$ is the rotated rectangle counterclockwise of an angle $\frac{\pi}{2}$.
In each R_{ij} we perform a rotation given by the flow

$$R_t^{ij} = \chi^{-1} \circ r_t \circ \chi,$$

where $\chi : R_{ij} \to K$ is the affine map, up to translation, sending each R_{ij} into the unit square K, namely

$$\chi x = \begin{pmatrix} \frac{N}{l_1} & 0 \\ 0 & \frac{N}{l_2} \end{pmatrix} x, \quad \forall x \in R_{ij},$$

whereas $r_t : K \to K$ is the rotation flow (2.2.5). Finally define $R_t : K \to K$ such that $R_{t\llcorner R_{ij}} = R_t^{ij}$. This flow rotates the interior of each rectangle R_{ij} by $\pi/2$ during the time evolution.

Now we choose $M \in \mathbb{N}$ large enough to refine the grid $\mathbb{N} \times \mathbb{N}\frac{1}{N}$ in such a way that for every subsquare $\kappa \in \mathbb{N} \times \mathbb{N}\frac{1}{N}$, $\forall i, j$, each rectangle $R_{ij} \subset \kappa$ is the union of squares of the grid $\mathbb{N} \times \mathbb{N}\frac{1}{M}$ and each rectangle $q = \sigma_1(\kappa)$ is union of subsquares of $\mathbb{N} \times \mathbb{N}\frac{1}{M}$, which is possible since the vertices of the squares and rectangles we are considering are all rationals.
We claim that the map $\sigma_1 \circ R_t : K \to K$ is a flow of invertible, measure-preserving maps such that $\sigma_1 \circ R_1 : K \to K$ is a permutation of subsquares of size $\frac{1}{M}$ up to a rotation of $\pi/2$. Indeed, fix R_{ij} and assume that it contains a_{ij} subsquares κ_{ij}^h of size $\frac{1}{M} \times \frac{1}{M}$ along the horizontal side and b_{ij} subsquares along the vertical one. The rotation R_1 stretches each square κ_{ij}^h into a rectangle r_{ij}^h whose size is $\frac{l_1}{Ml_2} \times \frac{l_2}{Ml_1}$, i.e., $\frac{1}{\lambda_1 M} \times \frac{\lambda_1}{M}$. Now it is clear that $\sigma_1(r_{ij}^h)$ is a square of size $\frac{1}{M} \times \frac{1}{M}$.

The Jacobian of R_1 is

$$JR_1 = \begin{pmatrix} 0 & -\lambda_2 \\ \lambda_1 & 0 \end{pmatrix}.$$

Thus the composition of the two maps acts in each square r_{ij}^h as

$$\begin{pmatrix} \lambda_1 & 0 \\ 0 & \lambda_2 \end{pmatrix} \begin{pmatrix} 0 & -\lambda_2 \\ \lambda_1 & 0 \end{pmatrix} = \begin{pmatrix} 0 & -1 \\ 1 & 0 \end{pmatrix},$$

i.e., a rotation of $\pi/2$.

Define then the map $\bar{R}_t$ as

$$\bar{R}_{t\llcorner \kappa_{ij}^h} = R_t \circ r_t^{-\pi/2},$$

where $r_t^{-\pi/2}$ is the rotation of the square κ_{ij}^h of $-\pi/2$: now the map has Jacobian id in each square κ_{ij}^h. This is the map of the statement. □

Remark 4.3.2. A completely similar construction can be done in dimension $d \geq 3$: in this case, in each cube $\kappa \in \mathbb{N}^d/N$ the piecewise affine map σ has the form (up to a translation)

$$\sigma = \mathrm{diag}(\lambda_1, \dots, \lambda_d), \quad \lambda_1 \lambda_2 \dots \lambda_d = 1.$$

Hence the subpartition of κ is done into parallelepipeds $\ell_1 \times \ell_2 \times \cdots \times \ell_d$ such that

$$\lambda_i = \frac{\ell_{i+1}}{\ell_i}.$$

The action of σ transform each of these parallelepipeds into the new ones $\ell_2 \times \ell_3 \times \cdots \times \ell_d \times \ell_1$, which is the range of the rotation

$$\begin{pmatrix} 0 & -1 & 0 & \cdots & 0 \\ 0 & 0 & -1 & \cdots & 0 \\ \vdots & \vdots & \vdots & \ddots & \vdots \\ 1 & 0 & 0 & \dots & 0 \end{pmatrix} = \begin{pmatrix} 1 & 0 & \cdots & 0 & 0 \\ 0 & 1 & \cdots & 0 & 0 \\ \vdots & \vdots & \mathrm{id} & \vdots & \vdots \\ 0 & 0 & \cdots & 0 & -1 \\ 0 & 0 & \dots & 1 & 0 \end{pmatrix} \cdots\cdots\cdots \begin{pmatrix} 0 & -1 & \cdots & 0 & 0 \\ 1 & 0 & \cdots & 0 & 0 \\ \vdots & \vdots & \mathrm{id} & \ddots & \vdots \\ 0 & 0 & \dots & 1 & 0 \\ 0 & 0 & \dots & 0 & 1 \end{pmatrix}.$$

(The above formula is the decomposition into $2d$ rotations.) Hence, as in Lemma 4.3.1 above, a rotation of the parallelpipeds $\ell_1 \times \cdots \times \ell_d$ and a counter-rotation of the subcubes of the parallelepipeds gives the transformation.

4.4 Main approximation theorem

We are ready to prove our main result.

Theorem 4.4.1. *Let $b \in L^\infty([0,1]; BV(K))$ be a divergence-free vector field and assume that there exists $\delta > 0$ such that for $\mathcal{L}^1$-a.e. $t \in [0,1]$, $\operatorname{supp} b_t \subset\subset K^\delta$. Then for every $\epsilon > 0$ there exist $\delta', C_1, C_2 > 0$ positive constants, $D \in \mathbb{N}$ arbitrarily large and a divergence-free vector field $b^\epsilon \in L^\infty([0,1]; BV(K))$ such that*

1. $\operatorname{supp} b^\epsilon_t \subset\subset K^{\delta'}$,
2. *it holds*

$$\|b - b^\epsilon\|_{L^\infty(L^1)} \leq \epsilon, \quad ||\text{Tot.Var.}(b^\epsilon)(K)||_\infty \leq C_1 ||\text{Tot.Var.}(b)(K)||_\infty + C_2, \tag{4.4.1}$$

3. *the map $X^\epsilon{}_{\llcorner t=1}$ generated by b^ϵ at time $t = 1$ translates each subsquare of the grid $\mathbb{N} \times \mathbb{N}\frac{1}{D}$ into a subsquare of the same grid, i.e., it is a permutation of squares.*

Remark 4.4.2. Observe that the theorem can be easily extended to vector fields $b \in L^\infty([0,1], \mathrm{BV}(\mathbb{R}^2))$ such that $\operatorname{supp} b_t \subset K$. We keep here the original setting of [43].

Remark 4.4.3. By inspection of the proof one can check that C_1, C_2 are independent of b. This is in any case not needed for the proof of the main theorem.

Remark 4.4.4. A possible approach would be to divide the time interval $[0,1]$ into sufficiently small time steps $\sim \tau$ in order to apply Lemmas 4.1.1 , 4.3.1 and hence to compose the resulting maps as done in [43], however by Lemma 2.2.13,

$$||\text{Tot.Var.}(\bar{R})(\kappa)||_\infty \sim \frac{\text{Area}(K)}{\tau}$$

so that the total variation blows up as the time step goes to zero.

Proof. We divide the proof into several steps.

Step 1. Let $\rho \in C^\infty_c(\mathbb{R}^2)$ be a mollifier, and define

$$b^\alpha_t \doteq b_t * \rho_\alpha,$$

where $\rho_\alpha(x) \doteq \alpha^{-2}\rho(\frac{x}{\alpha})$ and $\alpha << 1$ is chosen such that $\operatorname{supp} b_{\alpha,t} \subset\subset K$.

By well known estimates (see (1.0.1)) we obtain

$$\|b^\alpha_t - b_t\|_{L^1} \leq \alpha \text{Tot.Var.}(b_t)(K), \quad \text{Tot.Var.}(b^\alpha_t)(K) \leq \text{Tot.Var.}(b_t)(K).$$

then if α is chosen such that $\alpha \leq \frac{\epsilon}{2||\text{Tot.Var.}(b)(K)||_\infty}$, we conclude that

$$||b^\alpha_t - b_t||_1 \leq \frac{\epsilon}{2}, \quad \text{Tot.Var.}(b^\alpha_t)(K) \leq \text{Tot.Var.}(b_t)(K)$$

and we have to prove the theorem for b^α. Moreover b^α satisfies the estimates

$$||b^\alpha_t||_\infty \leq \frac{1}{\alpha^2}||b_t||_1, \quad \|\nabla^n b^\alpha_t\|_\infty \leq \frac{C_n}{\alpha^{1+n}}\|\text{Tot.Var.}(b_t)(K)\|_\infty.$$

From now on we will call $b^\alpha = b$ to avoid cumbersome notations.

Step 2. Let us consider a partition of the time interval $0 = t_0 < t_1 < \cdots < t_n = 1$ where $n \in \mathbb{N}$ and $t_i = \frac{i}{n}$, where n will be chosen later on. Let us call $X_j \doteq X(t_j, t_{j-1}, x)$ and $X_j(t) \doteq X(t, t_{j-1}, x)$ defined for $t \in [t_{j-1}, t_j]$. Then each flow $X_j(t)$ is close to the identity with its derivatives, indeed

$$X_j(t,x) = x + \int_{t_{j-1}}^{t} b(s, X(s, t_{j-1}, x))ds, \tag{4.4.2}$$

so that

$$\|X_j(t) - \mathrm{id}\|_{C^k} \leq C(k)(t - t_{j-1})\|b\|_{C^k}.$$

More precisely, if $\wp$ is the constant of (4.2.1), there exists $n \in \mathbb{N}$ such that

$$\|X_j(t) - \mathrm{id}\|_{C^3}, \|X_j^{-1} - \mathrm{id}\|_{C^3} \leq \wp, \quad \forall t \in [t_{j-1}, t_j], \quad \forall j = 1, \ldots, n.$$

Therefore we can apply Lemma 4.1.1 to each $X_j(t)$ finding $N_j = 2^{p_j}$ dyadic and $\tilde{X}_j : [t_{j-1}, t_j] \times K \to K$ with the property that, at time $t = t_j$, the map $\tilde{X}_j(t_j)$ sends subsquares of the grid $\mathbb{N} \times \mathbb{N}\frac{1}{N_j}$ into rational rectangles with vertices in $\frac{\mathbb{N}}{N_j R_j}$. In particular, the eigenvalues of all affine maps σ for $\tilde{X}_j(t_j)$ belongs to $\frac{\mathbb{N}}{R_j}$. We can moreover assume that $N_j = N$ for all maps $\tilde{X}_j(t_j)$ by taking N sufficiently large. Finally from Lemma 4.2.3 we have that in each interval $[t_{j-1}, t_j]$ it holds

$$\|b - \tilde{b}_j\|_{L^\infty(L^1)} \leq \frac{C\wp}{N}, \quad \|\mathrm{Tot.Var.}(\tilde{b}_j)\|_\infty \leq C\|\mathrm{Tot.Var.}(b_t)\|_\infty + \frac{C\wp}{N}.$$

so that for $N \gg 1$ we have

$$\|b - \tilde{b}_j\|_{L^\infty(L^1)} \leq \epsilon, \quad ||\mathrm{Tot.Var.}(\tilde{b}_j)(K)||_\infty \leq C||\mathrm{Tot.Var.}(b)(K)||_\infty + \epsilon,$$

where $\tilde{b}_j$ is the vector field associated with $\tilde{X}_j$.

We define $t \to \tilde{X}_t$ the *perturbed flow*

$$\tilde{X}(t) = \begin{cases} \tilde{X}_1(t) & 0 \leq t \leq t_1, \\ \tilde{X}_2(t) \circ \tilde{X}_1(t_1) & t_1 \leq t \leq t_2, \\ \cdots & \\ \tilde{X}_{i+1}(t) \circ \tilde{X}_i(t_i) \circ \cdots \circ \tilde{X}_1(t_1) & t_i \leq t \leq t_{i+1}, \\ \cdots & \\ \tilde{X}_n(t) \circ \tilde{X}_{n-1}(t_{n-1}) \circ \cdots \circ \tilde{X}_1(t_1) & t_{n-1} \leq t \leq 1. \end{cases}$$

The map is clearly piecewise affine, and the eigenvalues of each affine piece σ belong to $\frac{\mathbb{N}}{\prod_j R_j}$.

Step 3. The map $\tilde{X}(1)$ has the property of sending subsquares of the grid $\mathbb{N} \times \mathbb{N}\frac{1}{N}$ into union of rational rectangles. Let $D = N(\prod_j R_j)^2$: we now show that $\tilde{X}(1)$ maps subsquares of the grid $\mathbb{N} \times \mathbb{N}\frac{1}{D}$ into rational rectangles.

Let $R = \prod_j R_j$ and assume that the map $\tilde{X}(1, t_{j+1})$ maps the subsquares of the grid

$$\mathbb{N} \times \mathbb{N}\frac{1}{NR\prod_{k=j+1}^n R_k}$$

into rational rectangles. Since $\tilde{X}_j$ maps affinely the subsquares of $\mathbb{N}\times\mathbb{N}\frac{1}{N}$ into rectangles of the grid

$$\mathbb{N} \times \mathbb{N}\frac{1}{NR_j} \subset \mathbb{N} \times \mathbb{N}\frac{1}{NR\prod_{k=j+1}^n R_k},$$

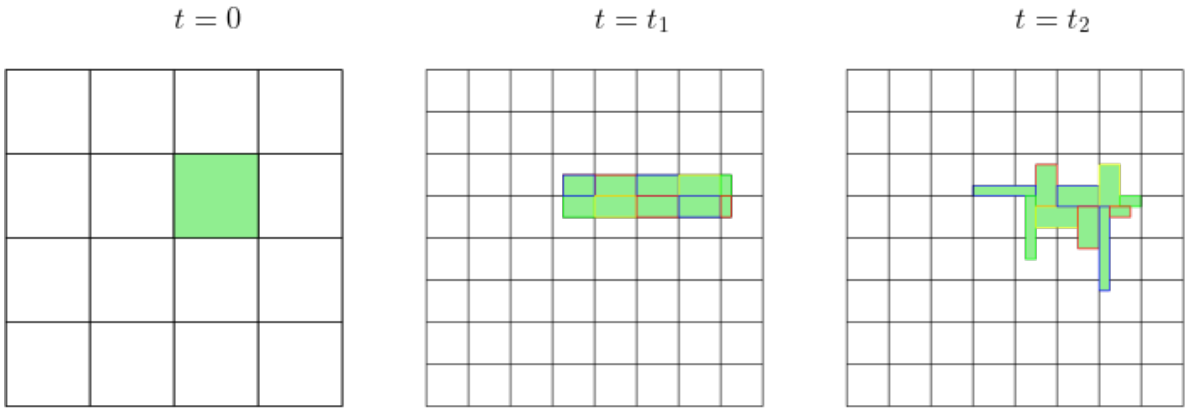

Figure 4.6: A square is sent into a union of rectangles by the map $\tilde{X}(1)$.

then

$$\tilde{X}_j^{-1}\left(\mathbb{N}\times\mathbb{N}\frac{1}{NR\prod_{k=j+1}^{n}R_k}\right)\subset\mathbb{N}\times\mathbb{N}\frac{1}{NR\prod_{k=j}^{n}R_k}.$$

In particular we obtain that

$$\tilde{X}^{-1}\left(\mathbb{N}\times\mathbb{N}\frac{1}{NR}\right)\subset\mathbb{N}\times\mathbb{N}\frac{1}{NR^2}.$$

We rename the flow $\tilde{X}_t^D$ to indicate the size of the grid on which it acts as a piecewise affine map. Note that the above estimates (as well as the next ones) improve whenever N becomes larger, so that the size of the grid D can be taken arbitrarily large.

Step 4. To conclude the proof we want to modify the flow $\tilde{X}_t^D$ slightly in such a way that the new flow $\check{X}_t^D$ evaluated at $t = 1$ sends subsquares into subsquares by translations. The key idea is to perform rotations as in Lemma 4.3.1 balancing two effects: one one hand the cost of a rotation is at least of the order of the area (Lemma 2.2.13), on the other hand if the squares are too much deformed the cost is exponentially large w.r.t. the total variation used to deform the square. The idea will be to use these rotations only when the deformation reaches a critical threshold.

First let us fix κ_0 a subsquare of the grid $\mathbb{N}\times\mathbb{N}\frac{1}{D}$ and call κ_i its images through the maps $\kappa_i = \tilde{X}^D_{t=t_i}(\kappa_0)$. Since each map $\tilde{X}_i(t_i)$ is affine and measure-preserving on κ_{i-1}, up to a translation it can be represented as

$$\begin{pmatrix}\sigma_i & 0\\ 0 & \frac{1}{\sigma_i}\end{pmatrix}$$

where $\sigma_i\in\mathbb{Q}$ and $|\sigma_i-1|, |\frac{1}{\sigma_i}-1|\leq\wp\ll 1$, where $\wp$ is the one given by the partition. Moreover, being

$$\nabla^2\tilde{X}^D_{t=t_j}(x) = 0 \tag{4.4.3}$$

whenever x belongs to the interior of the subsquares, we deduce that for the same x

$$|\nabla^2\tilde{X}_t^D(x)|\leq\wp.$$

We can also observe that, by (4.4.2)

$$|\sigma_i - 1|, \left|\frac{1}{\sigma_i} - 1\right| \leq \frac{C}{\mathcal{L}^2(\kappa_0)} \int_{t_{i-1}}^{t_i} \text{Tot.Var.}(b_s^D)(\kappa_0) ds.$$

By elementary computations one can prove that

$$\left|\prod_i \sigma_i - 1\right|, \left|\prod_i \frac{1}{\sigma_i} - 1\right| \leq \max\left\{\sigma, \frac{1}{\sigma}\right\} \sum_i |\sigma_i - 1|.$$

Hence if we have the bound

$$3 \leq \left(\sigma_{j+1} \cdot \ldots \cdot \sigma_i + \frac{1}{\sigma_{j+1} \cdot \ldots \cdot \sigma_i}\right) \leq 4,$$

then

$$\frac{3}{8}\mathcal{L}^2(\kappa_j) \leq \int_{t_j}^{t_i} \text{Tot.Var.}(b_s^D)(\kappa_0) ds. \tag{4.4.4}$$

The idea is to find now a new sequence of times $\{t_{i_j}\} \subset \{t_i\}$, $j = 1, \ldots, n'$ and $i = 1, \ldots, n$, in which we perform the rotations of Lemma 2.2.13 in order to have both the total variation is controlled be the total variation of $\tilde{b}^D$ and the property of sending subsquares into subsquares by translation.

Let us start defining $t_{i_0} = 0$ and

$$t_{i_1} = \min T_0,$$

where

$$T_0 = \left\{t_i > 0 : 3 \leq \left(\sigma_1 \cdot \cdots \cdot \sigma_i + \frac{1}{\sigma_1 \cdot \cdots \cdot \sigma_i}\right) \leq 4\right\}.$$

Then two situations may occur.

1. The set T_0 is empty, that is $\left(\sigma_1 \ldots \sigma_i + \frac{1}{\sigma_1 \ldots \sigma_i}\right) \leq 3$ for all i. In this case we perform a rotation in $[0,1]$, that is $R^1 : [0,1] \times K \to K$ (as in Lemma 4.3.1) where $R^1 \llcorner_{K \setminus \mathring{\kappa}_0}(x) = x$ and it is such that $X^D \circ R^1 \llcorner_{t=1}$ sends subsquares of κ_0 into subsquares of κ_n. In this case

$$\hat{X}_t^D = \tilde{X}_t^D \circ R_t^1$$

$$\hat{b}_t^D(x) = \tilde{b}_t^D(x) + \nabla \tilde{X}_t^D \circ (\tilde{X}_t^D)^{-1}(x) \dot{R}_t^1((\tilde{X}_t^D \circ R_t^1)^{-1}(x)) \quad x \in \kappa_0$$

(where we have recalled that all functions can be extended smoothly to κ_0) and

$$\begin{aligned}
\text{Tot.Var.}(\hat{b}_t^D - \tilde{b}_t^D)(\kappa_0) &\leq \|\nabla \tilde{X}_t^D\|_\infty^2 TV(\dot{R}_t(R_t^{-1}))(\kappa_0) \\
&\quad + \|\nabla \tilde{X}_t^D\|_\infty \|\dot{R}\|_\infty \text{Tot.Var.}(\nabla \tilde{X}_t^D)(\kappa_0) \\
&\leq \|\nabla \tilde{X}_t^D\|_\infty \frac{4}{D^2}\left(\sigma_1 \ldots \sigma_n + \frac{1}{\sigma_1 \ldots \sigma_n}\right) + \frac{\mathcal{O}(\wp)}{D^3} \quad (4.4.5) \\
&\leq \|\nabla \tilde{X}_t^D\|_\infty \frac{12}{D^2} + \frac{\mathcal{O}(\wp)}{D^3}.
\end{aligned}$$

We have observed that

$$\nabla^2 \tilde{X}_{t=t_j}^D(x) = 0 \quad \text{for } x \in \mathring{\kappa}_0 \text{ by (4.4.3)},$$

so that for $t \in [t_{j-1}, t_j]$

$$\|\nabla^2 \tilde{X}_t^D\|_\infty \leq \mathcal{O}(1) \int_{t_{j-1}}^t |\nabla^2 b(s, \tilde{X}_s^D)| ds = \frac{O(\wp)}{D^2}.$$

Since $\|\nabla \tilde{X}_t^D\|_\infty \leq C$ by the assumptions that these are sets with small deformations, we obtain

$$\text{Tot.Var.}(\hat{b}_t^D - \tilde{b}_t^D)(\kappa_0) \leq \frac{\mathcal{O}(1)}{D^2} = \mathcal{O}(1)\mathcal{L}^2(\kappa_0),$$

where we have used (4.4.4).

2. The set T_0 is non empty. Then if $t_{i_1} = 1$ the procedure stops and you perform a rotation as in Lemma 4.3.1 in $[0, 1]$ finding

$$\begin{aligned}\text{Tot.Var.}(\hat{b}_t^D - \tilde{b}_t^D)(\kappa_0) &\leq \|\nabla \tilde{X}_t^D\| \frac{4}{D^2} \left(\sigma_1 \dots \sigma_n + \frac{1}{\sigma_1 \dots \sigma_n}\right) + \frac{\mathcal{O}(\wp)}{D^3} \\ &\leq \mathcal{O}(1)\|\nabla \tilde{X}_t^D\| \int_0^1 \text{Tot.Var.}(\tilde{b}_s^D)(\kappa_0) ds + \frac{\mathcal{O}(\wp)}{D^3},\end{aligned}$$

where we have used (4.4.4) and we have estimated the higher order term as in (4.4.5).

If $t_{i_1} < 1$ we compute

$$t_{i_2} = \min T_1,$$

where

$$T_1 = \left\{ t_i > t_{i_1} : 3 \leq \left(\sigma_{i_1+1} \dots \sigma_i + \frac{1}{\sigma_{i_1+1} \dots \sigma_i}\right) \leq 4 \right\}.$$

If $T_1 = \emptyset$ we stop the procedure and we perform a rotation in $[t_{i_1-1}, 1] = [0, 1]$ finding, for $t \in [t_{i_1-1}, 1]$

$$\begin{aligned}\text{Tot.Var.}(\hat{b}_t^D - \tilde{b}_t^D)(\kappa_0) &\leq \|\nabla \tilde{X}_t^D\| \frac{4}{D^2} \frac{1}{1 - t_{i_0}} \left(\sigma_{i_1-1} \dots \sigma_n + \frac{1}{\sigma_{i_0} \dots \sigma_n}\right) \\ &\quad + \frac{\mathcal{O}(\wp)}{D^3} \\ &\leq \mathcal{O}(1) \frac{1}{1 - t_{i_0}} \int_{t_{i_0}}^{t_{i_1}} \text{Tot.Var.}(\tilde{b}_s^D)(\kappa_0) ds + \frac{\mathcal{O}(\wp)}{D^3} \\ &\leq \mathcal{O}(1) \int_{t_{i_0}}^1 \text{Tot.Var.}(\tilde{b}_s^D)(\kappa_0) ds + \frac{\mathcal{O}(\wp)}{D^3}.\end{aligned} \tag{4.4.6}$$

If T_1 is non empty we perform a rotation in $[0, t_{i_1}]$ finding for $t \in [0, t_{i_1}]$ the following estimate

$$\begin{aligned}\text{Tot.Var.}(\hat{b}_t^D - \tilde{b}_t^D)(\kappa_0) &\leq \|\nabla \tilde{X}^D\| \frac{4}{D^2} \frac{1}{t_{i_1} - 1} \left(\sigma_1 \dots \sigma_{i_1} + \frac{1}{\sigma_1 \dots \sigma_{i_1}}\right) + \frac{\mathcal{O}(\wp)}{D^3 t_{i_1}} \\ &\leq \mathcal{O}(1) \int_0^{t_{i_1}} \text{Tot.Var.}(\tilde{b}_s^D)(\kappa_0) ds + \frac{\mathcal{O}(n\wp)}{D^3}.\end{aligned}$$

Again if $t_{i_2} = 1$ the procedure stops and we perform another rotation in $[t_{i_1}, t_{i_2}]$. If not we consider the set T_2 and we proceed.

The general step if the following: we consider the set

$$T_{j+1} = \left\{ t_i > t_{i_j} : 3 \leq \left(\sigma_1 \cdot \cdots \cdot \sigma_i + \frac{1}{\sigma_1 \cdot \cdots \cdot \sigma_i} \right) \leq 4 \right\}.$$

If T_{j+1} is empty, then we perform a rotation in $[t_{i_{j-1}}, 1]$ finding for $t \in [t_{i_{j-1}}, 1]$ the same estimate as (4.4.6). If T_{j+1} is non empty, we perform a rotation in $[t_{i_{j-1}}, t_{i_j}]$ and we consider

$$T_{j+2} = \left\{ t_i > t_{i_{j+1}} : 3 \leq \left(\sigma_1 \cdot \cdots \cdot \sigma_i + \frac{1}{\sigma_1 \cdot \cdots \cdot \sigma_i} \right) \leq 4 \right\}.$$

At the end of this procedure there are two possible scenarios: let $n' = \sup\{j : T_j \neq \emptyset\}$. If $t_{i_{n'}} = 1$, the procedure ends by performing a rotation in $[t_{i_{n'-1}}, 1]$. If we find $t_{i_{n'}} < 1$ with the property that

$$\left(\sigma_{i_{n'}+1} \ldots \sigma_i + \frac{1}{\sigma_{i_{n'}+1} \ldots \sigma_i} \right) \leq 3$$

for all $i = i_{n'} + 1, \ldots, n$, the construction ends with a rotation in $[t_{i_{n'-1}}, 1]$ (as in the case of the estimate (4.4.6)).

In particular, for each subsquare κ_0 we find a sequence of times $\{t_{i_j}(\kappa_0)\}$, $j = 1, \ldots, n'(\kappa_0)$, where we are performing a rotation. There are two cases to be considered: if $T_0(\kappa_0)$ is empty then

$$\text{Tot.Var.}(\hat{b}_t^D - \tilde{b}_t^D)(\kappa_0) \leq \frac{\mathcal{O}(1)}{D^2},$$

otherwise

$$\text{Tot.Var.}(\hat{b}_t^D - \tilde{b}_t^D)(\kappa_0) \leq \mathcal{O}(1) \| \text{Tot.Var.}(\tilde{b}^D)(\kappa_0) \|_\infty + \frac{\mathcal{O}(n_\wp)}{D^3}.$$

Summing over all possible κ_0 we find that

$$\begin{aligned} \text{Tot.Var.}(\hat{b}_s^D)(K) &\leq \text{Tot.Var.}(\tilde{b}_s^D)(K) + D^2 \left(\frac{\mathcal{O}(n_\wp)}{D^3} + \frac{\mathcal{O}(1)}{D^2} \right) + C_2 \| \text{Tot.Var.}(\tilde{b}^D)(K) \|_\infty \\ &\leq \text{Tot.Var.}(\tilde{b}_s^D)(K) + C_1 + C_2 \| \text{Tot.Var.}(\tilde{b}^D)(K) \|_\infty \end{aligned}$$

if $D \gg 1$, therefore we can conclude the proof finding a positive constant $C > 0$ such that

$$\| \text{Tot.Var.}(\hat{b}^D)(K) \|_\infty \leq C_1 + C_2 \| \text{Tot.Var.}(\tilde{b}^D)(K) \|_\infty$$

which is the desired estimate. □

Remark 4.4.5. The same result can be obtained for the d-dimensional case, by using the maps of Section 4.1.1 and Remarks 4.2.4 and 4.3.2.

Appendix Mixing

Proof of Lemma 1.1.8. By the Ergodic Theorem, $T = X_{t=1}$ is ergodic iff

$$\frac{1}{n}\sum_{i=0}^{n-1} \chi_{T^i(A)} \to_{L^1} |A|$$

In particular, if T is ergodic, then by writing

$$\frac{1}{n}\int_0^n \chi_{X_t(A)} dt = \int_0^1 \frac{n-1}{n}\left(\frac{1}{n-1}\sum_{i=0}^{n-1} \chi_{T^i(X_s(A))}\right) ds$$

we see that

$$⨍_0^t \chi_{X_s(A)} ds \to_{L^1} |A|.$$

It is immediate to find a counterexample to the converse implication: just consider rotation of the unit circle with period 1.

The proof of the implication $\Rightarrow$ in the second point is analogous. For the converse, let $A, B \in \Sigma$ such that

$$\frac{1}{n}\sum_{i=0}^{n} \left[|T^i(A) \cap B| - |A||B|\right]^2 > \epsilon.$$

By the continuity of $s \mapsto X_s$ in the neighborhood topology we have that there exists $\bar{s}$ such that for $0 \le s \le \bar{s}$ it holds

$$\left|X_s(B) \triangle B\right| = \left|B \triangle (X_s)^{-1}(B)\right| < \frac{\epsilon}{2}.$$

Hence we can write

$$\begin{aligned}
⨍_0^n \left[|X_t(A) \cap B| - |A||B|\right]^2 dt &\ge \frac{n}{T}\int_0^{\bar{s}} \frac{1}{n}\sum_{i=0}^{n-1} \left[\left|X_s(T^i(A)) \cap B\right| - |A \cap B|\right]^2 ds \\
&= \int_0^{\bar{s}} \frac{1}{n}\sum_{i=0}^{n-1} \left[\left|T^i(A) \cap (X_s)^{-1}(B)\right| - |A \cap B|\right]^2 ds \\
&\ge \int_0^{\bar{s}} \frac{1}{n}\sum_{i=0}^{n-1} \left[\left|T^i(A) \cap B\right| - |A \cap B|\right]^2 ds - \bar{s}\frac{\epsilon}{2} > \bar{s}\frac{\epsilon}{2}
\end{aligned}$$

for $n \gg 1$. Hence

$$\liminf ⨍_0^T \left[|X_t(A) \cap B| - |A||B|\right]^2 dt \neq 0.$$

Finally, if T is strongly mixing, the continuity of $s \mapsto X_s$ in the neighborhood topology gives that $s \mapsto X_s^n = X_s \circ T^n$ is a family of equicontinuous functions, and since for all s fixed

$$\lim_{n\to\infty} |X_s(T^n(A)) \cap B| = |A||B|$$

we conclude that X_s^n converges to 0 uniformly in s. The opposite implication is trivial. □

Dynamic blocking problems of fire propagation

In this part of the thesis we study a dynamic blocking problem first proposed by Bressan in [12]. The problem is concerned with the model of wild fire spreading in a region of the plane $\mathbb{R}^2$ and the possibility to block it constructing some *barriers* in real time. If we denote by $R(t) \subset \mathbb{R}^2$ the region burned by the fire at time t, then we can describe it as the reachable set for a differential inclusion. More precisely, one considers the Cauchy Problem

$$\dot{x} \in F(x), \qquad x(0) \in R_0, \tag{4.4.7}$$

where the set $R_0 \subset \mathbb{R}^2$ represents the region burnt by the fire at the initial time $t = 0$ while the function F describes the speed of spreading of the fire. The set $R_0 \subset \mathbb{R}^2$ is assumed to be open, bounded, non empty and connected with Lipschitz boundary, whereas the standard assumptions on F are:

1. there exists $r > 0$ such that $B_r(0) \subset F(x) \quad \forall x \in \mathbb{R}^2$;
2. $F(x)$ is compact and convex $\forall x \in \mathbb{R}^2$;
3. $x \to F(x)$ is continuous in the Hausdorff topology.

If no barriers are present the *reachable set* for the differential inclusion is

$$R(t) = \Big\{ x(t), \quad x(\cdot) \text{ abs. cont.}, x(0) \in R_0, \dot{x}(\tau) \in F(x(\tau)) \text{ for a.e. } \tau \in [0,t] \Big\}.$$

When the fire starts spreading, a fireman can construct some barriers, modeled by a one-dimensional rectifiable set $\zeta \subset \mathbb{R}^2$, in order to block the fire. More in detail, we consider a continuous function $\psi : \mathbb{R}^2 \to \mathbb{R}_+$ together with a positive constant $\psi_0 > 0$ such that $\psi \geq \psi_0$. If we denote by $\zeta(t) \subset \mathbb{R}^2$ the portion of the barrier constructed within the time $t \geq 0$, we say that ζ is an admissible barrier (or admissible strategy) if

1. (H1) $\zeta(t_1) \subset \zeta(t_2)$, $\forall t_1 \leq t_2$;
2. (H2) $\int_{\zeta(t)} \psi d\mathcal{H}^1 \leq t, \quad \forall t \geq 0,$

where $\mathcal{H}^1$ denotes the one-dimensional Hausdorff measure. Once we have an admissible strategy ζ, then we define the reachable set for ζ at time t the set

$$R^\zeta(t) = \Big\{ x(t) : x \text{ abs. cont.}, \dot{x}(\tau) \in F(x(\tau)) \text{ for a.e. } \tau \in [0,t], x(\tau) \notin \zeta(\tau) \ \forall \tau \in [0,t] \Big\}. \tag{4.4.8}$$

Definition 4.4.6. Let $t \to \zeta(t)$ be an admissible strategy. We say that it is a *blocking* strategy if

$$R^\zeta_\infty \doteq \bigcup_{t \geq 0} R^\zeta(t)$$

is a bounded set.

We call *isotropic* the case in which the fire is assumed to propagate with unit speed in all directions, while the barrier is constructed at a constant speed $\sigma > 0$, namely

$$F \equiv \overline{B_1(0)}, \quad R_0 = B_1(0), \quad \psi \equiv \frac{1}{\sigma}, \tag{4.4.9}$$

where $\overline{B_1(0)}$ denotes the closure of the unit ball of the plane centered at the origin. The existence of admissible blocking (or winning) strategies for the isotropic blocking problem is a very challenging open problem and it has been addressed mainly in [12],[15].[1]. In particular, the following theorems hold:

Theorem 4.4.7. *Assume that* (4.4.9) *hold. Then if* $\sigma > 2$ *there exists an admissible blocking strategy.*

Theorem 4.4.8. *Assume that* (4.4.9) *hold. Then if* $\sigma \leq 1$ *no admissible blocking strategy exists.*

The two theorems are proved in [12] and they motivate the following Fire Conjecture [1]:

Conjecture 4.4.9. Let (4.4.9) hold. Then if $\sigma \leq 2$ no admissible blocking strategy exists.

For a survey of results related to the previous conjecture, see [13].

Equivalent formulation. Throughout the paper we will use the following equivalent formulation of the dynamic blocking problem (for a proof of the equivalence, see [18]): let $Z \subset \mathbb{R}^2$ be a rectifiable set. We denote by

$$R^Z(t) = \{x(t) : x \text{ abs. cont.}, \dot{x}(\tau) \in F(x(\tau)) \text{ for a.e. } \tau \in [0,t], x(\tau) \notin Z \ \forall \tau \in [0,t]\}. \tag{4.4.10}$$

We say that the strategy Z is *admissible* if

$$\mathcal{H}^1(Z \cap \overline{R^Z(t)}) \leq \sigma t. \tag{4.4.11}$$

Similarly to the previous formulation we denote by

$$R^Z_\infty = \bigcup_{t \geq 0} R^Z(t) \tag{4.4.12}$$

the burned region and we say that Z is an admissible blocking strategy if R^Z_∞ is bounded. The advantage of this description is that the barrier is fixed and it does not grow while the time evolves.

One can easily prove that if the strategy Z consists of a simple closed curve, then it is not admissible for $\sigma \leq 2$, but only partial results are present in the literature if the strategy has more complicated structures, as for example the presence of internal barriers that slow down the fire. One possible idea to prove the conjecture would be to investigate the shape of a strategy which is *optimal* among admissible strategies, allowing for the presence of some internal barriers.

Optimization problem. To define an optimization problem one introduces the following cost functional

$$J(Z) = \int_{R^Z_\infty} \kappa_1 d\mathcal{L}^2 + \int_Z \kappa_2 d\mathcal{H}^1, \tag{4.4.13}$$

[1] One can prove that the existence of blocking strategy does not depend on the starting set R_0 but only on the speed σ [13]

among all possible admissible blocking strategies, where $\kappa_1, \kappa_2 : \mathbb{R}^2 \to \mathbb{R}_+$ are two non-negative continuous functions. In [17] it is proved that, if the class of admissible blocking strategies is non-empty, then there exists an optimal strategy. Moreover, there exists an optimal strategy Z^* which is *complete*:

Definition 4.4.10. Let $Z \subset \mathbb{R}^2$ be a rectifiable set. Z is complete if it contains all its points of positive upper density, that is, let $x \in \mathbb{R}^2$ such that

$$\limsup_{r \to 0^+} \frac{\mathcal{H}^1(Z \cap B_r(x))}{2r} > 0 \Longrightarrow x \in Z.$$

The following corollary also holds [18]:

Corollary 4.4.11. *If there exists an admissible blocking strategy Z with $\mathcal{H}^1(Z) < \infty$, then there exists an optimal blocking strategy Z^* such that*

$$Z^* = (\cup_i Z_i) \cup \mathcal{N},$$

where Z_i are countably many compact rectifiable connected components and $\mathcal{H}^1(\mathcal{N}) = 0$.

We mention also the recent result in [16] where it is proved that the optimal strategy is nowhere dense. Giving necessary conditions for optimality is a hard question. Some results are obtained in [19] assuming some further regularity on the optimal strategy.

Minimum time function and Hamilton-Jacobi formulation. The propagation of fire can be described also in terms of the minimum time function

$$u(x) \doteq \inf\{t \geq 0; \quad x \in R^Z(t)\}. \tag{4.4.14}$$

The function u is the time needed for the fire to reach the point x in the burned region, without crossing the barrier. The minimum time function can be computed by solving an Hamilton-Jacobi equation with obstacles, namely

$$\begin{cases} |\nabla u(x)| \leq 1 & x \notin Z, \\ u(x) = 0 & x \in R_0. \end{cases} \tag{4.4.15}$$

For the properties of the solution of (4.4.15) we refer to [25].

4.5 Optimality conditions and a case study

The aim of this first part of the work is to present some new techniques that help to determine the shape of the optimal strategy Z without asking any further regularity assumption. These techniques can be used to prove the conjecture in the specific case the optimal Z is assumed to be the union of an external barrier Z^2 which is a simple closed curve and an internal barrier Z^1 which is a segment. We remark that our analysis is independent of the regularity of the barrier Z, which is assumed to be only rectifiable and complete, differently from what has been derived in [12], [19] where the $\mathcal{C}^1$ and $\mathcal{C}^2$ regularity were respectively required. For our result will be of key importance to assume that $\sigma < 2$, but this is enough. Indeed one can prove that if no admissible blocking strategy exists for $\sigma < 2$, then it cannot exist for $\sigma = 2$. To be more precise, if by contradiction there exists a blocking strategy for $\sigma = 2$, we can always consider a new strategy for the starting set $R_0 = B_{\frac{1}{2}}(0)$ which is constructed with a speed $\sigma' < 2$. Therefore, by using a rescaling argument, the confinement could be achieved for σ' starting from $R_0 = B_1(0)$. We remark that we will address mainly the optimization

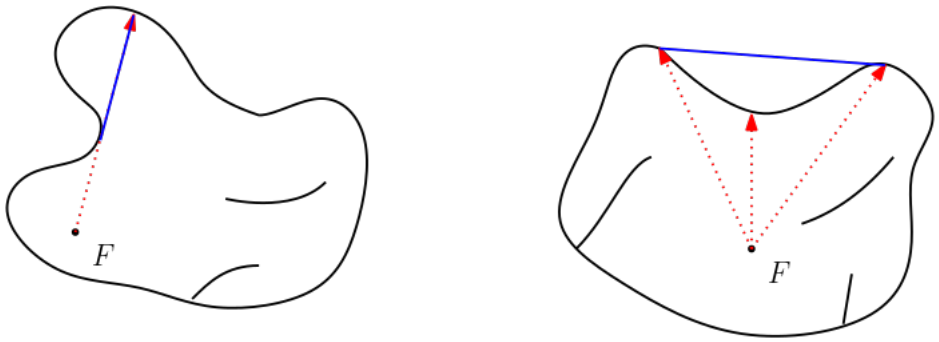

Figure 4.7: The new barrier obtained replacing the old one with the blue portion is still admissible and star shaped (left picture) and convex (right picture).

problem 4.4.13 with $\alpha = 0, \beta = 1$, that is we will find necessary conditions for optimal strategies that minimize the length functional.

Techniques. We start our analysis with the assumption of having an admissible blocking strategy Z (not necessarily optimal). As written above we will always write $Z = Z^2 \cup Z^1$ (see Chapter 5 for further details). We look for some deformations $(Z^2)'$ of the external barrier Z^2 that keep the new barrier admissible, but with shorter length. In particular we prove in Chapter 6 the following two results (see Figure 4.7):

- If $Z = Z^2 \cup Z^1$ is an admissible blocking strategy, then there exists an admissible blocking strategy $Z' = (Z')^2 \cup (Z')^1$ with the following property: $(Z^2)'$ is star-shaped with respect to the direction of fire rays. Moreover $\mathcal{H}^1(Z') \leq \mathcal{H}^1(Z)$ and $\mathcal{L}^2(\overline{R^{Z'}_\infty}) \leq \mathcal{L}^2(\overline{R^Z_\infty})$, where $\mathcal{L}^2$ is the two-dimensional Lebesgue measure.

- If $Z = Z^2 \cup Z^1$ is an admissible blocking strategy, then there exists an admissible blocking strategy $Z' = (Z^2)' \cup Z^1$ with the following property: $(Z^2)'$ is convex with respect to the direction of fire rays in the points of $(Z^2)'$ where it does not touch the internal barriers Z^1. Moreover $\mathcal{H}^1(Z') \leq \mathcal{H}^1(Z)$.

For the definitions of star-shaped/convex w.r.t. the direction of the fire rays we refer the reader to Chapter 6. Anyway, the main idea that will be used to derive some new interesting features of the optimal strategy is the following homotopy argument: assume that Z is an optimal blocking strategy. Then, if two portions of the external barrier Z^2 are burning *simultaneously*, they are two segments. With portions of the barrier we mean arcs $\eta : [0,1] \to \mathbb{R}^2$ whose images are subsets of the strategy Z. Two disjoint *boundary* arcs η_1, η_2 (that is, subsets of the external barrier Z^2) are burning simultaneously (see for example Figure 4.8) if

$$\eta_i([0,1]) \cap \overline{R^Z(\tau)} \setminus \cup_{\tilde{\tau}<\tau} R^Z(\tilde{\tau}) \neq \emptyset, \quad i = 1,2, \quad \forall \tau \in [t_0, t_1], \text{ for some } t_0, t_1 \in [0,T].$$

The homotopy argument (Proposition 6.0.5) states that every perturbation of $\eta_i([0,1])$ with endpoints $\eta_i(0)$ and $\eta_i(1)$ and with shorter length is still admissible, therefore it yields a strategy with shorter length. The reason of this fact can be heuristically understood in the following way: when one considers the function $t \to \mathcal{H}^1(Z \cap \overline{R^Z(t)})$ which describes the length of the set Z which is burned up to the time t, if two portions of the barrier are burning simultaneously, then the *burning rate*

$$\frac{d}{dt}\mathcal{H}^1(Z \cap \overline{R^Z(t)}) \geq 2 > \sigma,$$

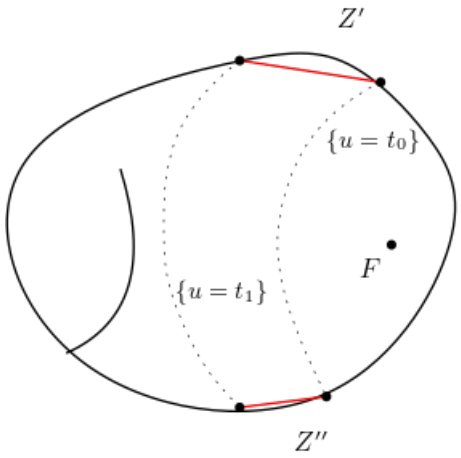

Figure 4.8: The two arcs Z', Z'' are burning simultaneously.

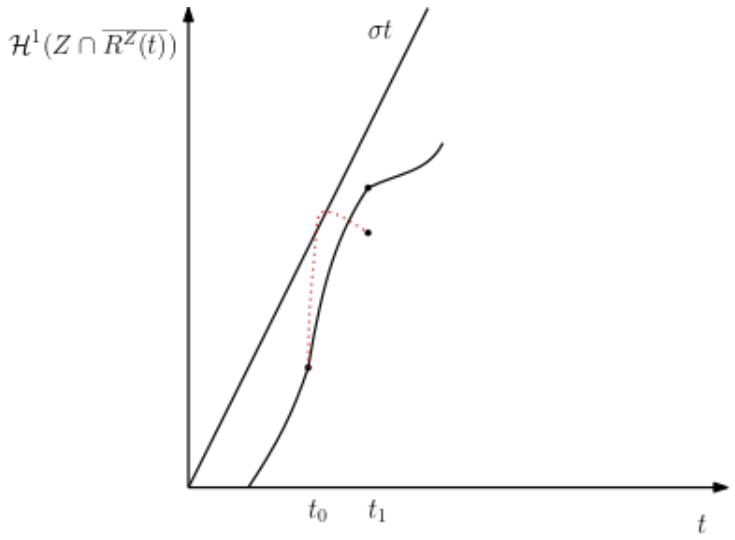

Figure 4.9: If a perturbation of the barrier that shortens the length is not admissible, then the burning rate should be lower than σ in some time interval, yielding a contradiction.

since the fire moves with speed 1 (this is the reason why we are focusing on the case $\sigma < 2$). Consider now a perturbation of the barrier (*homotopy*) that shortens the length (the red curve in Figure 4.9). If by contradiction the new curve is not admissible, then its burning rate should be lower than σ for some time interval, which contradicts the fact that we are still burning two branches of the barrier, thus with burning rate greater than 2 (which is strictly greater than σ).

Clearly the homotopy argument cannot be used on internal walls, since we have no way to take control of the admissibility of the barrier. This idea simplifies the understanding of the shape of the external barrier for the optimal strategy (where optimal refers to the curves with minimum length), but yields also an interesting byproduct. Let us assume that $Z = Z^2 \cup Z^1$ is the optimal strategy, where Z^2 is a simple closed curve and Z^1 is a single internal barrier. Then Z must be connected (see Lemma 6.1.2). One conjectures indeed that the optimal strategy should be connected, since constructing disconnected portions of walls seems a bad strategy, but this question is still wide open for more complicated strategies.

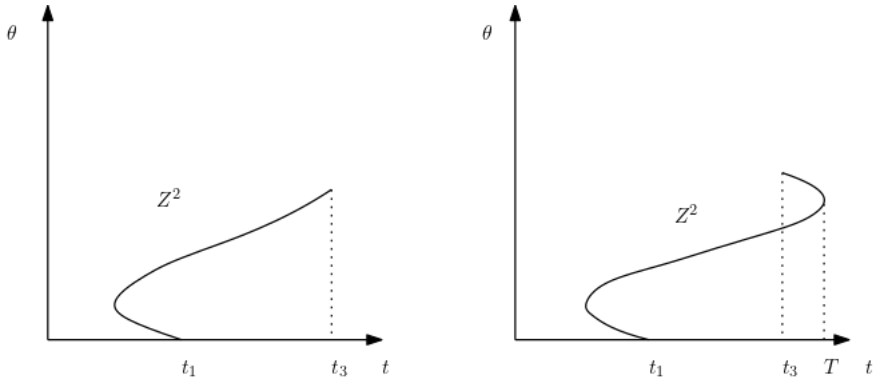

Figure 4.10: Shape of the optimal strategy, if the first point burning on Z^2 P is reached in a time $u(P) < t_1$.

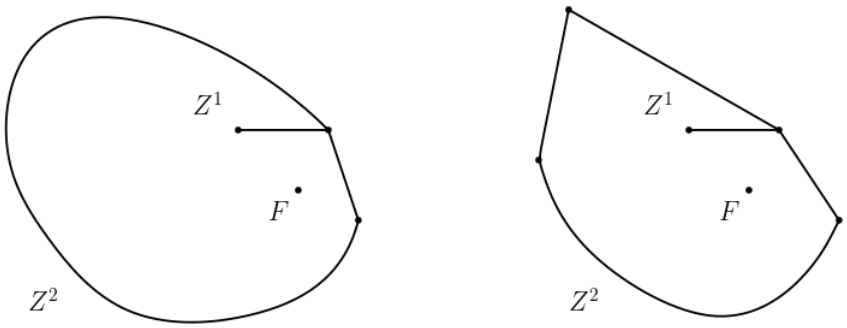

Figure 4.11: A segment and a branch of logarithmic spiral vs a segment, a branch of logarithmic spiral and two segments.

With these simplifications at hand we can treat a first case study in which the optimal strategy $Z = Z^2 \cup Z^1$ is the union of a single closed curve and of a segment Z^1 that touches Z^2 in some point O. Here the assumption is to work with the optimal strategy for the optimization problem $\alpha = 0$ and $\beta = 1$, allowing us to assume the convexity of the strategy and to use the homotopy.

It will be of key importance the following observation (which is valid not only in the assumption Z^1 is a segment but assuming Z^1 is a single curve): call $Z^2(t) = Z^2 \cap \{u = t\}$, where u is the minimum time function. Then we will prove (Chapters 6,10) that

$$\sharp Z^2(t) \leq 2.$$

This observation is fundamental: indeed, if one call $\zeta : [0, 2\pi] \to \mathbb{R}^2$ a parametrization for the external barrier Z^2, the only possibilities that one can have are the two of Figure 4.10. The analysis of Chapter 10 shows that the left picture consists of a segment and a branch of logarithmic spiral, while the right configuration is associated to a curve which is a union of a segment, a branch of logarithmic spiral and two segments, as in Figure 4.11. The analysis in Subsection 6.1.3 shows that the optimal barrier cannot have two segments joining at some points, excluding therefore the case of the second picture. Once we know exactly the shape of the optimal strategy, we can easily verify if it is admissible or not. In particular, the computations of Section 7.1 show that the branch of the spiral cannot close, giving a contradiction. Extending this analysis to the case in which Z^1 is any single curve is far from trivial and it is object of the next section.

4.6 Non admissibility of spiral-like strategies

This second part is devoted to the study of spiral-like strategies: namely, admissible barriers that are constructed putting all the effort on a single branch. The study of spiraling strategies is of key importance in the study of Bressan's Fire conjecture, indeed there is a strongly belief that these strategies are the best possible barriers that can be constructed when $\sigma \leq 2$. To be more precise,

Definition 4.6.1 (Spiral-like strategy)**.** Let $Z = \zeta([0,S]) \subset \mathbb{R}^2$ be an admissible strategy, where ζ is a parametrization by length. We say that it is a spiral-like strategy if it satisfies:

- $[0,S] \ni s \mapsto \zeta(s) \in \mathbb{R}^2$ is a Lipschitz curve, and $\zeta\llcorner_{[0,S)}$ is simple;
- $s \mapsto u \circ \zeta(s)$ is increasing.

Finally, we say that Z is an admissible spiral if it is a spiral-like strategy, the curve is locally convex, in the sense of Definition 8.0.2 and moreover it is admissible according to (H1) and (H2). In addition to the parametrization by arc-length, it is possible to parametrize any admissible spiral by $(r(\phi),\phi)$, where ϕ denotes the angle of rotation on the spiral, which is defined in Lemma 8.1.1 (see Equation (8.1.1)) while $r(\phi)$ represents the length of the final segment of the fire ray reaching the point $(r(\phi),\phi)$, as explained in Figure 8.2. See also Remark 8.0.3.

The only results known on these barriers can be found in [15] and [34]. In the two papers it is proved independently and with different techniques the following

Theorem 4.6.2. *Let $\sigma > 2.6144..$ (critical speed). Then there exists a spiral-like strategy which confines the fire.*

The proof of this result is obtained by the study of a particular spiral, that we will call *saturated spiral*. Let S be an admissible spiral. We say that S is a saturated spiral if

$$\mathcal{S}(S) = \{t \in [0,T] : \mathcal{H}^1(S \cap \overline{R^S(t)}) = \sigma t\} = [0,T]. \tag{4.6.1}$$

Saturated spirals (or portions of it) are thought to be building blocks for optimal strategies. Indeed, it has been proved in [20] that, if $\sigma > 2$, the optimal strategy (that minimizes the cost functional (4.4.13)) among simple closed curves is made by an arc of circle and two branches of logarithmic spirals. One can prove that there are intimate relations between logarithmic spirals and saturated spirals. Also, referring to the previous discussion, we will prove that for $\sigma < 2$, if a strategy Z is optimal ($\kappa_1 = 0, \kappa_2 = 1$) and its internal barrier is a segment, then the boundary ∂R^Z_∞ is made by a segment and a branch of logarithmic spiral.

The proof of Theorem 4.6.2 relies on the following fact: consider the parametrization of a saturated spiral S given by $(r(\phi),\phi)$ (Remark 8.0.3), where $r(\phi)$ represents the length of the fire ray that does not coincide with a portion of the barrier (see Figure 8.2). Then the radius of S satisfies the following Cauchy Problem

$$\frac{dr}{d\phi} = r(\phi)\cot\alpha - \frac{r(\phi-(2\pi+\alpha))}{\sin\alpha}, \tag{4.6.2}$$

with initial data

$$r(\phi) = \begin{cases} e^{\cot\alpha\,\phi} & \forall \phi \in [0,2\pi], \\ (e^{2\pi\cot\alpha}-1)e^{\cot\alpha(\phi-2\pi)} & \forall \phi \in [2\pi, 2\pi+\alpha]. \end{cases}$$

where α satisfies

$$\alpha = \arccos\left(\frac{1}{\sigma}\right), \tag{4.6.3}$$

(this is precisely the approach followed by [34]). Observe that for $\phi < 2\pi$ the solution is $r(\phi) = e^{\cot\alpha\phi}$ which is the logarithmic spiral. A study of the eigenvalues of the operator associated to the previous RDE (Section 8.1) gives the proof of Theorem 4.6.2 (see also Subsection 8.1.2). Actually, if a player constructs any admissible spiral and at some point it decides to construct a saturated spiral, that is a branch that satisfies the length constraint of Definition 4.6.1, then for $\sigma > 2.6144$ it manages to block the fire. This is the content of Proposition 8.1.6 and is due to the complex spectrum of the operator of (8.1.8). We are interested in the converse of Theorem 4.6.2, namely

Conjecture 4.6.3. If $\sigma \leq 2.6144...$ then no spiral-like strategy is admissible.

A partial answer to this conjecture has been given in [34] where the authors use a geometric argument to prove the following

Theorem 4.6.4. *If $\sigma \leq \frac{1+\sqrt{5}}{2}$ then no spiral-like strategy is admissible.*

The aim of this part of the thesis is to extend the previous theorem to higher values of σ and to provide a general framework for the study of spirals (or more complicated strategies). We will prove the following

Theorem 4.6.5. *No admissible spiral-like strategy confines the fire if $\sigma \leq 2.3$.*

We do not know if the bound 2.3 is sharp since it is obtained by purely numerical computations. We believe that a slightly different variation of the approach we propose may allow us to reach even higher values of σ: this is currently under investigation. The critical case $\sigma = 2.6144..$ at the present time seems out of reach and very delicate. We underline that Theorem 4.6.5 proves Bressan's Fire Conjecture in the case of spiral strategies.

We discuss here the general idea of our approach: let $Z = \zeta([0, S])$ be an admissible spiral-like strategy and let $(r(\phi), \phi)$ be its parametrization by angle (see Section 8, Remark 8.0.3). Assume that for every point $\zeta(s)$ of the barrier you can assign an element of the following family of generalized barriers, that is

Definition 4.6.6 (Family of Generalized Barriers)**.** We say that $f_s \in \mathrm{SBV}([0, +\infty); \mathbb{R})$, with $s \in [0, S]$, is an element of the family of generalized barriers $\mathcal{F}_Z$ if:

- $f_0(\phi) > 0$ for $\phi \in [0, +\infty)$;
- $f_s(\phi) = r(\phi)$ for every $\phi \leq \bar{\phi}$ whenever $\zeta(s) = (r(\bar{\phi}), \bar{\phi})$.

Moreover, we say that it is a *diverging family* if, calling

$$\bar{f}_s(\phi) = \lim_{h\to 0} \frac{f_{s+h}(\phi) - f_s(\phi)}{h}, \tag{4.6.4}$$

then $\bar{f}_s(\phi) \geq 0$ for every $\phi \in [0, \infty)$.

See Figure 4.12. We remark that the parametrization $(\phi, r(\phi))$ of the optimal barrier Z chosen at the beginning is an element of any family of generalized barriers, since it is f_S accordingly to the previous notation. A family of generalized barriers is NOT in general a family of admissible barriers, but it is a family of functions parametrized by the length parameter s. We are currently not able to write the right guess for the barrier of minimal radius at fixed $s \in [0, S]$, which would satisfy the definition naturally. Our main theorem is:

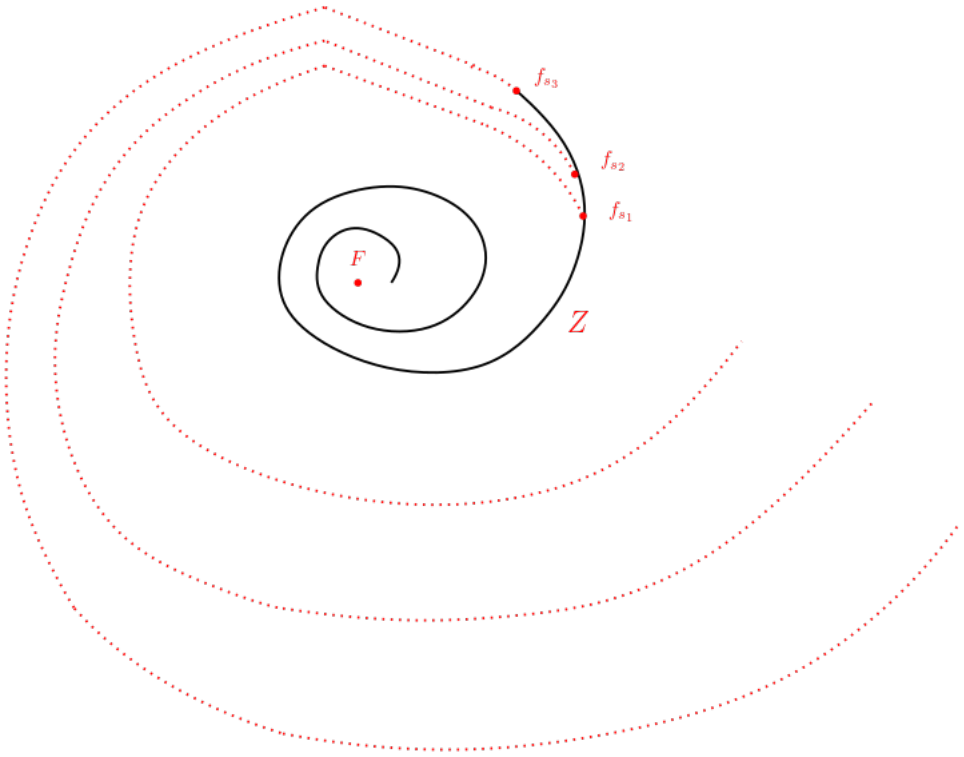

Figure 4.12: At every point an element of the family of generalized barriers is assigned.

Theorem 4.6.7. *Let Z be as before and assume that there exists a family of generalized barriers $\{f_s\} = \mathcal{F}_Z$ which is diverging. Then Z does not confine the fire.*

The proof of this fact is very easy and relies on the following observation: by the fundamental theorem of calculus we have that

$$f_s(\phi) = f_0(\phi) + \int_0^s \bar{f}_\eta(\phi) d\eta.$$

By the diverging condition on the family $\mathcal{F}_Z$ it holds then that

$$f_s(\phi) \geq f_0(\phi), \quad \forall \phi \geq 0, \forall s \in [0, S],$$

therefore

$$f_S(\phi) \geq f_0(\phi) > 0,$$

by the first assumption on the family. But since $f_S(\phi)$ is $r(\phi)$ one concludes that the radius of Z is always positive. This also proves that $f_0(\phi)$ is the best strategy we can do (even if it could be non-admissible, thus living in the family $\mathcal{F}_Z$). By Theorem 4.6.7, the proof of Theorem 4.6.5 follows by exhibiting a diverging family of generalized barriers for $\sigma \leq 2.3$.

The motivation for this construction can be explained as follows: given a spiral Z defined up to an angle $\bar{\phi}$, corresponding to a point $\zeta(s) = (\bar{\phi}, r(\bar{\phi}))$, the strategy $(\phi, f_s(\phi))$ with $\phi \geq \bar{\phi}$ represents the best spiral-like barrier that a player can place in order to enclose the fire. This gives a lower bound on the radius of any admissible spiral $r(\phi) \geq f_0(\phi) > 0$ which is strictly positive by definition of family of generalized barriers. Being $r(\phi) > 0$ strictly positive for every choice of ϕ, for every admissible spiral-like strategy, then no spiral can confine the fire.

Setting this framework for the study of spirals has been extremely hard. One of the main issues of this procedure is that, in general, finding a diverging family of generalized barriers is a difficult task. First of all, we did many guesses for the shape of f_s and the most reasonable failed to be correct (here the need to introduce the concept of generalized barriers). Moreover, the proofs of these results are based on numerical computations, which make hard to take under control how the strategies evolve. The possibility to perform an analytical proof of these results is currently under investigation, but we strongly believe that at some point one needs to use machine-based computations. Anyway, we are strongly convinced that this new method to prove the non-admissibility of strategies could be promising in the study of the fire problem and could be adapted to more general cases.

4.6.1 Construction of the family of generalized barriers.

Summarizing, in order to prove the non-admissibility of spiral-like strategies, we need to find a diverging family of generalized barriers. Let Z be an admissible spiral, then for every $P \in Z$ we define the Admissibility Functional $\mathcal{A}$ as

$$\mathcal{A}(P) = u(P) - \frac{1}{\sigma} L(P) \geq 0,$$

where $L(P)$ is the length of the spiral from the starting point until P. This is precisely the admissibility condition (H2) for spirals. Then we have the following geometric result (which is the content of Chapter 9):

Proposition 4.6.8. *Let Z be an admissible spiral-like strategy and let $(r(\phi), \phi)$ be its parametrization by angle. Fix any $\bar{\phi}$ and consider the following strategy $\hat{Z}$ parametrized by $(\hat{r}(\phi), \phi)$ such that:*

- *$\hat{r}(\phi) = r(\phi)$ for every $\phi \leq \bar{\phi}$;*
- *$(r(\phi), \phi) \subset \{u = u((r(\bar{\phi}), \bar{\phi})\}$ for $\phi \in [\bar{\phi}, \bar{\phi} + \Delta\bar{\phi}]$ (it is a subset of the level set of the minimum time function u);*
- *$(r(\phi), \phi))$ for $\phi \in [\bar{\phi} + \Delta\bar{\phi} = \phi_1, \phi_2]$ is a segment of endpoints P_1, P_2 such that $P_1 \in \{u = u((r(\bar{\phi}), \bar{\phi})\}$ and P_2 is saturated, that is $\mathcal{A}(P_2) = 0$. Moreover the segment P_1P_2 is tangent to $\{u = u((r(\bar{\phi}), \bar{\phi})\}$ in P_1.*
- *$r(\phi)$ is solution to the following RDE*

$$\dot{r}(\phi) = \cot\alpha r(\phi) - \frac{r(\phi - 2\pi - \alpha)}{\sin\alpha},$$

for $\phi \geq \phi_2$ (or, in other words, it is a saturated spiral).

Then we have that, for $\phi \in [\bar{\phi}, \bar{\phi} + 2\pi]$ it holds

$$r(\phi) \geq \hat{r}(\phi).$$

This result states that, for fixed Z admissible spiral and fixed angle $\bar{\phi}$, the following **optimization problem**

$$\min_{\tilde{Z} \in \mathcal{A}_S(Z, \bar{\phi})} r_{\tilde{Z}}(\phi), \qquad \text{for some } \phi \geq \bar{\phi}, \tag{4.6.5}$$

where $\mathcal{A}_S(Z, \bar{\phi})$ denotes the class of admissible spirals that coincide with Z up to the angle $\bar{\phi}$, and if $\tilde{Z} \in \mathcal{A}_S(Z, \bar{\phi})$, $(r_{\tilde{Z}}(\phi), \phi)$ will denote its parametrization by angle, admits

a minimizer if $\phi \in [\bar{\phi}, \bar{\phi} + 2\pi]$. In particular, it is possible to write down explicitly the shape of this minimizer, which is precisely given by the proposition. It is not clear at all if it is possible to determine the existence/uniqueness of the minimizer for bigger angles ϕ, and also to exhibit the explicit shape of it.

The above proposition is the main reason why we considered at the beginning the following family of generalized barriers: at each point $P = \zeta(s)$ of the spiral the element of the family $f_s(\phi)$ is the length of the radius of a spiral-like strategy Z_s (not necessarily admissible), with parametrization by angle given by $(f_s(\phi), \phi)$ with the following properties: it is a subset of the level set $\{u = u(P)\}$, then it continues as a segment whose last endpoint is saturated (in the sense the admissibility functional is zero at that point) and then it is a saturated spiral, in the sense it satisfies the RDE (8.1.8) (see again Figure 4.12). Actually, this construction did not produce a diverging family of generalized barriers since there was always a tiny region in which $\bar{f}_s < 0$. Inspired by this (negative) result, we found out instead that the best strategy a player can do in order to confine the fire is to speed up the construction up to the critical value, that is: from the point $\zeta(s)$, the strategy Z_s is an an arc (subset of the level set of u), a segment (whose last point is saturated for the admissibility functional defined in (11.1.1)) and then it is a saturated spiral, but this time for the critical value $\sigma = 2.6144....$ We remark that this is not a family of admissible barriers, since we are using a construction speed which is higher than the one available (≤ 2.3), but every element is a *generalized* barrier. Computations show that in this case $\bar{f}_s > 0$, therefore this family is diverging and it is the right one to consider for proving Theorem 4.6.5.

The construction of the diverging family of generalized barriers is provided in Chapter 11.

4.6.2 Plan of the discussion

In Chapter 5 we set the fire problem, giving some useful preliminaries and definitions. In Chapter 6 we study the problem of optimal barriers for the Length functional (see the Optimization Problem (4.4.13)) and we prove some qualitative properties of the optimal strategy (as being star-shaped and convex). We describe also how to perform homotopies in order to derive some important properties of the boundary of the burned region (see Subsection 6.1). Connectedness of the optimal strategy and properties of the external barriers are discussed. Differently from what was previously done, we do not use any further regularity assumption on the barrier. In Chapter 10 we study in detail the case of an optimal strategy whose internal barrier is a segment. In chapter 8 we give the definition of admissible spirals, and we study their description via an ODE formulation (Section 8.1). In Chapter 9 we present the geometric motivation for the study of family of generalized barriers. Instead in Chapter 10 we prove that the first element of the family of generalized barriers for the critical speed $\bar{\sigma} = 2.6144..$ does not confine the fire. Finally in Chapter 11 we construct a diverging family of generalized barriers which gives the proof the main theorem 4.6.5. The numerical computations can be found in the Appendix 11.2.2.

Chapter 5

Setting of the Fire Problem

In this chapter we set the fire problem and we give some basic definitions on barriers. For a survey of the results related to Bressan's Fire Conjecture, see [13].

We consider the following objects:

- Z is a rectifiable set with finite length (our admissible strategy).
- $R_0 \subset \mathbb{R}^2$ is an open set, we will assume that $R_0 = B_r(0)$ with $r << 1$ (being equivalent to assume $R_0 = B_1(0)$). We will call it the *starting set*.
- The set Γ of admissible curves (trajectories of the fire) is given by

$$\Gamma = \{\gamma \in \mathrm{Lip}([0,1], \mathbb{R}^2), \gamma((0,1)) \cap Z = \emptyset, \dot{\gamma}(t) \in \overline{B_1(\gamma(t))} \text{ a.e. } t\}. \tag{5.0.1}$$

- The distance of two points is

$$d(x,y) = \inf\{L(\gamma), \gamma \in \Gamma, \gamma(0) = x, \gamma(1) = y\}. \tag{5.0.2}$$

The function u (**minimum time function**) is defined as

$$u(x) = \inf\big\{L(\gamma) : \gamma \in \Gamma, \gamma(0) \in R_0, \gamma(1) = x\big\}. \tag{5.0.3}$$

is the minimum time function for reaching a point $x \in \mathbb{R}^2$ from the starting set R_0.

Definition 5.0.1 (Optimal ray)**.** Let us fix a point $x \in \mathbb{R}^2$. An optimal ray from the starting set R_0 to the point x is a path $\bar{\gamma} : [0,1] \to \mathbb{R}^2$, $\gamma \in \mathrm{Lip}([0,1]; \mathbb{R}^2)$ with the following property: there exists $\{\gamma_n\} \subset \Gamma$, a minimizing sequence for 5.0.3, with $\gamma(0) \in R_0$ and $\gamma(1) = x$ such that $\gamma_n \to \bar{\gamma}$ uniformly. We will denote by $\bar{\gamma}_x$ an optimal ray starting from R_0 and reaching some point $x \in \mathbb{R}^2$. We call $\bar{\Gamma}$ the set of optimal rays.

We give the following

Definition 5.0.2 (Complete Strategy)**.** Let $Z \subset \mathbb{R}^2$ be an admissible strategy, then we say that Z is *complete* if it contains all its points of positive upper density, that is, if $x \in \mathbb{R}^2$ is such that

$$\limsup_{r \to 0} \frac{\mathcal{H}^1(Z \cap B_r(x))}{2r} > 0 \implies x \in Z. \tag{5.0.4}$$

In [17] it is proved that for any admissible strategy Z there exists a complete strategy $\tilde{Z} \supset Z$ such that $\mathcal{H}^1(\tilde{Z} \setminus Z) = 0$. One of the advantages of this assumption is the Corollary 2.5 in [17]. We recall that a set $A \subset \mathbb{R}^n$ is a continuum if it is compact and connected.

Corollary 5.0.3. *Let E be a set with $\mathcal{H}^1(E) < \infty$, and let $\tilde{E}$ be its completion with the points of positive upper density. If $C \subset \tilde{E}$ is a connected component of $\tilde{E}$, then C is a continuum.*

From now on we will assume that, if Z is an admissible strategy, then Z is complete.

5.0.1 Classification of arcs

Here and in the following we will always write $Z = Z^2 \cup Z^1$ where $Z^2 = \partial R^Z_\infty$ is a simple closed curve (**blocking barrier**) and $Z^1 = \overline{Z \setminus Z^2}$ are the internal barriers (or **delaying arcs**). This decomposition is general.

We call *arc* any (Jordan) curve Z', that is the image of a continuous injection $\psi : [0,1] \to \mathbb{R}^2$, which is contained in Z.

Definition 5.0.4. Let Z be an admissible strategy. We say that an arc $Z' \subset Z$ compact is burning within the time interval $[s,t] \subset [0,T]$ if $\sharp Z' \cap \overline{R^Z(\tau)} \setminus \cup_{\tilde{\tau}<\tau} \overline{R^Z(\tilde{\tau})} = 1 \; \forall \tau \in [s,t]$, where

$$s = \inf\{\tau : u(x) = \tau, \forall x \in Z'\}, \qquad t = \sup\{\tau : u(x) = \tau, \forall x \in Z' \setminus \cup_{\tilde{\tau}<\tau} \overline{R^Z(\tilde{\tau})}\}.$$

Moreover there exists $\eta : [s,t] \to \mathbb{R}^2$ parametrization such that $\eta(\tau) = Z' \cap \overline{R^Z(\tau)}$.

This definition tells us that we are considering arcs burning only on one side. The following lemma establishes the rate at which every arc is burned by the fire. As it is intuitive, since the speed of the fire is 1, this rate is greater than 1.

Lemma 5.0.5. *Let Z be an admissible strategy and assume that an arc $Z' \subset Z$ is burning within $[s,t] \subset [0,T]$. Then*

$$\mathcal{H}^1(Z' \cap \overline{R^Z(t')} \setminus R^Z(s')) \geq t' - s', \quad \forall t' > s', t', s' \in [s,t]. \tag{5.0.5}$$

Proof. This is an easy consequence of the fact that $|\nabla u| = 1$, where u is the minimum time function. □

The previous lemma gives as an immediate result the following corollary, that states that the burning rate of n portions of the barrier burning simultaneously is greater than n.

Corollary 5.0.6. *Let Z be an admissible barrier and let $Z_1, \dots, Z_n$ disjoint arcs of the barrier burning simultaneously within the time interval $[s,t]$. Then*

$$\mathcal{H}^1(Z_1 \cup \cdots \cup Z_n \cap \overline{R^Z(t')} \setminus R^Z(s')) \geq n(t' - s'), \quad \forall t' > s', t', s' \in [s,t]. \tag{5.0.6}$$

We will call burning rate the function

$$b(t) = \frac{d}{dt} \mathcal{H}^1(Z \cap \overline{R^Z(t)}) \tag{5.0.7}$$

in the points of differentiability of $\mathcal{H}^1(Z \cap \overline{R^Z(t)})$. Then, if n portions of the barrier are burning simultaneously, $b(t) \geq n$.

Thanks to the next lemma, we can imagine the fire as a point source F and we can assume that the admissible strategy Z is at a positive distance from it. Indeed, the following holds:

Lemma 5.0.7. *Let $Z = Z^2 \cup Z^1$ be an admissible strategy. Assume that $Z^2 \cap F \neq \emptyset$, then the strategy Z is not admissible.*

Proof. The proof of this lemma relies on the condition $\sigma < 2$. Let $\epsilon > 0$ and let $B_\epsilon(F)$ be some closed ball centered at F. Then $\mathcal{H}^1(Z \cap \overline{B_\epsilon(F)}) \geq 2\epsilon$, since Z^2 is a continuum that intersects $B_\epsilon(F)$ in F and two points of $\partial B_\epsilon(F)$ (see Lemma 3.4 [28]). But this contradicts the admissibility of Z, since $\mathcal{H}^1(Z^2 \cap \overline{R^Z(\epsilon)}) \geq 2\epsilon > \sigma\epsilon$. □

Remark 5.0.8. We observe first that, given an admissible barrier for the any open set R_0, then this barrier is admissible for any ball contained in R_0 (and viceversa, if a strategy is admissible for any ball, then it is admissible for any bounded open set R_0). Therefore one can consider the problem for $R_0 = B_1(0)$ or even for $R_0 = (0,0)$ with the barrier at a positive distance (Lemma 5.0.7). A simple rescaling of the barrier then allows us to work in the following framework: we will always assume that the fire starts spreading in the point $(0,0)$ and the barrier is constructed in the point $(1,0)$ and

$$F \equiv \overline{B_1(0)}, \quad R_0 = \{(0,0)\}, \quad \psi \equiv \frac{1}{\sigma}. \tag{5.0.8}$$

Burning rate of segments

In this subsection we compute the burning rate of segments, that is we compute the quantity $b(t)$ if a portion of the barrier Z is a straight line. The following holds:

Lemma 5.0.9. *If Z is a straight line and the level sets of u are convex, then the burning rate is decreasing.*

Proof. Since $\nabla u = n$, where n is the outer normal, we have that the burning rate $b(t)$ is computed as

$$\dot{b}(t) = \sqrt{1 + |\dot{Z}|^2 - (\dot{Z} \cdot \nabla u)^2},$$

in particular

$$\ddot{b}(t) = \frac{\dot{Z} \cdot \ddot{Z} - \ddot{Z} \cdot \nabla u - \nabla^2 u : \dot{Z} \otimes \dot{Z}}{\sqrt{1 + |\dot{Z}|^2 - (\dot{Z} \cdot \nabla u)^2}}.$$

We have denoted by Z a parametrization for the segment. In the case of straight line, $\ddot{Z} = 0$, and

$$\nabla^2 u = \frac{1}{R} t \otimes t,$$

t being the tangent vector to the level set and R the radius of curvature: we thus obtain in general for any strategy without requiring to be a segment that

$$\nabla^2 u : \dot{Z} \otimes \dot{Z} + \nabla u \cdot \ddot{Z} = \frac{1}{R}(t \cdot \dot{Z})^2 + n \cdot \ddot{Z},$$

and observing that for θ angle w.r.t. n and R_Z curvature of Z

$$t \cdot \dot{Z} = \sin\theta, \quad n \cdot \ddot{Z} = \pm \frac{\cos\theta}{R_Z},$$

where the plus depends if bends toward n or on the other side, we write

$$\nabla^2 u : \dot{Z} \otimes \dot{Z} + \nabla u \cdot \ddot{Z} = \frac{\sin\theta^2}{R} \pm \frac{\cos\theta}{R_Z}.$$

For the straight line case we conclude

$$\ddot{b}(t) = -\frac{\sin\theta^2}{R\sqrt{1 + |\dot{Z}|^2 - (\dot{Z} \cdot \nabla u)^2}} < 0.$$

□

Remark 5.0.10. These computations show that the level sets of the minimum time function are convex in the points where they do not intersect the barrier.

Chapter 6

Qualitative Properties of the Optimal Strategy

In this chapter we study the qualitative properties of strategies minimizing the length functional in the optimization problem (4.4.13). Some geometric properties as being star-shaped and convex are analyzed, moreover it is given an homotopy argument to study the external boundary of the burned region. It is proved that among strategies with a single internal barrier the optimal one is connected and some further properties, as the number of intersections with the level sets of the minimum time function u are discussed.

Let $Z = Z^2 \cup Z^1 \subset \mathbb{R}^2 \backslash R_0$ be an admissible barrier. Let $\zeta : [0,1] \to \mathbb{R}^2$ be a clockwise parametrization of Z^2. We are interested in those perturbations of Z^2 that keep the new barrier admissible with shorter length. We fix two points $w_1 = \zeta(t_1), w_2 = \zeta(t_2) \in Z^2$ with $t_1 \leq t_2$. Assume also that $\zeta(t_1, t_2) \cap Z^1 = \emptyset$. Here and in the following we assume that the points $w \in Z$ are reached by an optimal ray $\bar{\gamma}_w$. We recall that the main assumption here is to work with $\sigma < 2$.

Lemma 6.0.1 (Star-shaped)**.** *Let $\bar{\gamma}_{w_2}$ be an optimal ray to w_2, and assume that $w_1 \in \bar{\gamma}_{w_2}$. Call $(Z')^2$ the closed curve obtained by replacing $\zeta([t_1, t_2])$ with the optimal ray from w_1 to w_2. Then the barrier $Z' = (Z')^2 \cup (Z')^1$, obtained by intersecting $Z \cap \overline{R_\infty^{Z'}}$, where $\overline{R_\infty^{Z'}} = \overline{int((Z')^2)}$ is an admissible strategy. Moreover, $\mathcal{H}^1(Z') \leq \mathcal{H}^1(Z)$, $\mathcal{L}^2(\overline{R_\infty^{Z'}}) \leq \mathcal{L}^2(\overline{R_\infty^{Z}})$.*

For this result see also the proof in [20] for strategies where $Z^1 = \emptyset$.

Proof. Clearly $\mathcal{H}^1(Z') \leq \mathcal{H}^1(Z)$, being the optimal ray by definition the shortest path from w_1 to w_2. The inequality for the area is immediate since we are cutting out some portions. For the proof we need to prove only the admissibility of the new strategy. We have that

$$R^{Z'}(t) \subset R^Z(t) \quad \forall t,$$

therefore

$$\mathcal{H}^1(Z' \cap \overline{R^{Z'}(t)}) \leq \mathcal{H}^1(Z' \cap \overline{R^Z(t)}).$$

We remark the following thing: we know that $\bar{\gamma}_{w_2}(t_1) = w_1$ and $\bar{\gamma}_{w_2}(t_2) = w_2$. Then, for every $t \in [t_1, t_2]$, $\bar{\gamma}_{w_2 \llcorner [0,t]}$ is an optimal path from w_1 to $\bar{\gamma}_{w_2}(t)$. In particular, $L(\bar{\gamma}_{w_2 \llcorner [t_1,t]}) = t - t_1$. Therefore, $\mathcal{H}^1(\zeta([t_1, t_2]) \cap \overline{R^Z(t)}) \geq \mathcal{H}^1(\bar{\gamma}_{w_2}([t_1, t_2]) \cap \overline{R^Z(t)})$, which implies that

$$\mathcal{H}^1(Z' \cap \overline{R^Z(t)}) \leq \mathcal{H}^1(Z \cap \overline{R^Z(t)}) \leq \sigma t,$$

Figure 6.1: Cutting out a portion of the barrier yields the new strategy admissible.

where the last inequality follows by the admissibility of the barrier Z. □

This analysis tells us that, in the optimal strategy, if the optimal ray touches the external barrier Z^2 in more than one point, then the external barrier coincides with it. Therefore, from now on, we can assume Z^2 to be star-shaped as in the previous lemma.

Definition 6.0.2. Let Z be an admissible blocking barrier. We say that Z^2 is *convex in the region not touching the internal barrier* Z^1 if $\forall w_1 = \zeta(t_1), w_2 = \zeta(t_2) \in Z^2$, such that $Z^1 \cap \zeta(t_1, t_2) = \emptyset$ the segment of endpoints w_1, w_2 is contained in $\overline{R^Z_\infty}$.

Lemma 6.0.3 (Convexity)**.** *Let Z be an admissible strategy, star-shaped. We fix $w_1 = \zeta(t_1), w_2 = \zeta(t_2) \in Z^2$ as in Definition 6.0.2. Let us call S the segment of endpoints w_1, w_2, and we assume that $S \subset (intR^Z_\infty)^c$. Then the strategy $Z' = (Z')^2 \cup Z^1$ obtained by replacing $\zeta([t_1, t_2])$ with S is still admissible, moreover $\mathcal{H}^1(Z') \leq \mathcal{H}^1(Z)$.*

Remark 6.0.4. If one considers an optimal strategy Z for the optimization problem (4.4.13) with $\kappa_1 = 0$, this result tells us that, up to increase the area burnt, we can consider Z convex in the sense of Definition 6.0.2. This result does not give the convexity for the optimization problem for $\kappa_1 \neq 0$. In the case of the area functional the optimal among simple closed curves [20] is not convex.

Proof. The inequality $\mathcal{H}^1(Z') \leq \mathcal{H}^1(Z)$ is immediate, so one has to prove only the admissibility of the new strategy Z'. Assume that $\zeta([t_1, t_2])$ burns within $[s, t]$. Then for every $\tau \in [s, t]$ consider the set $R^{Z'}(\tau)$ and call $z_1(t), z_2(t)$ the endpoints of the intersection of $Z \cap \overline{R^{Z'}(\tau)}$. We have that

$$\mathcal{H}^1(\zeta([t_1, t_2]) \cap \overline{R^Z(\tau)}) = \mathcal{H}^1(\zeta([t_1, t_2]) \cap \overline{R^{Z'}(t)}) \geq \overline{z_1(t)z_2(t)},$$

where the last quantity is the length of the segment of endpoints $z_1(t)$ and $z_2(t)$. If $z_1'(t)$ and $z_2'(t)$ are instead the endpoints of the intersection of the barrier Z' with $\overline{R^{Z'}(t)}$, then it holds $\overline{z_2(t)z_1(t)} \geq \overline{z_2'(t)z_1'(t)}$. This concludes the proof (Figure 6.2). □

6.0.1 Homotopy.

We present here one of the main tools that will be used throughout the paper. We are interested in those portions of the external barrier that can be shortened keeping the new barrier admissible. We saw that a barrier can be shortened cutting out some portions (Lemma 6.0.1) or replacing some regions in which it is concave (Lemma 6.0.3). Another important step towards this direction is the following: let $z_1, z_2 \in Z^2$ and assume that the arc $Z' \subset Z$ of endpoints z_1, z_2 is burning within the time interval $[t_1, t_2]$

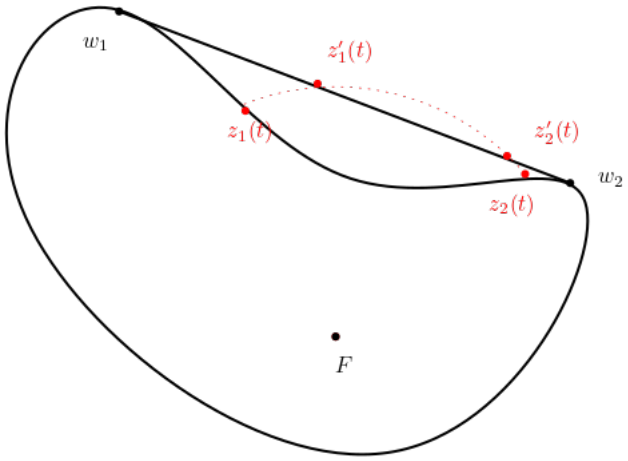

Figure 6.2: The selection of points $z_1(t), z_2(t)$ and $z_1'(t), z_2'(t)$ in the proof of the convexity.

(recall Definition 5.0.4), with the assumption that $z_1 \in Z' \cap \overline{R^Z(t_1)}$ and $z_2 \in Z' \cap \overline{R^Z(t_2)}$. Call $\eta : [0,1] \to \mathbb{R}^2$ an injective parametrization of Z', with $\eta(0) = z_1, \eta(1) = z_2$. Let now $h : [0,1]^2 \to \mathbb{R}^2$ be a Lipschitz homotopy with fixed points, that is

$$h(r,0) = z_1, \quad h(r,1) = z_2 \quad \forall r \in [0,1],$$

and

$$h(0,s) = \eta(s) \quad \forall s \in [0,1].$$

We call $Z^r = Z^{2,r} \cup Z^1$ the *perturbed* barrier obtained replacing $\eta([0,1])$ by $h(r,[0,1])$ (see Figure 6.3). Moreover we assume that

1. the homotopy does not affect the internal barrier, that is $h(r,(0,1)) \cap Z^1 = \emptyset$ for every r;

2. the burning rate of the barrier burned within $[t_1,t_2]$ is greater than σ, that is

$$\mathcal{H}^1(Z^r \cap \overline{R^{Z^r}(t)} \setminus R^{Z^r}(s)) > \sigma(t-s), \quad \forall r \in [0,1], \forall t > s, \text{ with } t,s \in [t_1,t_2]; \tag{6.0.1}$$

3. the homotopy shortens the lengths, that is

$$\mathcal{H}^1(Z^r) < \mathcal{H}^1(Z^{r'}) \quad \forall r' < r, \tag{6.0.2}$$

4. the set $Z^r \cap \overline{R^{Z^r}(t)} = Z \cap \overline{R^Z(t)}$ for every $t \le t_1$, and $Z^r \cap \overline{R^{Z^r}(t)} \setminus R^{Z^r}(t_2) = Z \cap \overline{R^Z(t)} \setminus R^Z(t_2)$ for $t \ge t_2$.

Proposition 6.0.5 (Homotopy.)**.** *Let $z_1, z_2 \in Z^2$ and h be as before satisfying* (1),(2),(3),(4). *Then Z^r is admissible for every $r \in [0,1]$.*

Proof. Assume by contradiction that there exists some $r \in [0,1]$ for which Z^r is not admissible. Therefore there exists $t \in [0,T]$ such that $\mathcal{H}^1(Z^r \cap \overline{R^{Z^r}(t)}) > \sigma t$. We claim that $t \in (t_1,t_2)$. Indeed, if $t \le t_1$, by (4) we have that

$$\mathcal{H}^1(Z^r \cap \overline{R^{Z^r}(t)}) = \mathcal{H}^1(Z \cap \overline{R^Z(t)}) \le \sigma t,$$

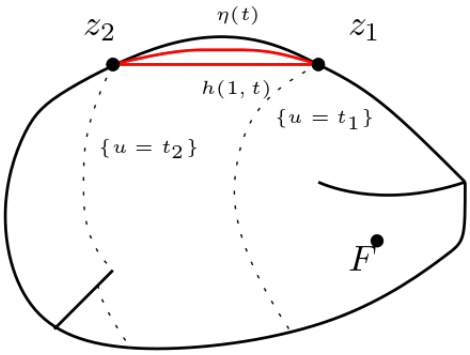

Figure 6.3: An example of some portion of the barrier that can be shortened by the homotopy remaining admissible.

since Z is admissible. If $t \geq t_2$ we have that, always by (4),

$$\begin{aligned}\mathcal{H}^1(Z^r \cap \overline{R^{Z^r}(t)}) &= \mathcal{H}^1(Z^r \cap \overline{R^{Z^r}(t_2)}) + \mathcal{H}^1(Z^r \cap \overline{R^{Z^r}(t)} \setminus R^{Z_r}(t_2)) \\ &\leq \mathcal{H}^1(Z^r \cap \overline{R^{Z^r}(t_2)}) + \mathcal{H}^1(Z \cap \overline{R^{Z}(t)} \setminus R^{Z}(t_2)),\end{aligned}$$

but since the homotopy shortens the lengths (3),

$$\mathcal{H}^1(Z^r \cap \overline{R^{Z^r}(t_2)}) \leq \mathcal{H}^1(Z \cap \overline{R^{Z}(t_2)}),$$

being

$$\begin{aligned}\mathcal{H}^1(Z^r \cap \overline{R^{Z^r}(t_2)}) &= \mathcal{H}^1(h(r,[0,1])) + \mathcal{H}^1(Z^r \setminus h(r,[0,1]) \cap \overline{R^{Z}(t_2)}) \\ &\leq \mathcal{H}^1(\eta([0,1])) + \mathcal{H}^1(Z \setminus \eta([0,1]) \cap \overline{R^{Z}(t_2)}) \\ &= \mathcal{H}^1(Z \cap \overline{R^{Z}(t_2)}) \leq \sigma t_2.\end{aligned}$$

So, since $t \in (t_1, t_2)$ we have that

$$\mathcal{H}^1(Z^r \cap \overline{R^{Z^r}(t_2)} \setminus R^{Z^r}(t)) = \mathcal{H}^1(Z^r \cap \overline{R^{Z^r}(t_2)}) - \mathcal{H}^1(Z^r \cap \overline{R^{Z^r}(t)}) \leq \sigma t_2 - \sigma t = \sigma(t_2 - t),$$

which contradicts (2). □

Remark 6.0.6. We observe that if two arcs $Z', Z'' \subset Z$ are burning simultaneously, that is they are burning within a time interval $[t_0, t_1]$, then their burning speed should be strictly greater than σ (being $\sigma < 2$) as proved in Corollary 5.0.6. In this case condition (2) is satisfied for $r = 0$. If we shorten the lengths of both Z', Z'' with a continuos homotopy h, we are still burning two arcs of the barrier, so condition (2) is satisfied for any other r (see Figure 6.4).

Remark 6.0.7. What is really crucial in the proof is that the last point (in the previous case z_2) remains admissible. One could also think to homotopies with no fixed points but that have this property, and the proposition would work in the same way. We will use this observation to prove the connectedness of the optimal strategy if Z^1 is a single internal barrier (see Lemma 6.1.2).

We remark also that thanks to the convexity proved before the homotopy allows to reduce the total burned area. This argument is powerful for the external barrier, since does not require any regularity assumption on Z^2, but it can not be used in the shortening of the internal barriers, since this would affect the barrier not only within the time interval $[t_1, t_2]$ as in the previous result, but also for later times.

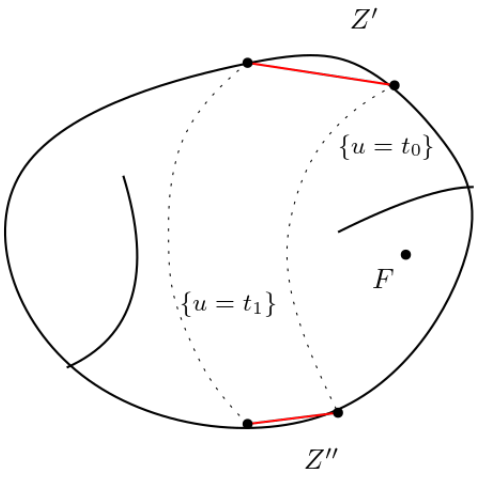

Figure 6.4: The new barrier obtained by substituting Z', Z'' with the red segments is still admissible by Proposition 6.0.5

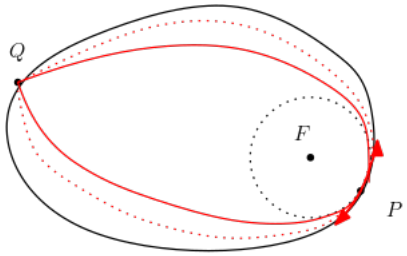

Figure 6.5: A single curve can be shortened remaining admissible since from the first point on the barrier P there are always at least two branches burning simultaneously.

Corollary 6.0.8. *Let Z be an admissible strategy and assume that Z is a simple curve, that is $Z = Z^2$. Then Z cannot be a blocking strategy.*

Proof. Any simple closed curve is characterized by the following property: let P be the first point on the curve Z reached by the fire, and let Q be the last point: then for $t \geq u(P)$ there are always at least two branches of the barrier burning simultaneosuly. If Z is admissible then any shortening of the curve that remains a simple closed curve passing through the point Q is still admissible (by Homotopy 6.0.5 and Remark 6.0.7), since it has shorter length and the property that the burning rate 5.0.7 is always greater than σ (Proposition 6.0.5). In particular the segment QF is still admissible, which is a contradiction (Lemma 5.0.7). □

6.1 Further Properties of Optimal Strategies

We consider an optimal strategy $Z = Z^2 \cup Z^1$ for the optimization problem (4.4.13) with $\kappa_1 = 0, \kappa_2 = 1$. We assume here that Z^1 is a single rectifiable curve. By the results of the previous section, we can assume Z being *star-shaped* and *convex* with the meaning of Lemmas 6.0.1,6.0.3. Moreover we can also assume that, if T is the time at which the fire is confined,

$$T \in \mathcal{S}(Z). \tag{6.1.1}$$

Indeed, if not, consider $\{u = T - \epsilon\}$ for $\epsilon << 1$. Consider the new barrier $\tilde{Z} = \partial \overline{R^Z(T-\epsilon)} \cup Z^1 \cap \overline{R^Z(T-\epsilon)}$. It has shorter length (since the level sets of u are

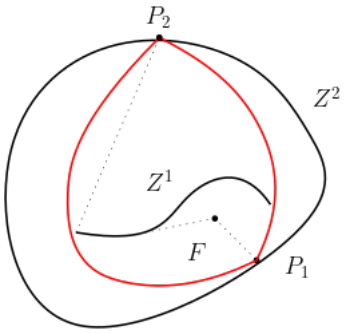

Figure 6.6: The new strategy given by the convex envelope is still admissible.

convex) and it is admissible, since $T \notin \mathcal{S}(Z)$ and $\epsilon << 1$. But this contradicts the hypothesis that Z is optimal.

Remark 6.1.1. The optimal strategy Z is not unique in general. If the initial burnt set R_0 is a ball, as in this case, then every rotation of Z is an optimal strategy.

6.1.1 Connectedness of the Optimal set.

Thanks to the homotopy argument, we can prove the following statement:

Corollary 6.1.2. *Let $Z = Z^2 \cup Z^1$ be an admissible blocking strategy and assume that Z^2 and Z^1 are two (disjoint) connected components. Then Z cannot be optimal.*

Proof. The proof of this result exploits the same idea of 6.0.8. Let us consider the first point P_1 reached by the fire on the external barrier, burning at time t_1, and the last one, let us say P_2, reached by the fire at time T. We claim that the burning rate of the strategy Z within $[t_1, T]$ is always strictly greater than σ. Indeed, when the fire reaches P_1 at least two branches (the left one and the right one with respect to P_1) start burning simultaneously. Consider the optimal ray $\bar{\gamma}_{P_2}$: if it does not intersect the internal barrier, then it is a segment: the same proof of Corollary 6.0.8 then gives us the statement. If it intersects the internal barrier Z^1 at some point P, consider the convex envelope of the set $C = Z^1 \cup \{F\} \cup \{P_2\}$. Consider the two arcs connecting F to P_2: call η_1 the one passing through P, η_2 the other one, touching Z^1 in some point Q. We observe that $\mathcal{H}^1(\partial C) = L(\eta_1) + L(\eta_2) \leq \mathcal{H}^1(Z^2)$, by convexity of the optimal strategy (lemma 6.0.3). Call η^ϵ a small perturbation of the curve $\eta = \eta_1 \cup \eta_2$ whose distance from Z^1 is ϵ. Consider the new strategy $Z^\epsilon = \eta^\epsilon \cup Z^1$. Now, since it burns with speed greater than σ (consider the first point and the last point on η^ϵ etc.), and since $L(\eta^\epsilon) < \mathcal{H}^1(Z^2)$, by Proposition 6.0.5, it is admissible. Since ϵ can be chosen arbitrarily small, we find that the curve obtained by the strategy $Z^1 \cup \eta = \tilde{Z}$ is admissible: contradiction. Indeed: for every ϵ we have that, by admissibility:

$$\mathcal{H}^1(Z^\epsilon \cap \overline{R^{Z^\epsilon}(t)}) \leq \sigma t.$$

Without loss of generality we can assume that $\eta^\epsilon \to \eta$ monotonically (that is, the set delimited by η is contained in the set delimited by η^ϵ). Then we observe that if $\epsilon_1 < \epsilon_2$, $R^{Z^{\epsilon_1}}(t) \subset R^{Z^{\epsilon_2}}(t)$. In particular, $\mathcal{H}^1(Z^\epsilon \cap \overline{R^{\tilde{Z}}(t)}) \leq \sigma t$. Now, since $Z^\epsilon \to \tilde{Z}$ w.r.t. the Hausdorff distance, and since $\mathcal{H}^1$ is lower semicontinuous for compact connected sets [28], we have that

$$\mathcal{H}^1(\tilde{Z} \cap \overline{R^{\tilde{Z}}(t)}) \leq \sigma t.$$

□

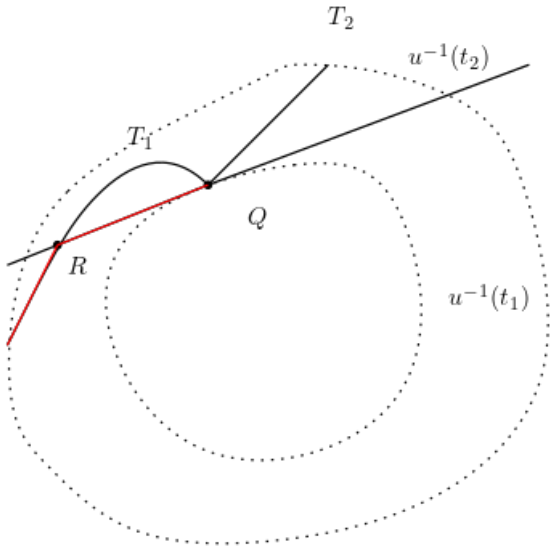

Figure 6.7: The intersection of T_1 or T_2 with r_-, r_+ would violate the optimality.

As told in the introduction, the hope would be to prove the connectedness of the optimal strategy, but we cannot simply use the homotopy argument to achieve it in the case we have more connected components. Anyway, we can prove the following

Corollary 6.1.3. *Let $Z = Z^2 \cup Z^1$ be an admissible strategy and assume that $Z^2 \cap Z^1 = \emptyset$. Then Z cannot be optimal.*

Proof. The proof is almost identical to the previous one. □

This collection of results tells us that there is always at least one internal barrier intersecting the external barrier.

6.1.2 Intersection with level sets

In this subsection we deal with the number of branches of the external barrier burning simultaneously. We recall that $\{u = t\}$ are convex in the points where it does not intersect the barriers (see Remark 5.0.10). We start with the following

Proposition 6.1.4. *Let Z be an optimal strategy. Assume that there exist $T_1, T_2 \subset Z^2$ sub arcs of the external barrier burning simultaneously within $[t_1, t_2]$. Then they are two segments. In particular, if $T_1 \cap T_2 = \{Q\}$ with $Q \in \{u = t_1\}$ and Q is a point of differentiability for $\{u = t_1\}$, then $\angle Q = \pi$ (they are a single segment).*

Proof. Consider the case in which $T_1 \cap T_2 = \{Q\}$ with $Q \in \{u = t_1\}$. Call r_-, r_+ the tangents in Q to the level set $\{u = t_1\}$. If by contradiction at least one of the two portions T_1, T_2 intersects r_- or r_+ in a point R different from Q, then by Proposition 6.0.5 the new strategy obtained replacing the portion of endpoints R, Q with the segment RQ would be admissible with shorter length, which contradicts the optimality (see Figure 6.7). Therefore, since no intersections can occur between T_1, T_2 with the two tangents, by homotopy one can replace the barrier with the two segments that start burning at Q and arrive at $\{u = t_2\}$. A similar argument can be used to conclude that T_1, T_2 are segments in the case they intersect at $P \in \{u = t_2\}$. Clearly, if $r_-, r_+ = r$, since the optimal barrier is convex (Lemma 6.0.3), the angle in Q is π. □

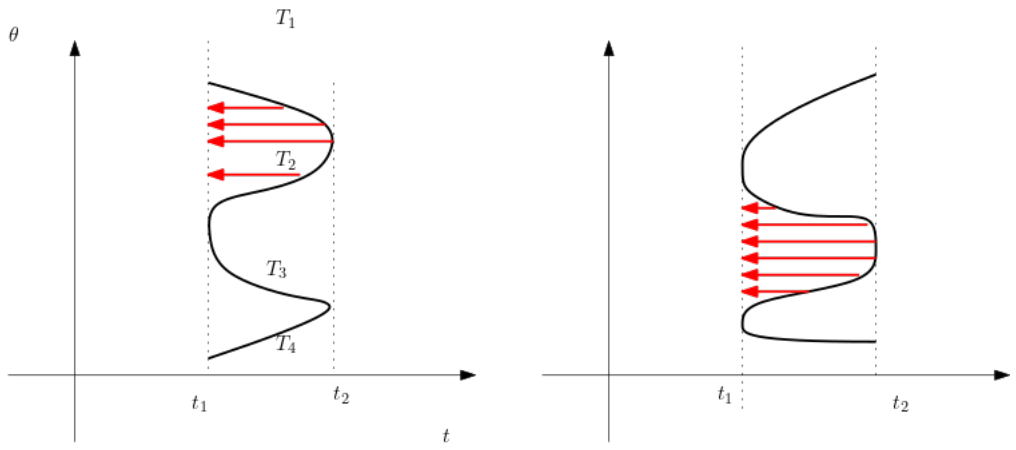

Figure 6.8: A representation of the boundary of Z through level sets. We push for example $T_1 \cup T_2$ on the level set $\{u = t_1\}$ since we are still burning two branches of the barrier (T_3, T_4), therefore the strategy remains admissible.

Remark 6.1.5. It is not necessary that the point Q is a point of differentiability. An alternative proof indeed would be the following: call $R_i = T_i \cap \{u = t_2\}$ for $i = 1, 2$. Then the segment R_1R_2 is shorter and its burning rate (5.0.6) is greater than σ, therefore by Proposition 6.0.5 with Remark 6.0.7 we would have the admissibility.

Finally we have the following

Proposition 6.1.6. *Let Z be an optimal strategy. If*

$$\sharp Z^2 \cap \{u = t\} < +\infty, \quad \text{for } t \in (t_1, t_2),$$

then

$$\sharp Z^2 \cap \{u = t\} \leq 3, \quad \text{for } t \in (t_1, t_2).$$

Proof. If $\sharp Z^2 \cap \{u = t\} \leq 3, \quad$ for $t \in (t_1, t_2)$, then there is nothing to prove. Therefore we assume to have T_1, T_2, T_3, T_4 burning simultaneously within $[t_1, t_2]$. By connectedness of Z^2 there exists T_i, T_j such that the intersection $T_i \cap T_j \in \{u = t_2\}$ and it is non-empty. Call R_i the point $T_i \cap \{u = t_1\}$ and R_j the point $T_j \cap \{u = t_1\}$. Call $\zeta : [0, 1] \to \mathbb{R}^2$ a clockwise parametrization of Z^2 and let $R_i = \zeta(t_i)$ and $R_j = \zeta(t_j)$ with $t_i \leq t_j$. Then the new strategy obtained by replacing $\zeta([t_i, t_j])$ with the portion of the level set $\{u = t\}$ of endpoints R_i, R_j is still admissible, by homotopy (Proposition 6.0.5), since by the convexity of level sets it has shorter length. But this contradicts the optimality of Z.

□

In particular optimal strategies are characterized by the fact that

$$\text{if } \sharp Z \cap \{u = t\} < +\infty \text{ then } \sharp Z \cap \{u = t\} \leq 3$$

.

Before the next result we define the *saturated set* as

$$\mathcal{S}(Z) = \{t \in [0, T] : \mathcal{H}^1(Z \cap \overline{R^Z(t)}) = \sigma t\}. \tag{6.1.2}$$

Proposition 6.1.7. *Let Z be an optimal strategy. Assume that there exist $T_1, T_2 \subset Z^2$ burning simultaneously within $[t_1, t_2]$ with $t_1 < t_2$ and assume that $T_1 \cap T_2 = \{Q\}$ with $Q \in \{u = t_2\}$. Then if $t_2 \notin \mathcal{S}(Z)$ the strategy is not optimal.*

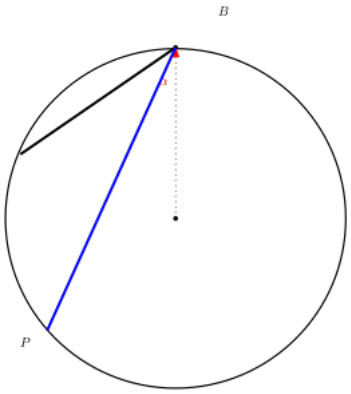

Figure 6.9: A purely geometric reason is behind Theorem 6.1.8: from one side $P \notin B_1$, since it is in the same level set of B, that is $\{u = t_1\}$. On the other side the angle between the segment PB with the fire ray should be less than α. Then $\overline{PB} \geq t_2 - t_0$. Here the worst case is $\alpha = \frac{\pi}{3}$ for $\sigma = 2$.

Proof. Assume $t_2 \notin S(Z)$, then there exists $\epsilon \ll 1$ such that $t_2 - \epsilon > t_1$ and

$$\mathcal{H}^1(Z \cap \overline{R^Z(t_3)}) < \sigma(t_2 - \epsilon). \tag{6.1.3}$$

Consider the level set $\{u = t_2 - \epsilon\}$ and call R_1, R_2 two intersections with T_1, T_2 respectively. We recall that, by Proposition 6.1.4, T_1, T_2 are segments. The new strategy Z' obtained by replacing the segments QR_1, PR_2 with the portion of the level set $\{u = t_2 - \epsilon\}$ of endpoints R_1, R_2 is shorter (by convexity) and admissible by condition (6.1.3). This contradicts the optimality hypothesis. □

Finally we have

Theorem 6.1.8 (Three branches)**.** *Let Z be an optimal strategy. Assume that there exist $T_1, T_2, T_3 \subset Z^2$ arcs burning simultaneously within $[t_1, t_2]$ and assume that $T_1 \cap T_2 = \{Q\}$ with $Q \in \{u = t_0\}$ where $t_0 < t_1$ and that $T_2 \cap T_3 = \{P\}$ with $P \in \{u = t_2\}$. If $t_0 \in \mathcal{S}(Z)$ and no internal barrier is burning within $[t_0, t_2]$, then the strategy is not optimal.*

This theorem will be of key importance in the study of Lemma 7.0.9.

Proof. By Proposition 6.1.4 T_1, T_2, T_3 are two segments AP, PB (see also Remark 6.1.5) burning within $[t_0, t_2]$ with the property that $P, B \in \{u = t_2\}$ and $A \in \{u = t_0\}$. By Proposition 6.1.7 it has to be $t_2 \in \mathcal{S}(Z)$. We assume that $t_0 \in \mathcal{S}(Z)$. We claim that the strategy is not optimal. By admissibility, since $t_0, t_2 \in \mathcal{S}(Z)$, the point P lies on the ellipse

$$\overline{AP} + \overline{PB} = \sigma(t_2 - t_0). \tag{6.1.4}$$

We claim that the angle $\angle(\bar{\gamma}_B, PB)$ is lower than $\alpha = \arccos\left(\frac{1}{\sigma}\right)$. This must be true, since, if by contradiction it is $> \alpha$ then the burning rate (5.0.7) would be greater than σ, and since $t_3 \in \mathcal{S}(Z)$ the strategy would not be admissible any more.

Clearly, since $|\nabla u| = 1$, we have that $\overline{AP} \geq (t_2 - t_0)$, being $P \in \{u = t_2\}$ and $A \in \{u = t_0\}$. Moreover, by definition of u, the level set $\{u = t_2\}$ contains a ball of radius $t_2 - t_0$, then we immediately find that $\overline{PB} \geq (t_2 - t_0)$, which is a contradiction (see Figure 6.9). This configuration cannot exist.

□

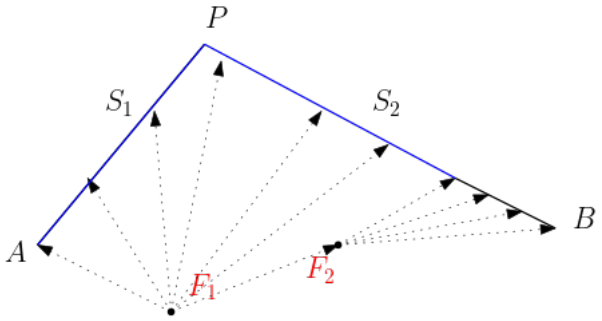

Figure 6.10: The fire source F_2 is emanated by F_1. The subset S (blue) of $S_1 \cup S_2$ is not burnt by the fire F_2, that is $\nexists x \in S$ for which F_2 is a source.

6.1.3 Double segment

We consider now an admissible barrier $Z = Z^2 \cup Z^1$ and we assume that two portions of the external barrier $S_1, S_2 \subset Z^2$ are segments joining at some point P. We will prove under which condition on the segments the strategy Z is optimal.

Definition 6.1.9 (Order of Sources)**.** Let $F_1, F_2 \in \overline{R^Z_\infty}$ and let $x \in Z$ such that $F_1, F_2 \in \bar\gamma_x([0, u(x)])$, where $\bar\gamma_x$ is an optimal ray to x. We say that F_2 is *subsequent* to F_1 if there exist $t_1 \le t_2$ with $t_1, t_2 \in [0, u(x)]$ such that $F_1 = \bar\gamma_x(t_1)$ and $F_2 = \bar\gamma(t_2)$.

We now assume to have two segments $S_1 = AP$ and $S_2 = PB$ joining at a point P, with $\angle APB < \pi$. We assume that for every $x \in S_1 \cup S_2$, $F_1 \in \bar\gamma_x([0, u(x)])$. We fix some $F_2 \in \overline{R^Z_\infty}$ with the following assumption: whenever $F_2 \in \bar\gamma_x([0, u(x)])$ for some $x \in S_1 \cup S_2$, then F_2 is subsequent to F_1 (see the Figure 6.10). We also assume that

C1) there exists $x \in S_1 \cup S_2$ such that $F_2 \in \bar\gamma_x([0, u(x)])$;

C2) consider the polygon $\mathcal{P}$ of vertices F_1APBF_2 and let $\mathrm{int}\mathcal{P}$ be its interior. Then $Z_1 \cap \mathrm{int}\mathcal{P} = \emptyset$, that is no internal barrier is contained inside $\mathcal{P}$;

We start with the following simple observation: consider the polygon $\mathcal{Q} = F_1APB$, then $F_2 \in \mathcal{Q}$, since F_2 is emanated by F_1. We exclude now some pathological cases requiring that

$$F_2 \in \mathrm{int}\,\mathcal{Q}. \tag{6.1.5}$$

Indeed, if F_2 lies on the boundary of $\mathcal{Q}$ then the two sources system F_1, F_2 behaves like a single source system F_1.

Proposition 6.1.10. *Let S_1 and S_2 be as before and assume that Conditions C1),C2), (6.1.5) hold. Assume also that $d(F_1, S_1) < d(F_1, S_2)$. If Z is an optimal strategy, then $\sharp S_2 \cap \{u = t\} \le 1$ or there exists a time t such that $S_1 \cup S_2 \cap \{u = t\} \ge 3$.*

Proof. Since $d(F_1, S_1) < d(F_1, S_2)$, it means that the segment S_1 starts burning before S_2. We start considering the two different cases: $\angle F_1PB \ge \frac{\pi}{2}$ and $\angle F_1PB < \frac{\pi}{2}$.

1. **Case** $\angle F_1PB \ge \frac{\pi}{2}$. It follows immediately that $\angle F_1BP < \frac{\pi}{2}$, therefore $\angle F_2BP < \frac{\pi}{2}$, since $F_2 \in \mathcal{Q}$.

   1.1 Assume that F_2 lives in the interior of the triangle F_1PB. We claim that $\sharp S_2 \cap \{u = t\} \le 1$ for all t such that $\sharp S_2 \cap \{u = t\} \neq \emptyset$. The claim follows by the easy observation that, called $\eta : [0, 1] \to \mathbb{R}^2$ the parametrization of the segment S_2, $\eta(s) = P + s(B - P)$, then the function $s \to d(F_1, \eta(s))$ is strictly increasing.

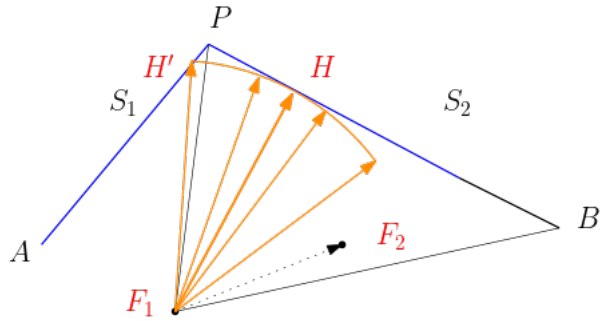

Figure 6.11: This figure represents the case 2.1 of Proposition 6.1.10.

1.2 Assume that F_2 lives in the interior of the triangle AF_1P. Also in this case we claim that $\sharp S_2 \cap \{u = t\} \leq 1$ for all t for which the intersection is non-empty. Assume by contradiction that there exist $x_1, x_2 \in S_2$ such that $d(F_1, x_1) = d(F_1, x_2)$. Then the triangle $F_2x_1x_2$ is isosceles, therefore $\angle F_2x_1x_2 < \frac{\pi}{2}$, which is a contradiction, since $\angle F_2x_1x_2 > \angle F_2PB > \frac{\pi}{2}$.

2. **Case** $\angle F_1PB < \frac{\pi}{2}$. Let H be the orthogonal projection of F_1 on S_2.

2.1 Assume F_2 inside the triangle F_1HB. Since $d(F_1, S_1) < d(F_1, S_2)$, there exists a point $H' \in S_1$ such that $d(F_1, H') = d(F_1, H)$, indeed, if one considers the following parametrization $\eta : [0, 1] \to \mathbb{R}^2$, defined by

$$\eta(s) = \begin{cases} A + 2s(P - A), & \text{for } s \in \left[0, \frac{1}{2}\right], \\ 2P - B + 2s(B - P), & \text{for } s \in \left[\frac{1}{2}, 1\right], \end{cases}$$

then the function $s \to d(F_1, \eta(s))$ is continuous and admits a local maximum at s_p, where $\eta(s_p) = P$. The existence of such H' implies now the existence of a time t for which $\sharp Z^2(t) \geq S_1 \cup S_2 \cap \{u = t\} = 3$.

2.2 We assume that the source F_2 is contained in the polygon F_1APH, and moreover $\angle F_2PB < \frac{\pi}{2}$. This case is similar to the case 2.1. Indeed, call K the orthogonal projection of F_2 on S_2, then by similar observations as before (since this time K has the role of H', one concludes with the existence of some time t for which $\sharp Z^2(t) \geq \sharp S_1 \cup S_2 \cap \{u = t\} = 3$.

2.3 We assume that the source F_2 is contained in the polygon F_1APH, but this time $\angle F_2PB > \frac{\pi}{2}$. In particular, this situation can occur when F_2 lives in the triangle F_1AP and $\angle APB > \frac{\pi}{2}$. In this case we have that $\sharp S_2 \cap \{u = t\} \leq 1$, concluding similarly to case 1.2.

□

Chapter 7

A case study

In this chapter we do a detailed analysis of the case a barrier has a single internal barrier which is a segment.

We consider an optimal strategy for the optimization problem (4.4.13) $Z = Z^2 \cup Z^1$ and we assume that Z^1 is a segment. By optimality, we know that Z is convex in the sense of Lemma 6.0.3. Moreover, by Lemma 6.1.2, we can also say that Z^1 intersects the external barrier Z^2. We assume that Z^1 is a segment of endpoints A and O, where $O \in Z^2$. We consider a coordinate system centered at O and we assume that the x-direction is along the segment OA, where, called (x_A, y_A) its coordinates, $x_A > 0$. Without loss of generality we can assume that the fire starts burning in the half plane $\mathbb{R} \times [0, +\infty)$ (see Figure 7.1). Moreover, if we call (x_F, y_F) the coordinates of the fire (recall Lemma 5.0.7), we can always assume that $y_F > 0$ by Lemma 5.0.7. We call A' the point on the external barrier reached by the optimal trajectory passing through A.

We define the following parameters:

- $t_1 = d(F, O)$;
- $t_2 = d(F, A')$;
- $t_3 = d(F, A) + \overline{AO}$.

Clearly $t_1 \leq t_3$ by the triangular inequality. From now on we will use some clockwise parametrization $\zeta : [0, 1] \to \mathbb{R}^2$ of Z^2 such that $\zeta(0) = \zeta(1) = O$. Let $s_{A'}$ be such that $\zeta(s_{A'}) = A'$. We recall that by $A(t)$ we will denote the set $A \cap \{u = t\}$. We start with the necessary conditions given by the admissibility of the barrier Z:

Lemma 7.0.1. *If $t_2 \leq t_1$, then the strategy Z is not admissible.*

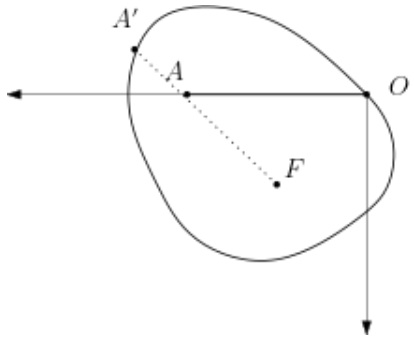

Figure 7.1: The simple case of a single segment with the correct orientation of the axes.

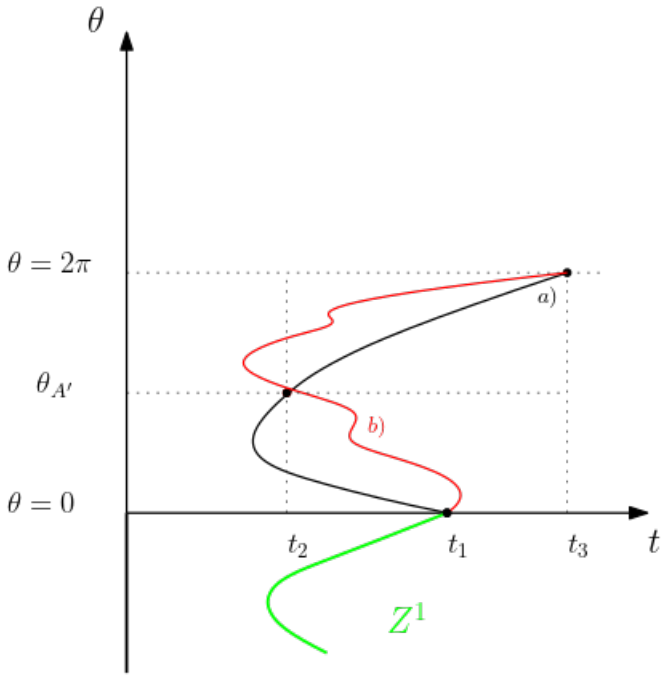

Figure 7.2: Parametrizations of two possible Z^2 a) and b). The green portion represents the segment Z^1. In any case the portion of the barrier $\zeta(s)$, with $s \in [0, s_{A'}]$ is always burning simultaneously with another portion of the barrier.

Proof. Let us assume that $t_2 \leq t_1$. We consider the *level set* graph of our admissible strategy Z (see Figure 7.2). Let $t_{\min} = \min d(F, \zeta(s))$ and $t_{\max} = \max d(F, \zeta(s))$ for $s \in [0, s_{A'}]$. Then we have $t_{\min} \leq t_2 \leq t_1 \leq t_{\max}$. We claim that the number of distinct branches of the external barrier Z^2 burning within $[t_{\min}, t_1]$ is greater than 2, that is, for every $t \in (t_2, t_1)$ the condition $\sharp Z(t) \geq 2$ holds (see Figure 7.2). This is clearly true, since the external internal barrier Z^1 starts burning in a time $t_2' \leq t_2$ and it stops burning in a time $t_1' \geq t_1$. By an homotopy argument (see Proposition 6.0.5), if we consider the portion $\zeta([0, s_{A'}])$ we can shorten it keeping the new barrier admissible. In particular, the new curve Z^A obtained by replacing $\zeta([0, s_{A'}])$ with a curve passing through F and the same endpoints is admissible. But this contradicts Lemma 5.0.7, since no portion of the external barrier can intersect F. □

7.0.1 Shape of the optimal strategy.

We add now the further assumption that Z is optimal meaning that it is the strategy with minimum length. We start with some lemmas describing the shape of Z^2. We will prove that Z^2 starts freely burning as a segment (far away from the fire) and then, when the fire reaches it, it is a branch of a logarithmic spiral. After the spiral has been burnt, the strategy is made by two segments joining in a point P: using Proposition 6.1.10, we conclude that the two segments are not optimal. Finally, an estimate of the angle covered by the logarithmic spiral (see Section 7.1) will show that the strategy cannot enclose the fire, yielding a contradiction.

Lemma 7.0.2. *Let Z be an optimal strategy. Assume that $d(F, O) \leq d(F, A)$. Then there exists $\bar{t}_1 \geq t_1$ such that, called t_{min} the first time the fire reaches the external barrier Z^2, $Z^2 \cap \operatorname{clos}(\overline{R^Z(\bar{t}_1)} \setminus R^Z(t_{min}))$ is a segment of endpoints O and Q with $d(Q, F) \geq d(F, O)$. Moreover, after $\bar{t}_1$ the segment OA has been burnt.*

Proof. Let us take $t_{\min}$ the first time the fire reaches the external barrier Z^2. Then $t_{\min} \leq t_1 \leq d(F, A) = t_A$. By connectedness of Z^2 (it is a simple closed curve) we have that $\sharp Z \cap \{u = t\} \geq 2$ for every $t \in (t_{\min}, t_A]$. Call $Q \in Z^2 \cap \{u = t_A\}$ such that $Q = \zeta(s_Q)$, with $s_Q = \sup\{s : \zeta(s) \in \{u = t_A\}\}$. By Proposition 6.0.5 the barrier Z' obtained by replacing the strategy from O to Q with the segment of endpoints O and Q is admissible, and the shortest possible curve, since within $[t_1, t_A]$ the internal barrier Z^1 is burning, keeping the number of barriers burning simultaneously greater than σ. Since Z is optimal, this means that $Z = Z'$. In particular $d(Q, F) = d(Q, A) = t_A \geq t_1 = d(F, O)$. □

Lemma 7.0.3. *Let Z be an optimal strategy. Assume that $d(F, O) \geq d(F, A)$. Then $Z^2 \cap \overline{R^Z(t_1)}$ is a segment of endpoints O and Q (eventually coinciding) such that $d(Q, F) = d(F, O)$.*

Proof. Again, let us fix $t_{\min}$ the minimum time for reaching the external barrier Z^2, then $t_{\min} \leq t_1$. Let $Q \in Z^2$ be the point on the external barrier such that $d(Q, F) = d(F, O)$ and such that $Q = \zeta(s_Q)$, with $s_Q = \sup\{s : \zeta(s) \in \{u = t_A\}\}$. As in the previous lemma we have that $\sharp Z \cap \overline{R^Z(t)} \geq 2$ for every $t \in [\max\{t_{\min}, t_A\}, t_1]$, and again by an homotopy argument (Proposition 6.0.5) we can shorten the barrier replacing it with a segment of endpoints O and Q. □

Lemma 7.0.4. *Let Z be an optimal strategy and let Q be the point of Lemmas 7.0.2,7.0.3. Then if $u(Q) \notin \mathcal{S}(Z)$ there exists a point Q' such that $u(Q') \in \mathcal{S}(Z)$ and $OQ' \supset OQ$ is a segment.*

Proof. If $u(Q) \notin \mathcal{S}(Z)$ we can shorten the length of the barrier keeping it admissible, therefore the optimal strategy should be made by a segment whose last point is saturated. □

Remark 7.0.5. By Lemma 7.0.4 we can assume that the point Q obtained in Lemmas 7.0.2,7.0.3 is saturated, that is $u(Q) \in \mathcal{S}(Z)$. Moreover $d(Q, F) \geq d(F, O)$.

Lemma 7.0.6. *The barrier Z is C^1 in the point Q given by Lemma 7.0.2 or by Lemma 7.0.3.*

Proof. As proved above, we can assume that $u(Q) \in \mathcal{S}(Z)$. By a blow up argument, by convexity of the barrier Z^2, we can consider the tangent cone at Z^2 in the point Q and the optimal rays from the fire F being parallel. If for simplicity we consider Q as the origin of a cartesian coordinate system, the two tangents are $y = \alpha_- x$ (the left one) and $y = \alpha_+ x$ (the right one), the convexity immediately gives $\alpha_- \geq \alpha_+$. Then, since the speed for burning the barrier is $\sqrt{1 + \frac{1}{\alpha_\pm^2}}$ (see Figure 7.3) the condition $u(Q) \in \mathcal{S}(Z)$ gives

$$\sqrt{1 + \frac{1}{\alpha_-^2}} \geq \sigma \geq \sqrt{1 + \frac{1}{\alpha_+^2}},$$

where the first inequality follows by the fact that before the fire reaches the point Q, the burning rate is greater than σ, while the second inequality means that, since Q is saturated, in order to be admissible the burning rate should be lower than σ. These two condition together yield $\alpha_- = \alpha_+$, which gives the C^1 regularity. Moreover, since

$$\sigma = \sqrt{1 + \frac{1}{\alpha^2}},$$

the angle $\angle FQO = \arccos\left(\frac{1}{\sigma}\right)$. □

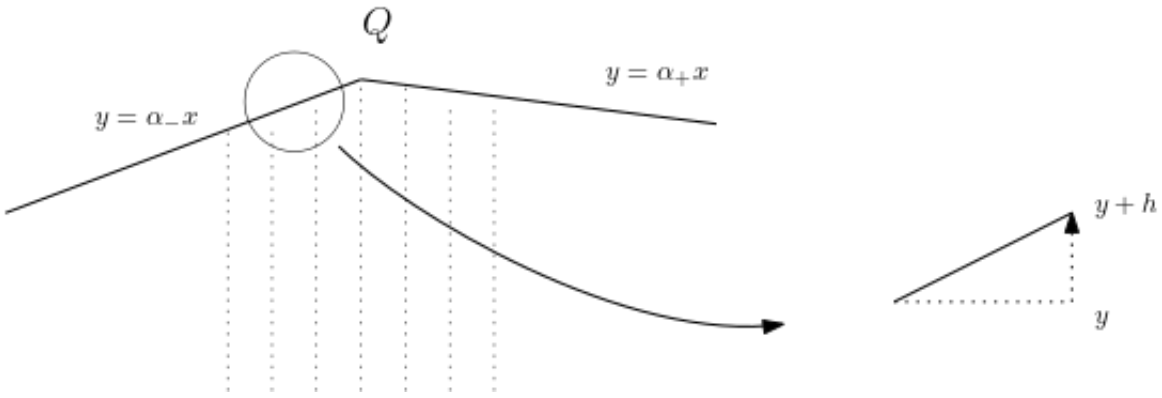

Figure 7.3: The fire moves with speed one while the speed for burning the barrier is $\sqrt{1 + \frac{1}{\alpha_\pm^2}}$.

We remark that the argument of the previous lemma applies to any point $P \in Z^2$ where the barrier is convex with respect to the direction of the fire rays, together with the local condition

$$\sqrt{1 + \frac{1}{\alpha_-^2}} \geq \sigma \geq \sqrt{1 + \frac{1}{\alpha_+^2}},$$

that holds in saturated points. This blow up argument is valid also for internal barriers.

The previous discussion gives the following

Corollary 7.0.7. *Let $Z' \subset Z^2$ and assume that it is burning within $[t_1, t_2] \subset \mathcal{S}(Z)$. Then it is $\mathcal{C}^1$.*

Corollary 7.0.8. *Call $\zeta(s_{P_1}) = P_1 = \sup\{s_P \in [s_Q, 1] : u(\zeta(s_P)) \in \mathcal{S}(Z)\}$, where s_Q is such that $Q = \zeta(s_Q)$. Then there exists $\epsilon > 0$ such that, if $\zeta(s_{P_2}) = P_2 \in \{u = u(P_1) + \epsilon\}$, then $\zeta([s_{P_1}, s_{P_2}])$ is a segment tangent to Z in P_1.*

Proof. Since P_1 is the last point saturated according to the definition in the statement, there exists $\epsilon > 0$ such that $u(P_1) + \delta \notin \mathcal{S}(Z)$ for all $\delta < \epsilon$. This tells us that, since the point P_1 is saturated, then we can burn only one single branch of the strategy (see Figure 7.4), that is the burning rate is lower than σ. This means that in the time interval $[u(P_1), u(P_1) + \epsilon]$ with $\epsilon << 1$ the fire is burning exactly one branch of the barrier (see Figure 7.4) and $\mathcal{H}^1(Z \cap \overline{R^Z(t)}) - \mathcal{H}^1(Z \cap \overline{R^Z(s)}) < \sigma(t - s)$ for every $t, s \in [u(P_1), u(P_1) + \epsilon]$. Call $P_2 = \zeta(s_{P_2}) \in Z^2 \cap \overline{R^Z(u(Q) + \epsilon)}$. Then, if the portion of the barrier $\zeta([s_{P_1}, s_{P_2}])$ is not a segment, we can shorten it a little bit keeping the new barrier admissible, since $u(P_2) \notin \mathcal{S}(Z)$. Therefore $\zeta([s_{P_1}, s_{P_2}])$ must be a segment, and since the barrier is $\mathcal{C}^1$ at P_1, this segment must be tangent to Z at P_1. □

Therefore, if Z is an optimal strategy, we call $[u(Q), T']$ the maximal time interval contained in the saturated set: here the barrier is a branch of logarithmic spiral, which is precisely the curve constructed at the edge of the advancing fire, in the assumption the level sets are union of arcs of circles, as in this case (see Section 5.2 of [13]).

Lemma 7.0.9 (Folding)**.** *Consider the level set graph of the optimal strategy Z. If the barrier Z^2 has a* folding*, that is there exists a time interval $[t_-, t_+]$ with $t_- \geq T'$ such that $\sharp Z^2(t) = 3$ for $t \in [t_-, t_+]$, then the strategy is not optimal (see Figure 7.5).*

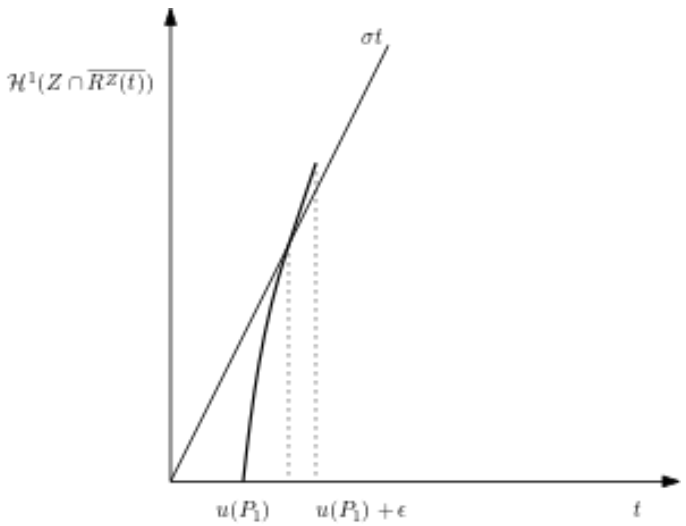

Figure 7.4: In the time interval $[u(P_1), u(P_1)+\epsilon]$ the fire is burning exactly one branch of the barrier, otherwise we would lose the admissibility.

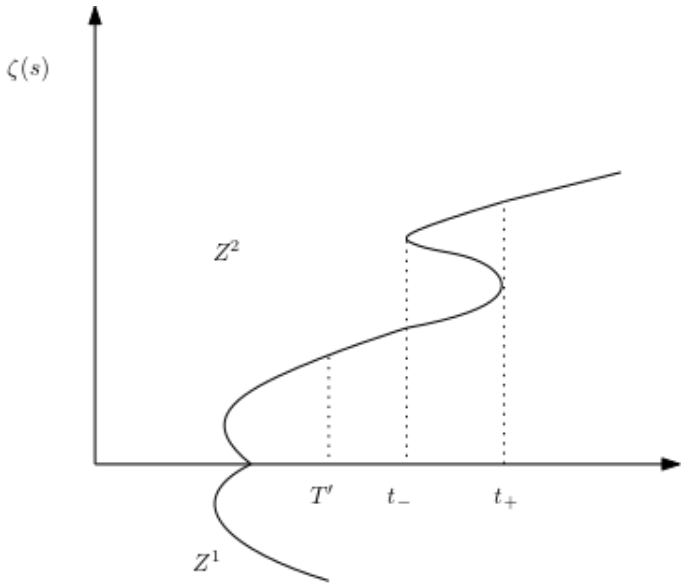

Figure 7.5: A folding in the level set graph is not optimal.

Proof. By Proposition 6.1.7 and by optimality $t_+ \in \mathcal{S}(Z)$. Since $t_- \notin \mathcal{S}(Z)$ (if not, since after t_- we are burning three branches the burning rate 5.0.7 would be greater than σ, violating the admissibility), the unique curve starting from the logarithmic spiral and connecting the point in $\{u = t_-\}$ has to be a segment (Corollary 7.0.8) which is tangent to the spiral in the point P_1. Call the endpoints of this segment P_1, N. Moreover, since, by Proposition 6.1.4 the tree branches burning within $[t_-, t_+]$ are two segments RL and RN with $R, L \in \{u = t_+\}$ and $N \in \{u = t_-\}$, then the angle $\angle RNP_1$ has to be π since again $t_- \notin \mathcal{S}(Z)$. We have obtained two segments P_1R and LR burning within $[T', t_+]$, with $t_+, T' \in \mathcal{S}(Z)$. This is not optimal by Theorem 6.1.8. □

Finally, we have the following

Lemma 7.0.10. *In the time interval $(T', T]$ the optimal strategy is a piece of logarithmic spiral or it is made by two segments joining at some point P.*

Proof. If $t_3 < T$ then two branches of the external barrier are burning within $[t_3, T]$ (they cannot be more than 2, by Proposition 6.1.6 and Theorem 6.1.8). In particular, by Proposition 6.1.4, they are two segments of endpoints P_2P and PO, with $P \in \{u = T\}$. Again, $t_3 \notin \mathcal{S}(Z)$ (if not, since for $t > t_3$ we are burning more than one segment, the burning rate would be greater than σ, contradicting the admissibility), therefore the branch of endpoints P_1P_2 (P_1 was the endpoint of the spiral) has to be a segment, and the angle $\angle P_1P_2P = \pi$. This concludes the proof in the case $t_3 < T$. If $t_3 = T$ then a single branch of the barrier is burning within $[T', T]$. We recall that $T \in \mathcal{S}(Z)$ (assumption (6.1.1)). Assume that it is not a logarithmic spiral, and compute the logarithmic spiral starting at P_1 (recall that P_1P_2 is tangent to the spiral). If the spiral does not intersect the curve, it is the optimal, since it has shorter length. If it intersects the curve in a point R, since the fire burns one branch, then the admissibility at R reads as

$$u(R) - \cos\alpha(\overline{AO} + \overline{OQ} + QP_1 + P_1R) \leq u(R) - \cos\alpha(\overline{AO} + \overline{OQ} + QP_1 + (P_1R)^s) = 0,$$

where $(P_1R)^s$ is the length of the saturated spiral between the points R_1S and the last equality is because the spiral satisfies the saturation condition (6.1.2) (see Figure 7.6), which is a contradiction.

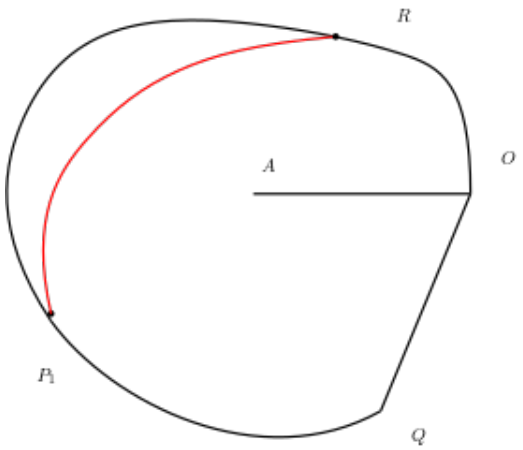

Figure 7.6: If the logarithmic spiral intersects a branch of the barrier that is touched only by one side of the fire, then it is the optimal spiral.

□

Remark 7.0.11. We remark that, even if in Lemma 7.0.10 we have a configuration made of two segments as in Theorem 6.1.8, the two are different, since in the one of the lemma we have that, if the two segments burn within $[t_1, t_2]$, we have a unique point in $\{u = t_2\}$, while in Theorem we have two points on $\{u = t_2\}$.

We summarize all the previous lemmas and propositions in the following characterization of the optimal strategy (Figure 4.11)

Theorem 7.0.12 (Optimal Shape)**.** *Let $Z = Z^2 \cup Z^1$ be an optimal strategy and assume that Z^1 is a segment AO. Then Z^2 is the union of*

- *a segment OQ with the property that $d(Q, F) \geq d(Q, O)$;*
- *is a piece of logarithmic spiral QP_1, tangent to the segment OQ;*
- *is the union of two segments P_1P and PO, where the first segment is tangent to the logarithmic spiral at the point P_1.*

7.1 Final computations

In this last section we use the tools and lemmas proved in the previous sections in order to show that an optimal strategy Z whose internal barrier is a segment does not exist. We will analyze the two different situations of Lemmas 7.0.2,7.0.3 showing that the last portion of the barrier, which is made by a branch of logarithmic spiral, cannot close, allowing the fire to escape. In the following computations $\sigma < 2$ and $\alpha = \arccos\left(\frac{1}{\sigma}\right)$.

Without loss of generality we assume that the internal barrier corresponds to a segment OA, where $O = (0; 0)$ and $A = (0; 1)$, that is it has length 1. The external barrier Z^2 starts from O and closes in O rotating clockwise. As in the previous section we call $\zeta = \zeta(\theta)$ its clockwise parametrization, for $\theta \in [0, 2\pi]$, where $\zeta(0) = \zeta(2\pi) = O$. We assume that the fire F starts burning from $F = (d\cos\alpha, d\sin\alpha)$, for some positive $d > 0$ and $\alpha \in [0, \pi]$. By the optimality conditions we recovered that Z^2 is convex in the regions not touching the segment OA (see Definition 6.0.2) and that

- $\zeta([0, 2\gamma])$ is a segment of endpoints O and Q of length L, for some $\gamma \in [0, \frac{\pi}{2}]$;
- $\zeta([2\gamma, \theta])$ is a piece of logarithmic spiral, for some $\theta \in [0, 2\pi]$.
- $\zeta([\theta, 2\pi])$ is made by two segments.

Our aim is to show that $2\gamma + \theta < \pi$. We will examine the following different situations:

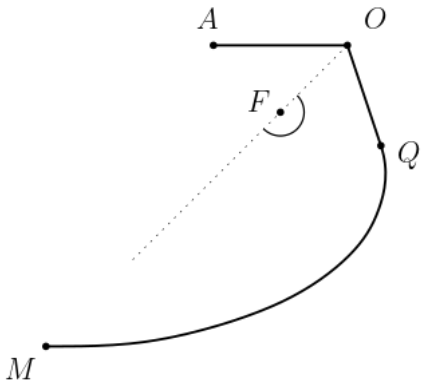

Figure 7.7: Situation of case a). From Q a single branch of spiral starts, and the angle around the fire $\theta + 2\gamma$ is strictly smaller than π.

7.1.1 Case a)

We assume that

$$d(F,Q) \geq d(F,A) \geq d(F,O) = d, \tag{7.1.1}$$

as in Lemma 7.0.2. Since $u(Q) \in \mathcal{S}(Z)$ (see Remark 7.0.5) we have that

$$L + 1 = \sigma d(F,Q). \tag{7.1.2}$$

By the theorem of sines applied to the triangle FOQ we get that

$$\frac{d(Q,F)}{\sin(2\gamma+\alpha)} = \frac{d}{\sin\alpha}, \tag{7.1.3}$$

being, by optimality, $\angle FQO = \alpha$. In particular we find that $2\gamma \leq \pi - 2\alpha$. By the admissibility condition we get that

$$\sigma d(F,Q)(e^{\theta\cot\alpha} - 1) + (L+1) \leq \sigma(d(F,A)+1) \leq \sigma(d(F,Q)+1),$$

where $\sigma d(F,Q)(e^{\theta\cot\alpha} - 1)$ is the length of the logarithmic spiral starting at the point Q and covering the angle θ. By equation (7.1.2) we find that

$$\sigma d(F,Q)(e^{\theta\cot\alpha} - 1) + \sigma d(F,Q) \leq \sigma(d(F,Q)+1),$$

therefore

$$\theta \leq \tan\alpha \log\left(1 + \frac{1}{d(F,Q)}\right) \leq \tan\alpha \log\left(1+\cos\alpha\right),$$

where the last inequality follows by the inequality $d(F,Q) \geq \sigma$. Therefore $2\gamma + \theta < \pi$.

7.1.2 Case b).

Similarly to the previous case:

$$d(F,Q) \geq d(F,O) = d \geq d(F,A), \tag{7.1.4}$$

(see Lemma 7.0.3). The admissibility condition gives

$$L + 1 = \sigma d(F,Q), \tag{7.1.5}$$

since after an amount of time equal to $d(Q,F)$ the fire has burnt both the segment OQ of length L and the segment OA of length 1, and it is starting burning a single branch of the external barrier Z^2 (see Figure 7.7). In particular $d(F,Q) \geq \frac{1}{\sigma}$. Similarly as before $2\gamma < \pi - 2\alpha$. Then we find that

$$\sigma d(F,Q)(e^{\theta\cot\alpha} - 1) + (L+1) \leq \sigma(d(F,A)+1) \leq \sigma(d(F,Q)+1).$$

Therefore, as before,

$$2\gamma + \theta < \pi. \tag{7.1.6}$$

Since in both cases $a), b)$ the angle $2\gamma + \theta < \pi$, we apply Proposition 6.1.10 on the optimality of the double segment. Here $F_1 = F$, $F_2 = A$, $A = P_1$ and $B = O$. Being $2\gamma + \theta < \pi$, condition (6.1.5) is satisfied, together with conditions C1),C2).

Proposition 7.1.1. *It holds $T' = T$.*

Proof. By Proposition 6.1.10 it holds $\sharp PO \cap \{u = t\} \leq 1$ for $t \in [t_3, T]$ or there exists t such that $P_1P \cup PO \cap \{u = t\} \geq 3$. This last situation cannot occur: at most two branches of the external barrier are burning from $[T', T]$. Let us analyze the first situation: if $\sharp PO \cap \{u = t\} \leq 1$, then $\angle AOP \geq \frac{\pi}{2}$ so that $\angle FPO < \frac{\pi}{2}$. Similarly $\angle FP_1P > \frac{\pi}{2}$ since $\sharp P_1P \cap \{u = t\} \leq 1$ for $t \leq t_3$. Then we are in the case 2.3 of Proposition 6.1.10, therefore it must be $\angle APO > \frac{\pi}{2}$, but since $\angle AOP \geq \frac{\pi}{2}$ we find a contradiction. □

Chapter 8

Admissible Spirals

In this chapter we give the definition of spiral-like strategies and we introduce their analytic description through RDE (Section 8.1). Here we study in detail the equation associated to the saturated spiral, with a careful analysis of its eigenvalues.

Let $Z = \zeta([0, S])$ be an admissible strategy parametrized by arc length. Since the problem is invariant by rigid transformations, we will assume that $\zeta(0) = (r_0, 0)$, with $r_0 \geq 1$. We call u the minimum time function of the strategy Z. Without loss of generality we can simplify the problem by considering the following setting: $\zeta(0) = (1, 0)$ and the fire starts spreading in the origin $(0, 0)$ (see Remark 5.0.8).

Among admissible strategies, we consider spiral-like strategies: namely barriers where the effort of construction is put on a single wall that keeps growing.

Definition 8.0.1 (Spiral-like strategy)**.** Let $Z = \zeta([0, S]) \subset \mathbb{R}^2$ be an admissible blocking strategy, where ζ is a parametrization by length. We say that it is a spiral-like strategy if it satisfies:

- $[0, S] \ni s \mapsto \zeta(s) \in \mathbb{R}^2$ is a Lipschitz curve, and $\zeta_{\llcorner [0,S)}$ is simple; 8.0.2;
- $s \mapsto u \circ \zeta(s)$ is increasing.

With this definition we exclude from our analysis those spirals that are touched simultaneously in more than one point by the fire (apart from those branches of the spiral that lie on the level sets of the minimum time function), while in the previous example (Chapter 10) the fire could touch the segment/the external barrier in more than one point.

From now on we will consider only admissible spiral-like strategies. Without loss of generality we can assume that $s \to \zeta(s)$ is oriented counterclockwise. We give a definition of (local) convexity for strategies:

Definition 8.0.2. We say that a spiral-like strategy $Z = \zeta([0, S])$ is locally convex if for every $x \in Z$ there exist an hyperplane $H = x + \lambda \mathbf{v}$ and $\epsilon > 0, \delta > 0$ and a function $f : [-\delta, \delta] \to \mathbb{R}$ convex such that, in the framework $\{\mathbf{v}, \mathbf{v}^\perp\}$ with $\mathbf{v}$ oriented in the direction of s increasing and $\{\mathbf{v}, \mathbf{v}^\perp\}$ oriented as the canonical base,

$$Z \cap \overline{B}_\epsilon(x) = \{(z, y) : y = f(z), z \in [-\delta, \delta]\}.$$

In particular, if $Z = \zeta([0, S])$ is a spiral-like strategy, then $\dot{\zeta}(s)$ exists a.e. and for a.e. $s \in [0, S)$ such that $\dot{\zeta}(s) \neq 0$ there exists $\epsilon > 0$ such that, for every $s' \in (s - \epsilon, s + \epsilon)$ it holds

$$\langle \dot{\zeta}^\perp(s), \zeta(s') - \zeta(s) \rangle \geq 0 \text{ a.e. } s,$$

where $\dot{\zeta}^\perp$ denote the normal vector to Z at $\zeta(s)$ such that $\{\dot{\zeta}(s), \dot{\zeta}^\perp(s)\}$ has the same orientation of the canonical basis, that is

$$\dot{\zeta}^\perp(s) = \begin{pmatrix} 0 & 1 \\ -1 & 0 \end{pmatrix} \zeta(s).$$

Moreover, if $\zeta(s)$ is a point of non differentiability of the curve Z, there exist two tangent vectors $t^+(s)$ and $t^-(s)$ (coinciding on regular points) defined as follows:

$$t^-(s) = \lim_{h\to 0^+} \frac{1}{h}(\zeta(s) - \zeta(s-h)),$$

$$t^+(s) = \lim_{h\to 0^+} \frac{1}{h}(\zeta(s+h) - \zeta(s)),$$

with the property that the function $s \to \dot{\zeta}(s) \doteq t^+(s) = e^{i\phi_s} \in \mathbb{S}^1$ is monotone, that is $\forall s, s'$ such that $s < s'$ it holds $\phi_s \leq \phi_{s'}$.

We remark that the function $s \to \dot{\zeta}(s)$ defined above is BV (right-continuous) and differentiable a.e. $s \in [0, S]$. In particular, there exists $\ddot{\zeta}(s)$ for $\mathcal{L}^1$- a.e. $s \in [0, S]$. In the assumption $\ddot{\zeta}(s) \neq 0$, there exists the radius of curvature:

$$R(\zeta(s)) = \frac{1}{|\ddot{\zeta}(s)|}. \tag{8.0.1}$$

We will use also the notation $\zeta(P), \dot{\zeta}(P), \ddot{\zeta}(P)$ if $P = \zeta(s) \in Z$ to indicate $\zeta(s), \dot{\zeta}(s), \ddot{\zeta}(s)$.

Remark 8.0.3 (Alternative description via angles)**.** If Z is an admissible spiral, as pointed out in the introduction, we will also use in addition a parametrization by angle $(\phi, r(\phi))$ to describe the strategy (see Figure 8.2), where, if $P = (r(\phi), \phi)$, $r(\phi)$ describes the length of the segment $\overline{PP_s}$, where P_s is the starting point of the fire ray $\bar{\gamma}_{P_s}$. In particular, we will have $\nabla u(P_s) = e^{i\phi}$. We will use both the descriptions, and we will develop a precise framework for characterizing spiral-like strategies in the next section. We will both use the notations $\beta(\phi) = \beta(s)$ whenever $(r(\phi), \phi) = \zeta(s)$. This description is possible thanks to the convexity assumption on admissible spirals, indeed it implies that the angle at the point P is monotonically increasing and so it is possible to parametrize the curve by the angle of rotation ϕ and the length of the radius.

Definition 8.0.4. Admissible spirals are admissible spiral-like blocking convex strategies. We will denote by $\mathcal{A}_S$ the set of admissible spirals.

Definition 8.0.5. Let $P \in Z$, where Z is an admissible spiral. The starting point of the optimal ray $\bar{\gamma}_P : [0, u(P)] \to \mathbb{R}^2$ is a point P_i with the following property: let

$$t_P = \inf\{t \in [0, u(P)] : \bar{\gamma}_{P\llcorner[t_p, u(P)]} \text{ is a segment}\}. \tag{8.0.2}$$

Then $P_i = \bar{\gamma}_P(t_P)$.

In general optimal rays (Definition 5.0.1) are segments where they do not touch the barrier: since the barrier is convex, these rays have an initial and a final segment and in the intermediate points they coincide with the barrier. If the final segment has length zero, then the barrier confines the fire. By definition of spiral-like strategies, the starting point is well-defined, since for every $P \in Z$ there exists unique $\bar{\gamma}_P$ optimal ray. Indeed, the solution to the Hamilton-Jacobi equation given by the Lax formula has a unique optimal ray starting from $O = (0, 0)$ and reaching any point $P \in R_\infty^Z$. Moreover, if $P_i \neq O = (0, 0)$, it lies on the barrier Z. We will denote the direction of

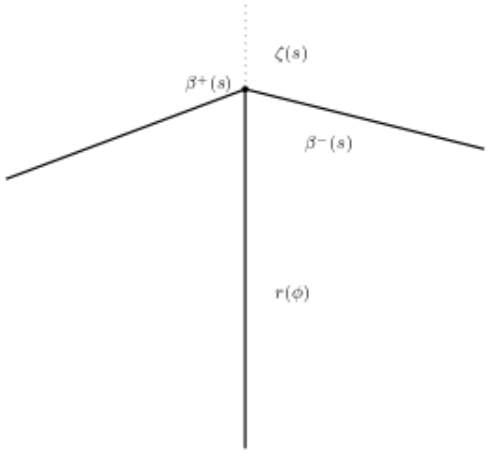

Figure 8.1: Here a point of non-differentiability of the convex barrier and the angles β^+ and β^-.

fire rays starting from $P_i = \zeta(s_i)$ and reaching a point $P \in Z$ as $\nabla u(\zeta(s_i))$ or $\nabla u(P_i)$ or $\frac{\dot\zeta(s_i)}{|\dot\zeta(s_i)|}$ alternatively. Moreover, if $\zeta(s) = P$ we will denote by $r(s) = \overline{P_s P}$.

Moreover, the level set of the fire is a convex curve and in particular $\mathcal{C}^{1,1}$. Now we consider a point $P \in Z$ and let $P_i = \zeta(s_i)$ be its starting point. We define the two following functions: $s \to \beta^+(s)$ and $s \to \beta^-(s)$ with values in $[0, \pi]$ representing the angles made by the the fire ray with the two tangents $t^+(s), t^-(s)$. More precisely:

$$\langle t^+(s), \nabla u(\zeta(s_i))\rangle = \cos\beta^+(s),$$

$$\langle t^-(s), \nabla u(\zeta(s_i))\rangle = -\cos\beta^-(s).$$

Here the convexity assumption reads as

$$\beta^+(s) \geq \beta^-(s). \tag{8.0.3}$$

The function $\beta^+(s)$ is BV and right-continuous. We remark that, by the third assumption in Definition 8.0.1, the angle $\beta^+(s) \leq \beta^+(s) \leq \frac{\pi}{2}$, otherwise the fire would touch the barrier in more than one point simultaneously. We denote by $s \to \beta(s) = \beta^+(s)$.

We recall that the admissibility condition reads as

$$\mathcal{H}^1(Z \cap \overline{R^Z(t)}) \leq \sigma t, \quad \forall t \leq T.$$

The function $t \to \mathcal{H}^1(Z \cap \overline{R^Z(t)})$ is monotone-increasing with countably many jumps, corresponding to the set of times t where the barrier is placed on the level set $\{u = t\}$, moreover it is right-continuous [16]. We define the burning rate as

$$b(t) = \frac{d}{dt}\mathcal{H}^1(Z \cap \overline{R^Z(t)}) \quad \text{a.e. t.} \tag{8.0.4}$$

More precisely, we have the following

Lemma 8.0.6. *The burning rate function b is* BV*.*

Proof. If $\zeta(s)$ is a point of non-differentiability of the curve, the computation of the right derivative of $\mathcal{H}^1(Z \cap \overline{R^Z(\zeta(s)})$ is

$$b^+(u(\zeta(s))) = \frac{1}{\cos(\beta^+(\zeta(s)))},$$

and similarly the left derivative. □

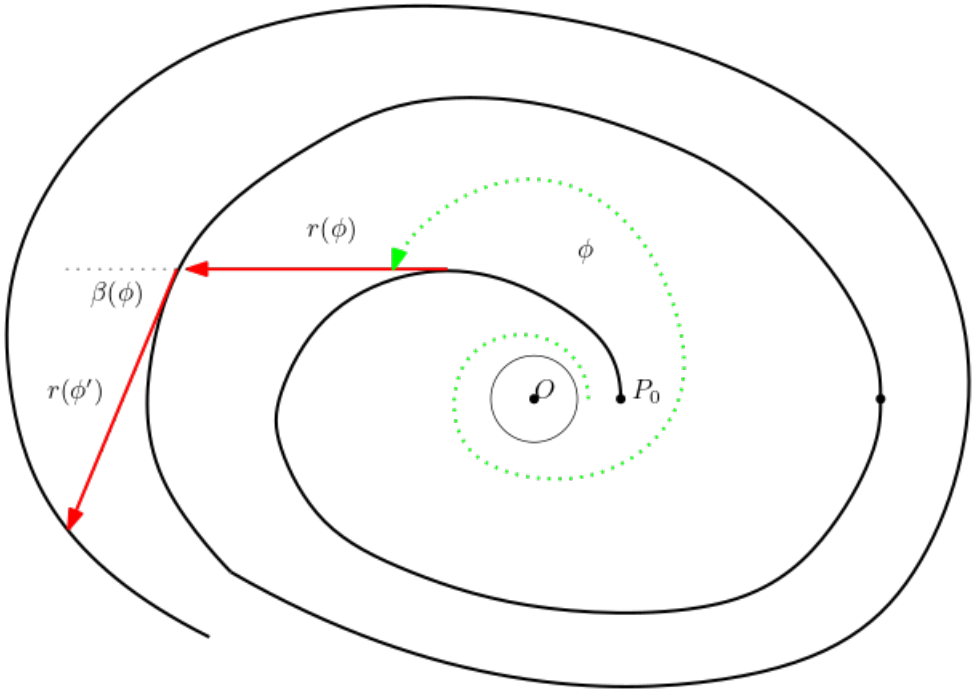

Figure 8.2: Parametrization of a spiral-like strategy. Any optimal ray $\bar{\gamma}$ is the union of a subset of the spiral and a final segment: this motivates the definition of a parametrization $(\phi, r(\phi))$ where the angle ϕ (green) is the angle of rotation of the optimal ray (defined in Equation (8.1.1)), while $r(\phi)$ is the length of the final segment of the optimal ray.

Remark 8.0.7. Fix $\zeta(s)$ a point of non-differentiability of the curve. Then, under the assumption of convexity we have that $b^+(u(\zeta(s))) \geq b^-(u(\zeta(s)))$.

Admissibility functional. We define also the Admissibility Functional related to a spiral-like strategy. Given Z an admissible spiral-like strategy, we define

$$\mathcal{A}(P) = u(P) - \frac{1}{\sigma} L(P), \quad \forall P \in Z, \tag{8.0.5}$$

where $u(P)$ is the minimum time function at P and $L(P)$ is the length of the spiral from $\zeta(0)$ until the point P.

8.1 ODE description of a spiral

In this section we will give an ODE description of spiral-like strategies. In the following, Z is an admissible spiral as in the previous section. As before, we will consider both a parametrization via length, namely $\zeta(s)$ where s is the length parameter, or $(r(\phi), \phi)$.

Lemma 8.1.1. *Let Z be an admissible spiral 8.0.4 and let $s \to \beta(s)$ (alternatively $\phi \to \beta(\phi)$) as before. Then one gets the following formulas:*

1. *The subsequent angle (see Figures 8.2, 8.3)*

$$\phi'(\phi) = \phi + \beta(\phi) + 2\pi, \tag{8.1.1}$$

(given ϕ we will denote by ϕ^{-1} the previous angle).

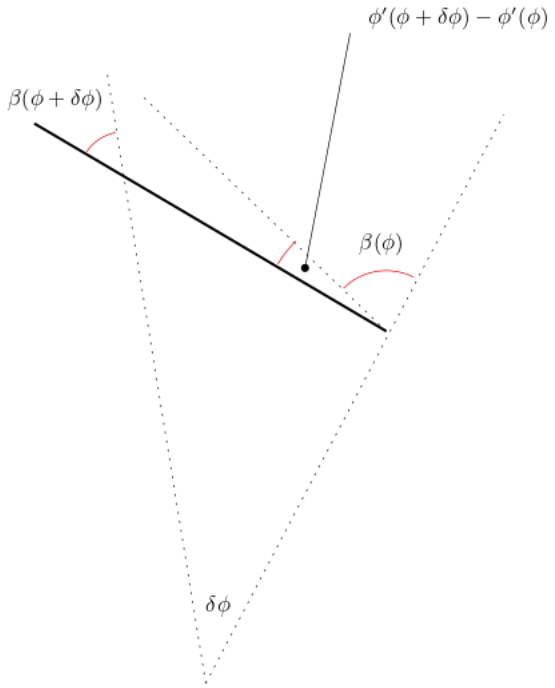

Figure 8.3: Computation of the subsequent angle $\phi'(\phi)$.

2. *If we call s the length parameter, the variation of the length is*

$$\frac{ds}{d\phi} = \frac{r(\phi)}{\sin\beta(\phi)}. \tag{8.1.2}$$

3. *In the points of differentiability of Z where $\ddot{\zeta}(s) \neq 0$ the curvature is given by*

$$\kappa = \frac{1}{R} = \frac{d\phi'}{ds}. \tag{8.1.3}$$

Finally the equation of the spiral is (by angle)

$$\frac{dr}{d\phi'} = \cot\beta(\phi')r(\phi') - R(\phi), \tag{8.1.4}$$

$$\frac{dr}{ds'} = \cos\beta(s') - \frac{ds}{ds'}. \tag{8.1.5}$$

Proof. We start computing the subsequent angle. With reference to Figure 8.3 one immediately observes that

$$\phi'(\phi+\delta\phi) - \phi'(\phi) = \beta(\phi+\delta\phi) - \beta(\phi) + \delta\phi.$$

This equation, coupled with the initial condition $\phi'(0) = 2\pi + \beta(0)$, gives the formula in the statement For point (2) observe that $\delta s = \frac{r(\phi)}{\sin(\beta(\phi))}\delta\phi$. For the point (3) one has to remember that the curvature is the modulus of $|\ddot{\zeta}(s)|$, where we indicated by $\zeta(s)$ the parametrization by arc-length. We assume that $|\ddot{\zeta}(s)| \neq 0$. The equation of the spiral is obtained in the following way:

$$r(\phi'+\delta\phi') - r(\phi') = \cot\beta(\phi')\delta\phi' r(\phi') - \int_{\phi}^{\phi+\delta\phi} \frac{r(\eta)}{\sin\beta(\eta)} d\eta,$$

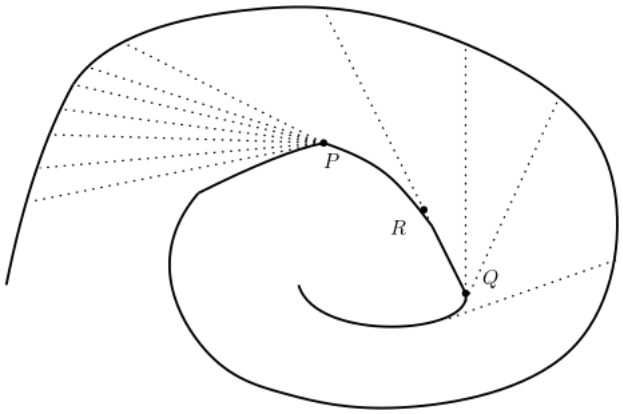

Figure 8.4: In a point of non-differentiability P the variation of the radius is computed as $\frac{d}{d\phi'}r(\phi') = \cot\beta(\phi')r(\phi')$. While the radius has a jump in the point R of the length of the segment QR.

therefore remembering (8.1.1) one gets

$$\frac{dr}{d\phi'}(\phi') = \cot\beta(\phi')r(\phi') - \frac{r(\phi)}{\sin(\beta(\phi))}\frac{1}{1+\frac{d\beta}{d\phi}(\phi)},$$

which is equivalent to

$$\frac{dr}{d\phi'}(\phi') = \cot\beta(\phi')r(\phi') - R(\phi'),$$

where R is the radius of curvature. Clearly, by equations (11.2.2),(8.1.3) one gets

$$\frac{dr}{ds'} = \frac{dr}{d\phi'}\frac{d\phi'}{ds'} = \cos\beta(s') - \frac{ds}{ds'}.$$

□

Remark 8.1.2. In the case of the first round of the equation of spiral reads as follows

$$\frac{dr}{ds} = \cos\beta(s). \tag{8.1.6}$$

Since in the assumption of the previous lemma we had $\ddot{\zeta}(s) \neq 0$, we have that, if $\ddot{\zeta}(s) = 0$ for all $s \in (s_1, s_2)$ (that is when the curve is a segment), and in the assumption of continuity of the function $s \to \beta(s)$ (that is $\beta^+ \equiv \beta^-$), the solution has a jump of the length of the segment. Instead in a point of non-differentiability the solution is computed as

$$\frac{d}{d\phi'}r(\phi') = \cot\beta(\phi')r(\phi').$$

See Figure 8.4.

8.1.1 Equation for the Saturated Spiral

We define the *Saturated Spiral* as the admissible spiral S with the following property:

$$\mathcal{S}(S) = \{t \in [0,T] : \mathcal{H}^1(S \cap \overline{R^S(t)}) = \sigma t\} = [0,T].$$

Saturated spirals are strategies built assuming the istantaneous speed of construction is constant and takes the maximum value σ, that is the burning rate function $b(t)$ is constantly equal to σ.

Proposition 8.1.3. *Any Saturated Spiral is $\mathcal{C}^1$.*

Proof. The proof exploits a blow-up argument and the convexity of the strategy S (see for the proof Lemma 7.0.6). □

The formula for burning rates tells us that, in case of saturated spirals, $\beta^+ = \beta^- = \arccos\left(\frac{1}{\sigma}\right)$. In this case (and in the following discussion) we will use the name α to indicate this angle.

Lemma 8.1.4. *Let S be a saturated spiral, and let $(r(\phi), \phi)$ its parametrization via angle. Then for $\phi \in [0, 2\pi]$ it is a logarithmic spiral.*

Proof. From the equations found in the previous section, we have that at first round

$$\frac{dr}{d\phi} = r(\phi)\cot\alpha,$$

which gives precisely the logarithmic spiral, since its radius is $r(\phi) = e^{\cot\alpha\phi}$. □

Lemma 8.1.5. *Let S be a saturated spiral. Then the radius of S satisfies the following Cauchy Problem*

$$\frac{dr}{d\phi'} = r(\phi')\cot\alpha - \frac{r(\phi' - (2\pi + \alpha))}{\sin\alpha}, \tag{8.1.7}$$

with initial data

$$r_0(\phi) = \begin{cases} e^{\cot\alpha\phi} & \forall\phi \in [0, 2\pi], \\ (r(2\pi) - 1)e^{\cot\alpha(\phi - 2\pi)} & \forall\phi \in [2\pi, 2\pi + \alpha]. \end{cases}$$

Proof. For $\phi \in [0, 2\pi]$ it is the content of the previous lemma. Assume $\phi \in [2\pi, 2\pi + \alpha]$, one easily computes that, calling $P = (1, 0)$, the saturated spiral is a logarithmic spiral centered at P with initial radius $r(2\pi) - 1$ For the computation of the angle $2\pi + \alpha$, see the computations of the subsequent angle in Lemma 8.1.1. □

8.1.2 A formulation as a retarded ODE

We consider the following RDE

$$\frac{d}{d\phi}r(\phi) = r(\phi)\cot\alpha - r(\phi - \phi_0)\frac{1}{\sin\alpha}, \tag{8.1.8}$$

where $\phi_0 \in \mathbb{R}_{>0}$ is any angle. In the assumption of saturated spirals it is $\phi_0 = 2\pi + \alpha$. (for the theory of RDEs see [29]). We observe that

$$\frac{d}{d\phi}\left(e^{-\cot\alpha\phi}r(\phi)\right) = -\frac{1}{\sin\alpha}r(\phi - \phi_0)e^{-\cot\alpha\phi}$$

therefore, if $\theta \in [0, \phi_0]$ we have that, for any $n \in \mathbb{N}$ it holds

$$r(\theta + n\phi_0) = e^{\cot\alpha\theta}r(n\phi_0) - \int_0^\theta \frac{1}{\sin\alpha}e^{\cot\alpha(\theta-\eta)}r(\eta + (n-1)\phi_0)d\eta.$$

If we call

$$\rho_n(\theta) = r(\theta + n\phi_0)$$

we get

$$\rho_n(\theta) = e^{\cot\alpha\theta}\rho_{n-1}(\phi_0) - \int_0^\theta \frac{1}{\sin\alpha}e^{\cot\alpha(\theta-\eta)}\rho_{n-1}(\eta)d\eta.$$

Therefore the retarded differential equation (8.1.8) defines a compact linear operator $T : \mathcal{C}([0, \phi_0]) \to \mathcal{C}([0, \phi_0])$

$$T\rho(\theta) = e^{\cot \alpha x}\rho(\theta) - \int_0^\theta \frac{1}{\sin \alpha} e^{\cot \alpha(\theta-\eta)}\rho(\eta)d\eta \tag{8.1.9}$$

By rescaling $x = \frac{\theta}{\phi_0}$ and $y = \frac{\eta}{\phi_0}$ and the solution $\tilde{\rho}_n(x) = \rho_n(x\phi_0)$ one gets the following compact linear operator $T : C([0, 1]; \mathbb{R}) \to C([0, 1]; \mathbb{R})$ defined by

$$T\rho(x) = e^{ax}\rho(1) - \int_0^x be^{a(x-y)}\rho(y)dy, \tag{8.1.10}$$

and its iterates, where

$$a = e^{\cot \alpha\phi_0}, \qquad b = \frac{\phi_0}{\sin \alpha}.$$

We reduce the problem to the study of the following operator

$$\tilde{T}g(x) = e^a g(1) - b\int_0^x g(y)dy,$$

observing that $e^{ax}\tilde{T}(g)(x) = T(e^{(a\cdot)}g)(x)$.

8.1.3 Computation of the eigenvalues

To find the eigenvalues of the compact operator T it is sufficient to find the eigenvalues of $\tilde{T}$ (which is still compact). We find the characteristic equation, computing $\tilde{T}g(x) = \zeta g(x)$. One finds that

$$\zeta g(x) = e^a g(1) - b\int_0^x g(y)dy. \tag{8.1.11}$$

We observe that $\zeta = 0$ is not in the point spectrum (it is not an eigenvalue). Therefore one has

$$\zeta g'(x) = -bg(x),$$

so

$$g(x) = g(1)e^{\frac{b}{\zeta}(1-x)}$$

and putting inside the equation (8.1.11) one finds

$$\zeta e^{\frac{b}{\zeta}} = e^a,$$

that is

$$\zeta e^{\frac{2\pi+\alpha}{\sin \alpha \zeta}} = e^{\cot \alpha(2\pi+\alpha)} \tag{8.1.12}$$

Calling $\tilde{\zeta} = \frac{b}{\zeta}$ one finds the equation

$$\frac{e^{\tilde{\zeta}}}{\tilde{\zeta}} = \frac{e^a}{b} = \frac{e^{\cot \alpha(2\pi+\alpha)}}{\frac{2\pi+\alpha}{\sin \alpha}}. \tag{8.1.13}$$

We study therefore the function

$$z \to \frac{e^z}{z},$$

with $z = x + iy$ complex number. We find that:

$$\frac{e^{x+iy}}{x+iy} = \frac{e^x}{x^2+y^2}(\cos y + i \sin y)(x - iy) = \frac{e^x}{x^2+y^2}\left[(x\cos y + y \sin y) + i\,(x \sin y - y \cos y)\right].$$

- If $y = 0$ we have real eigenvalues and the equation reads as

$$\frac{e^x}{x} = \frac{e^a}{b}. \tag{8.1.14}$$

In particular we find that

1. If $\alpha < \bar{\alpha} = 1.1783$ we have two solutions x_1, x_2 with $x_2 > 1$ and $x_1 < 1$.
2. If $\alpha = \bar{\alpha} = 1.1783$ we have a unique eigenvalue at $x = 1$ with multiplicity 2, corresponding to $\zeta = b$.
3. If $\alpha > \bar{\alpha}$ we have no real eigenvalues (this case corresponds to $\frac{e^a}{b} < e$).

- If $y \neq 0$ we have that $x = y \cot y$, in particular one has to study

$$f(y) = \frac{e^{y \cot y} \sin y}{y} = \frac{e^a}{b}.$$

The function $y \mapsto e^{y \cot y} \frac{\sin y}{y}$ has the properties:

– for $y \to 0$

$$\lim_{y \to 0} e^{y \cot y} \frac{\sin y}{y} = e;$$

– the function is even (being a real operator, the eigenvalues are complex conjugate), therefore we can limit our analysis to $y > 0$;

– the limits are (if $k \geq 1$)

$$\lim_{y \nearrow k\pi} e^{y \cot y} \frac{\sin y}{y} = 0,$$

$$\lim_{y \searrow k\pi} e^{y \cot y} \frac{\sin y}{y} = \infty.$$

Hence the following situation occurs:

1. if $\alpha > \bar{\alpha}$, then there are only complex eigenvalues, the ones with positive imaginary part in $y \in (2k, 2k+1)\pi$, $k > 1$, and a couple for $|y| < \pi$;
2. at $\bar{\alpha}$, the couple at $|y| < \pi$ converges to the point $y = 0$ (which is also real);
3. for $\alpha < \bar{\alpha}$, there is a couple of real roots and a family of complex roots for $|y| > \pi$, one in each interval $(k\pi, (k+1)\pi)$, $k \geq 1$.

8.1.4 Analysis on the complex eigenvalues

For the complex eigenvalues, we obtain

$$x = y \cot y, \quad \frac{e^{y \cot y} \sin y}{y} = \frac{e^a}{b}.$$

– There are eigenvalues for $y_k \in (2k\pi, (2k+1)\pi)$, $k \geq 1$, corresponding to the solution

$$\frac{e^{y \cot y} \sin y}{y} = \frac{e^a}{b}.$$

The corresponding eigenvalues are

$$\zeta_k = \frac{b}{x_k + i y_k},$$

that is

$$\zeta_k = \frac{b \sin y_k}{y_k}\big(\cos y_k - i \sin y_k\big).$$

Writing

$$y_k = 2\pi k + \frac{\pi}{2} - \delta_k,$$

we obtain the equation

$$\frac{e^{(2\pi k + \frac{\pi}{2} - \delta_k)\tan(\delta_k)} \cos \delta_k}{2\pi k + \frac{\pi}{2} - \delta_k} = \frac{e^a}{b}.$$

– For $k = 1$ we obtain that in the original formulation (the one with the angle α)

$$\delta_1 = \frac{\pi}{2} - \alpha, \quad y_1 = \phi_0 = 2\pi + \alpha, \quad x_1 = \phi_0 \tan \alpha, \quad \zeta_1 = \sin \alpha - \imath \cos \alpha.$$

– For general k, we observe that

$$\frac{d}{du} \frac{e^{(u-v)\tan v} \cos v}{u - v} \begin{cases} < 0 & u < v + \cot v, \\ 0 & u = v + \cot v, \\ > 0 & u > v + \cot v, \end{cases}$$

and then the critical points have value

$$e \sin v < e.$$

In particular all other complex eigenvalues have decreasing δ_k.

– As $k \to \infty$, $\delta_k \to 0$ and expanding

$$\frac{e^{2\pi k \delta_k}}{2\pi k} \simeq \frac{e^a}{b}, \quad \delta_k \simeq \frac{\ln(\frac{e^a 2\pi k}{b})}{2\pi k}.$$

In the original eigenvalues, we get

$$\zeta_k = \frac{b \cos \delta_k}{2\pi k + \frac{\pi}{2} - \delta_k}(\sin \delta_k - i \cos \delta_k) = \frac{b}{2\pi k + \frac{\pi}{2}} \left(\frac{\ln(\frac{e^a 2\pi k}{b})}{2\pi k} - i \right).$$

Hence the lie on the curve

$$x \simeq y^2 \ln(1/y).$$

– Note that the complex eigenvalues are simple and have eigenfunctions (computed for the original operator T)

$$\begin{aligned} \rho(x) &= \rho(0) e^{(a - \frac{b}{\zeta_k})x} = \rho(0) e^{(a - z_k)x} \\ &= e^{(a - x_k)x}\big(\cos(y_k x) - i \sin(y_k x)\big). \end{aligned}$$

In particular, since $y_k > 2\pi$ for $k > 1$, they change sign in the interval $[0, 1]$. These are solutions which already at the beginning are changing sign.

– For the first eigenvalue we have that $y_1 < \pi$, so that the real part of the initial solution ρ_1 is not changing sign. However by iteration we get

$$T^n \rho(x) = e^{(a - x_1)(x+n)}(\cos(y_1(x+n)) - i \sin(y_1(x+n))).$$

$$T^n \rho(x) = e^{(a - x_k)(x+n)}(\cos(y_k(x+n)) - i \sin(y_k(x+n))); \qquad (8.1.15)$$

An application to strategies.

We assume now that $\sigma > \bar{\sigma} = 2.614430844373.. = \frac{1}{\cos\bar{\alpha}}$. Consider the following situation: a firefighter construct any admissible spiral with construction speed σ up to some point Q, with the property that in the point Q it holds $\beta^-(Q) \leq \bar{\alpha}$ (recall the definitions in the previous section). From the point Q it starts constructing a spiral with constant angle $\bar{\alpha}$. With abuse of notation from now on we will call *saturated branches* the arcwise connected subsets of spiral-like strategies constructed with constant angle. The new spiraling strategy obtained in this way is still convex, moreover it is admissible: in this case, since the point Q is admissible by definition of admissible spirals (Definition 4.6.6), then any point on the saturated branch remains admissible. Indeed it holds that, if S is this particular strategy, then

$$\mathcal{H}^1(S \cap \overline{R^S(t)}) = \mathcal{H}^1(S \cap \overline{R^S(s_Q)}) + \sigma(t - s_Q) \leq \sigma t, \quad \forall t \geq s_Q,$$

with $s_Q = u(Q)$ (u is the minimum time function), where we have used that the burning rate (8.0.4) is constantly equal to σ and the fact that Q is admissible. An ODE point of view to look at these strategies is precisely the one given by the RDE (8.1.8), with initial data r_0 given by the radius of the strategy chosen at the beginning by the firefighter. The previous discussion on the complex spectrum of the operator justifies the following:

Proposition 8.1.6. *If $\sigma > \bar{\sigma}$, then for any initial data the saturated spiral confines the fire.*

Proof. We consider the change of variables

$$\rho(t) = r((2\pi + \alpha)t)e^{-(2\pi+\alpha)\cot\alpha t},$$

then the function ρ satisfies the following RDE:

$$\dot{\rho}(t) + \frac{(2\pi + \alpha)}{\sin(\alpha)} e^{-(2\pi+\alpha)\cot\alpha}\rho(t-1) = 0.$$

It is a well known fact that for RDE of the form $\dot{x} + c(x - r) = 0$ with $c > 0$ every solution is oscillating iff the characteristic equation $\lambda + ce^{-\lambda r} = 0$ has only complex eigenvalues (see for example [38]). □

8.1.5 A change of variables

In this subsection we study a change of variable of the solution of (8.1.8). This will be of key importance for the computations performed in the next sections, since exploiting this formulation allows, in a relatively simple manner, to prove that a spiral does not confine the fire (or, in other words, that the radius of any admissible spiral is always strictly positive). Here we will use these computations to prove that the saturated spiral (see (4.6.1)) does not confine the fire for $\sigma < \bar{\sigma}$ (Proposition 8.1.10).

We consider the following change of variable:

$$\rho(t) = r((2\pi + \alpha)t)e^{-c(2\pi+\alpha)t},$$

with

$$c = \cot\alpha - \frac{\log\left(\frac{a}{b}\right)}{2\pi + \alpha}.$$

The function ρ satisfies the following equation

$$\dot{\rho}(t) = \log\left(\frac{a}{b}\right)\rho(t) - \rho(t-1). \tag{8.1.16}$$

Observe that in the case $\alpha = \bar{\alpha}$ then the previous equation becomes

$$\dot{\rho}(t) = \rho(t) - \rho(t-1), \tag{8.1.17}$$

since $\frac{a}{b} = e$, and

$$\bar{c} = \cot\bar{\alpha} - \frac{1}{2\pi + \bar{\alpha}}, \tag{8.1.18}$$

with $\bar{c} = 0.27995$.

Lemma 8.1.7 (Change of variables)**.** *Let $\frac{a}{b} \geq e$. If $\rho(1) > \rho(t) > 0$ for every $t \in [0,1)$ and $\rho : [0,+\infty) \to \mathbb{R}$ is continuous, then $r(\phi) > 0$, for every ϕ.*

Proof. Since $\frac{a}{b} \geq e$ we have that $\log(\frac{a}{b}) \geq 1$. Consider the interval $[1,2]$ (the proof will be run inductively for any interval $[n, n+1]$), and define

$$\bar{t} = \sup\{t \in [1,2] : \rho(t) \geq \rho(1)\},$$

then since ρ is continuous, $\rho(\bar{t}) \geq \rho(1)$. Then

$$\dot{\rho}(\bar{t}) = \log\left(\frac{a}{b}\right)\rho(\bar{t}) - \rho(\bar{t}-1) > \rho(\bar{t}) - \rho(1) \geq 0,$$

where we have used that $\rho(\bar{t}-1) < \rho(1)$ and that $\rho(\bar{t}) \geq \rho(1)$. Since $\dot{\rho}(\bar{t}) > 0$, by continuity of the function $\dot{\rho}$ the supremum must be equal to 2. Moreover, the same inequality $\dot{\rho}(t) > 0$ holds for any $t \in [1,2]$: in particular ρ is monotonically increasing in $[1,2]$ and $\rho(2) > \rho(t) > 0$ for any $t \in [1,2)$. The induction is performed in the same way. Since this proves that $\rho > 0$, clearly $r(\phi)$ is positive for every ϕ. □

Remark 8.1.8. Note that (8.1.17) has the solutions 1 and t, corresponding to the two generalized eigenfunctions of the Delay DE.

Remark 8.1.9. The previous lemma proves also that the function $\rho \geq \kappa > 0$, in particular the function $r(\phi) \geq \kappa e^{c\phi}$ increases exponentially fast.

As an application of the previous discussion, we show how this lemma can be applied to a concrete case (the saturated spiral (4.6.1)) to prove that the strategy cannot confine the fire.

Proposition 8.1.10. *Let S be the saturated spiral. Then it does not confine the fire for $\sigma \leq \bar{\sigma}$.*

Proof. Recall the initial data for the saturated spiral is given in Lemma 8.1.5: it is

$$r_0(\phi) = \begin{cases} e^{\cot\bar{\alpha}\phi} & \forall\phi \in [0, 2\pi), \\ (e^{2\pi\cot\bar{\alpha}} - 1)e^{\cot\bar{\alpha}(\phi - 2\pi)} & \forall\phi \in [2\pi, 2\pi + \bar{\alpha}]. \end{cases}$$

We compute the solution of the RDE (8.1.8) for $\phi \in [2\pi + \bar{\alpha}, 4\pi + 2\bar{\alpha}]$ and we find that, for $\phi \in [2\pi + \bar{\alpha}, 4\pi + \bar{\alpha}]$

$$\begin{aligned} r(\phi) &= r(2\pi + \bar{\alpha})e^{\cot\bar{\alpha}(\phi - 2\pi - \bar{\alpha})} - \frac{1}{\sin\bar{\alpha}}\int_{2\pi+\bar{\alpha}}^{\phi} e^{\cot\bar{\alpha}(\phi-\eta)} r(\eta - 2\pi - \bar{\alpha})d\eta \\ &= r(2\pi + \bar{\alpha})e^{\cot\bar{\alpha}(\phi - 2\pi - \bar{\alpha})} - \frac{1}{\sin\bar{\alpha}} e^{\cot\bar{\alpha}(\phi - 2\pi - \bar{\alpha})}\int_{0}^{\phi - 2\pi - \bar{\alpha}} e^{-z\cot\bar{\alpha}} r(z)dz, \end{aligned}$$

and since $\phi \in [2\pi + \bar{\alpha}, 4\pi + \bar{\alpha}]$ we have that

$$r(\phi) = \left(r(2\pi + \bar{\alpha}) - \frac{1}{\sin \bar{\alpha}} (\phi - 2\pi - \bar{\alpha}) \right) e^{\cot \bar{\alpha}(\phi - 2\pi - \bar{\alpha})}, \quad \phi \in [2\pi + \bar{\alpha}, 4\pi + \bar{\alpha}].$$

The same computation can be performed for $\phi \in [4\pi + \bar{\alpha}, 4\pi + 2\bar{\alpha}]$, finding

$$r(\phi) = \left(r(4\pi + \bar{\alpha}) - \frac{e^{2\pi \cot \bar{\alpha}} - 1}{\sin \bar{\alpha}} (\phi - 4\pi - \bar{\alpha}) \right) e^{\cot \bar{\alpha}(\phi - 4\pi - \bar{\alpha})}, \quad \phi \in [4\pi + \bar{\alpha}, 4\pi + 2\bar{\alpha}];$$

In order to prove the positivity of the function $r(\phi)$ we apply Lemma 8.1.7: as before we define

$$\rho\left(\frac{\phi}{2\pi + \bar{\alpha}} \right) = r(\phi) e^{-\bar{c}\phi},$$

and we prove that the function ρ is increasing in the interval $[1, 2]$ (corresponding to $\phi \in [2\pi + \bar{\alpha}, 4\pi + \bar{\alpha}]$) proving that the derivative of $r(\phi)e^{-\bar{c}\phi}$ is strictly positive, so that r can never go to zero. Using the previous equations we find that for $\phi \in [2\pi + \bar{\alpha}, 4\pi + \bar{\alpha}]$

$$\begin{aligned} \frac{d}{d\phi} r(\phi) e^{-\bar{c}\phi} = & -\frac{1}{\sin \bar{\alpha}} e^{\cot \bar{\alpha}(\phi - 2\pi - \bar{\alpha}) - \bar{c}\phi} + \\ & + \frac{1}{2\pi + \bar{\alpha}} \left(r(2\pi + \bar{\alpha}) - \frac{1}{\sin \bar{\alpha}} (\phi - 2\pi - \bar{\alpha}) \right) e^{\cot \bar{\alpha}(\phi - 2\pi - \bar{\alpha}) - \bar{c}\phi}, \end{aligned}$$

where we have used (8.1.18) for the value $\bar{c}$.

In particular we have that the sign of the derivative depends on the following quantity:

$$Q_1(\phi) = r(2\pi + \bar{\alpha}) - \frac{1}{\sin \bar{\alpha}} \phi,$$

and performing the same computations for the interval $\phi \in [4\pi + \bar{\alpha}, 4\pi + 2\bar{\alpha}]$ we find

$$Q_2(\phi) = r(4\pi + \bar{\alpha}) - \frac{e^{2\pi \cot \bar{\alpha}} - 1}{\sin \bar{\alpha}} (\phi - 2\pi).$$

If we prove that these two quantities are positive then the derivative of $r(\phi)e^{-\bar{c}\phi}$ is positive and therefore the spiral can never confine the fire.

Estimates on Q_1 and Q_2. We observe that

$$\begin{aligned} Q_1 = r(2\pi + \bar{\alpha}) - \frac{1}{\sin \bar{\alpha}} \phi & \geq r(2\pi + \bar{\alpha}) - \frac{1}{\sin \bar{\alpha}} (4\pi + \bar{\alpha}) \\ & = (e^{2\pi \cot \bar{\alpha}} - 1) e^{\bar{\alpha} \cot \bar{\alpha}} - \frac{1}{\sin \bar{\alpha}} (4\pi + \bar{\alpha}) \geq 5. \end{aligned}$$

Similarly,

$$Q_2 \geq r(4\pi + \bar{\alpha}) - \frac{e^{\cot \bar{\alpha}(2\pi)} - 1}{\sin \bar{\alpha}} (\phi - 2\pi) \geq r(4\pi + \bar{\alpha}) - \frac{e^{\cot \bar{\alpha}(2\pi)} - 1}{\sin \bar{\alpha}} (2\pi + 2\bar{\alpha}) \geq 65.$$

□

Chapter 9

Existence of optimal closing barriers

In this chapter we give the main geometric motivation for the study of families of generalized barriers.

Here and in the following, we fix $Z \in \mathcal{A}_S$ an admissible spiral-like strategy (Definition 8.0.4). We call $(r(\phi), \phi)$ its parametrization by angle (see Remark 8.0.3), and $\zeta(s)$ its parametrization by arc-length, but we will use alternatively the notation $\zeta(\phi)$ to denote the point $(r(\phi), \phi)$ (if there is no risk of confusion). We remark that in this section we will work with any construction speed $\sigma > 0$ and we recall that the angle α is defined as

$$\alpha = \arccos\left(\frac{1}{\cos\alpha}\right).$$

In this section we will address the following **optimization problem**: fix any admissible strategy Z and any angle $\bar{\phi}$, then the minimization problem is

$$\min_{\tilde{Z} \in \mathcal{A}_S(Z,\bar{\phi})} r_{\tilde{Z}}(\phi), \qquad \text{for some } \phi \geq \bar{\phi}, \tag{9.0.1}$$

where $\mathcal{A}_S(Z, \bar{\phi})$ denotes the class of admissible spirals that coincide with Z up to the angle $\bar{\phi}$, and if $\tilde{Z} \in \mathcal{A}_S(Z, \bar{\phi})$, $(r_{\tilde{Z}}(\phi), \phi)$ will denote its parametrization by angle. Differently from what stated for the optimization problem (4.4.13), for which it has been proved that the minimum exists among admissible blocking strategies (therefore in a class that could be empty) [17], here the class of strategies is non-empty, since we are not assuming in general that the spiral-like strategies they confine the fire.

Here, for any angle $\bar{\phi}$ fixed, we also want to determine the best strategy $\hat{Z}$ parametrized by $(\hat{r}(\phi), \phi)$ with the following properties:

- $\hat{r}(\phi) = r(\phi)$ for $\phi \leq \bar{\phi}$;
- $\hat{Z}$ is optimal in $[\bar{\phi}, \bar{\phi} + 2\pi]$, where optimal means that $\hat{r}(\phi) \leq \tilde{r}(\phi)$ for every admissible spiral-like strategy $\tilde{Z}$ parametrized by $(\tilde{r}(\phi), \phi)$ which coincides with Z up to the angle $\bar{\phi}$.

The position $\zeta(\bar{\phi})$ is reached by the fire at time $t(\bar{\phi}) = u(\zeta(\bar{\phi}))$, where u is the minimum time function, and the *admissibility functional* reads therefore as

$$\mathcal{A}(\bar{\phi}) = t(\bar{\phi}) - \frac{L(\zeta([0, \bar{\phi}]))}{\sigma} \geq 0.$$

The aim of this section is to prove that $\hat{Z}$ has the following structure, starting from $\zeta(\bar{\phi})$:

1. it follows the level set $\{u = u(\zeta(\bar\phi))\}$ for $\phi \in [\bar\phi, \bar\phi + \Delta\phi = \phi_1]$;
2. for $\phi \in [\phi_1, \phi_2]$ it is a segment tangent to the level set and its endpoint $\zeta(\phi_2)$ not lying on the level set $\{u = u(\zeta(\bar\phi))\}$ is saturated (which means that $\mathcal{A}(\phi_2) = 0$);
3. for $\phi \geq \phi_2$ it is a saturated spiral, in the sense that the angle $\beta(\phi) = \alpha$ for every $\phi \geq \phi_2$ (see the previous section for the definitions). In particular the constraint $\mathcal{H}^1(\hat Z \cap \overline{R^{\hat Z}(t)}) = \sigma t$ for every $t \geq u(\zeta(\phi_2))$ is satisfied since the point $\zeta(\phi_2)$ is saturated for point (2).

Even if it is possible to give the shape of the best strategy $\hat Z$ minimizing $r(\phi)$ with $\phi \in [\bar\phi, \bar\phi + 2\pi]$, it is an open question if it is possible to write down explicitly the shape of a minimizer for the problem (9.0.1). The computations that we will perform in this section suggest that the natural guess for the minimizer is the following strategy: it is a circle, starting from the point $(1, 0)$, a segment whose last point is saturated, and then a saturated spiral, meaning that the angle with the fire rays is constantly equal to α, as in Figure 10.2. Actually it turned out it is not the right one (we will discuss this point in the next chapter).

9.0.1 Study of the distance function u

The function u is the solution to HJ equation,

$$u(x) = \operatorname{dist}(x, 0) = \min\big\{L(\gamma), \gamma \text{ admissible}\big\}.$$

Without loss of generality we call with the same name $\zeta(s)$ the parametrization of the spiral by arc-length. If $x \in Z$, then $s(x)$ is the length of the spiral Z up to the point where the optimal ray $\bar\gamma_x$ becomes a segment.

Lemma 9.0.1. *The function u is convex in $\mathbb{R}^2 \setminus Z$, and if $\zeta(s(x))$ is the last point where $\bar\gamma_x$ is a segment (recall $\bar\gamma_x$ is an optimal ray), then*

$$\nabla u = \frac{x - \zeta(s(x))}{|x - \zeta(s(x))|} = \mathbf{t}(s), \quad \nabla^2 u = \frac{1}{|x - \zeta(s(x))|}\mathbf{n}(s) \otimes \mathbf{n}(s),$$

where $n(s)$ is the normal vector at $\zeta(s)$. The case $\kappa(s(x)) = 0$ is analogous, and $\nabla^2 u$ is locally BV with jumps on the directions where Z is flat, since the radius of curvature $x - \zeta(s(x))$ has jumps.

Proof. All statements follows from the computation of the formulas. We consider only the case where $\zeta(s(x))$ is a differentiability point of Z and $\zeta''(s) = 1/R(s)\mathbf{n}(s) \neq 0$. Denote also $\mathbf{t} = \zeta'(s)$.

Using the parametrization

$$s, r \mapsto x(s, r) = \zeta(s) + r\mathbf{t}(s),$$

we have that

$$u(s, r) = \text{const} + s + r.$$

Then

$$\begin{aligned} Du &= (1,1) \cdot (Dx)^{-1} \\ &= (1,1)^T \left\{ \begin{bmatrix} \mathbf{t} & \mathbf{n} \end{bmatrix} \begin{bmatrix} 1 & 1 \\ r/R & 0 \end{bmatrix} \right\}^{-1} \\ &= (1,1)^T \begin{bmatrix} 0 & R/r \\ 1 & -R/r \end{bmatrix} \begin{bmatrix} \mathbf{t} & \mathbf{n} \end{bmatrix}^T \\ &= \mathbf{t}^T. \end{aligned}$$

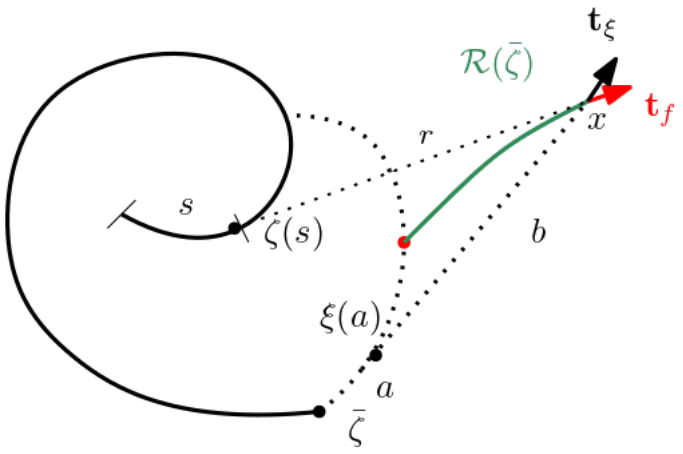

Figure 9.1: The green line is the set $\mathcal{R}(\bar\zeta)$ where all the points are saturated. It divides the region into the admissible and the non admissible part.

This proves the first formula.

Differentiating $\nabla u(x(s,r)) = \zeta'(s)$, one obtains

$$\nabla^2 u(x(s,r))\mathbf{t}(s) = 0, \qquad \nabla^2 u(x(s,r))(\mathbf{t}(s) + \frac{r}{R}\mathbf{n}(s)) = \frac{1}{R}\mathbf{n}(s),$$

i.e.

$$\nabla^2 u = \frac{1}{R}\mathbf{n}\otimes\mathbf{n},$$

which is the second formula. □

9.0.2 Construction of the curve of minimal reachable points

Definition 9.0.2. The set $\mathcal{R}(\bar\zeta)$, $\bar\zeta = \zeta(\bar\phi)$, of minimal reachable points is the set of end points of curves made of a piece of fire level set passing by $\zeta(\bar\phi)$ plus a tangent segment to the level set: all the points should be admissible, not crossing Z and the last point is saturated (meaning that the admissibility functional in the last point is zero).

It is possible that none of the points on the fire level set $\xi = u^{-1}(u(\bar\zeta))$ is saturated : in this case there is no starting point of the curve. We thus assume that there is a point $\xi(a)$ such that

$$u(\xi(a)) = u(\bar\zeta) \geq \frac{L(\zeta([0,\bar\phi])) + L(\xi([0,\bar a]))}{\sigma} = \frac{L(\zeta([0,\bar\phi])) + a}{\sigma}.$$

Clearly such a point is unique, (see Figure 9.1). Let $x \in \mathcal{R}(\bar\zeta)$, and $[\zeta(s), x]$ the last segment part of the optimal ray, $[\xi(a), x]$ the segment part of the admissible curve, with respective length r, b. Denote also

$$\mathbf{t}_f = \nabla u(x) = \frac{x-\zeta(s)}{|x-\zeta(s)|},\ \mathbf{n}_f = \mathbf{t}_f^\perp, \quad \mathbf{t}_\xi = \dot\xi(a) = \frac{x-\xi(a)}{|x-\xi(a)|},\ \mathbf{n}_\xi = \mathbf{t}_\xi^\perp.$$

Proposition 9.0.3. *The tangent to $\mathcal{R}(\bar\zeta)$ in x is given by*

$$\mathbf{v} = \frac{\mathbf{n}_f - \mathbf{n}_\xi/\sigma}{|\mathbf{n}_f - \mathbf{n}_\xi/\sigma|},$$

oriented according to $u_f \circ \mathcal{R}, u_\xi \circ \mathcal{R}$ increasing, where

$$u_f(\zeta(s) + r\zeta'(s)) = s + r, \quad u_\xi(\xi(a) + b\xi'(a)) = a + b,$$

$\dot\zeta$ is the tangent to the spiral and $\dot\xi$ denotes the tangent to the level set.

The minimal slope of $\mathcal{R}$ is the slope of the saturated spiral, and starting from the point $\xi(a)$ up to this point of the curve is admissible, the quantity $(\nabla u_f \cdot \nabla u_\xi) \circ \mathcal{R}$ is increasing.

After this point the curve is not admissible, in the sense that the segment has points outside the admissibility region. Moreover the curve is convex in the direction of $\mathbf{v}^\perp$ in the admissibility part.

Proof. Let u_f, u_ξ be the HJ solutions defined by

$$u_f(\zeta(s) + r\zeta'(s)) = s + r, \quad u_\xi(\xi(a) + b\xi'(a)) = a + b.$$

The admissibility functional reads as

$$\mathcal{A}(x) = \text{const} + s + r - \frac{a+b}{\sigma} = \text{const} + u_f(x) - \cos(\alpha)u_\xi(x) = 0.$$

Differentiating and using Lemma 9.0.1 we obtain

$$\nabla\mathcal{A} = \mathbf{t}_f - \cos(\alpha)\mathbf{t}_\xi,$$

and

$$\big(\nabla u_f - \cos(\alpha)\nabla u_\xi\big) \cdot \mathbf{v} = \big(\mathbf{t}_f - \cos(\alpha)\mathbf{t}_\xi\big) \cdot \mathbf{v} = 0,$$

with $\mathbf{v}$ the vector of the statement, which is the tangent to the curve $\mathcal{R}(\bar\zeta)$, and this gives precisely the statement. The orientation follows because we assume a counterclockwise rotation, and in the starting point on the level set $\{u = u(\bar\zeta)\}$ we obtain $\mathbf{n}_\xi = -\mathbf{t}_f$, so that the vector of the statement becomes

$$\mathbf{v} = \frac{\mathbf{n}_f + \cos(\alpha)\mathbf{t}_f}{|\mathbf{n}_f + \cos(\alpha)\mathbf{t}_f|}.$$

In particular the initial angle in the fire frame, that is $\angle(\mathbf{v}, \mathbf{t}_f)$ in this point is greater than α. The derivative of $u_f \circ \mathcal{R}$ is

$$(u_f \circ \mathcal{R})' = -\cos(\alpha)\frac{(\mathbf{t}_f \cdot \mathbf{n}_\xi)}{|\mathbf{n}_f - \mathbf{n}_\xi/\sigma|}$$

which is positive (we chose the orientation such that $u \circ \mathcal{R}$ was increasing) unless $\mathbf{t}_f \perp \mathbf{n}_\xi$, which means that the lines are parallel, and then $\mathcal{R} \to \infty$ (or it hits the barrier Z). Similarly,

$$(u_\xi \circ \mathcal{R})' = \frac{(\mathbf{t}_\xi \cdot \mathbf{n}_f)}{|\mathbf{n}_f - \mathbf{n}_\xi/\sigma|} = -\frac{(\mathbf{t}_f \cdot \mathbf{n}_\xi)}{|\mathbf{n}_f - \mathbf{n}_\xi/\sigma|} > 0,$$

as the saturation condition requires. One could also prove that $\mathbf{v} \cdot \mathbf{t}_f$ decreases.

In general, in the fire frame $(\mathbf{t}_f, \mathbf{n}_f)$ the position of $\mathbf{n}_f - \cos(\alpha)\mathbf{n}_\xi$ is contained in $(0,1) + \{|z| = \cos(\alpha)\}$, and the minimal slope is when $\mathbf{v} = e^{i\alpha}$. This point is in the cone $\alpha\mathbf{t}_f + \beta\mathbf{t}_\xi$ up to this tangent point, giving that the gradient of the two functions are approaching. Writing the derivative explicitly one gets

$$\begin{aligned}(\nabla u_f \cdot \nabla u_\xi \circ \mathcal{R})' &= \mathbf{v}^T \frac{\mathbf{n}_f \otimes \mathbf{n}_f}{r_f}\mathbf{t}_\xi + \mathbf{v}^T \frac{\mathbf{n}_\xi \otimes \mathbf{n}_\xi}{r_\xi}\mathbf{t}_f \\ &= \frac{\mathbf{t}_\xi \cdot \mathbf{n}_f}{|\mathbf{n}_f - \cos(\alpha)\mathbf{n}_\xi|}\left(\frac{1 - \cos(\alpha)\mathbf{n}_f \cdot \mathbf{n}_\xi}{r_f} - \frac{\mathbf{n}_f \cdot \mathbf{n}_\xi - \cos(\alpha)}{r_\xi}\right) > 0,\end{aligned}$$

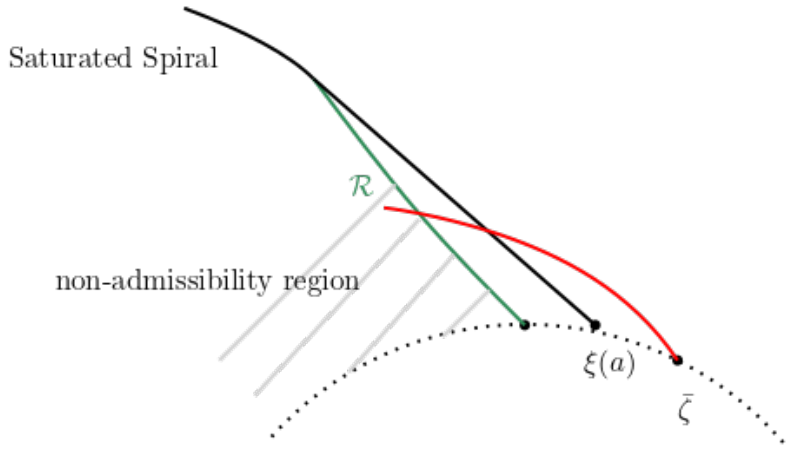

Figure 9.2: If by contradiction an admissible spiral (the red curve) crosses the strategy made by an arc, a segment whose last point is saturated and then a saturated spiral, it would enter the non-admissibility region. For the proof of this result see Corollary 9.0.4

so that

$$\frac{1-\cos(\alpha)\mathbf{n}_f\cdot\mathbf{n}_\xi}{r_f}-\frac{\mathbf{n}_f\cdot\mathbf{n}_\xi-\cos(\alpha)}{r_\xi}>0.$$

In particular, the angle $\angle(\mathbf{t}_f,\mathbf{t}_\xi)$ along the curve $\mathcal{R}$ decreases. We call $\bar{x}$ the point at which this angle is α, (the critical point). In the point $\bar{x}$ we have that $\mathbf{v}\parallel\mathbf{t}_\xi$.

After the critical angle, the vector $\mathbf{t}_\xi$ moves counterclockwise, which means that we are going to take values of a already used. However the derivative of the admissibility functional satisfies

$$\nabla\mathcal{A}=\mathbf{t}_f-\cos(\alpha)\mathbf{t}_\xi,$$

and thus for directions with angle $>\alpha$

$$\nabla\mathcal{A}\cdot\mathbf{t}_\xi=\cos(\psi_\mathbf{v})-\cos(\alpha)<0.$$

Hence in this part the functional is not admissible.

The second derivative of $\mathcal{A}$ along v gives

$$\begin{aligned}\mathbf{v}^T\nabla^2\mathcal{A}\mathbf{v}&=\frac{(\mathbf{n}_f\cdot\mathbf{v})^2}{r_f}-\cos(\alpha)\frac{(\mathbf{n}_\xi\cdot\mathbf{v})^2}{r_f}\\&=\frac{1}{|\mathbf{n}_f-\cos(\alpha)\mathbf{n}_\xi|^2}\left(\frac{(1-\cos(\alpha)\mathbf{n}_f\cdot\mathbf{n}_\xi)^2}{r_f}-\frac{(\mathbf{n}_f\cdot\mathbf{n}_\xi-\cos(\alpha))^2}{r_\xi}\right)\\&\geq\frac{1}{|\mathbf{n}_f-\cos(\alpha)\mathbf{n}_\xi|^2}\frac{\mathbf{n}_f\cdot\mathbf{n}_\xi-\cos(\alpha)}{r_\xi}\big(1-\cos(\alpha)\mathbf{n}_f\cdot\mathbf{n}_\xi-\mathbf{n}_f\cdot\mathbf{n}_\xi+\cos(\alpha)\big)>0.\end{aligned}$$

Hence the curve is convex in the direction of $\mathbf{v}^\perp$. □

The curve $\mathcal{R}$ has 3 possibilities:

1. there is no starting point on the fire level set;
2. the curves starts on the fire level set and touches Z;
3. there is a starting point on the level set $\xi(a)$. The point W is the one where the angle is α ($\bar{x}$ of the previous proof).

Corollary 9.0.4. *Assume that there is a starting point of the curve $\mathcal{R}(\bar{\zeta})$ on the level (case 3 above, see Figure 9.2), and let ς be the saturated spiral passing though W. Call θ_0 the angle that the spiral Z makes with the optimal ray $\bar{\gamma}_{\bar{\zeta}}$ and call $\hat{r}$ the radius of the strategy given by the arc (subset of $\{u = u(\bar{\zeta})\}$), the segment up to the point W and the saturated spiral (we will call this strategy $\hat{Z}$). Then $r(\phi) \geq \hat{r}(\phi)$ for every $\phi \in [\bar{\phi}, \bar{\phi} + 2\pi + \theta_0]$.*

This discussion tells us that the points on $\mathcal{R}$ are admissible and are the ones giving the shortest $r(\phi)$ for the angle ϕ.

Proof. Assume that the admissible strategy crosses the segment: then it must cross the curve $\mathcal{R}$ in a point $\bar{z}$ by convexity. In particular it must be an arc and a segment up to the point $\bar{z}$ (if not, it would be longer than this strategy and therefore not anymore admissible in the point $\bar{z}$). This strategy is characterized by the fact that $\angle(\mathbf{v}(\bar{z}), \mathbf{t}_\xi(\bar{z})) > \alpha$, so that the burning rate (8.0.4) of the strategy is greater than σ (by the convexity assumption on spiral-like strategies): this is not admissible. If instead the admissible strategy Z crosses the saturated spiral ς for $\phi \leq \bar{\phi} + 2\pi + \theta_0$ in a point $\bar{z}'$ then we would have

$$u(\bar{z}') - \frac{1}{\sigma} L(\bar{z}') < u(\bar{z}') - \frac{1}{\sigma} \hat{L}(\bar{z}') = 0,$$

where $\hat{L}(z')$ is the length of the strategy $\hat{Z}$ up to the point $\bar{z}'$. Here we have used $u(\bar{z}') = \hat{u}(\bar{z}')$. The last equality is because the point $\bar{z}'$ is saturated (living on a saturated spiral). In particular $\bar{z}'$ would not be admissible. Here it is crucial that $\phi \leq \bar{\phi} + 2\pi + \theta_0$ since the optimal rays of the two strategies Z and $\hat{Z}$ "coincide" up to the angle $\bar{\phi} + 2\pi + \theta_0$, so that, in the intersection points $\bar{z}'$, it holds $u(\bar{z}') = \hat{u}(\bar{z}')$. □

Chapter 10

A case study

Here the construction speed $\bar{\sigma} = 2.6144..$ is the critical speed, and $\bar{\alpha} = \arccos\left(\frac{1}{\bar{\sigma}}\right)$. The computations of the previous section suggest to study the following case study: assume that the fire spreads in a ball $B_a(0)$ with $a \in (0, 1]$ and that a player starts constructing a spiral S_a starting from a point $(1, 0) = P_0$ with the following property: in $\phi \in [0, 2\pi]$ it is the union of a circle (eventually consisting of a single point), a segment of endpoints $P_1(a), P_2(a)$ tangent to the circle in $P_1(a)$ such that the point $P_2(a)$ is saturated, that is

$$\mathcal{A}(P_2(a)) = u(P_2(a)) - \frac{1}{\bar{\sigma}} L(P_2(a)) = 0,$$

where $L(P_2(a))$ is the length of the spiral S_a up to the point $P_2(a)$. From the point $P_2(a)$ it is a saturated spiral, that is the angle β made by the spiral and the fire rays (see Section 8) is constantly equal to $\bar{\alpha}$.

The relevant equations are the following:

- the length of the arc of circle is $P_0P_1(a) = \Delta\phi_a$;
- the length of the segment is $\overline{P_1(a)P_2(a)} = \frac{1}{\sin\bar{\alpha}}$;
- **Saturation condition on $P_2(a)$:**

$$u(P_2(a)) - \frac{1}{\bar{\sigma}} L(P_2(a)) = \left(\frac{1}{\sin\bar{\alpha}} - a\right) - \frac{1}{\bar{\sigma}}\left(\Delta\phi_a + \frac{\cos\bar{\alpha}}{\sin\bar{\alpha}}\right) = 0.$$

In particular,

$$\Delta\phi_a = \bar{\sigma}\left(\frac{1}{\sin\bar{\alpha}} - a\right) - \frac{\cos\bar{\alpha}}{\sin\bar{\alpha}} = \tan\bar{\alpha} - \frac{a}{\cos\bar{\alpha}}, \tag{10.0.1}$$

since $\bar{\sigma} = \frac{1}{\cos\bar{\alpha}}$. Depending on the value of a we have the following situation: $\Delta\phi_a \leq 0$ or $\Delta\phi_a > 0$.

Case $\Delta\phi_a > 0$: Here the formula for $\Delta\phi_a$ is given by (10.0.1), corresponding to $a < \sin\bar{\alpha}$ and $\theta_a = \angle P_2(a)OP_1(a) = \frac{\pi}{2} - \bar{\alpha}$.

Case $\Delta\phi_a \leq 0$: if $\Delta\phi_a \leq 0$ (corresponding to $a \geq \sin\bar{\alpha}$) it means that $P_1(a) \equiv P_0$, in particular, by the Theorem of Sines, it holds

$$\overline{P_1(a)P_2(a)} = \frac{\sin\theta_a}{\sin\bar{\alpha}},$$

Figure 10.1: The two cases with $\Delta\phi_a > 0$ and $\Delta\phi_a \leq 0$.

.

where $\theta_a = \angle P_2(a)OP_1(a)$. Here the saturation condition on $P_2(a)$ is the following

$$(\overline{P_2(a)O} - a) - \frac{1}{\bar\sigma}\overline{P_1(a)P_2(a)} = \frac{\sin(\theta_a + \bar\alpha)}{\sin\bar\alpha} - a - \frac{1}{\bar\sigma}\frac{\sin\theta_a}{\sin\bar\alpha} = 0, \qquad (10.0.2)$$

which gives implicitly the value of θ_a. Indeed since $\frac{1}{\bar\sigma} = \cos\bar\alpha$ we have that:

$$\cos\theta_a = a,$$

and since $a \geq \sin\bar\alpha$ we find that $\theta_a \in [0, \frac{\pi}{2} - \bar\alpha]$.

The two cases are explained in Figure 10.1. We will prove the following

Theorem 10.0.1. *For any value of $a \in (0,1]$, the spiral S_a does not confine the fire.*

The proof of this theorem relies on a careful application of Lemma 8.1.7. Before proving the previous theorem, we give the proof of the following two lemmas on properties of the solution of RDEs.

Lemma 10.0.2. *Let $r(\phi)$ such that*

$$\frac{d}{d\phi}r(\phi) = \lambda r(\phi) - \gamma r(\phi - \phi_0),$$

for some $\lambda, \gamma, \phi_0 > 0$, and, given $\phi_0 \leq \phi_1 \leq \phi_2$, assume that

$$r(\phi) = \kappa e^{\lambda(\phi - \phi_1 + \phi_0)}, \quad \forall \phi \in [\phi_1 - \phi_0, \phi_2 - \phi_0],$$

for some constant κ. Then

$$r(\phi) = \left(r(\phi_1) - \gamma r(\phi_1 - \phi_0)(\phi - \phi_1)\right) e^{\lambda(\phi - \phi_1)}, \quad \forall \phi \in [\phi_1, \phi_2].$$

Proof. The proof follows easily by the following fact:

$$\begin{aligned} r(\phi) &= e^{\lambda(\phi-\phi_1)}r(\phi_1) - \gamma\int_{\phi_1}^{\phi} e^{\lambda(\phi-\eta)}r(\eta - \phi_0)d\eta \\ &= e^{\lambda(\phi-\phi_1)}r(\phi_1) - \gamma\int_{\phi_1-\phi_0}^{\phi-\phi_0} e^{\lambda(\phi-z-\phi_0)}\kappa e^{\lambda(z-\phi_1+\phi_0)}dz \\ &= \left(r(\phi_1) - \gamma\kappa(\phi - \phi_1)\right) e^{\lambda(\phi-\phi_1)}, \end{aligned}$$

which is the statement. □

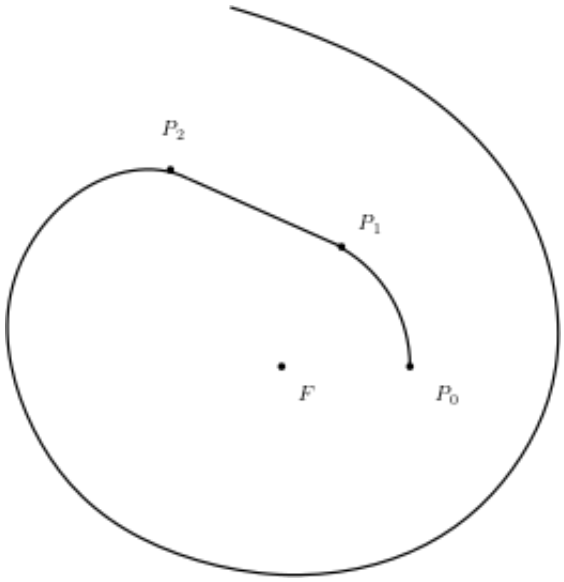

Figure 10.2: Here f_0 is made by an arc, a segment and a saturated spiral.

Lemma 10.0.3. *Let $r(\phi)$ such that*

$$\frac{d}{d\phi}r(\phi) = \lambda r(\phi) - \gamma r(\phi - \phi_0),$$

for some $\lambda, \gamma, \phi_0 > 0$, and, given $\phi_0 \leq \phi_1 \leq \phi_2$, assume that

$$r(\phi) = \left(r(\phi_1) - \gamma r(\phi_1 - \phi_0)(\phi - \phi_1)\right) e^{\lambda(\phi - \phi_1)}, \quad \forall \phi \in [\phi_1, \phi_2].$$

Call

$$\bar{d} = \lambda - \frac{1}{\phi_0}.$$

Then if $r(\phi_1), r(\phi_1 - \phi_0) \geq 0$ the function

$$\rho(\phi) = r(\phi)e^{-\bar{d}\phi}$$

is monotonically increasing in $[\phi_1, \phi_2]$ if

$$r(\phi_1) - \gamma r(\phi_1 - \phi_0)(\phi_2 - \phi_1 + \phi_0) \geq 0. \tag{10.0.3}$$

Proof. The computation of the derivative of $\rho(\phi)$ is straightforward, in particular

$$\operatorname{sign}(\rho'(\phi)) = \operatorname{sign}\left(\frac{r(\phi_1)}{\phi_0} - \gamma\left(r(\phi_1 - \phi_0) + \frac{1}{\phi_0}r(\phi_1 - \phi_0)(\phi - \phi_1)\right)\right),$$

and the conclusion follows observing that $r(\phi_1), r(\phi_1 - \phi_0) \geq 0$. □

We are ready to give the proof of Theorem 10.0.1.

Proof. We divide the proof in the study of the two cases $\Delta\phi_a > 0$ and $\Delta\phi_a \leq 0$.

- **Case $\Delta\phi_a > 0$.**This case is described in Figure 10.2. We remark that from (10.0.1) we find that $\Delta\phi_a \in (0, \tan\bar{\alpha}]$, the worst possible case is $\tan\bar{\alpha}$ corresponding to $a = 0$.

  $$\Delta\phi = \tan\bar{\alpha}. \tag{10.0.4}$$

  We call r_a the radius of the spiral S_a (see Remark 8.0.3). Then it can be computed as follows:

– for $\phi \in [\Delta\phi_a, \Delta\phi_a + \frac{\pi}{2} - \bar{\alpha})$ we have that

$$r_a(\phi) = \frac{1}{\cos(\phi - \Delta\phi_a)},$$

in particular we call

$$\kappa_1(a) = r_a\left(\Delta\phi_a + \frac{\pi}{2} - \bar{\alpha}\right) = \frac{1}{\sin\bar{\alpha}};$$

– for $\phi \in [\Delta\phi_a + \frac{\pi}{2} - \bar{\alpha}, 2\pi)$ it holds

$$\frac{d}{d\phi} r_a(\phi) = \cot\bar{\alpha} r_a(\phi),$$

since the spiral is saturated, that is

$$r_a(\phi) = \kappa_1(a) e^{\cot\bar{\alpha}(\phi - \frac{\pi}{2} + \bar{\alpha} - \Delta\phi_a)},$$

– the radius r_a has a jump at $\phi = 2\pi$, that is

$$r_a(2\pi) - r_a(2\pi-) = -1,$$

in particular we denote by

$$\kappa_2(a) = r_a(2\pi) = \kappa_1(a) e^{\cot\bar{\alpha}\left(2\pi - \frac{\pi}{2} + \bar{\alpha} - \Delta\phi_a\right)} - 1;$$

– for $\phi \in [2\pi, 2\pi + \frac{\pi}{2} + \Delta\phi_a)$ it holds

$$\frac{d}{d\phi} r_a(\phi) = \cot\bar{\alpha} r_a(\phi),$$

therefore

$$r_a(\phi) = \left[\frac{1}{\sin\bar{\alpha}} e^{\cot\bar{\alpha}(2\pi - \frac{\pi}{2} + \bar{\alpha} - \Delta\phi_a)} - 1\right] e^{\cot\bar{\alpha}(\phi - 2\pi)}; \tag{10.0.5}$$

– the radius r_a has a jump in $\phi = 2\pi + \frac{\pi}{2} + \Delta\phi_a$, that is

$$r_a\left(2\pi + \frac{\pi}{2} + \Delta\phi_a\right) - r_a\left(2\pi + \frac{\pi}{2} + \Delta\phi_a-\right) = -\cot\bar{\alpha},$$

and also here we denote by

$$\kappa_3(a) = r_a\left(2\pi + \frac{\pi}{2} + \Delta\phi_a\right) = \kappa_2(a) e^{\cot\bar{\alpha}\left(\frac{\pi}{2} + \Delta\phi_a\right)} - \cot\bar{\alpha}.$$

– for $\phi \geq 2\pi + \frac{\pi}{2} + \Delta\phi$ the function solves

$$\frac{d}{d\phi} r_a(\phi) = \cot\bar{\alpha} r_a(\phi) - \frac{r_a(\phi - 2\pi - \bar{\alpha})}{\sin\bar{\alpha}}.$$

Optimization w.r.t. a. We optimize with respect to the parameter a, computing the ODE satisfied by $\partial_a r_a(\phi)$. We find that

– for $\phi \in [0, \Delta\phi_a]$ it is $\partial_a r_a(\phi) = 0$;

– for $\phi \in [\Delta\phi_a, \Delta\phi_a + \frac{\pi}{2} - \bar{\alpha}]$ it holds

$$\partial_a r_a(\phi) = \frac{\sin(\phi - \Delta\phi_a)}{\cos\bar{\alpha}\cos^2(\phi - \Delta\phi_a)};$$

– for $\phi \in [\Delta\phi_a + \frac{\pi}{2} - \bar{\alpha}, \Delta\phi_a + \frac{\pi}{2} + 2\pi]$ it satisfies

$$\frac{d}{d\phi}\partial_a r_a(\phi) = \cot\bar{\alpha}\partial_a r_a(\phi);$$

– for $\phi \geq \Delta\phi_a + \frac{\pi}{2} + 2\pi$ it satisfies

$$\frac{d}{d\phi}\partial_a r_a(\phi) = \cot\bar{\alpha}\partial_a r_a(\phi) - \frac{\partial_a r_a(\phi - 2\pi - \bar{\alpha})}{\sin\bar{\alpha}}.$$

Similar computations to the ones performed in Section 8, Proposition 8.1.10 show that $\partial_a r_a(\phi) \geq 0$. Indeed, by Lemma 10.0.2 we have that

$$\partial_a r_a(\phi) = \left(\frac{1}{\sin^2\bar{\alpha}} e^{\cot\bar{\alpha}(2\pi+\bar{\alpha})} - \frac{1}{\sin^3\bar{\alpha}}(\phi - \Delta\phi_a - \frac{\pi}{2} - 2\pi)\right) e^{\cot\bar{\alpha}(\phi - \Delta\phi_a - \frac{\pi}{2} - 2\pi)},$$

for $\phi \in [\Delta\phi_a + \frac{\pi}{2} + 2\pi, 4\pi + \bar{\alpha} + \frac{\pi}{2} + \Delta\phi_a]$. In order to apply Lemma 8.1.7 we use Lemma 10.0.3 and we have that $\partial_a r_a(\phi) \geq 0$ if the following quantity

$$\frac{1}{\sin\bar{\alpha}^2} e^{\cot\bar{\alpha}(2\pi+\bar{\alpha})} - \frac{1}{\sin\bar{\alpha}^3}(4\pi + 2\bar{\alpha}) \geq 0.$$

But this is clearly true, since the previous quantity is ≥ 6.7. In particular this reduces our analysis to the case $a = 0$.

From now on we will assume $a = 0$ therefore $\Delta\phi_0 = \tan\bar{\alpha}$. We remark that the function r_0 is continuous for every $\phi \geq 2\pi + \frac{\pi}{2} + \tan\bar{\alpha}$. To use Lemma 8.1.7, we first need to compute $r_0(\phi)$ for $\phi \in \left[2\pi + \frac{\pi}{2} + \tan\bar{\alpha}, 4\pi + \frac{\pi}{2} + \tan\bar{\alpha} + \bar{\alpha}\right]$, such that the change of variable $\rho_0(\phi) = r_0(\phi)e^{-\bar{c}\phi}$ is continuous, where $\bar{c}$ is given in (8.1.18). We apply Lemma 10.0.2 and we find that for $\phi \in \left[2\pi + \frac{\pi}{2} + \tan\bar{\alpha}, 4\pi + \bar{\alpha}\right]$ it holds

$$r_0(\phi) = \left(\kappa_3(0) - \frac{1}{\sin\bar{\alpha}}\kappa_1(0)\left(\phi - \left(2\pi + \frac{\pi}{2} + \tan\bar{\alpha}\right)\right)\right) e^{\cot\bar{\alpha}\left(\phi - \left(2\pi + \frac{\pi}{2} + \tan\bar{\alpha}\right)\right)},$$

and called $\kappa_4(0) = r_0(4\pi + \bar{\alpha})$ one gets in the same way

$$r_0(\phi) = \left(\kappa_4(0) - \frac{1}{\sin\bar{\alpha}}\kappa_2(0)\left(\phi - (4\pi + \bar{\alpha})\right)\right) e^{\cot\bar{\alpha}(\phi - (4\pi + \bar{\alpha}))}.$$

Thanks to Lemma 10.0.2, in order to prove the monotonicity of the function ρ we need to prove that the two following quantities:

$$Q_1 = \kappa_3(0) - \frac{1}{\sin\bar{\alpha}}\kappa_1(0)\left(4\pi + 2\bar{\alpha} - \frac{\pi}{2} - \tan\bar{\alpha}\right) \geq 0,$$

$$Q_2 = \kappa_4(0) - \frac{1}{\sin\bar{\alpha}}\kappa_2(0)\left(2\pi + \frac{\pi}{2} + \tan\bar{\alpha} + \bar{\alpha}\right) \geq 0.$$

We evaluate numerically these two quantities finding that they are positive. Indeed one can check that

$$\kappa_1(0) = 1.0823, \qquad \kappa_2(0) = 3.56172, \qquad \kappa_3(0) = 18.1369, \qquad \kappa_4(0) = 59.2869,$$

and that

$$Q_1 = 5.32605, \qquad Q_2 = 15.157.$$

Thanks to Lemma 8.1.7 this proves that the spiral S_a does not confine the fire in the case $\Delta\phi_a \geq 0$.

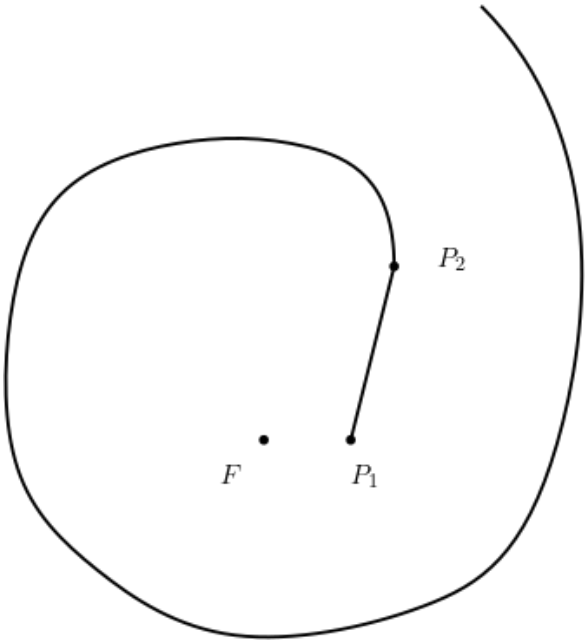

Figure 10.3: The function $\phi \to f_0(\phi)$.

- **Case $\Delta\phi_a \leq 0$.** This case is described in Figure 10.3. We compute $r_a(\phi)$ explicitly. We call $\bar{\theta}_a = \theta_a + \bar{\alpha}$, then
  - for $\phi \in [0, \bar{\theta}_a - \bar{\alpha}]$ we have that
    $$r_a(\phi) = \frac{\sin \bar{\theta}_a}{\sin(\bar{\theta}_a - \phi)},$$
    and we call
    $$\kappa_1'(a) = r_a(\bar{\theta}_a - \bar{\alpha}) = \frac{\sin \bar{\theta}_a}{\sin \bar{\alpha}};$$
  - for $\phi \in [\bar{\theta}_a - \bar{\alpha}, 2\pi)$ it holds
    $$\frac{d}{d\phi} r_a(\phi) = \cot \bar{\alpha} r_a(\phi),$$
    that is
    $$r_a(\phi) = \kappa_1'(a) e^{\cot \bar{\alpha}(\phi - \bar{\theta}_a + \bar{\alpha})};$$
  - the function $r_a(\phi)$ has a jump at $\phi = 2\pi$, indeed
    $$r_a(2\pi) - r_a(2\pi-) = -1,$$
    and we call
    $$\kappa_2'(a) = r_a(2\pi) = \frac{\sin \bar{\theta}_a}{\sin \bar{\alpha}} e^{\cot \bar{\alpha}(2\pi - \bar{\theta}_a + \bar{\alpha})};$$
  - for $\phi \in [2\pi, 2\pi + \bar{\theta}_a)$ it holds
    $$\frac{d}{d\phi} r_a(\phi) = \cot \bar{\alpha} r_a(\phi),$$
    so that
    $$r_a(\phi) = \kappa_2'(a) e^{\cot \bar{\alpha}(\phi - 2\pi)};$$

– in $\phi = 2\pi + \bar\theta_a$ the function r_a has a jump, computed as

$$r_a(2\pi + \bar\theta_a) - r_a(2\pi + \bar\theta_a -) = -\frac{\sin(\bar\theta_a - \bar\alpha)}{\sin\bar\alpha},$$

and we call

$$\kappa_3'(a) = r_a(2\pi + \bar\theta_a) = \kappa_2'(a)e^{\cot\bar\alpha\bar\theta_a} - \frac{\sin(\bar\theta_a - \bar\alpha)}{\sin\bar\alpha};$$

– finally, for $\phi \geq 2\pi + \bar\theta_a$ the function solves

$$\frac{d}{d\phi}r_a(\phi) = \cot\bar\alpha r_a(\phi) - \frac{r_a(\phi - 2\pi - \bar\alpha)}{\sin\bar\alpha}.$$

Optimization w.r.t. a. We optimize with respect to the parameter a, computing the ODE satisfied by $\partial_a r_a(\phi)$. We recall that $\bar\theta_a = \theta_a + \bar\alpha$ and $\cos\theta_a = a$. Thereofre we find that

– for $\phi \in [0, \bar\theta_a - \bar\alpha]$ it holds

$$\partial_a r_a(\phi) = \frac{\sin\phi}{\sin(\bar\theta_a - \bar\alpha)\sin^2(\bar\theta_a - \phi)};$$

– for $\phi \in [\bar\theta_a - \bar\alpha, 2\pi + \bar\theta_a]$ it satisfies

$$\frac{d}{d\phi}\partial_a r_a(\phi) = \cot\bar\alpha\partial_a r_a(\phi);$$

– in the point $\phi = 2\pi + \bar\theta_a$ the derivative has a jump, namely

$$\partial_a r_a(2\pi + \bar\theta_a) - \partial_a r_a(2\pi + \bar\theta_a -) = \frac{\cot(\bar\theta_a - \bar\alpha)}{\sin\bar\alpha};$$

– for $\phi \geq 2\pi + \bar\theta_a$ it satisfies

$$\frac{d}{d\phi}\partial_a r_a(\phi) = \cot\bar\alpha\partial_a r_a(\phi) - \frac{\partial_a r_a(\phi - 2\pi - \bar\alpha)}{\sin\bar\alpha}.$$

By using Lemma 10.0.2 one finds that, for $\phi \in [2\pi + \bar\theta_a, 4\pi + \bar\theta_a + \bar\alpha]$

$$\begin{aligned}\partial_a r_a(\phi)e^{-\cot\bar\alpha(\phi - 2\pi - \bar\theta_a)} = {} & \frac{\sin\phi}{\sin(\bar\theta_a - \bar\alpha)\sin^2(\bar\theta_a - \phi)}e^{\cot\bar\alpha(2\pi + \bar\alpha)} + \frac{\cot(\bar\theta_a - \bar\alpha)}{\sin\bar\alpha} \\ & - \frac{1}{\sin\bar\alpha}\frac{\sin\phi}{\sin(\bar\theta_a - \bar\alpha)\sin^2(\bar\theta_a - \phi)}(\phi - 2\pi - \bar\theta_a).\end{aligned}$$

We observe that

$$\frac{\sin\phi}{\sin(\bar\theta_a - \bar\alpha)\sin^2(\bar\theta_a - \phi)} \llcorner_{\phi = \bar\theta_a - \bar\alpha}, \frac{\cot(\bar\theta_a - \bar\alpha)}{\sin\bar\alpha} \geq 0;$$

by applying Lemma 10.0.3, we have that the sign of the function $\partial_a r_a(\phi)$ in the interval $[2\pi + \bar\theta_a, 4\pi + \bar\theta_a + \bar\alpha]$ depends on the following quantity (recall Lemma 8.1.7 and the change of variables):

$$Q(a) = \partial_a r_a(2\pi + \bar\theta_a) - \frac{1}{\sin\bar\alpha}\partial_a r_a(\bar\theta_a - \bar\alpha)(4\pi + 2\bar\alpha).$$

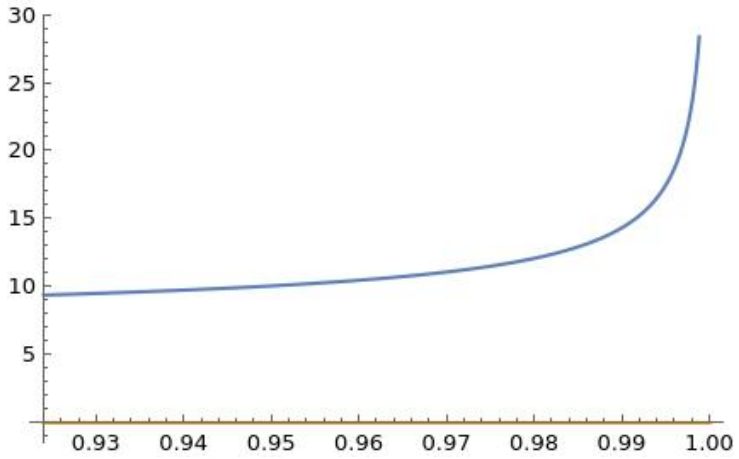

Figure 10.4: On the x-axis the parameter $a \in [\sin\bar{\alpha}, 1)$, and the blue function is $Q(a)$, which is positive. The orange line represents the axis $y = 0$.

The numerical evaluation of this quantity is positive (see Figure 10.4), which tells us that $\partial_a r_a(\phi) \geq 0$. In particular, this implies that the only case to study corresponds to $a = \sin\bar{\alpha}$. The discussion on the case $\Delta\phi_a \geq 0$ allows us to further reduce this case to $a = 0$. This concludes the proof of the theorem, since this proves that $r_a(\phi) \geq r_0(\phi)$, for every angle ϕ, and $r_0(\phi) \geq 0$ by the computations on the previous case.

□

Corollary 10.0.4. *The element Z_0 with parametrization $(r_0(\phi), \phi)$ does not confine the fire, moreover $r_0(\phi) \to +\infty$ exponentially fast.*

Proof. The proof follows by Remark 8.1.9. □

Chapter 11

Family of generalized barriers

> In this chapter we construct the family of generalized barriers: in the first section we consider elements of the family made by an arc (a subset of the level set of the minimum time function u), a segment whose endpoint is saturated and a saturated spiral (arc case). In the second section we assume that the arc is made by a single point (segment case). The numerical evidence shows that the derivative of the family $\bar{f}_s$ is positive.

In this chapter we will exhibit an example of a diverging family of generalized barriers. The computations that the construction requires rely on the evaluation of some algebraic-type functions, in the spirit of what has been done in Theorem 10.0.1 of the previous section, where we have analyzed concrete examples of admissible barriers and we have proved that they do not confine the fire. Here, we fix $\hat{\sigma} = 2.3$ and

$$\hat{\alpha} = \arccos\left(\frac{1}{\sigma}\right),$$

while $\bar{\sigma} = 2.6144..$ is the critical speed and α denotes the corresponding angle. We consider also $Z = \zeta([0, S]) \in \mathcal{A}_S$ an admissible spiral, where $(r(\phi), \phi)$ denotes its parametrization by angle (Remark 8.0.3). For every point $\zeta(s)$ of the barrier we can assign an element of a family of generalized barriers, namely

Definition 11.0.1 (Family of Generalized Barriers)**.** We say that $f_s \in \mathrm{SBV}([0, +\infty); \mathbb{R})$, with $s \in [0, S]$, is an element of the family of generalized barriers $\mathcal{F}_Z$ if:

- $f_0(\phi) > 0$ for $\phi \in [0, +\infty)$;
- $f_s(\phi) = r(\phi)$ for every $\phi \leq \bar{\phi}$ whenever $\zeta(s) = (r(\bar{\phi}), \bar{\phi})$.

Moreover, we say that it is a *diverging family* if, calling

$$\bar{f}_s(\phi) = \lim_{h \to 0} \frac{f_{s+h}(\phi) - f_s(\phi)}{h}, \tag{11.0.1}$$

then $\bar{f}_s(\phi) \geq 0$ for every $\phi \in [0, \infty)$.

We recall that exhibiting an example of a diverging family of generalized barriers is necessary for the proof of Theorem 4.6.5, whose proof follows by Theorem 4.6.7. In this section we will prove the following

Theorem 11.0.2. *If $\hat{\sigma} \leq 2.3$ there exists a diverging family $\{f_s\} = \mathcal{F}_Z$ of generalized barriers.*

A possible candidate for the family is given following the geometric intuition of Section 9. We recall that we have proved that, fixed any angle $\bar{\phi}$, the best strategy we can construct for $\phi \in [\bar{\phi}, \bar{\phi} + 2\pi + \theta_0]$ where $\beta(\bar{\phi}) = \theta_0$ (Corollary 9.0.4) is the one given by the union of a subset of the level set $u^{-1}(u(r(\bar{\phi}), \bar{\phi}))$, a segment tangent to it whose last point is saturated and then a saturated spiral. In Chapter 10 we have then proved that the strategy made by a circle, a segment tangent to it and a saturated spiral, does not confine the fire, which gives precisely the proof that f_0, which is the first element of the family of generalized barriers, is always strictly positive. Even if perfectly reasonable, this family f_s turned out to be non-diverging (see Definition 4.6.6), since $\bar{f}_s \leq 0$ in a small region. And this inequality was true even for the value $\hat{\sigma} = \frac{1+\sqrt{5}}{2}$ of Theorem 4.6.4.

The idea to overcome this issue was to change a slightly bit the family suggested by Section 9. Since Theorem 4.6.7 yields the inequality

$$r(\phi) \geq f_0(\phi), \quad \forall \phi,$$

it states in other words that f_0 is the best strategy (the one minimizing $r(\phi)$ for every ϕ) a player can do: it can decide to put some barrier on a level set, continue as a segment tangent to the level set and then it can construct a saturated spiral for the maximum speed available: the critical speed. This strategy is clearly not admissible, and this is the reason for considering *generalized* barriers.

The idea here is that at any point $\zeta(s) = (r(\bar{\phi}), \bar{\phi})$ of the spiral the strategy that confines better the fire is the union of a subset of the level set $u^{-1}(\zeta(s))$, a segment tangent to it and a saturated spiral for the critical speed $\sigma = 2.6144...$ In some sense it corresponds to slowing down the fire at the speed $\frac{\hat{\sigma}}{\sigma}$ and then having at our disposal the construction speed $\hat{\sigma}\left(\frac{\sigma}{\hat{\sigma}}\right) = \sigma$. We will prove that this new family is diverging, and its explicit construction will give the proof of Theorem 11.0.2. The heuristic motivations behind this choice of the family is not satisfactory: it is not clear while this method stops working with higher values of the speed $\hat{\sigma}$. Moreover, even if we strongly believe that variations of this procedure can be explored in order to increase the value of $\hat{\sigma}$ ($\sim 2.4 - 2.5$), the critical case seems to us very difficult to solve with such techniques.

Clearly, a key ingredient of the proof of Theorem 11.0.2 is to show that the first element f_0 of the family is always strictly positive (and actually we will see that it increases exponentially). This is the content of the first subsection. Then, we need to construct a generic element of the family $\mathcal{F}_Z$. In the second subsection we will consider generic elements f_s of the family made by an arc (a subset of the level set of the minimum time function u), a segment whose endpoint is saturated and a saturated spiral for the critical speed σ (**arc case**). In the third subsection we will assume that the arc is made by a single point (**segment case**).

We give an idea of the proof of Theorem 11.0.2: we first construct two elements of the family f_s and $f_{s+\delta s}$. We then compute the derivative

$$\bar{f}_s(\phi) = \lim_{\delta s \to 0} \frac{f_{s+\delta s}(\phi) - f_s(\phi)}{\delta s} \qquad \text{a.e } s.$$

The main observation here is the following: since both $f_{s+\delta s}$ and f_s for $\phi >> \bar{\phi}$ are saturated spirals, that is they satisfy the RDE (8.1.8) for $\bar{\alpha}$, then by linearity also their difference satisfies the same RDE. Therefore the study of the derivative $\bar{f}_s$ relies on a careful study of the solution of the same RDE. Numerical computations prove that $\bar{f}_s(\phi) \geq 0$. We will see indeed that the study of this problem relies on the evaluation of some explicit algebraic-type functions, that we will perform numerically (all the plots

are available in the Appendix 11.2.2). We use the software Mathematica to simply verify that all the quantities we are interested in are positive.

11.0.1 Construction of the element f_0.

We assume that the fire starts spreading in $(0,0)$ and that we start constructing our barrier in $(1,0)$ (this choice is motivated by the analysis performed in the proof of Theorem 10.0.1). We give the explicit construction of the element f_0. It is the union of a circle of endpoints P_0, P_1, a segment tangent to the circle of endpoints P_1, P_2 where P_2 is saturated for the following functional

$$\mathcal{A}_{\bar{\sigma},\hat{\sigma}}(P_2) = u(P_2) - \frac{1}{\sigma}\overline{P_1P_2} - \frac{1}{\sigma}P_0P_1 - \frac{1}{\hat{\sigma}}L(P_0) = 0, \tag{11.0.2}$$

where P_0P_1 denotes the length of the arc. We put $L(P_0) = 0$ since the point P_0 must be admissible for the Admissibility Functional (8.0.5) for $\hat{\sigma}$. If we call $\Delta\phi = \Delta\phi_{\bar{\sigma},\hat{\sigma}}$ the angle covered by the circle, then Equation (11.0.2) reads as

$$\frac{1}{\sin\alpha} - \frac{1}{\sigma}\cot\alpha - \frac{1}{\sigma}\Delta\phi = 0,$$

in particular

$$\Delta\phi = \tan\alpha, \tag{11.0.3}$$

since $\bar{\sigma} = \frac{1}{\cos\alpha}$. This is precisely the case study of Section 10 (see Equation (10.0.4)), whose parametrization was denoted by $(r_0(\phi), \phi)$. The discussion of the previous section (Theorem 10.0.1, Corollary 10.0.4) is clearly the proof of

Theorem 11.0.3 (Base case)**.** *The first element of the family does not confine the fire, that is $f_0(\phi) > 0$ for every $\phi \geq 0$ and $f_0(\phi) \to \infty$ exponentially fast.*

11.1 Analysis of Perturbations - Arc Case

We fix ϕ_0 and we consider an element of the family $f_{\zeta^{-1}(r(\phi_0,\phi_0))} = f_{\phi_0}$ defined in the following way:

- $f_{\phi_0}(\phi) = r(\phi)$ for every $\phi \leq \phi_0$;
- $(f_{\phi_0}(\phi), \phi) \subset \{u = u((r(\phi_0), \phi_0)\}$ for $\phi \in [\phi_0, \phi_0 + \Delta\phi]$;
- $(f_{\phi_0}(\phi), \phi))$ for $\phi \in [\phi_0 + \Delta\phi = \phi_1, \phi_2]$ is a segment of endpoints P_1, P_2 such that $P_1 \in \{u = u((r(\bar{\phi}), \bar{\phi})\}$ and P_2 is saturated for the following functional:

  $$u(P_2) - \frac{1}{\sigma}|P_2 - P_1| - \frac{1}{\sigma}P_0P_1 - \frac{1}{\hat{\sigma}}L(P_0) = 0, \tag{11.1.1}$$

  where u is the minimum time function, P_1P_0 denotes the length of the subset of the level set and $L(P_0)$ denotes the length of the spiral from the starting point until the point P_0. Moreover the segment P_1P_2 is tangent to $\{u = u((r(\bar{\phi}), \bar{\phi})\}$ in P_1. Here we use (11.1.1) because in the case $P_2 \equiv P_1$ the previous expression becomes the admissibility functional $\mathcal{A}$ (see (8.0.5)) for $\hat{\sigma}$.
- $r(\phi)$ is solution to the following RDE

  $$\dot{r}(\phi) = \cot\alpha r(\phi) - \frac{r(\phi - 2\pi - \alpha)}{\sin\alpha},$$

  for $\phi \geq \phi_2$.

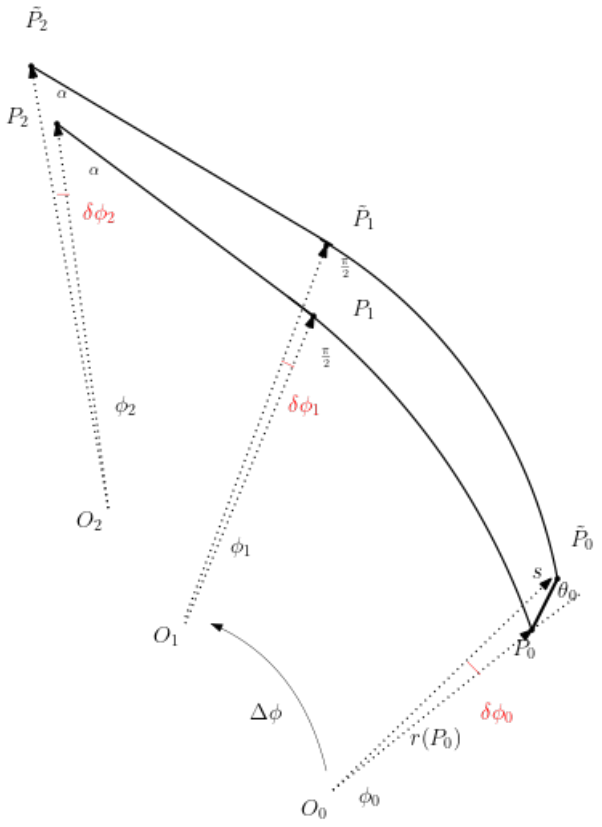

Figure 11.1: Perturbation of the family.

We want to study the new closest spiral obtained by perturbing the initial point P_0, that is

$$P_0 \to P_0 + se^{i\theta_0} = \tilde{P}_0,$$

where θ_0 is the angle with respect to the direction of fire rays at P_0 (see Figure 11.1) (it is β^+ according to the notations of Chapter 8). Here and in the following we will denote by $\mathbf{n}(P)$ the unit vector in the direction of the fire rays at a point P and $\mathbf{t}(P)$ will denote the tangent at the level sets. This means that we follow the level set for a positive angle $\Delta\phi$ up to a point P_1, and then a segment with direction $\mathbf{t}(P_1)$, up to a point P_2. The point P_2 is saturated (in the sense of equation (11.1.1)) and it holds $\angle\mathbf{n}(P_2), \mathbf{t}(P_1) = \alpha$. More precisely, we have:

- P_0 the point on the level set $\{u = u(P_0)\}$ from which we put an amount of barrier on the same level set. The point $O_0 \in Z$ is the point of the spiral from which the fire ray towards P_0 starts.
- P_1 is the point on the same level set as P_0 such that from P_1 a segment is constructed, that is $u(P_0) = u(P_1)$. The point $O_1 \in Z$ is the point of the spiral from which the fire ray towards P_1 starts.
- $\Delta\phi$ is the angle covered by the arc P_0P_1.
- P_2 is the saturated point ((11.1.1)) from which a saturated spiral is constructed. $O_2 \in Z$ is the point of the spiral from which the fire ray towards P_2 starts.
- $\theta_0 \in [0, \frac{\pi}{2}]$ is the angle that the barrier forms with the fire ray $\bar{\gamma}_{P_0}$;
- we call $\mathbf{n}(P_1) = \frac{\nabla u(P_1)}{|\nabla u(P_1)|}$, $\mathbf{n}(P_2) = \frac{\nabla u(P_2)}{|\nabla u(P_2)|}$, $\mathbf{t}(P_1) = \frac{P_2 - P_1}{|P_2 - P_1|}$;

- $s = \overline{P_0\tilde{P}_0}$, with $s << 1$, and
$$h = s\cos\theta_0. \tag{11.1.2}$$
- We will call $\delta P_i = \tilde{P}_i - P_i$, $i = 0, 1, 2$.
- Call ϕ_0 the angle corresponding to the point P_0 and ϕ_1 the angle corresponding to P_1, that is $\Delta\phi = \phi_1 - \phi_0$.

Remark 11.1.1. We remark that the starting point on the spiral of the rays for P_i and $\tilde{P}_i$ is the same: indeed, if the ray $\bar{\gamma}_{P_i}$ is not tangent to the curve, it is clearly true. If it is tangent, then if $P_i\tilde{P}_i = \mathcal{O}(\delta s)$, if we call the two starting points $O_i, \tilde{O}_i$ then $O_i\tilde{O}_i = o(\delta s)$, therefore we can assume that the starting point is the same.

Here the computations are performed with the parameter h instead of the parameter s of the family, since it is the difference in time between the points $\tilde{P}_0$, P_0, for which the computations are more easier to perform. In the following we will reconvert all the formulas in order to deal directly with $\bar{f}_s$. We have the following relations:

Relations at point P_0:
$$u(\tilde{P}_0) = u(P_0) + h, \tag{11.1.3}$$
$$L(\tilde{P}_0) = L(P_0) + \frac{h}{\cos\theta_0}, \tag{11.1.4}$$
where $L(P)$ is the length of the spiral up to the point P. The variation of the angle ϕ_0 reads as
$$r(P_0)\delta\phi_0 = h\tan\theta_0, \tag{11.1.5}$$
therefore the position of the new point $\tilde{P}_0$ is
$$\tilde{P}_0 = h\mathbf{n}(P_0) + r(P_0)\delta\phi_0\mathbf{t}(P_1) + o(h). \tag{11.1.6}$$

Relations at point P_1: the point P_1 is on the same level set as P_0.
$$u(\tilde{P}_1) = u(\tilde{P}_0) = u(P_0) + h = u(P_1) + h.$$
The position of the perturbed point as
$$\tilde{P}_1 = P_1 + h\mathbf{n}(P_1) + r(P_1)\delta\phi_1\mathbf{t}(P_1) + o(h).$$
We observe that the slope of the segment $\tilde{P}_1\tilde{P}_2$ is $e^{i(\phi_1+\delta\phi_1+\frac{\pi}{2})}$. Indeed here we cannot a priori assume that the fire rays arrive parallel at the points $P_1, \tilde{P}_1$.

Relations at point P_2: In the perturbed point $\tilde{P}_2$ a new saturated spiral starts. The slope of the segment arriving at $\tilde{P}_2$ is $e^{i(\phi_1+\delta\phi_1+\frac{\pi}{2})}$, and the slope of the starting spiral is $e^{i(\phi_2+\delta\phi_2+\alpha)}$. Therefore, since we require them to be parallel, the condition on the angles reads as
$$\phi_1 + \delta\phi_1 + \frac{\pi}{2} = \phi_2 + \delta\phi_2 + \alpha.$$
Since we know that
$$\phi_1 + \frac{\pi}{2} = \phi_2 + \alpha,$$
the condition on the variation of angles becomes
$$\delta\phi_1 = \delta\phi_2.$$

The difference in slope between the two vectors

$$\frac{\tilde{P}_2-\tilde{P}_1}{|\tilde{P}_2-\tilde{P}_1|} \text{ and } \frac{P_2-P_1}{|P_2-P_1|}$$

is $\delta\phi_1=\delta\phi_2$, therefore the position of the perturbed point $\tilde{P}_2$ can be computed as

$$\tilde{P}_2=P_2+(h-|P_2-P_1|\delta\phi_1)\mathbf{n}(P_1)+\left((h-|P_2-P_1|\delta\phi_1)\cot\alpha+\frac{f_{\phi_0}(P_2)}{\sin\alpha}\delta\phi_1\right)\mathbf{t}(P_1)+o(h).$$

We use the saturation condition, i.e. $\tilde{P}_2$ is a saturated point, knowing P_2 is saturated. In particular, we have:

Saturation: P_2 is a saturated point:

$$u(O_2)+\overline{O_2P_2}=\cos\alpha\overline{P_1P_2}+\cos\alpha P_0P_1+\cos\hat{\alpha}L(P_0); \tag{11.1.7}$$

We write the same equation for the perturbed point.

Saturation perturbed: $\tilde{P}_2$ is a saturated point:

$$u(O_2)+\overline{O_2\tilde{P}_2}=\cos\alpha\overline{\tilde{P}_1\tilde{P}_2}+\cos\alpha P_0P_1+\cos\hat{\alpha}L(P_0)+\cos\hat{\alpha}s. \tag{11.1.8}$$

We have that (recall r is the radius of the original spiral):

$$\begin{aligned}\tilde{P}_1\tilde{P}_0&=\int_{\phi_0+\delta\phi_0}^{\phi_1+\delta\phi_1}(r(\eta)+h)d\eta\\&=P_0P_1+h\Delta\phi-\int_{\phi_0}^{\phi_0+\delta\phi_0}(r(\eta)+h)d\eta+\int_{\phi_1}^{\phi_1+\delta\phi_1}(r(\eta)+h)d\eta\\&=P_0P_1+h\Delta\phi-h\tan\theta_0+r(P_1)\delta\phi_1+o(h),\end{aligned}$$

where we have used (11.1.5). Moreover,

$$\overline{\tilde{P}_1\tilde{P}_2}=\overline{P_2P_1}-r(P_1)\delta\phi_1+(h-|P_2-P_1|\delta\phi_1)\cot\alpha+\frac{f_{\phi_0}(P_2)}{\sin\alpha}\delta\phi_1+o(h),$$

and

$$\overline{\tilde{P}_2O_2}=\overline{P_2O_2}+\frac{h-|P_2-P_1|\delta\phi_1}{\sin\alpha}+f_{\phi_0}(P_2)\delta\phi_1\cot\alpha+o(h).$$

Subtracting equation (11.1.7) to equation (11.1.8) we get

$$\begin{aligned}&\frac{h-|P_2-P_1|\delta\phi_1}{\sin\alpha}+f_{\phi_0}(P_2)\delta\phi_1\cot\alpha-\\&\cos\alpha\left(h\Delta\phi-h\tan\theta_0+r(P_1)\delta\phi_1\right)+\\&-\cos\alpha\left(-r(P_1)\delta\phi_1+(h-|P_2-P_1|\delta\phi_1)\cot\alpha+\frac{f_{\phi_0}(P_2)}{\sin\alpha}\delta\phi_1\right)-\cos\hat{\alpha}\frac{h}{\cos\theta_0}=0,\end{aligned}$$

that is, expliciting $\delta\phi_1$ we obtain

$$\delta\phi_1=\frac{h}{|P_2-P_1|}\left(1-\cot\alpha\Delta\phi+\cot\alpha\tan\theta_0-\frac{\cos\hat{\alpha}}{\sin\alpha}\frac{1}{\cos\theta_0}\right) \tag{11.1.9}$$

$$=\frac{s}{|P_2-P_1|}\left(\cos\theta_0-\cot\alpha\Delta\phi\cos\theta_0+\cot\alpha\sin\theta_0-\frac{\cos\hat{\alpha}}{\sin\alpha}\right). \tag{11.1.10}$$

In particular, the variation of the angle of the level set arc is then

$$\begin{aligned}\delta\Delta\phi &= \Delta\phi + \delta\phi_1 - \delta\phi_0 \\ &= \Delta\phi + \frac{h}{|P_2 - P_1|}\left(1 - \cot\alpha\Delta\phi + \cot\alpha\tan\theta_0 - \frac{\cos\hat{\alpha}}{\sin\alpha}\frac{1}{\cos\theta_0} - \frac{|P_2 - P_1|}{r(P_0)}\tan\theta_0\right).\end{aligned}$$

Call $P(\phi)$ any point on the segment, with $P(\phi_1) = P_1$ and $P(\phi_2) = P_2$. Then we recover that, for any ϕ, $\phi + t = \phi_1 + \frac{\pi}{2}$.

$$\begin{aligned}\tilde{P}(\phi) &= P(\phi) + (h - |P(\phi) - P_1|\delta\phi_1)\mathbf{n}(P_1) \\ &\quad + \left((h - |P(\phi) - P_1|\delta\phi_1)\tan(\phi - \phi_1) + \frac{f_{\phi_0}(P(\phi))}{\cos(\phi - \phi_1)}\delta\phi_1\right)\mathbf{t}(P_1),\end{aligned}$$

and recall that

$$\mathbf{n}(P(\phi)) = \cos(\phi - \phi_1)\mathbf{n}(P_1) + \sin(\phi - \phi_1)\mathbf{t}(P_1). \tag{11.1.11}$$

Finally, if we call $\tilde{f}_{\phi_0}$ the element of the family of generalized barrier which is a perturbation of f_{ϕ_0} we find that: $\tilde{f}_{\phi_0} - f_{\phi_0}(\phi) = \delta r(\phi)$ with

$$\delta r(\phi) \sim \begin{cases} \frac{h}{\delta\phi_0}(\phi - \phi_0) & \phi_0 \le \phi < \phi_0 + \delta\phi_0, \\ h & \phi_0 + \delta\phi_0 \le \phi < \phi_1 + \delta\phi_1, \\ \frac{h - |P(\phi) - P_1|\delta\phi_1}{\cos(\phi - \phi_1)} & \phi_1 + \delta\phi_1 \le \phi < \phi_2 + \delta\phi_2. \end{cases}$$

The derivative in the parameter h reads as

$$\bar{g}_{\phi_0}(\phi) = \begin{cases} 1 & \phi_0 \le \phi < \phi_0 + \Delta\phi = \phi_1, \\ \frac{1 - \frac{|P(\phi) - P_1|}{|P_2 - P_1|}\left(1 - \cot\alpha\Delta\phi + \cot\alpha\tan\theta_0 - \frac{\cos\hat{\alpha}}{\sin\alpha}\frac{1}{\cos\theta_0}\right)}{\cos(\phi - \phi_1)}, & \phi_1 \le \phi < \phi_2 = \phi_1 + \frac{\pi}{2} - \alpha. \end{cases} \tag{11.1.12}$$

In particular to get $\bar{f}_{\phi_0}$ we need simply to multiply $\cos\theta_0\bar{g}_{\phi_0}(\phi)$.

11.1.1 Analysis of the initial data

In this subsection we analyze the initial data obtained in the previous section. We found that

$$\bar{g}_{\phi_0}(\phi) = \begin{cases} 1 & \phi_0 \le \phi < \phi_0 + \Delta\phi = \phi_1, \\ \frac{1 - \frac{|P(\phi) - P_1|}{|P_2 - P_1|}(1 - \cot\alpha\Delta\phi + \cot\alpha\tan\theta_0 - \frac{\cos\hat{\alpha}}{\sin\alpha}\frac{1}{\cos\theta_0})}{\cos(\phi - \phi_1)}, & \phi_1 \le \phi < \phi_2 = \phi_1 + \frac{\pi}{2} - \alpha. \end{cases} \tag{11.1.13}$$

Since after the point P_2 it is a saturated spiral, by linearity we can compute the RDE that the derivative $\bar{g}_{\theta_0}$ satisfies. In this subsection we study precisely the RDE satisfied by the initial data in the arc case.

It holds:

- In the interval $\phi \in [\phi_1 + \frac{\pi}{2} - \alpha, \phi_1 + 2\pi + \theta_0)$ it holds

$$\frac{d\bar{g}_{\phi_0}(\phi)}{d\phi} = \bar{g}_{\phi_0}(\phi)\cot\alpha.$$

  In particular the solution reads as

$$\bar{g}_{\phi_0}(\phi) = \bar{g}_{\phi_0}\left(\Delta\phi + \phi_0 + \frac{\pi}{2} - \alpha\right) e^{\cot\alpha(\phi - (\Delta\phi + \phi_0 + \frac{\pi}{2} - \alpha))}.$$

  We remark that $\bar{g}_{\phi_0}\left(\Delta\phi + \phi_0 + \frac{\pi}{2} - \alpha\right)$ can be easily computed: indeed it is

$$\bar{g}_{\phi_0}\left(\Delta\phi + \phi_0 + \frac{\pi}{2} - \alpha\right) = \frac{\cot\alpha}{\sin\alpha}\left(\Delta\phi - \tan\theta_0\right) + \frac{\cos\hat{\alpha}}{(\sin\alpha)^2}\frac{1}{\cos\theta_0}, \qquad (11.1.14)$$

  in particular there is no need for the computation of the formula $|P(\phi) - P_1|$ here.

- In the point $\phi = \phi_0 + 2\pi + \theta_0$ there is a downward jump, that is

$$\bar{g}_{\phi_0}(\phi_0 + 2\pi + \theta_0) - \bar{g}_{\phi_0}(\phi_0 + 2\pi + \theta_0 -) = -\frac{1}{\cos\theta_0}.$$

- In the interval $\phi \in [\phi_0 + 2\pi + \theta_0, \phi_0 + 2\pi + \frac{\pi}{2})$ it holds

$$\frac{d\bar{g}_{\phi_0}(\phi)}{d\phi} = \bar{g}_{\phi_0}(\phi)\cot\alpha.$$

  In particular the solution reads as

$$\bar{g}_{\phi_0}(\phi) = \left(\bar{g}_{\phi_0}\left(\Delta\phi + \phi_0 + \frac{\pi}{2} - \alpha\right) e^{\cot\alpha(2\pi + \theta_0 - \Delta\phi - \frac{\pi}{2} + \alpha)} - \frac{1}{\cos\theta_0}\right) e^{\cot\alpha(\phi - (\phi_0 + 2\pi + \theta_0))}.$$

- In the point $\phi = \phi_0 + 2\pi + \frac{\pi}{2}$ there is an upward jump, that is

$$\bar{g}_{\phi_0}(\phi_0 + 2\pi + \frac{\pi}{2}) - \bar{g}_{\phi_0}(\phi_0 + 2\pi + \frac{\pi}{2} -) = \tan\theta_0. \qquad (11.1.15)$$

  Indeed

$$f_{\phi_0}\left(2\pi + \frac{\pi}{2} + \delta\phi_0\right) = f_{\phi_0}\left(2\pi + \frac{\pi}{2}\right) + \frac{h\tan\theta_0}{r(P_0)}\left(f_{\phi_0}\left(2\pi + \frac{\pi}{2}\right)\cot\alpha - r(P_0)\right) + o(h),$$

  while

$$\tilde{f}_{\phi_0}\left(2\pi + \frac{\pi}{2} + \delta\phi_0\right) = \tilde{f}_{\phi_0}\left(2\pi + \frac{\pi}{2}\right)\left(1 + \frac{h\tan\theta_0}{r(P_0)}\cot\alpha\right) + o(h).$$

- In the interval $\phi \in [\phi_0 + 2\pi + \frac{\pi}{2}, \phi_0 + 2\pi + \frac{\pi}{2} + \Delta\phi)$ it holds

$$\frac{d\bar{g}_{\phi_0}(\phi)}{d\phi} = \bar{g}_{\phi_0}(\phi)\cot\alpha - 1.$$

  In particular the solution reads as

$$\bar{g}_{\phi_0}(\phi) = \left[\left(\bar{g}_{\phi_0}\left(\Delta\phi + \phi_0 + \frac{\pi}{2} - \alpha\right) e^{\cot\alpha(2\pi + \theta_0 - \Delta\phi - \frac{\pi}{2} + \alpha)} - \frac{1}{\cos\theta_0}\right) e^{\cot\alpha(\frac{\pi}{2} - \theta_0)} + \tan\theta_0\right] \cdot$$
$$\cdot\, e^{\cot\alpha(\phi - (\phi_0 - 2\pi - \frac{\pi}{2}))}.$$

- In the point $\phi = \phi_0 + 2\pi + \frac{\pi}{2} + \Delta\phi$ there is a downward jump, that is

$$\bar{g}_{\phi_0}\left(\phi_0 + 2\pi + \frac{\pi}{2} + \Delta\phi\right) - \bar{g}_{\phi_0}\left(\phi_0 + 2\pi + \frac{\pi}{2} + \Delta\phi-\right) = -\cot^2\alpha\left(\Delta\phi + \left(\frac{1-\sin\theta_0}{\cos\theta_0}\right)\right).$$

  To prove this quantity, observe that

$$f_{\phi_0}\left(\Delta\phi + \frac{\pi}{2} + 2\pi + \delta\phi_1\right) = f_{\phi_0}\left(\Delta\phi + \frac{\pi}{2} + 2\pi\right) - |P_2 - P_1| + \\ + \left(f_{\phi_0}\left(\Delta\phi + \frac{\pi}{2} + 2\pi\right) - |P_2 - P_1|\right))\cot\alpha\delta\phi_1 - \frac{r(P_2)}{\sin\alpha}\delta\phi_1,$$

  while

$$\tilde{f}_{\phi_0}\left(\Delta\phi + \frac{\pi}{2} + 2\pi + \delta\phi_1\right) = \tilde{f}_{\phi_0}\left(\Delta\phi + \frac{\pi}{2} + 2\pi\right) - |\tilde{P}_2 - \tilde{P}_1| + \\ + \left(\tilde{f}_{\phi_0}\left(\Delta\phi + \frac{\pi}{2} + 2\pi\right) - |\tilde{P}_2 - \tilde{P}_1|\right)\cot\alpha\delta\phi_1 - \tilde{r}(P_1)\delta\phi_1.$$

- For $\phi \geq \phi_0 + \Delta\phi + 2\pi + \frac{\pi}{2}$ the function $\bar{g}_{\phi_0}$ satisfies:

$$\frac{d\bar{g}_{\phi_0}}{d\theta} = \cot\alpha\bar{g}_{\phi_0}(\theta) - \frac{\bar{g}_{\phi_0}(\phi - 2\pi - \alpha)}{\sin\alpha}.$$

We compute then the same quantities for $\bar{f}_{\phi_0} = \cos\theta_0\bar{g}_{\phi_0}$ (the derivative with respect to the length parameter s).

Optimizing with respect to $\Delta\phi$.

Before starting with the computations of the solution we optimize w.r.t. $\Delta\phi$ exploiting the linearity of the problem, finding out that the worst case to analyze is the one of $\Delta\phi = 0$ (which we will see correspond to the case of the segment). We compute the derivative of $\bar{g}_{\phi_0} = \partial\bar{g}_{\phi_0}$ with respect to $\Delta\phi$. We have the following relations

- The derivative of $\bar{g}_{\phi_0}$ in the point $\phi_1 + \Delta\phi + \frac{\pi}{2} - \alpha$ is (see (11.1.14))

$$\partial\bar{g}_{\phi_0}\left(\phi_1 + \Delta\phi + \frac{\pi}{2} - \alpha\right) = \frac{\cot\alpha}{\sin\alpha}.$$

- For $\phi \in [\Delta\phi + \frac{\pi}{2} - \alpha, 2\pi + \frac{\pi}{2} + \Delta\phi)$ it satisfies the equation

$$\frac{d}{d\phi}\partial\bar{g}_{\phi_0} = \cot\alpha\partial\bar{g}_{\phi_0}.$$

- In $\phi = 2\pi + \frac{\pi}{2} + \Delta\phi$ there is a downward jump, that is

$$\partial(\bar{g}_{\phi_0})_{\Delta\phi}(2\pi + \frac{\pi}{2} + \Delta\phi) - \partial(\bar{g}_{\phi_0})_{\Delta\phi}(2\pi + \frac{\pi}{2} + \Delta\phi-) = -\cot^2\alpha.$$

- For $\phi \geq 2\pi + \Delta\phi + \frac{\pi}{2}$ it satisfies

$$\frac{d}{d\phi}\partial\bar{g}_{\phi_0} = \cot\alpha\partial\bar{g}_{\phi_0} - \frac{\partial\bar{g}_{\phi_0}(\phi - 2\pi - \alpha)}{\sin\alpha}.$$

To prove some positivity of the derivative we use observation in Subsection 8.1.5. First we compute the solution for $\phi \in [\Delta\phi + \frac{\pi}{2} - \alpha + (2\pi+\alpha), 2\pi + \frac{\pi}{2} + \Delta\phi + (2\pi+\alpha))$: (see Lemma 10.0.2) it is

$$\left(\frac{\cot\alpha}{\sin\alpha}e^{\cot\alpha(2\pi+\alpha)} - \cot^2\alpha - \frac{\cot\alpha}{\sin\alpha^2}\left(\phi - (\Delta\phi + \frac{\pi}{2} + 2\pi)\right)\right)e^{\cot\alpha\left(\phi-(\Delta\phi+\frac{\pi}{2}+2\pi)\right)}.$$

We recall that the following change of variable

$$\rho(t) = r\left(\frac{(2\pi+\alpha)}{\log\lambda}t\right)e^{-c\frac{(2\pi+\alpha)}{\log\lambda}t},$$

with c solution of (8.1.18), satisfies

$$\dot\rho(t) = \rho(t) - \rho(t - \log\lambda).$$

Here $\lambda = e$ (for $\sigma = 2.6144$) and $c = 0.27995$. We need to compute therefore

$$\frac{d}{d\phi}\partial\bar g_{\phi_0}e^{-c\phi}.$$

An easy computation shows that it is

$$\frac{1}{(2\pi+\alpha)}\left(\frac{\cot\alpha}{\sin\alpha}e^{\cot\alpha(2\pi+\alpha)} - \cot^2\alpha - \frac{\cot\alpha}{\sin\alpha^2}(\phi - \Delta\phi - \frac{\pi}{2} - 2\pi)\right) - \frac{\cot\alpha}{\sin\alpha^2}.$$

In particular for determining its sign we have to study the function (Lemma 10.0.3)

$$\begin{aligned}&-\frac{\cot\alpha}{\sin\alpha^2}\left(2\pi+\alpha-\phi+\Delta\phi+\frac{\pi}{2}+2\pi\right) + \frac{\cot\alpha}{\sin\alpha}e^{\cot\alpha(2\pi+\alpha)} - \cot\alpha^2\\ &\geq -\frac{\cot\alpha}{\sin\alpha^2}(2\pi+\alpha) + \frac{\cot\alpha}{\sin\alpha}e^{\cot\alpha(2\pi+\alpha)} - \cot\alpha^2 \geq 6.\end{aligned}$$

This proves that it is an increasing function in $\Delta\phi$, that is $\partial\bar g_{\phi_0} \geq 0$, therefore the worst case scenario is represented by $\Delta\phi = 0$. The previous computations are the proof of the following

Proposition 11.1.2. *The worst possible scenario is $\Delta\phi = 0$, that is the study of the segment case.*

11.1.2 Diverging family: arc case

Here we study the case $\Delta\phi = 0$. The numerical plots of the results presented here are in the Appendix. Even if all the formulas for $\bar f_s$ are explicit, the computation of the values of $\bar f_s$ is onerous, therefore we use the software Mathematica in order to provide them. See Section 11.3 in the appendix. We have the following:

Theorem 11.1.3. *Let $\sigma \leq 2.3$ and let f_{ϕ_0} be an element of the family made by a piece of arc, a segment and a saturated spiral, with the constraint that if the arc is a single point P_1, then $\bar\gamma_{P_1}$ is orthogonal to the segment P_1P_2. Then $\bar f_{\phi_0} \geq 0$.*

Proof. By the previous discussion we can assume $\Delta\phi = 0$. We write the solution:

- We call
$$\bar f_{\phi_0}(\phi_0 + \frac{\pi}{2} - \alpha) = \kappa_1(\theta_0) = \frac{\cos\hat\alpha - \cos\alpha\sin\theta_0}{\sin\alpha^2};$$

- then
$$\bar{f}_{\phi_0}(\phi_0 + 2\pi + \theta_0) = \kappa_2(\theta_0) = \kappa_1(\theta_0)e^{\cot\alpha(2\pi+\theta_0-\frac{\pi}{2}+\alpha)} - 1;$$

- $$\bar{f}_{\phi_0}(\phi_0 + 2\pi + \theta_0) = \kappa_3(\theta_0) = \kappa_2 e^{\cot\alpha(\frac{\pi}{2}-\theta_0)} + \sin\theta_0 - \cot\alpha^2(1-\sin\theta_0);$$

- finally for $\phi \in [\phi_0 + 2\pi + \frac{\pi}{2}, \phi_0 + 4\pi + \alpha + \theta_0]$ the solution reads as
$$\bar{f}_{\phi_0}(\phi) = \left(\kappa_3(\theta_0) - \frac{\kappa_1(\theta_0)}{\sin\alpha}(\phi - \phi_0 - 2\pi - \frac{\pi}{2})\right) e^{\cot\alpha(\phi-\phi_0-2\pi-\frac{\pi}{2})}$$

- call
$$\kappa_4(\theta_0) = \bar{f}_{\phi_0}(\phi_0 + 4\pi + \alpha + \theta_0);$$

- for $\phi \in [\phi_0 + 4\pi + \alpha + \theta_0, \phi_0 + 4\pi + \alpha + \frac{\pi}{2}]$ the solution reads as
$$\bar{f}_{\phi_0}(\phi) = \left(\kappa_4(\theta_0) - \frac{\kappa_2(\theta_0)}{\sin\alpha}(\phi - \phi_0 - 4\pi - \theta_0 - \alpha)\right) e^{\cot\alpha(\phi-\phi_0-4\pi-\theta_0-\alpha)}.$$

In order to use the ideas of Subsection 8.1.5 we consider again
$$\rho(t) = r((2\pi+\alpha)t)e^{-c(2\pi+\alpha)t}.$$

To prove that the derivative is positive one has to evaluate the two quantities (the procedure is precisely the same of Subsection 11.1.1: when computing $\frac{d}{d\phi}r(\phi)e^{-c\phi}$ one gets:

- for $\phi \in [\phi_0 + 2\pi + \frac{\pi}{2}, \phi_0 + 4\pi + \theta_0 + \alpha]$ it is
$$-\frac{\kappa_1}{\sin\alpha} + \frac{1}{2\pi+\alpha}\left(\kappa_3 - \frac{\kappa_1}{\sin\alpha}(\phi - \phi_0 - 2\pi - \frac{\pi}{2})\right).$$

- For $\phi \in [\phi_0 + 4\pi + \theta_0 + \alpha, \phi_0 + 4\pi + \frac{\pi}{2} + \alpha]$ it is
$$-\frac{\kappa_2}{\sin\alpha} + \frac{1}{2\pi+\alpha}\left(\kappa_4 - \frac{\kappa_2}{\sin\alpha}(\phi - \phi_0 - 4\pi - \theta_0 - \alpha)\right).$$

  Numerical computations (that can be found in the appendix) shows that $\kappa_i \geq 0$ for $i = 1, 2, 3, 4$. (Analytically one could show that κ_i are all increasing functions). In particular to have that they are positive it is enough to show that
$$-\frac{\kappa_1}{\sin\alpha}\left(4\pi + \theta_0 + 2\alpha - \frac{\pi}{2}\right) + \kappa_3 \geq 0$$
  and
$$-\frac{\kappa_2}{\sin\alpha}\left(2\pi + \alpha + \frac{\pi}{2} - \theta_0\right) + \kappa_4 \geq 0.$$
  Again, this is performed via numerical computations (see Appendix, Section 11.3 for the plots).

□

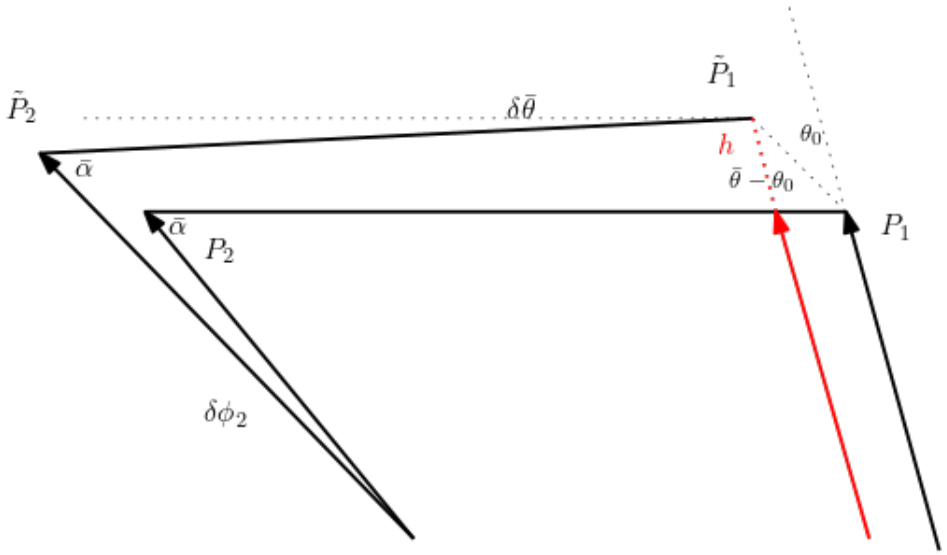

Figure 11.2: Analysis of perturbations for the segment case.

11.2 Analysis of Perturbations - Segment Case

The analysis of this section refers to Figure 11.2. In this case the point $P_0 \equiv P_1$. Call $\pi - \bar{\theta} = \angle O_0 P_1 P_2$. The analysis in Chapter 9 implies that there are no convex curves with an angle $\theta_0 > \bar{\theta}$: indeed any admissible curve will cross the segment. Since the last point is saturated, the starting angle must satisfy some bounds, that is:

$$\alpha < \bar{\theta}.$$

Here again we will perform the computations for

$$h = \frac{s \sin(\bar{\theta} - \theta_0)}{\sin \bar{\theta}}.$$

We have that the time difference for reaching the point $\tilde{P}_1$ is:

$$\delta t = h.$$

Therefore (see Figure 11.2)

$$r(P_1)\delta\phi_0 = h \frac{\sin\theta_0 \sin\bar{\theta}}{\sin(\bar{\theta} - \theta_0)}, \tag{11.2.1}$$

and the length is

$$|\tilde{P}_1 P_1| = h \frac{\sin\bar{\theta}}{\sin(\bar{\theta} - \theta_0)}. \tag{11.2.2}$$

Call $\mathbf{n}(P_1)$ the direction orthogonal to the segment P_1P_2 and $\mathbf{t}(P_1)$ the tangent such that $(\mathbf{t}(P_1), \mathbf{n}(P_1)) = (-e_1, e_2)$. We have that

$$\tilde{P}_1 = P_1 + h \sin\bar{\theta}\mathbf{n}(P_1) + h \sin\bar{\theta} \cot(\bar{\theta} - \theta_0)\mathbf{t}(P_1). \tag{11.2.3}$$

Point P_2. The new angle is $\angle O_0 \tilde{P}_1 \tilde{P}_2 = \pi - \bar{\theta} - \delta\bar{\theta}$ satisfying

$$\phi_0 + \bar{\theta} + \delta\bar{\theta} = \phi_2 + \delta\phi_2 + \alpha \tag{11.2.4}$$

but since $\phi_0 + \bar\theta = \phi_2 + \alpha$ we have that $\delta\bar\theta = \delta\phi_2$. We find that

$$\tilde P_2 = P_2 + \big(h\sin\bar\theta - |P_2 - P_1|\delta\phi_1\big)\,\mathbf{n}(P_1) + \left(\big(h\sin\bar\theta - |P_2 - P_1|\delta\bar\theta\big)\cot\alpha + \frac{f_{\phi_0}(P_2)\delta\bar\theta}{\sin\alpha}\right)\mathbf{t}(P_1). \tag{11.2.5}$$

In particular, the variation of the length of the segment P_1P_2 is as follows:

$$\delta|P_2 - P_1| = h(\sin\bar\theta - |P_2 - P_1|\delta\bar\theta)\cot\alpha - h\sin\bar\theta\cot(\bar\theta - \theta_0) + \frac{f_{\phi_0}(P_2)\delta\phi_2}{\sin\alpha}. \tag{11.2.6}$$

The time difference $\delta t = \tilde u(\tilde P_2) - u(P_2)$ is

$$\delta t = f_{\phi_0}(P_2)\delta\bar\theta\cot\alpha + (h\sin\bar\theta - |P_2 - P_1|\delta\bar\theta)\frac{1}{\sin\alpha}.$$

Finally the admissibility condition reads as

$$\begin{aligned}
&\big(h\sin\bar\theta - |P_2 - P_1|\delta\bar\theta\big)\,\frac{1}{\sin\alpha} + f_{\phi_0}(P_2)\delta\bar\theta\cot\alpha\\
&- \cos\alpha\left(\big(h\sin\bar\theta - |P_2 - P_1|\delta\bar\theta\big)\cot\alpha + \frac{f_{\phi_0}(P_2)\delta\bar\theta}{\sin\alpha} - h\sin\bar\theta\cot(\bar\theta - \theta_0)\right) - \cos\hat\alpha h\frac{\sin(\bar\theta)}{\sin(\bar\theta - \theta_0)}\\
&= \big(h\sin\bar\theta - |P_2 - P_1|\delta\bar\theta\big)\sin\alpha + \cos\alpha\sin\bar\theta\cot(\bar\theta - \theta_0) - \cos\hat\alpha\frac{\sin\bar\theta}{\sin(\bar\theta - \theta_0)} = 0.
\end{aligned}$$

This leads to

$$\delta\bar\theta = \frac{h}{|P_2 - P_1|}\left(\sin\bar\theta + \cot\alpha\sin\bar\theta\cot(\bar\theta - \theta_0) - \frac{\cos\hat\alpha}{\sin\alpha}\frac{\sin\bar\theta}{\sin(\bar\theta - \theta_0)}\right)$$

Compare with the previous case with $\bar\theta = \frac{\pi}{2}$ and $\Delta\phi = 0$. In this case the initial data (where we are deriving w.r.t. the parameter h) is the following:

$$\begin{aligned}
\bar g_{\phi_0}(\phi) &= \frac{\sin\bar\theta}{\sin(\bar\theta - \phi)} - \frac{|P(\phi) - P_1|\frac{\delta\bar\theta}{h}}{\sin(\bar\theta - \phi)}\\
&= \frac{1}{\sin(\bar\theta - \phi)}\left(\sin\bar\theta - \frac{|P(\phi) - P_1|}{|P_2 - P_1|}\left(\sin\bar\theta + \cot\alpha\sin\bar\theta\cot(\bar\theta - \theta_0) - \frac{\cos\hat\alpha}{\sin\alpha}\frac{\sin\bar\theta}{\sin(\bar\theta - \theta_0)}\right)\right).
\end{aligned}$$

As before we are interested in the final point, that is for $\phi = \bar\theta - \alpha$. We find that

$$\bar f_{\phi_0}(\bar\theta - \alpha) = \left(\frac{\cos\hat\alpha - \cos\alpha\cos(\bar\theta - \theta_0)}{\sin\alpha^2}\right)\frac{\sin\bar\theta}{\sin(\bar\theta - \theta_0)}, \tag{11.2.7}$$

(compare with the computations for the segment case, that is $\Delta\phi = 0$ and $\bar\theta = \frac{\pi}{2}$.

11.2.1 RDE satisfied by the initial data

In this subsection we study the RDE satisfied by the initial data. It holds:

- In the interval $\phi \in [\phi_0 + \bar\theta - \alpha, \phi_0 + 2\pi + \theta_0)$ it holds

$$\frac{d\bar f_{\phi_0}(\phi)}{d\phi} = \bar f_{\phi_0}(\phi)\cot\alpha.$$

  In particular the solution

$$\bar g_{\phi_0}(\phi) = \bar g_{\phi_0}\left(\phi_0 + \bar\theta - \alpha\right)e^{\cot\alpha(\phi - (\phi_0 + \bar\theta - \alpha))}.$$

  where $\bar g_{\phi_0}\left(\phi_0 + \bar\theta - \alpha\right)$ is given by the formula (11.2.7).

- In the point $\phi = \phi_0 + 2\pi + \theta_0$ there is a downward jump, that is

$$\bar{g}_{\phi_0}(\phi_0 + 2\pi + \theta_0) - \bar{g}_{\phi_0}(\phi_0 + 2\pi + \theta_0 -) = -\frac{\sin\bar{\theta}}{\sin(\bar{\theta} - \theta_0)}, \tag{11.2.8}$$

  which is computed by subtracting the length $\frac{|P_1\tilde{P}_1|}{h}$.

- In the interval $\phi \in [\phi_0 + 2\pi + \theta_0, \phi_0 + 2\pi + \bar{\theta})$ it holds

$$\frac{d\bar{g}_{\phi_0}(\phi)}{d\phi} = \bar{g}_{\phi_0}(\phi)\cot\alpha.$$

- In the point $\phi = \phi_0 + 2\pi + \bar{\theta}$ the jump is computed as follows:

$$f_{\phi_0}(\phi_0{+}2\pi{+}\bar{\theta}{+}\delta\bar{\theta}) = f_{\phi_0}(2\pi{+}\bar{\theta}{+}\phi_0){+}\delta\bar{\theta}f_{\phi_0}(2\pi{+}\bar{\theta}{+}\phi_0)\cot\alpha{-}\frac{f_{\phi_0}(P_2)\delta\bar{\theta}}{\sin\alpha}{-}|P_2{-}P_1|;$$

$$\tilde{f}_{\phi_0}(\phi_0 + 2\pi + \bar{\theta} + \delta\bar{\theta}) = \tilde{f}_{\phi_0}(2\pi + \bar{\theta} + \phi_0) + \delta\bar{\theta}\tilde{f}_{\phi_0}(2\pi + \bar{\theta} + \phi_0)\cot\alpha - |\tilde{P}_2 - \tilde{P}_1|;$$

  therefore, using (11.2.6), we get

$$\begin{aligned}
&\bar{g}_{\phi_0}(\phi_0 + 2\pi + \bar{\theta}) - \bar{g}_{\phi_0}(\phi_0 + 2\pi + \bar{\theta}-) = \\
&= -\delta|P_2 - P_1| + \frac{f_{\phi_0}(P_2)}{\sin\alpha}\delta\bar{\theta} \\
&= \frac{\cot(\bar{\theta} - \theta_0)\sin\bar{\theta}}{\sin^2\alpha} - \cot^2\alpha\frac{\sin\bar{\theta}}{\sin(\bar{\theta} - \theta_0)}.
\end{aligned}$$

- For $\phi \geq \phi_0 + 2\pi + \bar{\theta}$ the function $\bar{g}_{\phi_0}$ satisfies:

$$\frac{d\bar{g}_{\phi_0}}{d\theta} = \cot\alpha\bar{g}_{\phi_0}(\theta) - \frac{\bar{g}_{\phi_0}(\phi - 2\pi - \alpha)}{\sin\alpha}.$$

We have then that $\bar{f}_{\phi_0} = \frac{\sin(\bar{\theta}-\theta_0)}{\sin\bar{\theta}}\bar{g}_{\phi_0}$. Then we have that

- In the point $\phi = \phi_0 + 2\pi + \theta_0$ the downward jump is

$$\bar{f}_{\phi_0}(\phi_0 + 2\pi + \theta_0) - \bar{f}_{\phi_0}(\phi_0 + 2\pi + \theta_0 -) = -1; \tag{11.2.9}$$

- In the point $\phi = \phi_0 + 2\pi + \bar{\theta}$ the jump is

$$\bar{f}_{\phi_0}(\phi_0 + 2\pi + \bar{\theta}) - \bar{f}_{\phi_0}(\phi_0 + 2\pi + \bar{\theta}-) = \frac{\cos(\bar{\theta} - \theta_0)}{\sin^2\alpha} - \cot^2\alpha.$$

11.2.2 Diverging family: segment case

In this subsection we finally compute the solution as we previously did in the arc case. The numerical plots can be found in the Appendix Section 11.4

Theorem 11.2.1. *Let $\sigma \leq 2.3$ and let f_{ϕ_0} be an element of the family made by a segment and a saturated spiral. Then $\bar{f}_{\phi_0} \geq 0$.*

Proof. Without loss of generality we can assume $\phi_0 = 0$. We compute the solution $\bar{f}_{\phi_0}$. Call

-

$$\bar{f}_{\phi_0}\left(\bar{\theta} - \alpha\right) = \kappa_1(\bar{\theta}, \theta_0) = \frac{\cos\hat{\alpha} - \cos\alpha\cos(\bar{\theta} - \theta_0)}{\sin\alpha^2}.$$

- For $\phi \in [\bar{\theta} - \alpha, 2\pi + \theta_0)$ we have that

$$\bar{f}_{\phi_0}(\phi) = \kappa_1(\bar{\theta}, \theta_0) e^{\phi - (\bar{\theta} - \alpha)}.$$

- For $\phi \in [2\pi + \theta_0, 2\pi + \bar{\theta})$

$$\bar{f}_{\phi_0}(\phi) = \left(\kappa_1(\bar{\theta}, \theta_0) e^{\cot\alpha(2\pi + \theta_0 - \bar{\theta} + \alpha)} - 1\right) e^{\cot\alpha(\phi - 2\pi - \theta_0)} = \kappa_2(\bar{\theta}, \theta_0) e^{\cot\alpha(\phi - 2\pi - \theta_0)}. \tag{11.2.10}$$

- Then we have

$$\bar{f}_{\phi_0}(2\pi + \bar{\theta}) = \kappa_2(\bar{\theta}, \theta_0) e^{\cot\alpha(\bar{\theta} - \theta_0)} + \frac{\cos(\bar{\theta} - \theta_0)}{\sin\alpha^2} - \cot^2\alpha = \kappa_3(\bar{\theta}, \theta_0).$$

Finally, in the interval where it is continuous we have:

- So for $\phi \in [2\pi + \bar{\theta}, 4\pi + \theta_0 + \alpha)$

$$\bar{f}_{\phi_0}(\phi) = \left(\kappa_3(\bar{\theta}, \theta_0) - \frac{\kappa_1(\bar{\theta}, \theta_0)}{\sin\alpha}(\phi - 2\pi - \bar{\theta})\right) e^{\cot\alpha(\phi - 2\pi - \bar{\theta})}. \tag{11.2.11}$$

- Call then

$$\kappa_4(\bar{\theta}, \theta_0) = \bar{f}_{\phi_0}(4\pi + \theta_0 + \alpha);$$

- So that for $\phi \in [4\pi + \theta_0 + \alpha, 4\pi + \bar{\theta} + \alpha]$ the solution reads as

$$\bar{f}_{\phi_0}(\phi) = \left(\kappa_4(\bar{\theta}, \theta_0) - \frac{\kappa_2(\bar{\theta}, \theta_0)}{\sin\alpha}(\phi - 4\pi - \theta_0 - \alpha)\right) e^{\cot\alpha(\phi - 4\pi - \theta_0 - \alpha)}, \tag{11.2.12}$$

  and so on. Again, numerical computations shows that $\kappa_i \geq 0$ for $i = 1, 2, 3, 4$. The proof proceeds exactly in the same way as the one of the arc case (see Theorem 11.1.3). Indeed it is enough to show that the two following quantities are positive (Lemma 10.0.3) (see Appendix 11.2.2, Section 11.4).

$$-\frac{\kappa_1}{\sin\alpha}\left(4\pi + \theta_0 + 2\alpha - \bar{\theta}\right) + \kappa_3 \geq 0$$

  and

$$-\frac{\kappa_2}{\sin\alpha}\left(2\pi + \alpha + \bar{\theta} - \theta_0\right) + \kappa_4 \geq 0.$$

□

Remark 11.2.2. It is compatible with the computations done for the arc case in the case $\Delta\phi = 0$ and $\bar{\theta} = \frac{\pi}{2}$.

Remark 11.2.3. It would be interesting to investigate the optimization w.r.t. $\bar{\theta}$ and θ_0.

Appendix Fire

Here the code provides the evaluation of the relevant quantities related to the function $\bar{f}_s$: we do not ask the program to solve any PDE or ODE. The evaluation of these functions are hard to perform by hand, and even if we do a careful analysis (like the study of minima and maxima of the functions), at some point one needs to use a calculator.

11.3 Numerical Computations for the Arc Case

In this section we present the numerical computations for the arc case (see Chapter 11, Section 11.1). The orange line represents $y = 0$

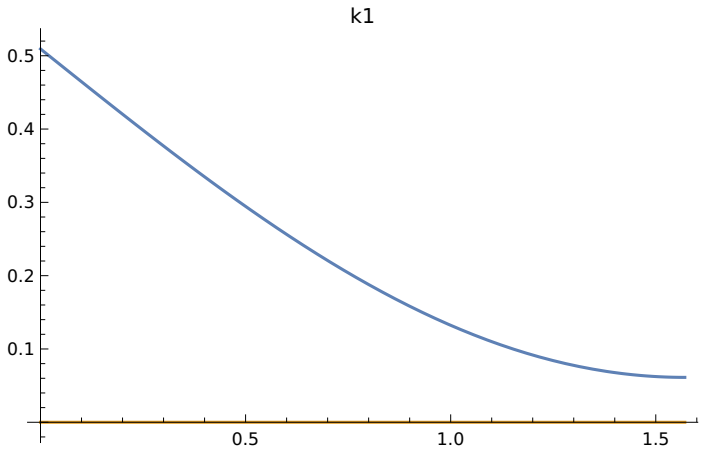

Figure 11.3: Computations for the arc case: κ_1.

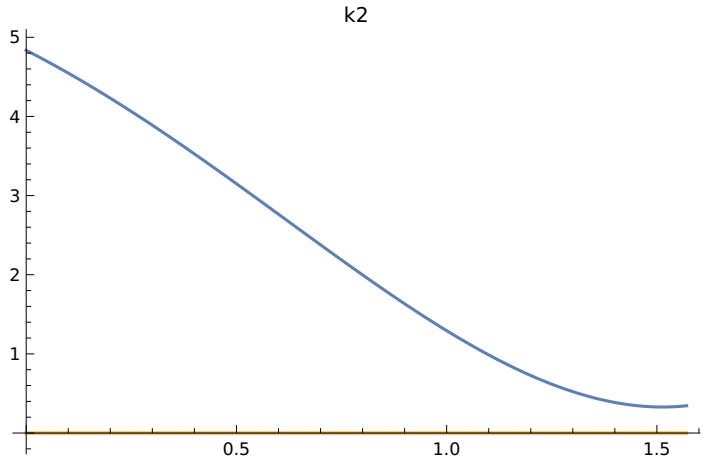

Figure 11.4: Computations for the arc case: κ_2.

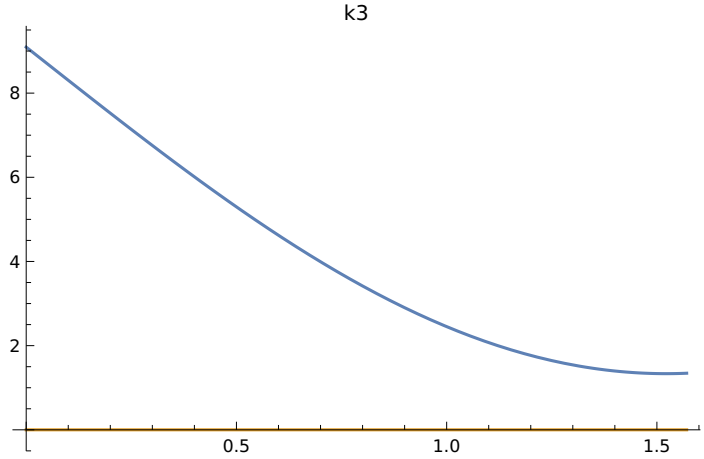

Figure 11.5: Computations for the arc case: κ_3.

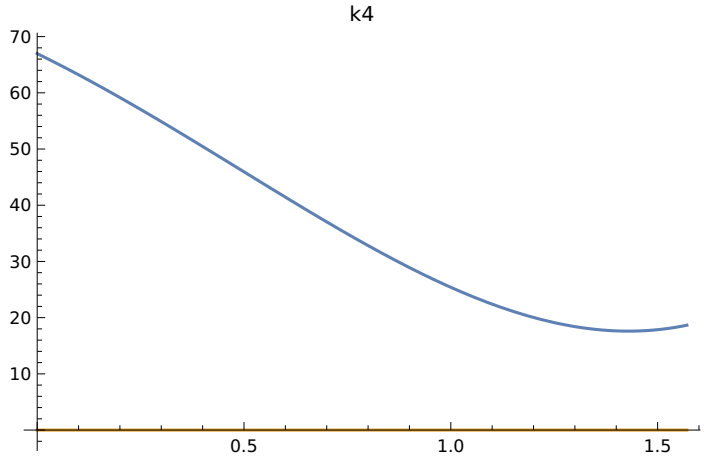

Figure 11.6: Computations for the arc case: κ_4.

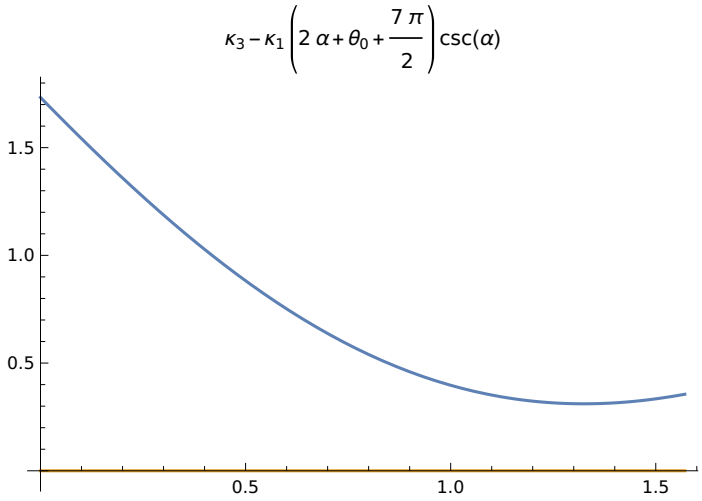

Figure 11.7: Computations for the arc case: $\kappa_3 - \frac{\kappa_1}{\sin\alpha}\left(2\alpha + \theta_0 + 7\frac{\pi}{2}\right)$.

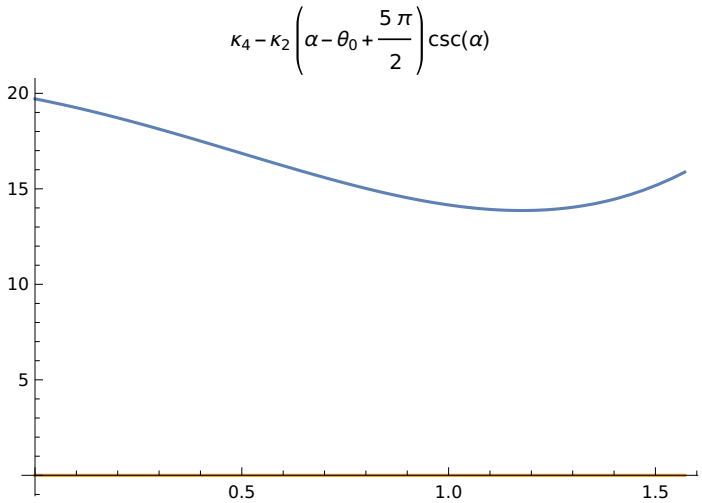

Figure 11.8: Computations for the arc case: $\kappa_4 - \frac{\kappa_2}{\sin\alpha}\left(\alpha - \theta_0 + 5\frac{\pi}{2}\right)$.

11.4 Numerical Computations for the Segment Case

In this section we present the numerical computations for the segment case (see Chapter 11, Section 11.2). The blue plane corresponds to $z = 0$.

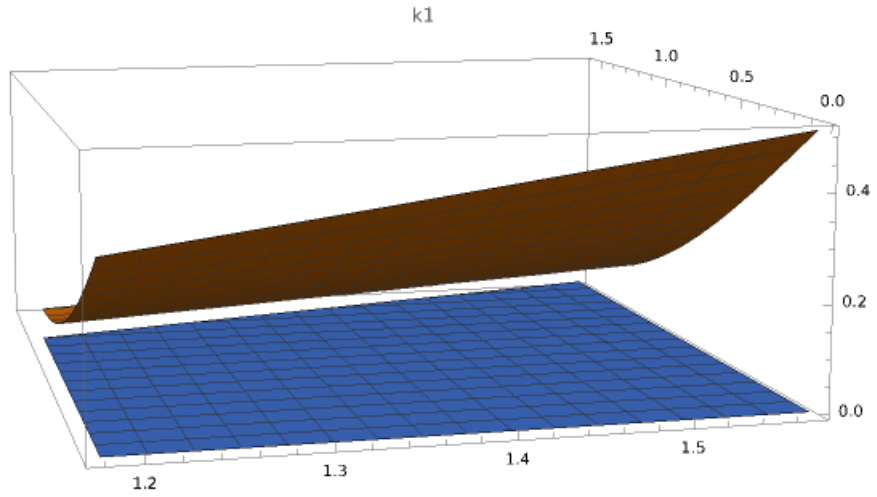

Figure 11.9: Computations for the segment case: κ_1.

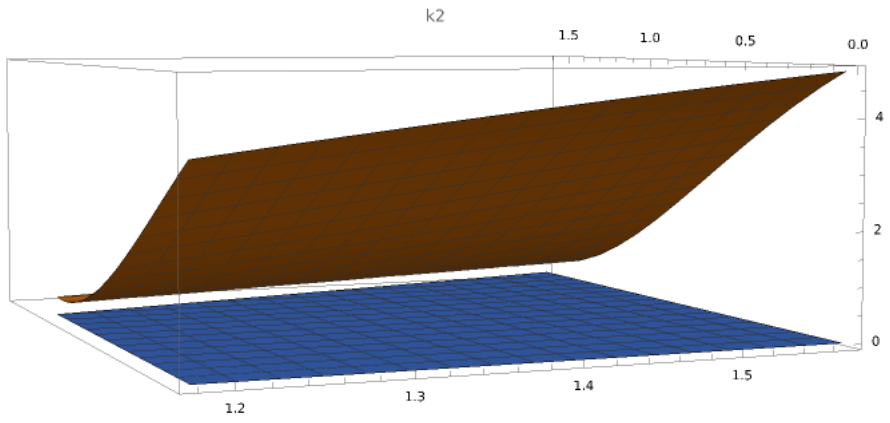

Figure 11.10: Computations for the segment case: κ_2.

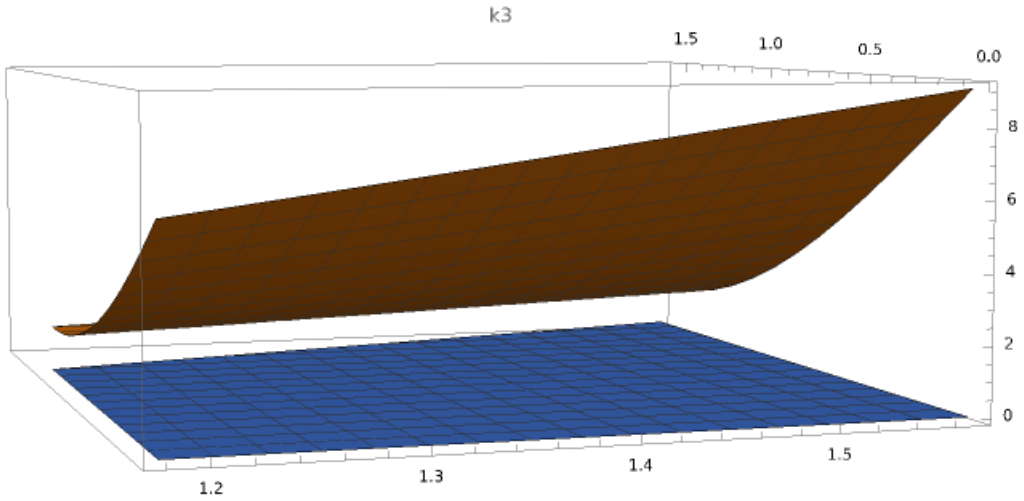

Figure 11.11: Computations for the segment case: κ_3.

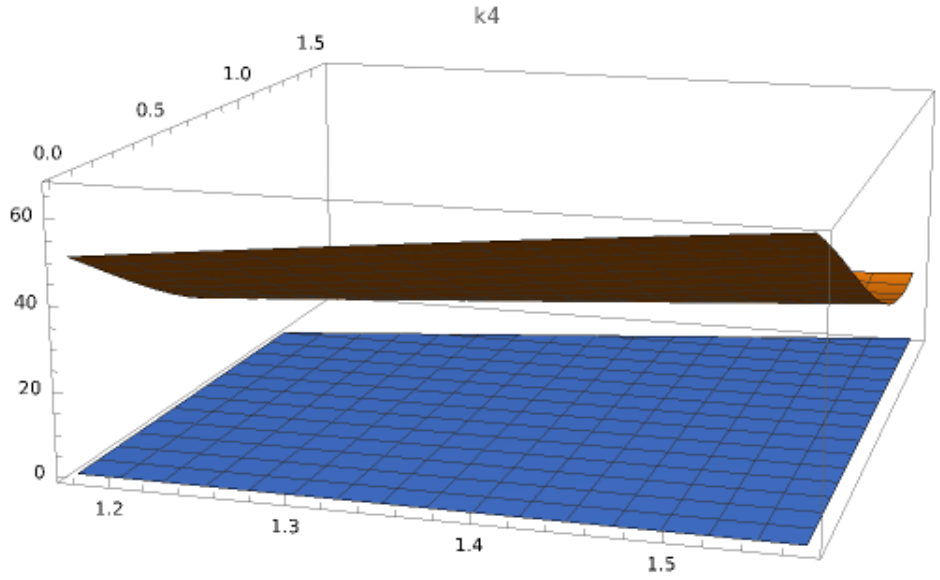

Figure 11.12: Computations for the segment case: κ_4.

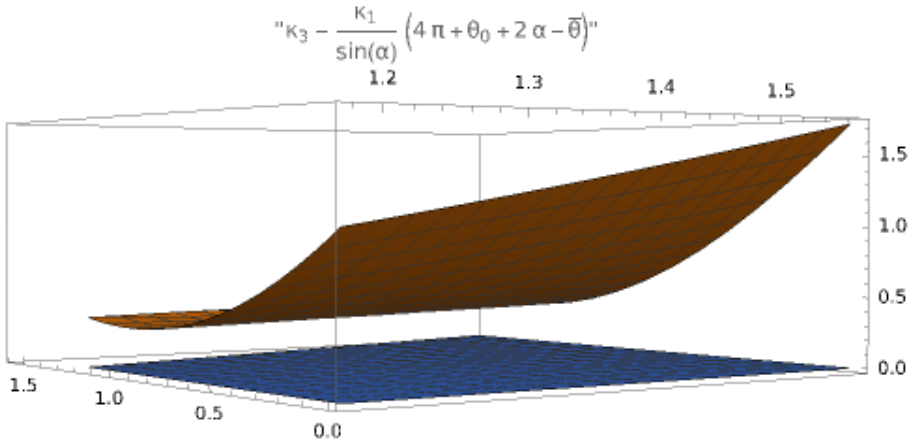

Figure 11.13: Computations for the segment case: $\kappa_3 - \frac{\kappa_1}{\sin\alpha}\left(4\pi + 2\alpha + \theta_0 - \bar{\theta}\right)$.

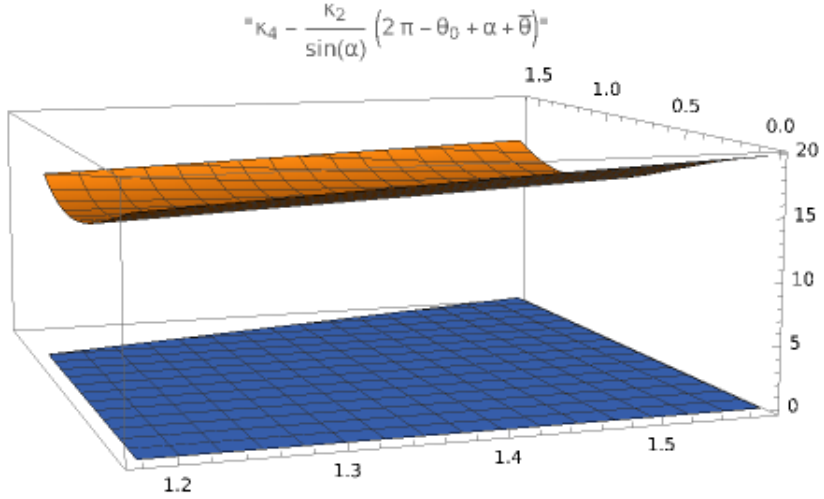

Figure 11.14: Computations for the segment case: $\kappa_4 - \frac{\kappa_2}{\sin\alpha}\left(2\pi + \alpha - \theta_0 + \bar{\theta}\right)$.

Ringraziamenti

Voglio ringraziare il mio relatore, il Prof. Stefano Bianchini, per tutto ciò che mi ha insegnato. Mi ha dato l'opportunità di entrare nel suo mondo matematico e farmi vedere qualche volta quello che lui vede con tanta chiarezza, oltre ad avermi dato la piena libertà di esprimermi come meglio credessi. Sono stata molto fortunata a essere sua studentessa, e il suo esempio mi farà da guida per tutta la vita.

Bibliography

[1] Bressan A. "A lemma and a conjecture on the cost of rearrangements." In: *Rend. Sem. Mat. Univ. Padova* 110 (2003), pp. 97–102.

[2] Bressan A. "An Ill Posed Cauchy Problem or a Hyperbolic System in Two Space Dimensions." In: *Rend. Sem. Mat. Univ. Padova* 110 (2003), pp. 103–117.

[3] Alberti G., Crippa G., Mazzucato, Anna M. "Exponential Self-similar mixing by incompressible flows." In: *J. Amer. Math. Soc. (JAMS)* 2 (2019), pp. 445–490.

[4] Alpern S. "New Proofs that Weak Mixing is Generic." In: *Inventiones Mathematicae* 32 (1976), pp. 263–278. URL: http://eudml.org/doc/142373.

[5] Ambrosio L. "Lecture notes on transport equation and Cauchy problem for BV vector fields and applications." In: (2004). URL: https://cvgmt.sns.it/paper/1573/.

[6] Ambrosio L. "Transport equation and Cauchy problem for BV vector fields." In: *Inventiones Mathematicae* 158 (2004), pp. 227–260.

[7] Ambrosio L., Fusco N., Pallara D. *Functions of Bounded Variations and Free Discontinuity Problems*. Oxford University Press, 2000. ISBN: 0198502451.

[8] Bedrossian J., Blumenthal A., Punshon-Smith S. "Almost-sure exponential mixing of passive scalars by the stochastic Navier-Stokes equations". In: *Annals of Probability* (2019).

[9] Bedrossian, J., Blumenthal, A., Punshon-Smith, S. "Almost-sure exponential mixing of passive scalars by the stochastic Navier-Stokes equations". In: *Annals of Probability. 2019* (2019).

[10] Bianchini S., Zizza M. "Properties of Mixing BV vector fields." In: *Communications in Mathematical Physics* (2023).

[11] Bonicatto P., Marconi E.. "Regularity estimates for the flow of BV autonomous divergence free vector fields in $\mathbb{R}^2$." In: *Communications in Partial Differential Equations* (2021).

[12] Bressan A. "Differential inclusions and the control of forest fires." In: *J. Differ. Equ.* 243 (2007), pp. 179–207.

[13] Bressan A. "Dynamic Blocking Problems for a Model of Fire Propagation." In: *Advances in Applied Mathematics, Modeling, and Computational Science* (2013), pp. 11–40.

[14] Bressan A. "Prize offered for the solution of a dynamic blocking problem." In: (). URL: %7Bhttp://personal.psu.edu/axb62/PSPDF/prize2.pdf%7D.

[15] Bressan A., Burago M., Friend A., Jou J. "Blocking strategies for a fire control problem." In: *Analysis and Applications* 6 (2008), pp. 229–246.

[16] Bressan A., Chiri M. T., "On the Regularity of Optimal Dynamic Blocking Strategies." In: *Calc. Var. Partial Diff. Equations* 61.36 (2022).

[17] Bressan A., De Lellis C. "Existence of optimal strategies for a fire confinement problem." In: *Comm. Pure Appl. Math.* 62 (2009), pp. 789–830.

[18] Bressan A., Wang T. "Equivalent formulation and numerical analysis of a fire confinement problem". In: *ESAIM; Control Optim. Calc. Var* 16 (2010), pp. 974–1001.

[19] Bressan A., Wang T. "Global necessary conditions for a dynamic blocking problem". In: *ESAIM; Control Optim. Calc. Var* 18 (2012), pp. 124–145.

[20] Bressan A., Wang T. "On the optimal strategy for an isotropic blocking problem." In: *Calc. Var.* 45 (2011), pp. 125–145.

[21] Chacon R. V. "Weakly mixing transformations which are not strongly mixing." In: *Proceedings of the American Mathematical Society* 22.3 (1969), pp. 559–562.

[22] Chen W. "THE NOTION OF MIXING AND RANK ONE EXAMPLES". In: 2015. URL: %7Bmath.uchicago.edu/~may/REU2015/REUPapers/Chen,Wenyu.pdf%7D.

[23] Cornfeld I. P., Fomin S.V., Sinai Y. G., Sossinski A.B. *Ergodic Theory.* Grundlehren der mathematischen Wissenschaften 245. Springer, 1982.

[24] Crippa G., De Lellis C. "Estimates and regularity results for the DiPerna-Lions flow." In: *J. Reine Angew. Math.* 616 (2008), pp. 15–46.

[25] De Lellis C.,Robyr R. "Hamilton-Jacobi equation with obstacles." In: *Archive for Rational Mechanics and Analysis* 200 (2011), pp. 1051–1073.

[26] Diperna R. J., Lions P. L. "Ordinary differential equations, transport theory and Sobolev spaces." In: *Inventiones Mathematicae* 98 (1989), pp. 511–547.

[27] Elgindi T. M., Zlatoš A. "Universal Mixers in All Dimensions." In: *Advances in Mathematics* 356 (2019).

[28] Falconer, K.J. *The geometry of fractal sets.* Cambridge University Press, 1986.

[29] Hale, J.K., Verduyn Lunel, S.M. *Introduction to functional differential equations.* Springer-Verlag, 1993.

[30] Halmos P. R. "Approximation theories for measure preserving transformation." In: *Transactions of the A. M. S.* 55 (1944), pp. 1–18.

[31] Halmos P. R. "In General a Measure Preserving Transformation is Mixing." In: *Annals of Mathematics* 45.4 (1944), pp. 786–792. URL: https://www.jstor.org/stable/1969304.

[32] Halmos P. R. *Lectures in Ergodic Theory.* AMS Chelsea Publishing, 1956.

[33] Katok A., Stepin A. "Metric properties of measure-preserving homeomorphisms." In: *Russ. Math. Surv.* 25.191 (1970).

[34] Klein, R., Langetepe E., Levcopoulos C., Lingas A., Schwarzwald B. "On a Firefighter's problem." In: *Int. J. Foundations of Computer Science* 30.02 (2019), pp. 231–246.

[35] Srivastava S. M. *A course on Borel sets.* Graduate texts in Mathematics. Springer, 1989.

[36] Mañé R. *Ergodic Theory and Differentiable Dynamics.* A series of modern surveys in Mathematics. Springer-Verlag, 1987.

[37] Mathew G., Mezic I., Petzold L. "A multiscale measure for mixing." In: *Phys. D* 211.1-2 (2005), pp. 23–46.

[38] Myshkis, A.D. "Linear Differential Equations with Retarded Argument". In: *GITTL, Moscow-Leningrad* (1951).

[39] Depauw N. "Non unicité des solutions bornées pour un champ de vecteurs BV en dehorsd'un hyperplan." In: *C. R. Math. Acad. Sci. Paris* 337(4) (2003), pp. 249–252.

[40] Oxtoby J. C., Ulam S. M. "Measure-Preserving Homeomorphisms and Metrical Transitivity." In: *Annals of Mathematics* 42.4 (1941), pp. 874–920. URL: http://www.jstor.com/stable/1968772.

[41] Pierrehumbert R. "Tracer microstructure in the large-eddy dominated regime." In: *Chaos, Solitons and Fractals* 4.6 (1994).

[42] Rokhlin V. "A 'general' measure preserving transformation is not mixing." In: *Dokl. Akad. Nauk SSSR* 60 (1948), pp. 349–351.

[43] Shnirelman A.I. "The geometry of the group of diffeomorphisms and the dynamics of an ideal incompressible fluid". In: *Math. USSR Sb.* 56 (1985), pp. 82–109. URL: https://iopscience.iop.org/article/10.1070/SM1987v056n01ABEH003025/pdf.

[44] Viana M., Olivera K. *Foundations of Ergodic Theory.* Cambridge Studies in Advanced Mathematics. Cambridge University Press, 2016. DOI: https://doi.org/10.1017/CBO9781316422601.

[45] Weiss B. "On the work of Rokhlin in ergodic theory." In: *Ergodic theory and dynamical systems* 9 (1989), pp. 619–627.

[46] Zizza, M. "An example of a BV weakly mixing vector field which is not strongly mixing". In: *Preprint* (2022).